INFORMATION TO USERS

This manuscript has been reproduced from the microfilm master. UMI films the text directly from the original or copy submitted. Thus, some thesis and dissertation copies are in typewriter face, while others may be from any type of computer printer.

The quality of this reproduction is dependent upon the quality of the copy submitted. Broken or indistinct print, colored or poor quality illustrations and photographs, print bleedthrough, substandard margins, and improper alignment can adversely affect reproduction.

In the unlikely event that the author did not send UMI a complete manuscript and there are missing pages, these will be noted. Also, if unauthorized copyright material had to be removed, a note will indicate the deletion.

Oversize materials (e.g., maps, drawings, charts) are reproduced by sectioning the original, beginning at the upper left-hand corner and continuing from left to right in equal sections with small overlaps.

Photographs included in the original manuscript have been reproduced xerographically in this copy. Higher quality 6" x 9" black and white photographic prints are available for any photographs or illustrations appearing in this copy for an additional charge. Contact UMI directly to order.

ProQuest Information and Learning
300 North Zeeb Road, Ann Arbor, MI 48106-1346 USA
800-521-0600

Characterization of the Catalytic Mechanisms of Two Aminoglycoside Phosphotransferases: APH(3')-IIIa from *Enterococcus faecalis* and APH(9)-Ia from *Legionella pneumophila*

By

Paul R. Thompson, B.Sc.

A Thesis

Submitted to the School of Graduate Studies

In Partial Fulfillment of the Requirements

For the Degree

Doctor of Philosophy

McMaster University

REGIOSPECIFICITY & CATALYTIC MECHANISM OF APH(3')-IIIa

Doctor of Philosophy (1999)
(Biochemistry)

McMaster University
Hamilton, Ontario

TITLE: Characterization of the Catalytic Mechanisms of Two Aminoglycoside Phosphotransferases: APH(3')-IIIa from *Enterococcus faecalis* and APH(9)-Ia from *Legionella pneumophila*

AUTHOR: Paul R. Thompson, B.Sc. (McMaster University)

SUPERVISOR: Associate Professor G.D. Wright

NUMBER OF PAGES: xix, 305

ABSTRACT

While the aminoglycoside antibiotics continue to be useful chemotherapeutic agents, the appearance and dissemination of high level aminoglycoside resistant strains is a threat to the future clinical relevance of these antibiotics. Since there are only a limited number of alternative antibiotics, and resistance to all of these therapies has been observed, there is an urgent need to either introduce new classes of antibiotics or to 'rehabilitate' the ones currently employed. The development of drugs that inhibit the resistance mechanism is one method to 'rehabilitate' the usefulness of these antibiotics. As such, we are employing structure based drug design techniques for the development of inhibitors to several enzymatic aminoglycoside resistance mechanisms. A prerequisite for this method of drug design is a thorough knowledge of the catalytic mechanism of the enzyme, and as such I have characterized the regiospecificity and phosphoryl transfer mechanism of two aminoglycoside phosphotransferases: APH(3')-IIIa and APH(9)-Ia. From these studies, described herein, it is now known that the APH(3')-IIIa enzyme catalyzes the direct transfer of the γ-phosphate of ATP to either the 3'-hydroxyl of 4,6-disubstituted aminoglycosides, or the 3'- and 5"-hydroxyl of 4,5-disubstituted aminoglycosides, providing that both hydroxyl groups are present. It is also now known that APH(9)-Ia catalyzes the transfer of the γ-phosphate of ATP to the 9-hydroxyl of spectinomycin. Site directed mutagenesis, kinetic, metal, solvent isotope, and solvent viscosity studies of these two enzymes indicate that a dissociative-like transition state is employed, and that phosphate transfer occurs through a biomechanical process.

Acknowledgements

I would like to begin by thanking my entire family for their kind and generous support, both financial and most importantly emotional, during these last six years. I would particularly like to thank my parents, Judy and Neil, for taking me in again during the last year and a half of my doctoral studies. I owe them a great deal for this and many others.

I would next like to thank all of the members of my lab for their intellectual support during our time together. I would particularly like to mention those people in the lab that contributed the most to the progression of my thesis work: David Boehr, Denis Daigle, Byron Delabarre, Kari Draker, and Geoff McKay. I would further like to thank my supervisory committee members, Albert Berghuis, G.E. Gerber, and T. Finan for their helpful comments and criticisms.

I would finally and most especially like to thank Gerry Wright for his patience with me and, as well, his ability to get the best out of me. Under his supervision I felt less like an automaton, and more like an equal. For this I am truly grateful, as it is a wonderful way to learn.

TABLE OF CONTENTS

		PAGE
ABSTRACT		iii
ACKNOWLEDGEMENTS		iv
TABLE OF CONTENTS		v
ABBREVIATIONS		x
LIST OF FIGURES		xii
LIST OF TABLES		xvi
LIST OF PDB FILES		xviii
PERSONAL PUBLICATIONS		xix
CHAPTER 1:	**INTRODUCTION**	1
1.1	Antibiotics and resistance	2
1.2	Identification and general chemical characteristics of aminoglycoside/aminocyclitol antibiotics	10
1.3	Mechanism of aminoglycoside action	13
1.4	Aminoglycoside resistance	21
1.4.1	Resistance by altered uptake	21
1.4.2	Altered targets I: resistance by mutation	22
1.4.3	Altered targets II: enzymatic modification of 16S rRNA	23
1.4.4	Enzyme catalyzed covalent modification of aminoglycosides	25
1.4.4.1	AACs	27
1.4.4.2	ANTs	29
1.4.4.3	APHs	32
1.4.4.3.1	AAC(6')-APH(2")	37
1.4.4.3.2	APH(3')-Ia	40
1.4.4.3.3	APH(3')-IIa	40
1.4.4.3.4	APH(3')-IVa	45
1.4.4.3.5	APH(3')-IIIa	46
1.4.5	Effect of covalent modification on aminoglycoside binding to 16 S rRNA	51
1.5	Reversing aminoglycoside resistance	53
1.6	Summary	58
1.7	References	60
CHAPTER 2:	**REGIOSPECIFICITY OF APH(3')-IIIa**	74
2.1	Introduction	75
2.2	Materials and methods	78

2.2.1 Chemicals 78
2.2.2 Preparation of an *aph(3')-IIIa* protein expression construct 78
2.2.3 Purification of APH(3')-IIIa 80
2.2.4 Preparation and purification of phosphorylated aminoglycosides 81
2.2.5 HPLC analysis of neomycin bis-phosphorylation 86
2.2.6 Mass spectrometry of phosphorylated aminoglycosides 87
2.2.8 Sample Preparation for NMR analysis 87
2.2.7 Enzyme assay 87
2.3 Results 88
2.3.1 Stoichiometry of aminoglycoside phosphorylation 88
2.3.2 Aminoglycoside phosphorylation in the steady state 89
2.3.3 HPLC analysis of aminoglycoside bis-phosphorylation 91
2.4 Discussion 93
2.5 Conclusions 98
2.6 References 99

CHAPTER 3: APH(3')-IIIa EMPLOYS A DIRECT IN-LINE PHOSPHATE TRANSFER MECHANISM. 101
3.1 Introduction 102
3.2 Materials and methods 108
3.2.1 Chemicals 108
3.2.2 Survey of chemical modifying agents 113
3.2.3 Site directed mutagenesis 114
3.2.4 Purification of mutant APH(3')-IIIa proteins 115
3.2.5 Western analysis 115
3.2.6 Positional isotope exchange 116
3.3 Results 116
3.3.1 Survey of chemical modifying agents 117
3.3.2 Analysis of the inactivation of APH(3')-IIIa by DEPC 118
3.3.3 Kinetic analysis of APH(3')-IIIa His mutants 120
3.3.3.1 Histidine 78 121
3.3.3.2 Histidine 82 121
3.3.3.3 Histidine123 121
3.3.3.4 Histidine 188 124
3.3.4 DEPC inactivation of the four His mutants 125
3.3.5 Analysis of positional isotope exchange experiments 126
3.4 Discussion 126
3.4.1 Role of histidines in the catalytic mechanism of APH(3')-IIIa 128

3.4.2 Role of His188 130
3.4.3 The mechanism of APH(3')-IIIa catalyzed phosphate transfer 131
3.58 Conclusions 132
3.6 References 136

CHAPTER 4: STRUCTURE/FUNCTION ANALYSIS OF APH(3')-IIIa 139
4.1 Introduction 140
4.2 Materials and methods 152
4.2.1 Chemicals 152
4.2.2 Site directed mutagenesis 152
4.2.3 Purification of mutant APH(3')-IIIa proteins 155
4.2.4 Kinetic assay 158
4.2.5 Metal ion dependence 159
4.2.6 Measurement of solvent isotope, solvent viscosity and thio effects for APH(3')-IIIa 159
4.2.7 Partial proteolysis of wild type APH(3')-IIIa 161
4.2.8 Amino terminal sequencing of peptide fragments 162
4.3 Results 162
4.3.1 Kinetic analysis of APH(3')-IIIa mutants 163
4.3.1.1 Glutamate 60 163
4.3.1.2 Serine 27 168
4.3.1.3 Aspargine 195 170
4.3.1.4 Aspartate 190 171
4.3.1.5 Aspartate 208 173
4.3.2 Metal ion effects 174
4.3.3 The effect of ATPγS on APH(3')-IIIa activity 183
4.3.4 Proteolysis results 184
4.4 Discussion 186
4.4.1 Kinetic analyses of APH(3')-IIIa mutants 186
4.4.2 Role of the magnesium ions in the catalytic mechanism of APH(3')-IIIa 192
4.4.3 Is the role of Ser27 conserved in ePKs? 198
4.4.4 The effect of ATPγS on APH(3')-IIIa activity 201
4.4.5 Proteolysis studies on APH(3')-IIIa 202
4.4.6 Model for the catalytic mechanism of APH(3')-IIIa 204
4.4.7 How could a conformational change be transmitted to Asp208? 207
4.5 Conclusions 209
4.6 References 210

CHAPTER 5: THE EXTREME C-TERMINUS OF APH(3')-IIIA IS REQUIRED FOR SUBSTRATE BINDING AND CATALYSIS 216
5.1 Introduction 217
5.2 Materials and methods 219
5.2.1 Chemicals 219
5.2.2 Site directed mutagenesis 219
5.2.3 Protein purification 220
5.2.4 Kinetic analysis of mutant APH(3')-IIIa proteins 221
5.2.5 Purification of phosphorylated aminoglycosides 222
5.2.6 Sample preparation for NMR analysis of phosphoribostamycin 223
5.2.7 Mass spectral analysis of phosphoaminoglycosides phosphorylated by mutant APH(3')-IIIa proteins 223
5.2.8 Determination of minimal inhibitory concentrations 223
5.2.9 Expression of wild type and mutant enzymes 224
5.3 Results 225
5.3.1 Kinetic analysis of APH(3')-IIIa mutants 225
5.3.1.1 Tyrosine 55 225
5.3.1.2 Arginine 211 226
5.3.1.3 Aspartate 261 232
5.3.1.4 Glutamate 262 233
5.3.1.5 Phenylalanine 264 234
5.3.2 Regiospecificity of aminoglycoside binding pocket mutants 237
5.3.3 *In vivo* role of aminoglycoside binding pocket mutants 240
5.4 Discussion 243
5.5 Conclusions 251
5.6 References 253

CHAPTER 6: CHARACTERIZATION OF THE CATALYTIC MECHANISM OF APH(9)-IA. A NOVEL SPECTINOMYCIN KINASE FROM LEGIONELLA PNEUMOPHILA. 255
6.1 Introduction 256
6.2 Materials and methods 258
6.2.1 Chemicals 258
6.2.2 Preparation of the spectinomycin kinase overproducing construct 259
6.2.3 Site directed mutagenesis 259

6.2.4 Overexpression and purification of wild type and mutant spectinomycin kinase proteins 260
6.2.5 Spectinomycin kinase assay 261
6.2.6 Inactivation of spectinomycin kinase with FSBA 262
6.2.7 Preparation and purification of phosphorylated spectinomycin 263
6.2.8 Sample preparation for NMR analysis of phosphorylated spectinomycin 264
6.2.9 Miscellaneous methods 264
6.3 Results 264
6.3.1 Overexpression and purification of spectinomycin kinase 264
6.3.2 Characterization of spectinomycin phosphate 265
6.3.3 Steady state kinetic characterization of spectinomycin kinase 266
6.3.4 The catalytic mechanisms of spectinomycin kinase and APH(3')-IIIa are similar 268
6.3.4.1 The ATP binding pocket of spectinomycin kinase 268
6.3.4.2 Kinetic analysis of spectinomycin kinase mutants 272
6.3.4.3 Metal and solvent isotope effects 273
6.4 Discussion 275
6.5 Conclusions 280
6.6 References 283

CHAPTER 7: CONCLUSIONS, IMPLICATIONS, AND PROSPECTS FOR THE FUTURE DESIGN OF AMINOGLYCOSIDE PHOSPHOTRANSFERASE INHIBITORS. 287
7.1 From the past to the present – 1993-1999 288
7.2 Where do we go from here? 293
7.3 What does it all mean? 302
7.4 A final word 303
7.5 References 303

ABBREVIATIONS

AAC	- aminoglycoside acetyltransferase
ADP	- adenosine diphosphate
AG	- aminoglycoside
ANT	- aminoglycoside nucleotidyltransferase
APH	- aminoglycoside phosphotransferase
ATP	- adenosine triphosphate
ATP-γ-S	- adenosine 5'-*O*-(3-thiotriphosphate)
CCD	- core catalytic domain
CSK	- C-terminal sarc kinase
DCC	- dicyclohexlcarbodiimide
DEPC	- diethylpyrocarbonate
DMSO	- dimethyl sulfoxide
DTT	- dithiothreitol
EDPI	- energy dependent phase I
EDPII	- energy dependent phase II
EDTA	- *N,N,N',*N'-ethylenediaminetetraacetic acid
EGTA	- ethylene glycol bis(*β*-aminoethylether) *N,N'*-tetraacetic acid
ePKs	- eukaryotic protein kinases
ESI-MS	- electrospray ionization mass spectrometry
ETC	- electron transport chain
FSBA	- 5'-[*p*-(fluorosulfonyl)benzoyl]adenosine
H9	- *N*-(2-aminoethyl)-5-isoquinoline sulfonamide
HEPES	- *N*-(2-hydroxyethyl)piperazine-*N'*-2-ethanesulfonic acid
HPLC	- high pressure liquid chromatography
IPTG	- β-D-thiogalactopyranoside

LB	- Luria broth
MAPK	- mitogen activated protein kinase
MIC	- minimal inhibitory concentration
NADH	- nicotinamide adenine dinucleotide reduced form
NPL	- nucleotide positioning loop
PCR	- polymerase chain reaction
PDB	- protein data base
PIK	- phosphatidylinositol kinases
PIX	- positional isotope exchange
PhK	- phosphorylase kinase
PKA	- cyclic AMP-dependent protein kinase
PMSF	- phenylmethanesulfonyl fluoride
SDS-PAGE	- sodium dodecyl sulfate-polylacrylamide gel electrophoresis
SK	- spectinomycin kinase
TEAB	- triethylammonium bicarbonate buffer
TLC	- thin layer chromatography
Tris	- tris-(hydroxymethyl)aminomethane
TS	– Transition State

LIST OF FIGURES

Chapter 1		PAGE
1.1	**Antibiotic targets and potential mechanisms of resistance.**	4
1.2	**Structures of AGs described in this thesis.**	12
1.3	**Proposed mechanism for the bactericidal activity of AG antibiotics.**	17
1.4	**Classes of AG-modifying enzymes.**	25
1.5	**Naming scheme for AG-modifying enzymes.**	26
1.6	**Regiospecificity of the reactions catalyzed by the known AACs.**	28
1.7	**Regiospecificity of the reactions catalyzed by the known ANTs.**	30
1.8	**Regiospecificity of the reactions catalyzed by the known APHs.**	33
1.9	**Phylogeny of APHs and related proteins.**	38
1.10	**Kinetic mechanism of APH(3')-IIIa.**	48
1.11	**Redesigning AG antibiotics to avoid resistance.**	54
1.12	**Aminols that bind A-site rRNA (Tok & Rando, 1998).**	55
1.13	**Mechanism-based inactivation of APH(3') enzymes. A.**	56

Chapter 2		PAGE
2.1	**Figure 2.1. Progress curves for the phosphorylation of the 4,5-disubstituted AGs.**	90
2.2	**Figure 2.2. HPLC chromatograms monitoring the progress of the neomycin B bis-phosphorylation reaction.**	92
2.3	**Figure 2.3. Analysis of HPLC chromatograms.**	93

2.4	**Figure 2.4. Regiospecificity of APH(3')-IIIa, a paradigm.**	97
Chapter 3		
3.1	**Regions of APH(3') homology.**	102
3.2	**The two possible phosphate transfer mechanisms employed by APH(3')-IIIa.**	104
3.3	**Positional isotope exchange in a double displacement phosphate transfer mechanism.**	106
3.4	**Synthesis of ADP-morpholidate.**	110
3.5	**Coupling of ADP-morpholidate to $P^{18}O_4$.**	111
3.6	**Wavelength scans of wild type APH(3')-IIIa, after either treatment with DEPC in ethanol, or ethanol alone.**	118
3.7	**Figure 3.7. Overexpression of APH(3')-IIIa and the APH(3')-$IIIa^{H188A}$ mutant.**	125
3.8	**PIX experiments.**	127
3.9	**Structure of the APH(3')-IIIa monomer, bound to ATP.**	135
Chapter 4		
4.1	**Sequence Homology between 3'-Aminoglycoside Phosphotransferases and eularyotic Protein Kinases.**	141
4.2	**Potential mechanisms of Phosphoryl Transfer.**	144
4.3	**The Active Site of APH(3')-IIIa**	153
4.4	**Crystal structure of the APH(3')-IIIa monomer bound to ADP (Hon, *et al*, 1997).**	164

4.5	**Magnesium and manganese metal ion dependencies of APH(3')-IIIa and the APH(3')-IIIa^{N195A} mutant.**	175
4.6	**Measurement of the solvent viscosity effect for the APH(3')-IIIa^{N195A} mutant.**	178
4.7	**Magnesium ion dependencies of Wild Type and mutant APH(3')-IIIa proteins.**	180
4.8	**Partial Proteolysis of APH(3')-IIIa.**	185
4.9	**Model of the Catalytic Mechanism of APH(3')-IIIa.**	206
Chapter 5		
5.1	**Relative specificity constants, $(k_{cat}/K_{m(mut)})/(k_{cat}/K_{m(WT)})$, of wild type and mutant APH(3')-IIIa enzymes.**	231
5.2	**Progress curves for the phosphorylation of neomycin, by the wild type APH(3')-IIIa enzyme (— · —), and the Phe264Δ mutant (- - -).**	238
5.3	**Expression of mutant APH(3')-IIIa proteins.**	241
5.4	**AGs modeled into the AG binding pocket of APH(3')-IIIa.**	245
Chapter 6		
6.1	**Structures of spectinomycin**	257
6.2	**Purification of spectinomycin kinase**	266
6.3	**Inactivation of spectinomycin kinase by FSBA.**	269
6.4	**Primary sequence alignment of spectinomycin kinase and APH(3')-IIIa.**	271
6.5	**Regiospecificity of spectinomycin kinase**	276
6.6	**Catalytic mechanism of APH(9)-Ia**	281

Chapter 7

7.1	**Regiospecific mechanism-based inactivators**	294
7.2	**Bi-substrate analogues for the APH(3') family of enzymes.**	296
7.3	**Derivatives of bisubstrate analogues.**	298
7.4	**Structures of H9 (A) and potential higher affinity H9 derivatives (B).**	300

LIST OF TABLES

Chapter 1		PAGE
1.1	**General mechanisms of antibiotic action and resistance.**	3
1.2	**Effects of various aminoglycosides on translation, and on the fidelity of translation.**	15
1.3	**APH homologues.**	35
Chapter 2		
2.1	**R_fs of AGs and phospho-AGs described in this study.**	83
2.2	**Stoichiometry of aminoglycoside phosphorylation by APH(3')-IIIa.**	89
Chapter 3		
3.1	**Survey of chemical modifying agents.**	117
3.2	**Stoichiometry and rate of APH(3')-IIIa inactivation by DEPC.**	119
3.3	**Steady state kinetic parameters for wild type APH(3')-IIIa and His mutant proteins.**	122
Chapter 4		Page
4.1	**Steady state kinetic parameters for the wild type and mutant APH(3')-IIIa proteins.**	165
4.2	**Metal and solvent effects on APH(3')-IIIa-Asn195Ala**	176
4.3	**Kinetic parameters for Mg^{2+} titrations**	179
4.4	**Steady state kinetic parameters determined for Wild Type APH(3')-IIIa in 1 mM $MgCl_2$**	181

Chapter 5

5.1	**Steady state kinetic parameters for wild type and C-terminal mutant APH(3')-IIIa proteins**	227
5.2	**Regiospecificity of aminoglycoside binding pocket mutants**	238
5.3	**Minimal inhibitory concentrations of *aph(3')-IIIa* aminoglycoside binding site mutants when expressed in *E. coli* BL 21(DE3)**	241

Chapter 6

6.1	**Purification of spectinomycin kinase**	265
6.2	**Steady state kinetic parameters for spectinomycin kinase**	267
6.3	**Other structurally unrelated AGs are neither substrates nor inhibitors of spectinomycin kinase**	267
6.4	**Inactivation of the SK^{K52A} mutant by FSBA**	270
6.5	**Steady state kinetic parameters for mutant spectinomycin kinase proteins**	272
6.6	**Metal and solvent isotope effects**	274

Chapter 7

7.1	**Bi-substrate analogue inhibition of APH(3')-IIIa**	297

LIST OF PROTEIN DATA BASE CODES

PDB Code	PDB Description	Reference
1PBR	Paromomycin bound to A-site RNA	Fourmy, *et al*, 1996[1]
1JST	CDK2	Russo, *et al*, 1996[2]
1AD5	HCK	Sicheri, *et al*, 1997[2]
1PHK	phosphorylase kinase γ	Owen, *et al*, 1995[2]
1ATP	PKA	Zheng, 1993[2]

[1] Referenced in Chapter 1.
[2] Referenced in Chapter 4.

PUBLICATIONS:

1. G.A. McKay, P.R. Thompson, & G.D. Wright (1994). Broad spectrum aminoglycoside phosphotransferase type III from enterococcus: Overexpression, purification and substrate specificity. *Biochemistry* **33:** 6936-6944.

2. P.R. Thompson, D.W. Hughes,& G.D. Wright (1996). Regiospecificity of aminoglycoside phosphotransferase from *Enterococci and Staphylococci* (APH(3')-IIIa). *Biochemistry* **35:** 8686-8695.

3. P.R. Thompson, D.W. Hughes, & G.D. Wright (1996). Mechanism of 3'-aminoglycoside 3'-phosphotransferase type IIIa: His188 is not a phosphate accepting residue. *Chemistry and Biology* **3:** 747-755.

4. W.C. Hon, G.A. McKay, P.R. Thompson, R.M. Sweet, D.S. Yang, G.D. Wright, & A.M. Berghuis (1997). Structure of an enzyme required for aminoglycoside antibiotic resistance reveals homology to eukaryotic protein kinases. *Cell* **89:** 887-895.

5. P.R. Thompson, D.W. Hughes, N.P. Cianciotto, & G.D. Wright (1998). Spectinomycin kinase from *Legionella pneumophila*. Characterization of substrate specificity and identification of catalytically important residues. *J. Biological Chemistry* **273:** 14788-14795.

6. G.D. Wright & P.R. Thompson (1999). Aminoglycoside Phosphotransferases: Proteins, Structure, and Mechanism. *Frontiers in BioScience* **4:** D9-21.

7. D.M. Daigle, G.A. McKay, P.R. Thompson, & G.D. Wright (1999). Aminoglycoside antibiotic phosphotransferases are also serine protein kinases. *Chemistry and Biology* **6**: 11-18.

8. P.R. Thompson, J.D. Schwartzenhauer, D.W. Hughes, A.M. Berghuis, & G.D. Wright (1999) COOH terminus of aminoglycoside phosphotransferase (3')-IIIa is critical for antibiotic recognition and resistance. *J. Biol. Chem.* **274**, 30697-30706.

Chapter 1

Introduction

Chapter: Introduction.

1.1. Antibiotics and Resistance.

At the turn of this century, Paul Ehrlich first conceptualized the idea of designing chemotherapeutic agents to take aim at the microbial world, and thereby thwart the devastating impact bacterial infections have on humankind. Ehrlich likened this approach to his study of antibodies, which he had previously termed 'magic bullets', and thus the concept of treating bacterial infections with a 'well aimed magic bullet' was born (Marquardt, 1949). Since that time, a number of antimicrobial compounds have been identified, the most notable being Alexander Fleming's discovery of penicillin (Fleming, 1929) (For representative examples see Table 1.1). Since the time of Fleming, with the discovery of greater than 100 antibiotics (Neu, 1992), many felt that we had entered a 'golden age', where the threat of bacterial infection as a cause of human mortality was a thing of the past. However, the rising incidence of bacterial resistance, to **all** of the antimicrobial agents discovered so far, threatens that golden age. Much like the prognosticators of the past, who forecasted a 'golden age', there are many, that are now forecasting an age, where human populations are once again susceptible to the horrific impact of diseases caused by microbial agents (Neu, 1992; Cohen, 1992; Schlaes *et al*, 1993).

As is clearly evident from Table 1.1, there are a number of antibiotic resistance mechanisms employed by bacteria. The major mechanisms of resistance fall into one of three categories (Neu, 1992) that involve i) alterations in antibiotic uptake; ii) alterations

to the targets of antibiotics, or; iii) the bacterial expression of enzymes that alter the chemical structures of specific antibiotics (reviewed, respectively, in Nikaido, 1994; Spratt, 1994; Davies, 1994) (see Figure 1.1).

Table 1.1: General mechanisms of antibiotic action and resistance.

Antibiotic Class	Site of Action	Resistance Mechanisms	References
Streptamine Aminoglycosides (e.g. Streptomycin)	Protein Synthesis –16S rRNA and ribosomal protein S12 of the 30S ribosomal subunit	Enzymatic modification (adenylation or phosphorylation) -mutations in genes for 16S rRNA and ribosomal protein S12	Benveniste & Davies (1973a); Musser (1995)
Deoxystreptamine Aminoglycosides (e.g. kanamycins, and neomycins)	Protein Synthesis –16S rRNA of the 30 S ribosomal subunit	Primarily enzymatic -acetylation, adenylation, or phosphorylation of these antibiotics	Moazed & Noller (1987); Miller et al (1997)
Macrolides (e.g. erythromycin)	Protein Synthesis –23S rRNA of the 50S ribosomal subunit	Altered target -mutations in 23S rRNA and 50S subunit proteins -Enzymatic methylation of 23S rRNA or glycosylation of the antibiotic	Cundliffe (1987); Leclercq & Courvalin (1991); Benveniste & Davies (1973a); Cundliffe (1992)
Tetracyclines	Protein Synthesis –16S rRNA of 30S ribosomal subunit	Active efflux –specific transporters 'pump' these antibiotics out of the cell	Moazed & Noller (1987); Nikaido (1994)
Rifampin	Transcription –DNA dependent RNA polymerase	Altered target –mutations in pol β subunit	Musser (1995)
Penicillins and Cephalosporins	Cell wall synthesis –inhibits transpeptidation	Enzymatic -β-lactamases hydrolyze the β-lactam ring Altered target -low affinity penicillin binding proteins.	Benveniste & Davies (1973a); Spratt (1994)
Quinolones (e.g. ciprofloxacin)	DNA Synthesis -inhibits DNA gyrase and topoisomerase IV	Altered target -mutations in DNA gyrase and topoisomerase IV Active efflux	Spratt (1994); Nikaido (1994); Hooper (1998)
Chloramphenicol	Protein Synthesis –inhibits fMet-tRNA binding	Enzymatic -acetylation	Benveniste & Davies (1973a);

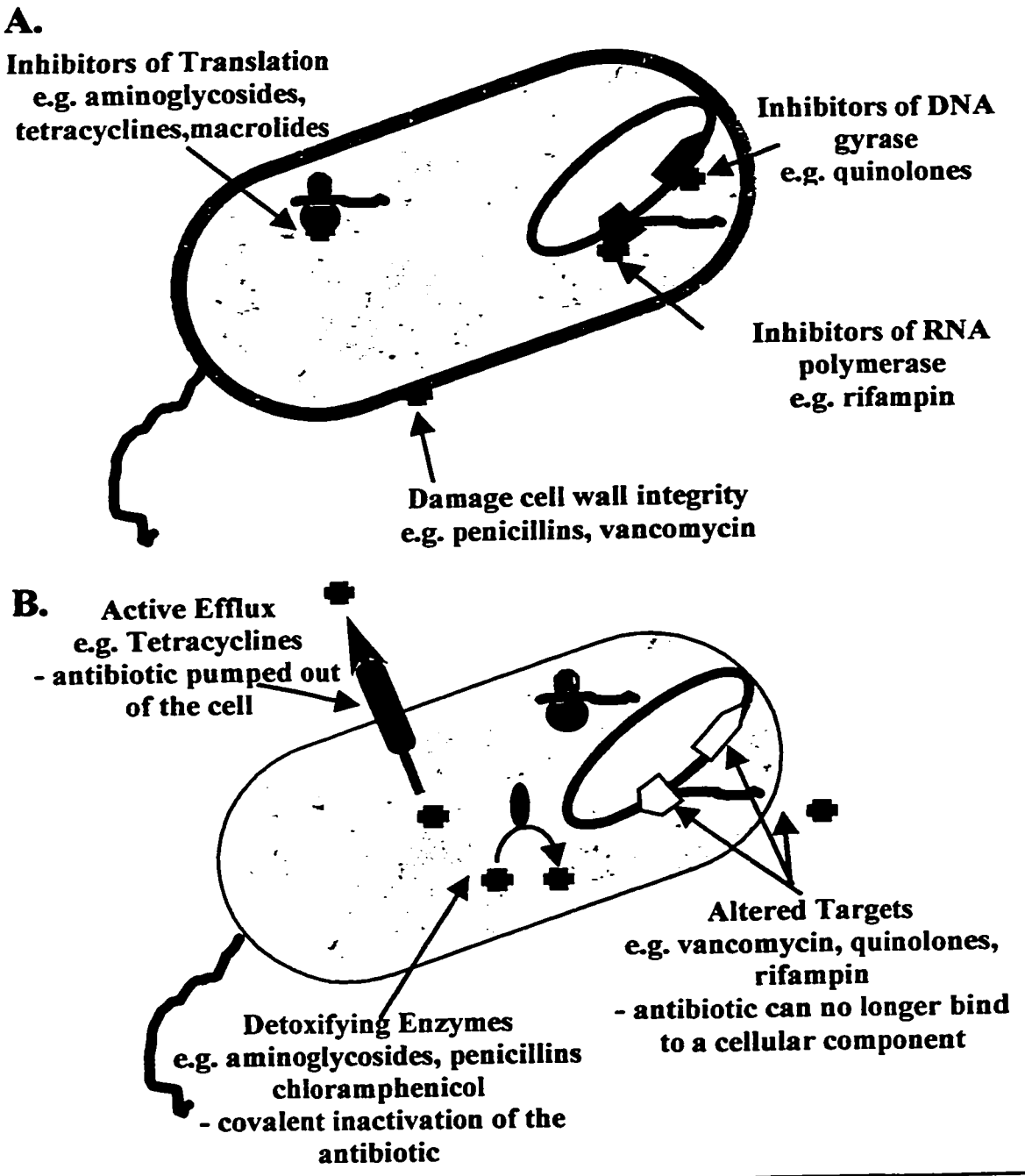

Figure 1.1. Antibiotic targets and potential mechanisms of resistance. **A.** The 3 major targets of current antimicrobial therapies, namely cell wall biosynthesis, protein synthesis, and DNA/RNA synthesis, are highlighted, as are examples of antibiotics that target these processes. **B.** The 3 main mechanisms that bacteria employ to resist the toxic effects of antibiotics, namely, altered uptake, target alteration, and drug modification, are also highlighted, and examples given.

The genetic elements required to mediate a particular type of resistance mechanism can arise either by mutation or by the acquisition of entire antibiotic resistance determinants, which are often present on plasmids and transposons (Neu, 1992). While the resistance mechanisms, described above, are not limited to either Gram positive or Gram negative bacteria (Neu, 1992), it was once thought that bacterial antibiotic resistance, of clinical relevance, was limited to the Gram negatives (Howe *et al*, 1996). However, the use, or misuse, of antimicrobial compounds has resulted in the selection of antibiotic resistant strains of Gram positive organisms (Howe *et al*, 1996). Thus, with the development of antibiotic resistant Gram positive organisms, these organisms have 're-emerged' as a serious threat to the health and welfare of humankind (Howe *et al*, 1996; Neu, 1992; Schlaes *et al*, 1993). Of the Gram positives, the enterococci and staphylococci are a major threat, and organisms of these genera account for one third of all hospital acquired infections (Weinstein, 1998).

In staphylococci, resistance to β-lactam antibiotics can be due to the expression of either a β-lactamase or an altered penicillin binding protein (Schlaes *et al*, 1993; Spratt, 1994). However, penicillin resistant staphylococci, that employ a β-lactamase, are generally susceptible to the semi-synthetic penicillins, for example methicillin and the cephalosporins (Schlaes *et al*, 1993). Unfortunately, the same cannot be said of penicillin resistant strains of staphylococci that have acquired a transposon encoded penicillin binding protein, PBP2', which has very low affinity for β-lactam containing antibiotics (Spratt, 1994). Such strains are resistant to methicillin, the cephalosporins, and the carbapenems, and are generally referred to as methicillin resistant staphylococci (MRS)

(Schlaes *et al*, 1993). Methicillin resistant *Staphylococcus aureus* are therefore termed MRSA, although this term is also used to describe *S. aureus* strains that are resistant to multiple antibiotics, for example, methicillin and the aminoglycosides (AGs). Vancomycin, a glycopeptide antibiotic, is the only effective therapy for MRSA (Brighty *et al*, 1993; Schlaes *et al*, 1993), and the recent identification of vancomycin tolerance in clinical isolates of MRSA (Hiramatsu *et al*, 1997) is therefore, particularly alarming. If vancomycin tolerance is a prelude to acquiring high level vancomycin resistance in MRSA isolates, then there will be no antibiotics left to treat this pathogenic organism (Brighty *et al*, 1993). Thus, the redesign of antibiotics, or the design of drugs that will inhibit the resistance mechanisms in staphylococci are critical areas of research. The AGs, which were once a mainstay of staphylococcal therapy, having since been replaced by less toxic antimicrobial compounds, are nonetheless excellent targets for the latter approach, as 90% of gentamicin resistance in MRSA is due to the expression of a single bifunctional AG-modifying enzyme, AAC(6')-APH(2") (Miller *et al*, 1997). The discovery of agents that will inhibit this enzyme should result in the continued efficacy of this AG antibiotic.

For enterococcal infections, the problem of AG resistance is said to be of even greater concern (Schlaes *et al*, 1993) because enterococci are generally resistant to low levels of most antibiotics, especially those that target the cell wall (Murray, 1990; Schlaes *et al*, 1993). The problem of antibiotic resistant enterococci is further compounded by the fact that these organisms seem to readily acquire antibiotic resistance determinants, affording high level resistance, for many classes of antibiotics (Moellering, 1991).

Traditionally, the combined treatment of enterococci with an AG and an antibiotic that targets the cell wall, such as penicillin, led to the synergistic killing of organisms belonging to this genus (Leclercq *et al*, 1992; Moellering *et al*, 1979). However, in 1992, at least 25% of enterococci were shown to be resistant to AG antibiotics, through the expression of an AG-modifying enzyme (Neu, 1992). This is frightening because AG β-lactam synergism is required for the effective treatment of enterococcal endocarditis and meningitis (Moellering, 1991), and β-lactam containing antibiotics, generally, do not afford killing of enterococci, and are simply bacteriostatic (Murray, 1990). Since resistance to AGs obviates that synergism (Leclercq *et al*, 1992), these infections are difficult to treat, and for endocarditis of enterococcal origin, valve replacement surgery may be the most appropriate therapeutic option (Moellering, 1991).

Vancomycin resistant enterococci (VRE) are also of particular concern (Leclercq & Courvalin, 1997). While vancomycin resistance is rarely associated with *E. faecalis*, the most frequent cause of enterococcal infections (79%), greater than 50% of *E. faecium* clinical isolates, which account for 21% of enterococcal infections, are resistant to high levels of vancomycin (Huycke *et al*, 1998). VRE infections are normally treated with a combination of a β-lactam and an AG (Leclercq & Courvalin, 1997). This treatment regimen is complicated by the fact that enterococci are generally resistant to low levels of β-lactams (Leclercq *et al*, 1992), and the fact that greater than 80% of isolates are resistant to high levels of ampicillin (Huycke *et al*, 1998). For the treatment of VRE, in patients infected with *E. faecium*, this drug regimen is further complicated by the presence of a chromosomally encoded AAC(6)-Ii enzyme (Leclercq & Courvalin,

1997). Thus, gentamicin is the only suitable AG (Leclercq & Courvalin, 1997). If such an isolate is also resistant to gentamicin, which occurs in greater than 50% of infections caused by *E. faecium* (Howe *et al*, 1996), streptomycin can be used in place of gentamicin. However, a streptomycin resistance mechanism can also be present in enterococcus (Leclercq *et al*, 1992). Thus, one can see the inherent difficulty in treating patients infected with VRE.

Another troubling aspect of VRE, is the steep rise in the number of patients infected with this organism. Cases of VRE caused by *E. faecium* have nearly doubled in the years between 1995 and 1997 (Huycke *et al*, 1998). Should this trend continue, and occur concomitantly with an increase in the incidence of vancomycin resistance in *E. faecalis*, vancomycin, will virtually be eliminated as an effective anti-enterococcal agent.

Thus, with the limited number of chemotherapeutic options available for combating enteroccocal and staphylococcal infections and the much-anticipated emergence of vancomycin-resistant Staphylococci, one can see the need for new more potent antibiotics. While there has been some progress in this area (Service, 1995), it can be assumed, based on the precedents of the past, that the introduction of such novel antibiotics will ultimately result in the emergence of bacteria that are resistant to even the newest and most potent antibiotics. Thus, there is an ever-present need for continued research into antibiotic development. There are a number of methods that can be used to expand the medical practitioner's 'arsenal' of anti-bacterial compounds. These methods include the aforementioned discovery of novel classes of antibiotic compounds, as well as the identification of novel targets. The latter method uses the information contained in

the sequenced bacterial genomes to identify genes that are of known, predicted, or unknown function, but are critical for bacterial cell growth. The characterization of the protein products of such genes should, in theory, lead to the development of compounds that can inhibit the activity of such a protein, and thereby inhibit bacterial cell growth. A more traditional method of expanding our antibiotic arsenal has been the modification of existing antibiotics, in such ways that the modified drugs remain anti-bacterial, but are no longer, or more accurately put, poorly, recognized by the various resistance mechanisms employed by pathogenic bacteria. Another traditional method is the development of drugs that inhibit particular resistance mechanisms. The successful development of such inhibitors would lead to their inclusion in a drug 'cocktail', which would also include the antibiotic that is the target of the resistance mechanism. This combined therapy should result in the inhibition of the resistance enzyme with a concomitant return of the antibacterial properties of the included antibiotic. Such an approach has led to the successful development of the β-lactamase inhibitors clavulinic acid and sulbactam (Sutherland, 1991).

The application of the latter two approaches to the different classes of antibiotics that possess an antibacterial activity towards susceptible enterococci or staphylococci, including the AGs, vancomycin, or the β-lactams, should reverse resistance to these antibiotics. The potential for thwarting AG resistance in enterococci and staphylococci, through the design of specific inhibitors to the resistance mechanisms, is high because the primary mechanism of AG resistance in these organisms is the expression of a similar subset of AG-modifying enzymes (Leclercq *et al*, 1992), and of

these enzymes, a single bifunctional enzyme, AAC(6')-APH(2"), accounts for most cases of high level AG resistance (Brighty *et al*, 1993; Miller *et al*, 1997). Thus, one focus of our research group has been to study the catalytic mechanisms of a number of AG-modifying enzymes, from such Gram positive organisms as *S. aureus, E. faecium,* and *E. faecalis.* The long-term goals of this project are the design and subsequent testing of inhibitors to these enzymes, such that successful inhibitors could be co-prescribed with an AG antibiotic, and thereby thwart AG resistance.

The primary focus of my research has been the characterization of the catalytic mechanism of the AG-modifying enzyme AG 3'-phosphotransferase type IIIa (APH(3')-IIIa). While this resistance determinant does not mediate resistance to the gentamicin C complex (McKay *et* al, 1994), it was initially felt that a study of the catalytic mechanism of APH(3')-IIIa would aid our understanding of the phosphate transfer mechanism of the bifunctional enzyme, AAC(6')-APH(2"), and as we shall see, they have. Before I begin a discussion of the various mechanisms of AG resistance and the strategies that have been employed to combat these resistance mechanisms, it is only appropriate that I first discuss the identification and chemical characteristics of the AGs, as well as their mode of action.

1.2. Identification and general chemical characteristics of aminoglycoside antibiotics.

While Fleming's identification of penicillin as an antimicrobial agent is said to have occurred by a chance observation in the laboratory, Selman A. Waksman's discovery of streptomycin, in 1944, was the result of a systematic search for organisms that produce antimicrobial agents. The search included bacterial strains that had been isolated from soil and composted material. Eventually, the streptomycin-producing

strain, *Streptomyces griseus*, was isolated from a 'heavily manured field' (Schatz *et al*, 1944). In 1949, the structurally related AG, neomycin, was similarly identified (Waksman & Lechevalier, 1949), and since that time at least a dozen AGs have seen clinical use (Wright *et al*, 1999). All AGs possess an aminocyclitol ring to which a wide variety of substituents can be attached. These include amino groups, hydroxyl groups, hexoses, aminohexoses, and pentoses (Figure 1.2).

Particular AGs can be grouped together according to the type of aminocyclitol ring they possess. For the majority of AG antibiotics, the aminocyclitol ring is a 2-deoxystreptamine ring, whereas for the others, such as streptomycin, the aminocyclitol ring is simply a streptamine ring (Wright *et al*, 1999). For spectinomycin, a structurally related antibiotic, the aminocyclitol ring is an actinamine ring. The 2-deoxystreptamine AGs are either substituted at the 4 and 6 positions of the aminocyclitol ring with aminohexoses (e.g. kanamycin), or at the 4 and 5 positions of the aminocyclitol ring with an aminohexose and a pentose, respectively (e.g. neomycin). The former class of AGs has variably been termed the kanamycins, the 4,6-disubstituted deoxystreptamine AGs, or the **4,6-disubstituted AGs**, whereas the latter class has been termed the neomycins, the 4,5-disubstituted deoxystreptamine AGs, or the **4,5-disubstituted AGs**. For the sake of consistency, I will use the latter term given for both cases (in bold).

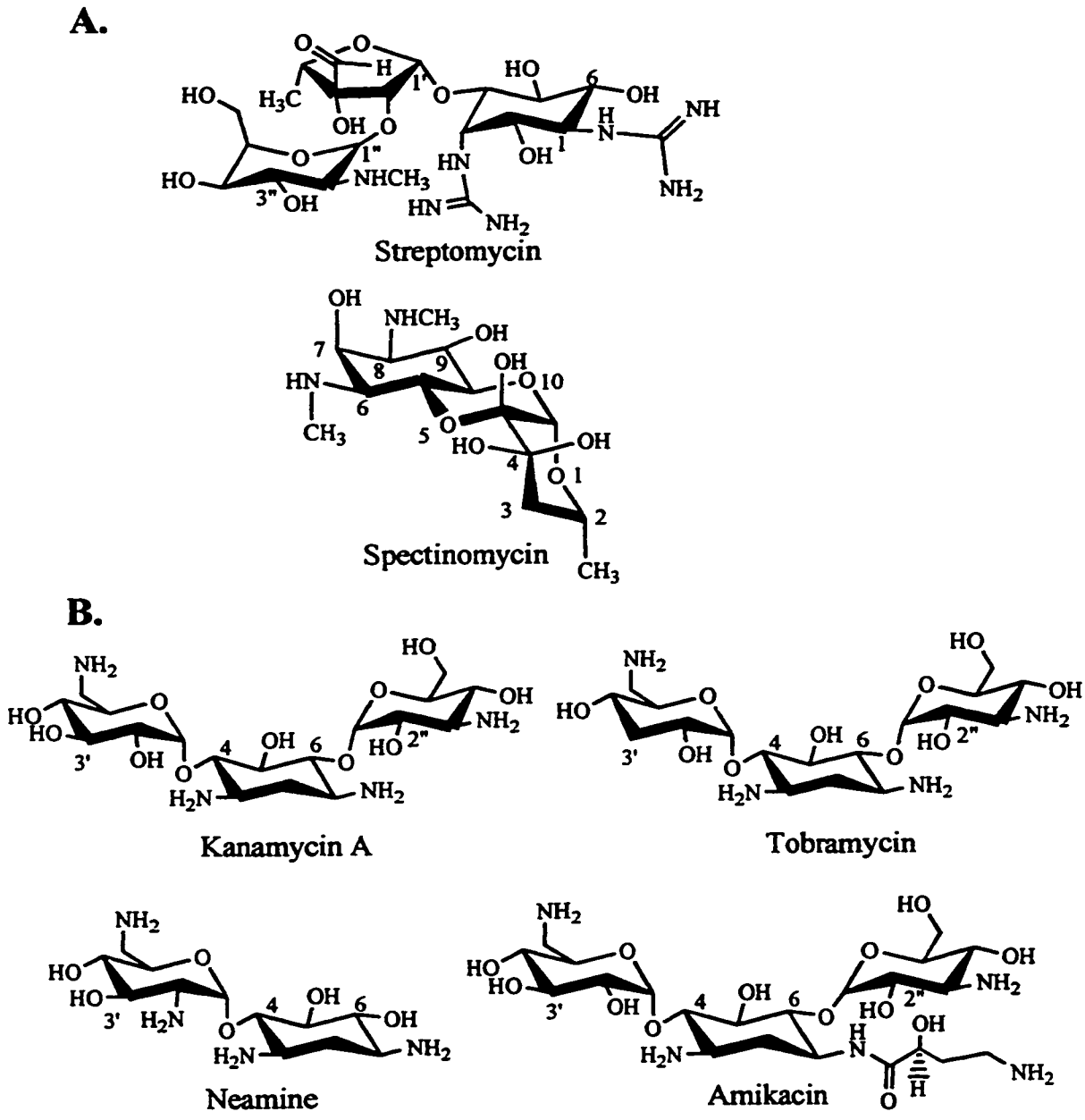

Figure 1.2. Structures of AGs/aminocyclitols described in this thesis. A. Structures of streptomycin and spectinomycin. **B.** Representative structures of 4,6-disubstituted AGs. **C.** Representative structures of 4,5-disubstituted AGs. All AGs possess an aminocyclitol ring and this ring is typically number 1-6. Sugar rings attached to the aminocyclitol ring are numbered 1'-6', and 1"-5"(or 6"). Additional ring structures are designated by ''', and ''''.

C.

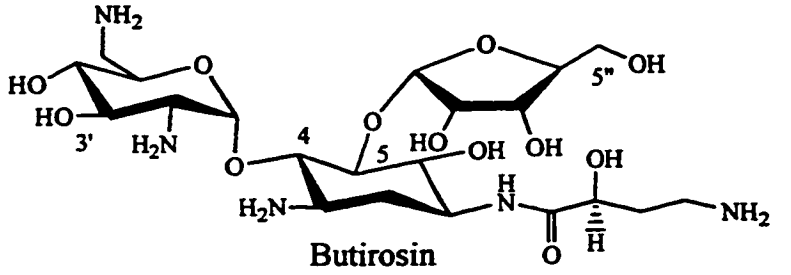

Butirosin

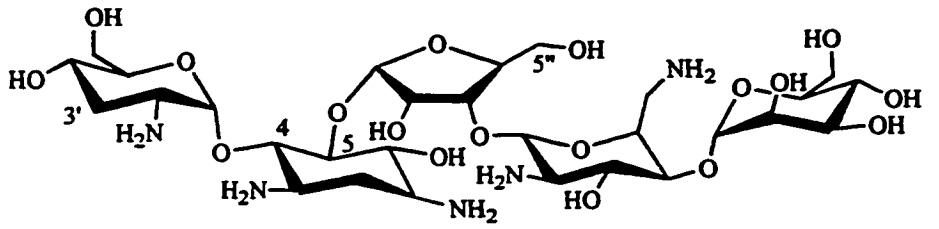

Lividomycin A

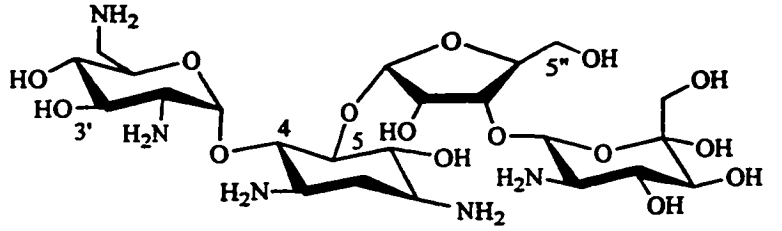

Neomycin B

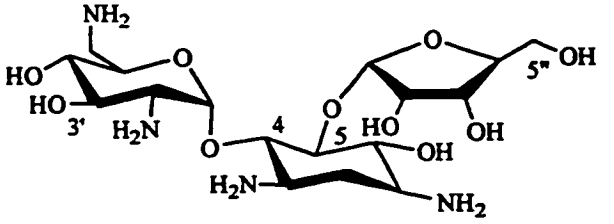

Ribostamycin

Figure 1.2. Continued.

1.3. Mechanism of aminoglycoside action.

The ribosome is the main site of AG action (Gale *et al*, 1981), and a number of AGs, including streptomycin, neomycin and paromomycin have been shown, by

chemical footprinting, to bind to the A^- site of the 16S rRNA subunit (Moazed & Noller, 1987; Miyaguchi *et al*, 1996). Aminoglycoside binding to the A^- site, in general, results in the inhibition of either the initiation of translation, or the transition of an initiating ribosome to a ribosome involved in chain elongation (Gale *et al*, 1981), more specifically the translocation step (Misumi *et al*, 1978; Cabanas *et al*, 1978). Certain AGs also permit the recognition of incorrect aminoacyl tRNAs during chain elongation, which effectively leads to the production of *misread* proteins (Davies, *et al*, 1964; Gorini & Kataja, 1964; Lando *et al*, 1973; Tai *et al*, 1978).

Lando *et al* have categorized a number of AGs according to the ability of these compounds to cause misreading (Table 1.2) (Lando *et al*, 1973). In general, an AG that is bacteriostatic, for example spectinomycin, inhibits translation (Anderson *et al*, 1967), but does not cause misreading (Lando *et al*, 1973). Conversely, the bactericidal activity of an AG, correlates well with the ability to effect misreading (Bakker, 1992). For example, such bactericidal AGs as streptomycin, neomycin and gentamicin promote misreading (Lando *et al*, 1973; Tai *et al*, 1978). Interestingly, the level of misreading appears to be AG dependent, and AGs possessing a 2-deoxystreptamine ring, for example kanamycin A, promote misreading to a greater extent than those AGs, such as streptomycin, that possess a streptamine ring (Lando *et al*, 1973; Tai *et al*, 1978). For kanamycin A, the 2-deoxystreptamine ring has been shown to be the main source of the misreading caused by this drug (Tanaka *et al*, 1967).

Table 1.2: Effects of various aminoglycosides on translation, and on the fidelity of translation.

Aminoglycoside	Effect on translation	References
Streptomycin	Misreading and inhibition of translation	Lando, *et al* (1973); Davies, *et al* (1964)
Neomycin B	Misreading and inhibition of translation	Lando, *et al* (1973)
Neomycin C	Misreading and inhibition of translation	Lando, *et al* (1973); Davies, *et al* (1964)
Neamine	Misreading and inhibition of translation	Lando, *et al* (1973)
Kanamycin A	Misreading and inhibition of translation	Lando, *et al* (1973); Davies, *et al* (1964)
Paromomycin	Misreading and inhibition of translation	Lando, *et al* (1973)
Hygromycin	Inhibition of translation	Bakker (1992)
Spectinomycin	Inhibition of translation	Lando, *et al* (1973)

Presumably, misreading is the result of a bactericidal AG enhancing the non-specific binding of tRNA to the A site. Such a conclusion has previously been suggested (Woodcock *et al*, 1991). Reduced fidelity and translation inhibition are both presumed to be due to the interaction of these drugs with the A^- site region of the 16S rRNA subunit (Moazed & Noller, 1987; Yoshizawa *et al*, 1998; Recht *et al*, 1999a; 1999b).

How the combined effects of a reduced fidelity and an inhibition of translation are translated into a bactericidal activity is not completely understood. However, several hypotheses have been put forward (reviewed in Davis, 1987; Taber *et al*, 1987), these are summarized here, and in Figure 1.3. Since the bactericidal activity of the AG antibiotics

appears to be linked to the way in which these antibiotics make their way into the cell, it is important that one first understands the process of AG uptake.

There are three phases that govern AG uptake (Bryan & Van Den Elzen, 1976). The first phase of AG uptake occurs rapidly and involves the adsorption of the polycationic AGs to the anionic surface of the plasma membrane. Thus, the driving force for this first phase is simply electrostatic, and as such this phase of uptake is reversible; streptomycin can be washed away from the cell surface with increasing amounts of salt (Davis, 1987; Taber *et al*, 1987). It has been suggested that AG binding to the anionic bacterial surface could disrupt the architecture of the outer membrane of Gram negative cells, and thereby causes cell lysis and death (Kadurugamuwa *et al*, 1993). This suggestion is based upon electron microscopy studies that have shown that a bovine serum albumin-gentamicin conjugate binds, but does not penetrate, the *Pseudomonas aueruginosa* membrane and causes membrane blebbing. While the gentamicin conjugate was bactericidal, the concentrations required to achieve a bactericidal effect are on the order of 10^3 fold higher than those obtained with unconjugated gentamicin (Kadurugamuwa *et al*, 1993). Thus, AG binding to the outer membrane is unlikely to be the primary cause of bacterial cell death.

The second phase of AG uptake has been termed Energy Dependent Phase I (EDPI). During EDPI a small amount of the drug makes its way into the cell through a poorly understood mechanism that likely involves some sort of facilitated transport (reviewed in Taber *et al*, 1987). A passive diffusion mechanism is unlikely, owing to both the large size (~ 500 Da) and polycationic nature of these antibiotics.

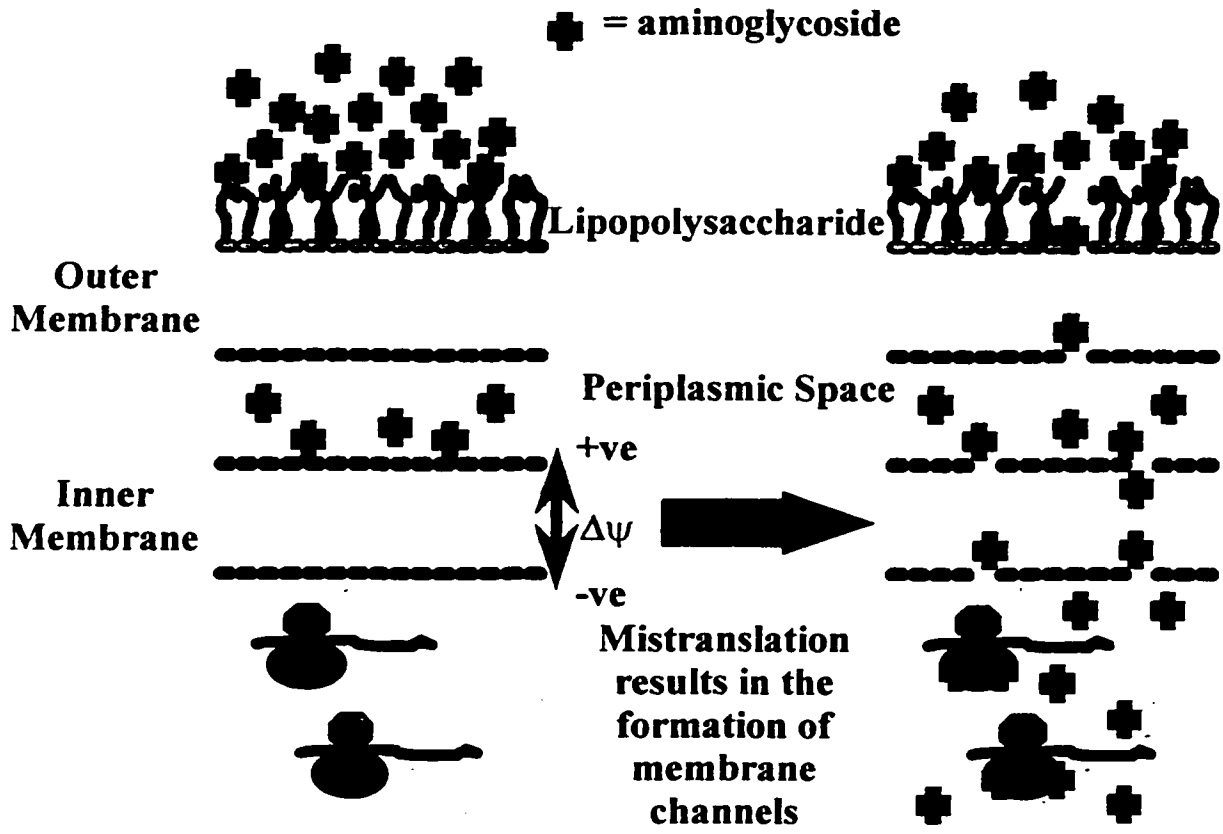

Figure 1.3. Proposed mechanism for the bactericidal activity of AG antibiotics. Initial binding of AGs to the anionic, lipopolysaccharide, surface of the outer bacterial membrane, is followed by a slow phase of uptake known as EDPI. Once inside the cell, bactericidal AGs cause misreading, which by an unknown mechanism, results in the rapid phase of AG uptake known as EDPII. Subsequently, the protein synthesis machinery is completely inhibited, further membrane damage occurs, and the initiation of DNA synthesis is inhibited. Consequently, the bacterial cell dies. This figure has been adapted from Wright, *et al* (1999). Note the cell wall structure shown is that for a Gram negative organism, but the general properties of AG entry are shared with Gram positive bacteria, as well.

While AG uptake during EDPI is not completely understood, there appears to be a role for an intact membrane potential. The role of the membrane potential is poorly

understood, but the $\Delta\psi$ portion of the membrane potential appears to be the most important (reviewed in Taber *et al*, 1987). A threshold value of $\Delta\psi$ is required for AG uptake in *E. coli* and *S. aureus* (Mates *et al*, 1982; Bryan & Kwan, 1983; Eisenberg *et al*, 1984). While one might expect that an increasingly negative $\Delta\psi$ would aid the influx of these polycationic antibiotics, it should be noted that an increasingly negative $\Delta\psi$ does not in all cases lead to an increased uptake of AG antibiotics (Taber *et al*, 1987).

The role of $\Delta\psi$, in AG uptake, is further complicated by the fact that a threshold level is not sufficient, as the $\Delta\psi$ portion of the electrochemical gradient is maintained when the electron transport chain (ETC) is inhibited by cyanide, but gentamicin uptake does not occur (Bryan & Kwan, 1983). Other ETC inhibitors also prevent streptomycin uptake (Bryan and Van Den Elzen, 1976). Further evidence to support the involvement of ETC components in AG uptake comes from the fact that AG uptake into wild type *E. coli* cells, when grown anaerobically, is poor relative to the same cell strain grown under aerobic conditions (Muir *et al*, 1985). It should be noted that drug accumulation in cells grown anaerobically eventually reaches the level accumulated in cells grown aerobically (Muir *et al*, 1985), which suggests that a poorly functioning ETC can slow the initial influx of drug. Thus, the results described in the preceding two paragraphs indicate that an intact electrochemical potential and a functional ETC are both required for AG uptake during EDPI. Bryan and Kwan (1983) have suggested that ubiquinone may have a role in shuttling gentamicin across the membrane, as uptake of this drug in ubiquinone deficient strains appears to be impaired. However, this suggestion is highly speculative. Kashiwagi *et al* (1998), have identified the oligopeptide transport system as a possible

AG transport system, as a decrease in the level of oligopeptide binding protein A is associated with AG resistance. However, it is not known how this transport system is linked to the requirement of either an intact $\Delta\psi$ or a functional ETC.

The third phase of AG uptake has been termed EDPII (Taber *et al*, 1987). A role for protein synthesis, in the EDPI to EDPII transition, is indicated by the fact that AG uptake into *E. coli* membrane vesicles does not occur unless the protein synthesis machinery is present in vesicle preparations (Bryan & Kwan, 1983). The requirement of new proteins, for AG uptake, is further supported by the lack of EDPII in *E. coli* cells that possess an R-factor encoded AG modifying enzyme (Dickie *et al*, 1978), as AGs modified in this manner do not bind the ribosome (Yamada *et al*, 1968).

Since bactericidal AGs are known to cause misreading, the role of protein synthesis, in AG uptake, is thought to be one where misread proteins accumulate in the plasma membrane during EDPI and EDPII (Davis, 1987). It should be noted that these proteins are not limited to integral membrane proteins, as it has been shown that alkaline phosphatase, normally a periplasmic protein, can be found in a membrane associated fraction, after the treatment of *E. coli* with streptomycin (Davis *et al*, 1986). The accumulation of misread proteins in the plasma membrane is believed to cause membrane damage, and this damage is associated with the efflux of nucleotides and K^+ ions into the surrounding medium, which is a hallmark of cells entering the third phase of AG uptake (Anand & Davis, 1960; Roth *et al*, 1960; Dubin & Davis, 1961; Busse *et al*, 1992; Bakker, 1992). The efflux of ions is thought to be a direct consequence of misreading, as ion and nucleotide efflux does not occur when antibiotics that are simply inhibitors of

translation, for example chloramphenicol, spectinomycin, and hygromycin, are coincubated with streptomycin in uptake assays (Anand & Davis, 1960; Busse, 1992). Thus, it is believed that streptomycin induced misreading causes the formation of some sort of facilitated transport system, possibly the un-gating of channels, by the misread proteins. Support for this type of system comes from the fact that nucleotide leakiness occurs even in the face of an inhibited ETC, but streptomycin uptake does not (Bryan & Van Den Elzen, 1976), which should occur if the misread proteins simply formed pores. Pore formation is also unlikely because the membrane potential is only modestly affected by the addition of streptomycin (Busse, 1992). Whatever the exact nature of the transport system, clearly misreading plays a role. The formation of aberrantly folded proteins from misread polypeptides likely converts a slow transport mechanism to a rapid one, where AG uptake is greatly enhanced.

Once a catastrophic amount of an AG antibiotic enters the cell translation is completely inhibited, and the cell undergoes a number of poorly understood changes. These include the aforementioned inhibition of protein synthesis, misreading, and membrane damage, as well as the inhibition of the initiation of DNA synthesis (Tanaka *et al*, 1984; Matsunaga *et al*, 1986). Regardless of whether or not the actions of AGs on membrane structure and DNA synthesis can be directly correlated to their ability to cause misreading during protein synthesis, it is likely that a combination of these effects causes cell death.

1.4. Aminoglycoside Resistance.

The preceding section is meant to provide a better understanding of the mechanism of AG uptake and their mode of action. Such an understanding is useful to appreciate the different mechanisms that bacteria employ to resist the AG class of antibiotics. It is therefore apparent that AG resistance could arise from an alteration in the energy dependence of AG uptake or from alterations to the primary target of these antibiotics, the ribosome. While these forms of resistance are currently found only rarely in resistant pathogens, Nikaido (1994) has pointed out that a successful reversal of one of the other more common resistance mechanisms would likely select for these non-specific mechanisms of resistance. In addition to non-enzymatic AG resistance mechanisms, I will also discuss the enzyme-catalyzed modification of both the ribosome, and the antibiotics themselves.

1.4.1. Resistance by altered uptake.

Alterations to AG uptake are generally the result of a failure to initiate uptake during EDPII (Schlessinger, 1988). Multiple-AG resistant strains of *S. aureus*, which fail to initiate any significant uptake of gentamicin have been identified as menadione auxotrophs (Miller *et al*, 1980). Menadione is a precursor for certain quinones that are important for electron transport, and as such the mechanism of resistance employed by these bacteria appears to be a poorly functioning ETC, as AG resistance can be abolished by the addition of menadione to the growth medium (Miller *et al*, 1980). Similar examples of ETC deficient AG resistant bacteria have been observed in *E. coli*, a Gram negative bacteria (Bryan & Van Den Elzen, 1977; Muir *et al*, 1981). An *E. coli* clinical

isolate, resistant to gentamicin, has also been described (Humber & Altendorff, 1989). Gentamicin resistance in this isolate is associated with a 2 nucleotide insertion into the gene that codes for the γ-subunit of the F_1 ATPase. This mutation is thought to result in a membrane with an increased permeability to protons, the result of which would be a less negative $\Delta\psi$. As described above, a threshold $\Delta\psi$ is required for AG entry, thus this mutation would inhibit AG entry. These two examples therefore make it readily apparent that AG resistance can arise from mutations that affect the requirement of AG uptake on an intact membrane potential and an intact ETC.

Alterations in AG uptake have also been shown to be the cause of resistance in *Burkholderia*, although these resistance mechanisms are not the result of a failure to initiate uptake during EDPII. In *Burkholderia cepacia*, changes in the outer membrane are believed to prevent AG binding to the anionic surface of the bacteria, the initial phase of AG uptake. These antibiotics bind poorly to the outer membranes of intact cells, but do bind to partially purified lipopolysaccharide, a prime component of the negatively charged outer membrane (Moore & Hancock, 1986). In *Burkholderia pseudomallei*, Moore *et al* (1999), have identified a multi-drug efflux pump, encoded by the *AmrA-AmrB-OprA* operon, that confers high level resistance to AG and macrolide antibiotics.

1.4.2 Altered targets I: resistance by mutation.

While target alteration is the most prevalent form of resistance to such synthetic antibiotics as the quinolones and sulfonamides (Spratt, 1994), there are some examples where this type of mechanism is employed to resist the antibacterial effects of the AG antibiotics (see below). Since the primary target of AG antibiotics is the ribosome, it is

not surprising that mutations of either rRNA or ribosomal proteins decrease the affinity that AGs have for these molecules, and the mutant bacteria are consequently resistant to the drug. For *Mycobacterium tuberculosis*, mutations that cause resistance to streptomycin can occur in the ribosomal protein S12 gene, *rpsL*. The most frequent sites of mutation occur at codons 43 and 88. Mutation at these codons, often results in the generation of S12-Lys43Arg and S12- Lys88Arg mutant proteins (Musser, 1995). Mutation of the 16S rRNA gene, *rrs*, also causes resistance to streptomycin, although it appears that base substitutions at a variety of positions can contribute to streptomycin resistance (Musser, 1995). Mutations in *rrs*, A913G, C912A/G (*E. coli* numbering) (Honore & Cole, 1994; Meier *et al*, 1994), which mediate *M. tuberculosis* resistance to streptomycin, are present in a region, identified by chemical footprinting that is important in streptomycin binding (Moazed & Noller, 1987). While streptomycin resistance, in the clinically relevant pathogen *M. tuberculosis*, is most commonly the result of ribosomal mutation, such mutations are rarely employed, as a method to resist AG antibiotics, by other clinically relevant pathogens (Spratt, 1994; Musser, 1995). With regard to mutations in the 16S rRNA gene that afford AG resistance, it has been suggested that this mechanism is precluded by the presence of multiple copies of this gene in eubacteria. In contrast, resistance of this type in mycobacteria is facile, as bacteria of this genera only encode a single copy of this gene (Musser, 1995).

1.4.3. Altered targets II: enzymatic modification of 16S rRNA.

While AG resistance can be due to mutations in the *rrs* and *rpsL* genes, some bacteria express enzymes that catalyze the S-adenosylmethionine dependent methylation

of 16S rRNA (reviewed in Cundliffe, 1989). The synthesis of 16S rRNA methyltransferases appears to be a common mechanism of self protection for AG synthesizing bacteria, as the sisomicin producers *Micromonospora zionensis* (Kojic *et al*, 1992) and *Micromonospora rosea*, as well as the gentamicin producer *Micromonospora purpurae* (Keleman *et al*,1991) and the istamycin producer *Streptomyces tenjimariensis* (Beauclerk & Cundliffe, 1987) all encode 16S rRNA methyltransferases. Methylation of 16S rRNA has also been shown to be the mechanism by which *Streptomyces tenebrarius* achieves high level resistance to the toxic effects of gentamicin (Thompson *et al*, 1985; Cundliffe, 1992). The 16S rRNA methyltransferase from this organism had originally been reported to be from *M. purpurae* (Thompson *et al*, 1985), however, Cundliffe (1992) has since corrected this error. The methyltransferase from *S. tenebrarius* has been shown to catalyze the methylation of 16S rRNA at the N7 position of guanine 1405 (*E. coli* numbering) (Beauclerk & Cundliffe, 1987). Similarly, the methyltransferase from *S. tenjimariensis* methylates 16S rRNA at the N1 position of adenine 1408 (*E. coli* numbering) (Beauclerk & Cundliffe, 1987). Both of these sites of modification are within the region of 16S rRNA that binds the 4,5- and 4,6- disubstituted AGs (Moazed & Noller, 1987). Interestingly, the methyltransferase from *S. tenebrarius*, which methylates guanine 1405, mediates resistance to both kanamycin and gentamicin in *Streptomyces lividans*, whereas the methyltransferase from *S. tenjimariensis*, which methylates adenine 1408, mediates resistance, in *S. lividans*, to kanamycin and apramycin, but not gentamicin (Beauclerk & Cundliffe, 1987). Such a finding, coupled with the chemical footprinting studies that indicate that chemically related AGs have different footprinting

patterns (Moazed & Noller, 1987), suggests that AGs bind to similar regions of the A site in the 16S rRNA, but that they do so in subtly different ways.

1.4.4. Enzyme Catalyzed Covalent Modification of Aminoglycosides.

The second enzymatic method of AG resistance, AG modification, is the predominant method of resistance employed by clinically relevant bacteria (Miller *et al*, 1997). There are 3 general classes of enzymes that can modify AG antibiotics (reviewed in Wright *et al*, 1999) (Figure 1.4).

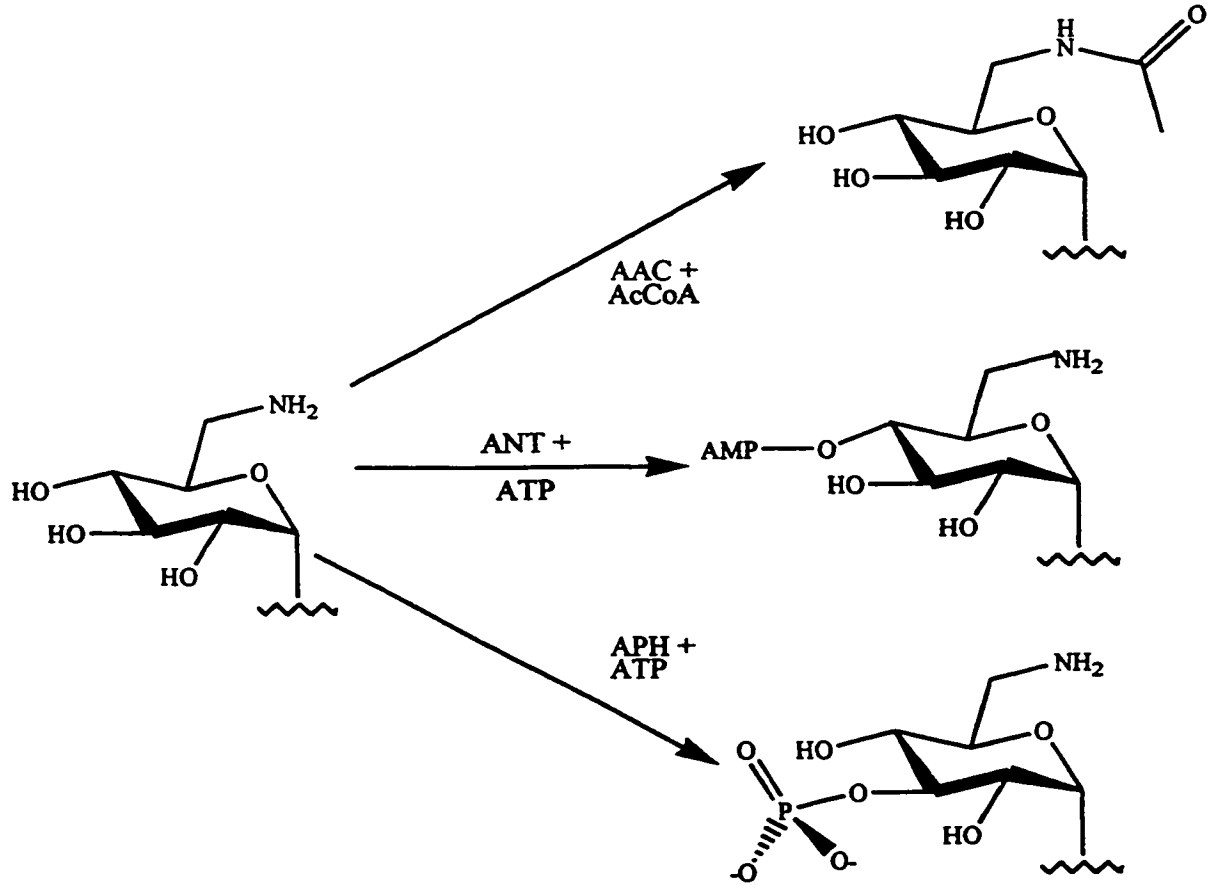

Figure 1.4. Classes of AG-modifying enzymes. The AACs catalyze the acetyl coenzyme A dependent N-acetylation of AG antibiotics. The ANTs catalyze the ATP dependent O-adenylation of AG antibiotics. The APHs catalyze the ATP dependent O-phosphorylation of AG antibiotics.

The first class of AG modifying enzymes is the AG acetyltransferases (AACs) and these enzymes catalyze the transfer of the acetyl moiety of acetyl-Coenzyme A (AcCoA) to specific amino groups present on these drugs. The second class of AG modifying enzymes is the AG nucleotidyltransferases (ANTs). These enzymes catalyze the transfer of the adenosyl moiety of ATP to specific AG hydroxyls. The second product of this reaction is pyrophosphate. The third class of AG modifying enzymes is the AG phosphotransferases (APHs) and these enzymes catalyze the transfer of the γ-phosphate of ATP to specific AG hydroxyls.

As will become apparent below, the terms AAC, ANT or APH are each used to describe a diverse class of AG-modifying enzymes. Individual members of a particular class can afford significantly different patterns of resistance, and therefore, to avoid confusion, Shaw *et al* (1993) have proposed a systematic method for naming AG-modifying enzymes (Figure 1.5).

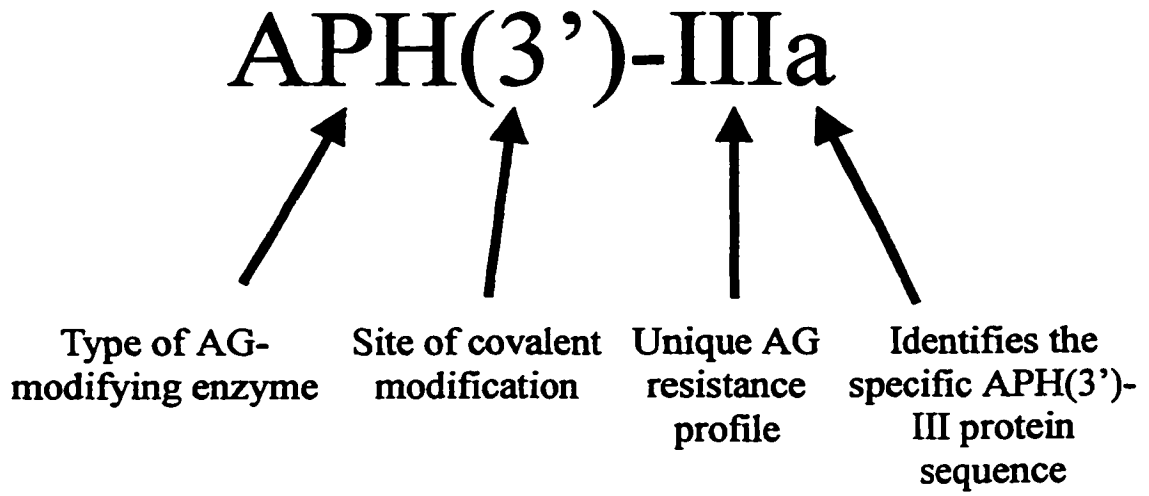

Figure 1.5. Naming scheme for AG-modifying enzymes. As originally proposed by Shaw, *et al* (1993).

The class of AG-modifying enzyme is first designated (e.g. APH, ANT, or AAC), and this is followed by a numerical description of the site of modification (e.g. 3'). Since different AG-modifying enzymes afford different patterns of resistance *in vivo* (e.g. kanamycin and gentamicin versus kanamycin and neomycin, but not gentamicin), a Roman numeral then designates the specific pattern of resistance observed *in vivo*. Since different genes, for a given resistance pattern, have been identified, the specific protein sequence is designated next using an uncapitalized letter. Thus, the APH from *E. faecalis* (Trieu-Cuot & Courvalin, 1983; Gray & Fitch, 1983), which modifies the 3' position of 4,6- and 4,5-disubstituted AG antibiotics, and mediates resistance to kanamycin and amikacin, is designated *aph(3')-IIIa*, whereas the APH from *Bacillus circulans* (Herbert *et al*, 1986), which modifies the 3' position of 4,6- and 4,5-disubstituted AG antibiotics, and mediates resistance to kanamycin and neomycin, but not amikacin, is designated *aph(3')-IVa*.

Since the primary focus of this thesis is a greater understanding of the catalytic mechanism of an APH, specifically APH(3')-IIIa, a detailed discussion of either the AACs or ANTs is not appropriate. Therefore, the catalytic mechanisms of these AG-modifying enzymes will not be discussed in great detail. For a more detailed discussion of these two classes of AG modifying enzymes, please see the excellent reviews of Umezawa & Kondo, 1982; Wright *et al*, 1999; Mingeot-Leclercq *et al*, 1999.

1.4.4.1 AACs

The earliest identification of an AAC activity occurred in 1965 (Okamoto & Suzuki, 1965). Since then, greater than 35 AACs have been identified (Wright *et al*,

1999), and these enzymes are a primary cause of AG resistance in virtually all clinically relevant bacteria (Miller *et al*, 1997). The genes encoding these enzymes are located primarily on plasmids, however a number have been found on transposable elements, and in the genomes of pathogenic bacteria (Shaw *et al*, 1993). Examples of chromosomally encoded *aac* genes can be found in the genomes of *M. tuberculosis* (Cole *et al*, 1998), *E. faecium* (Costa *et al*, 1993) and *Providencia stuartii* (Rather *et al*, 1993).

As a class, the AACs catalyze the acetylation of a diverse array of AG substrates, including kanamycin, gentamicin, amikacin, neomycin and isepamicin (Wright *et al*, 1999). Resistance is associated with acetylation at the N3, N2' and N6' positions of 4,6- and 4,5-disubstituted AG antibiotics (Figure 1.6) (Umezawa & Kondo, 1982; Wright *et al*, 1999; Mingeot-Leclercq *et al*, 1999).

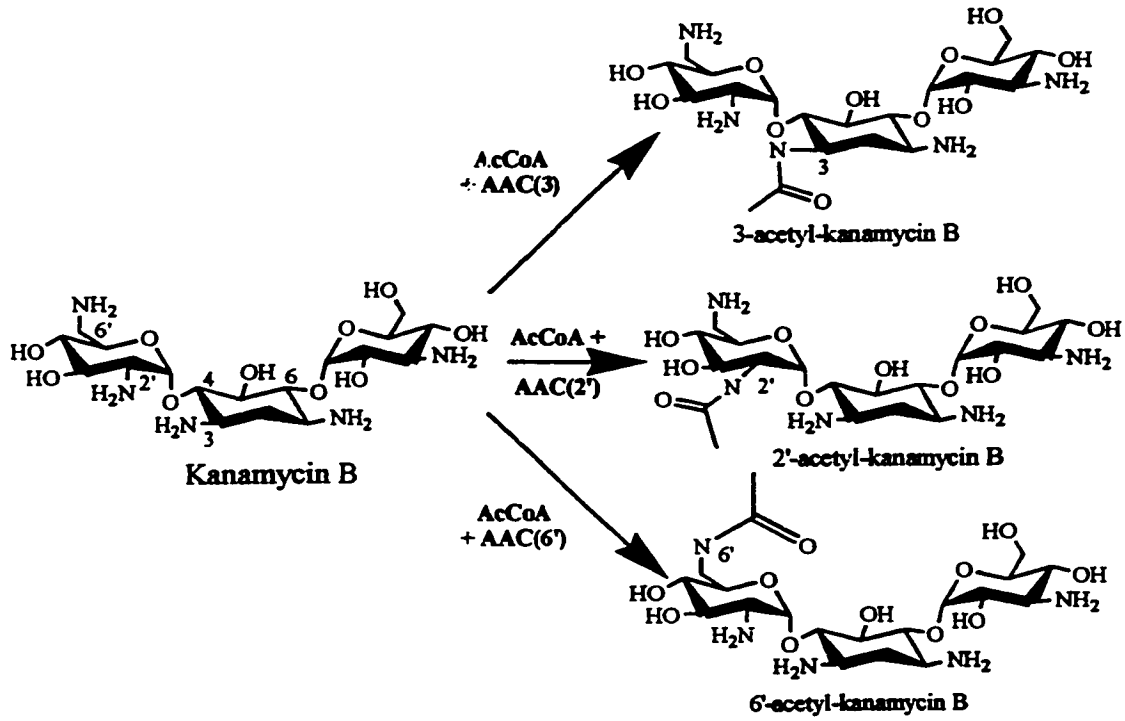

Figure 1.6. Regiospecificity of the reactions catalyzed by the known AACs.

The AACs are a well-studied class of enzymes. For example, the kinetic mechanisms of at least three AACs, AAC(6')-Ib (Radika & Northrop, 1984), AAC(3)-I (Williams & Northrop, 1978) and AAC(6')-APH(2") (Martel *et al*, 1983), have been determined and all these enzymes employ ternary complex mechanisms, where both the substrates and products can bind or be released in a random manner. The crystal structures of AAC(6')-Ii, from *Enterococcus faecium* (Wybenga-Groot, 1999) and the AAC(3)-Ia from *Serratia marcescens* (Wolf *et al*, 1998) have also been determined. Unfortunately, little is known about the roles of specific amino acid residues in promoting catalysis. The structural studies, described above, should quickly help ameliorate this deficiency. Such studies will be important for the development of AAC inhibitors. While there is a lack of information on the catalytic mechanism of these enzymes, the structures of AAC(6')-Ii and AAC(3)-Ia have revealed that these enzymes are structurally homologous to eukaryotic protein histone acetyltransferases, specifically *Saccharomyces cerevisiae* histone acetyltransferase 1 (yHAT1) and yeast GCN5 (yGCN5) transcriptional coactivator (Dutnall *et al*, 1998; Trieval *et al*, 1999). The successful design of inhibitors to the AACs will have to take this structural homology into account, in order to minimize non-specific inhibition and any resultant toxicity.

1.4.4.2. ANTs

The ANTs are also an important cause of AG resistance (Miller *et al*, 1997). Similar to the AACs, the genes encoding these resistance enzymes are also present on plasmids and transposable elements (Shaw *et al*, 1993). A number of ANTs have been identified, and these have been shown to mediate resistance to a variety of

AG/aminocyclitol antibiotics. These include streptomycin, spectinomycin, gentamicin, kanamycin, and neomycin (Wright *et al*, 1999). ANT mediated resistance to streptomycin has been shown to result from the *O*-adenylation of either the 6 or 3" hydroxyl, whereas resistance to spectinomycin can result from the adenylation of the 9 hydroxyl group of this AG (Figure 1.7). Resistance to 4,5- and 4,6-disubstituted AGs is due to the modification of hydroxyl groups at either the 4' or the 2" position of these antibiotics. Modification of O2", by the ANT(2")-I enzyme, is a prominent cause of gentamicin and tobramycin resistance in *Enterobacteriaceae, Pseudomonas, Serratia,* and *Providencia* species (Miller *et al*, 1997).

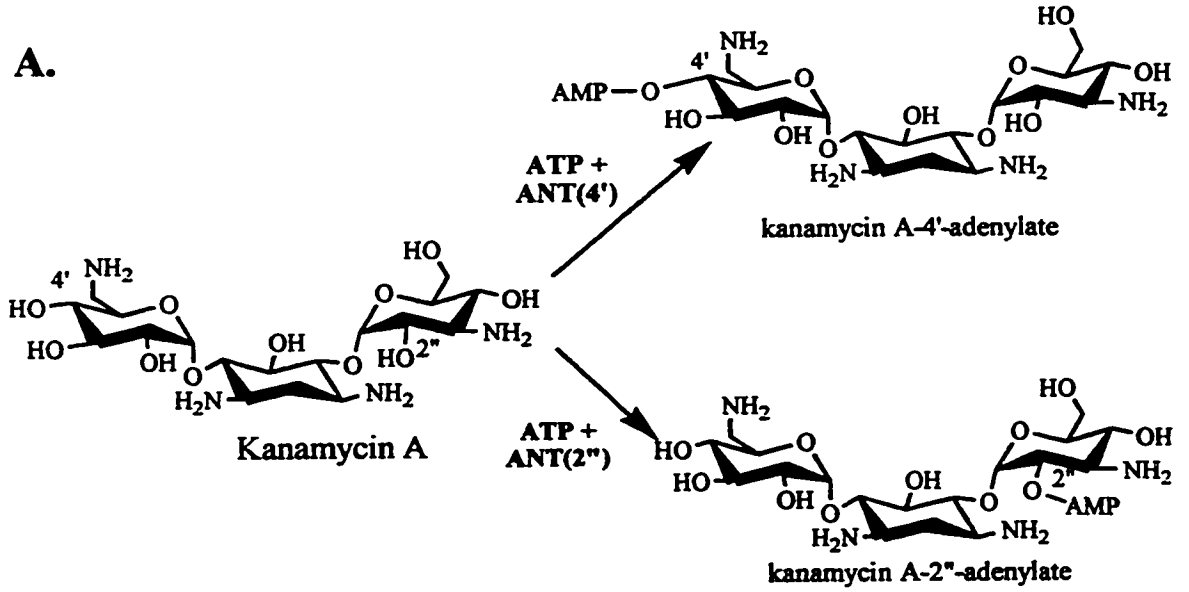

Figure 1.7. Regiospecificity of the reactions catalyzed by the known ANTs. **A.** Adenylation of 4,6-disubstituted AGs. This figure is continued on the following page.

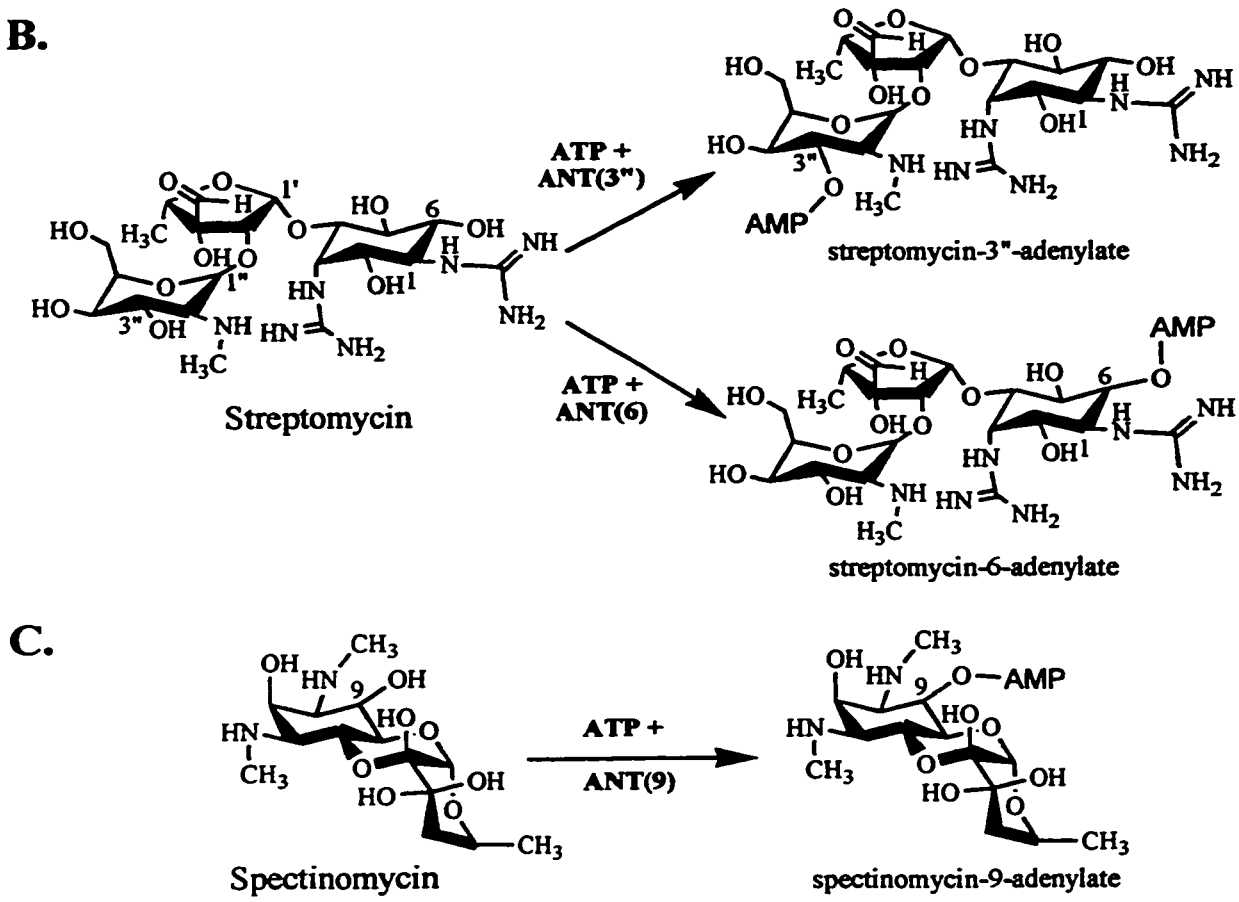

Figure 1.7. Regiospecificity of the reactions catalyzed by the known ANTs. Continued. B. Adenylation of streptomycin. **C.** Adenylation of spectinomycin.

The ANTs are also a well-characterized group of enzymes. For example, Van Pelt *et al* (1986) have established that the ANT(2")-I enzyme catalyzes the direct transfer of the adenylyl moiety of ATP to the O2" of an AG, whereas Gates and Northrop (1988) have established the kinetic mechanism of this enzyme to be a Theorell-Chance ordered bi bi reaction. A crystal structure of the ANT(4')-I apoenzyme (Sakon *et al*, 1993), from *S. aureus*, is available, and reveals that two individual protein subunits make up a head-to-tail dimer. The structure of this enzyme bound to kanamycin and the non-

ATP analogue AMPPCP has also been determined (Pedersen *et al*, 1995). While each monomer possesses an AG and ATP binding site, the second structure revealed that there are two active sites per dimer. However, these active sites are not independent, and adenyl transfer occurs between an AG bound to one subunit and a nucleotides to the other subunit (Pedersen *et al*, 1995). Despite the availability of a crystal structures for the ANT(4')-I enzyme there is paucity of biochemical information, which would confirm the suspected role(s) of specific amino acids. For a description of the predicted roles of specific amino acids please see the review of Wright *et al*, 1999.

1.4.4.3. APHs

Since the earliest identification of an APH activity (Umezawa *et al* 1967), greater than 40 APHs have been identified in such **pathogenic** bacteria as *E. coli, E. faecalis*, and *S. aureus* (Shaw *et al*, 1993). These genes are primarily located on plasmids and transposons (Shaw *et al*, 1993), however, APHs of chromosomal origin have been identified in the genomes of *Legionella pneumophila* and *Pseudomonas aueruginosa* (Suter *et al*, 1997; Hachler *et al*, 1996). Two proteins that show primary structure homology to the APHs were also identified during the sequencing of the *M. tuberculosis* genome, although their function is unknown (Cole *et al*, 1998). Chromosomally encoded APHs are also present in **non-pathogenic** bacteria. Such APHs have been identified in the AG producing organisms *Streptomyces fradiae, Bacillus circulans* and *Micromonospora chalcea* (reviewed in Wright & Thompson, 1999). The APHs identified to date catalyze the transfer of the γ-phosphate of ATP to a diverse set of regiospecific sites, which include the 3', 2", and 5" hydroxyls present on 4,5- and 4,6-

disubstituted AGs; the 3" and 6 hydroxyls present on streptomycin; the 9 hydroxyl on spectinomycin; and the 4 and 7" hydroxyls present on hygromycin (Wright & Thompson, 1999). These reactions are summarized in Figure 1.8.

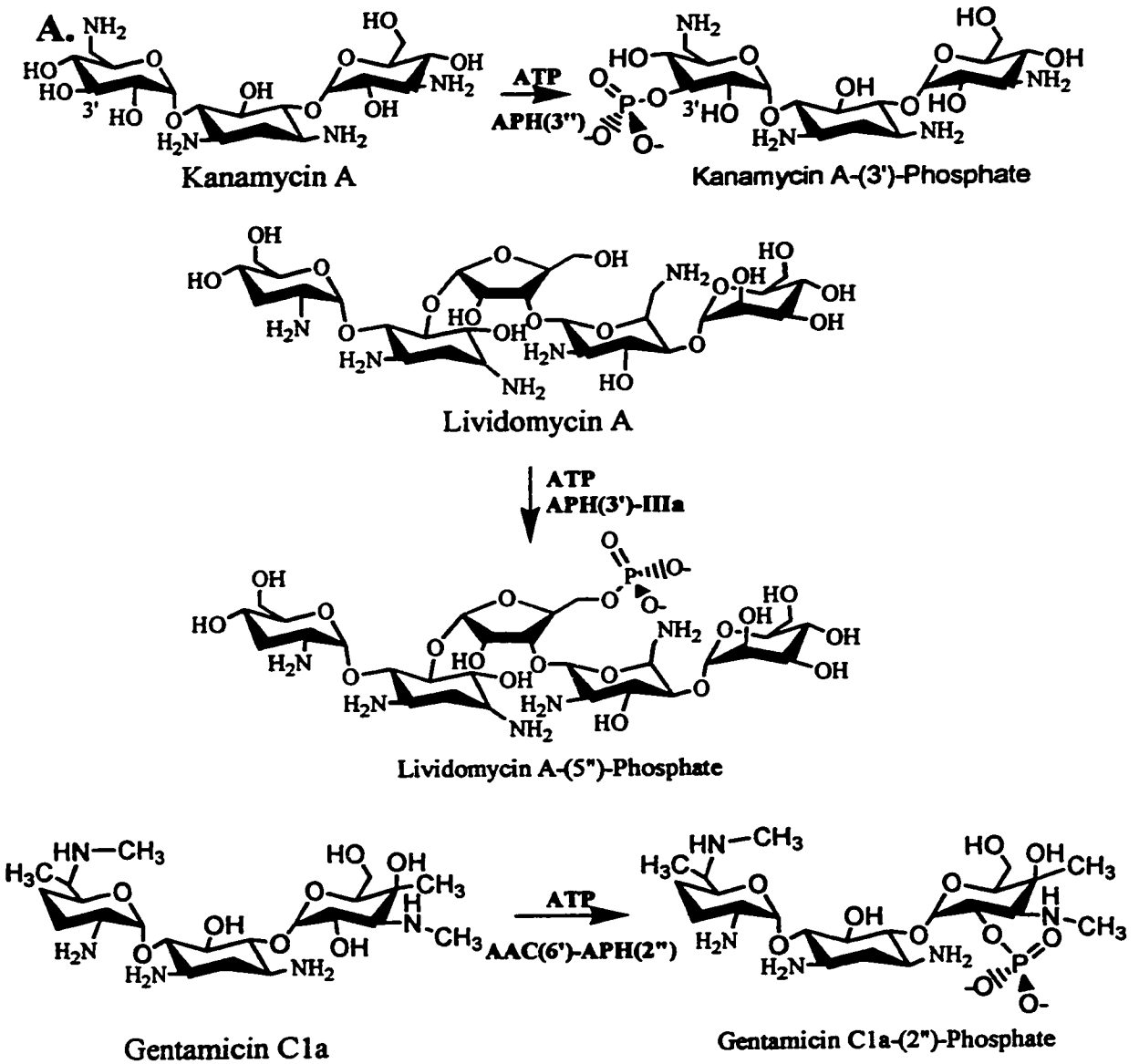

Figure 1.8. Regiospecificity of the reactions catalyzed by the known APHs. A. Phosphorylation of 4,5- and 4,6-disubstituted AGs. **B.** Phosphorylation of streptomycin. **C.** Phosphorylation of spectinomycin. **D.** Phosphorylation of hygromycin.

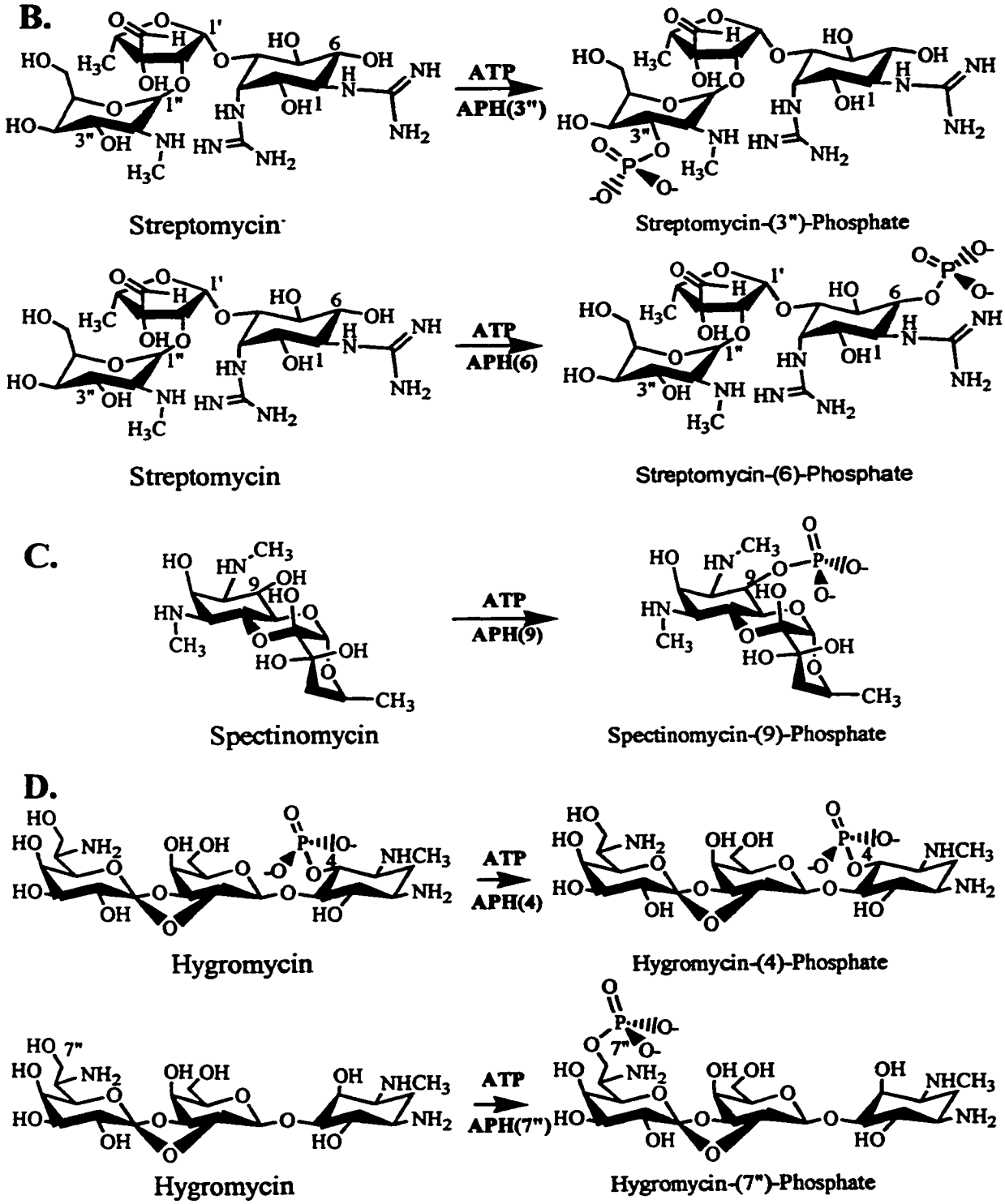

Figure 1.8: Continued.

Wright & Thompson (1999) have grouped the known APHs (Table 1.3) into one of four families (A-D), based upon primary structure homology (Figure 1.9). The APHs within families C, and D, generally, catalyze the phosphorylation of AGs that do not possess a 2-deoxystreptamine ring, whereas the majority of the APHs, in family A, do phosphorylate AGs of this type. It should be noted that the APH(2")s, which also phosphorylate 2-deoxystreptamine containing AGs, are not closely related to the APH(3') (family B versus family A) at the level of their primary structures.

Table 1.3. APH homologues[1].

APH homologue	Substrate/ Resistance Pattern	Host Organism	Reference
APH(3')-Ia	Gent B, Kan, Liv, Neo, Par, Rib	*Escherichia coli*	Oka *et al*, 1981
APH(3')-Ib	Gent B, Kan, Liv, Neo, Par, Rib	*E. coli*	Pansegrau *et al*, 1987
APH(3')-Ic	Gent B, Kan, Liv, Neo, Par, Rib	*Klebsiella pneumonia*	Lee *et al*, 1991
APH(3')-IIa	But, Gent B, Kan, Neo, Par, Rib	*E. coli*	Beck *et al*, 1982
APH(3')-IIIa	Ami, But, Gent B, Ise, Kan, Liv, Neo, Par, Rib	*Enterococcus faecalis* & *Staphylococcus aureus*	Gray & Fitch 1983; Trieu-Cout & Courvalin, 1983
APH(3')-IVa	But, Kan, Neo, Par	*Bacillus circulans*	Herbert *et al*, 1986
APH(3')-Va	Kan, Neo, Par	*Streptomyces fradiae*	Thompson & Gray, 1983
APH(3')-Vb	Kan, Neo, Par	*Streptomyces ribosidificus*	Hoshiko *et al*, 1988
APH(3')-Vc	Kan, Neo, Par	*Micromonospora chalcea*	Salauze & Davies, 1991
APH(3')-VIa	But, Gent B, Kan, Neo, Par, Rib	*Acinetobacter baumani*	Martin *et al*, 1988
APH(3')-VIIa	Ami, But, Gent B, Ise, Kan, Liv, Neo, Par, Rib	*Campylobacter jejuni*	Tenover *et al*, 1988
AAC(6')-APH(2")-Ia	Gent C, Kan, Liv, Neo, Tob	*E. faecalis* & *S. aureus*	Ferretti *et al*, 1986; Rouch *et al*, 1987

[1] This table has been adapted from Wright & Thompson (1999). Substrate short forms are as follows: Ami, amikacin; But, butirosin; Gent B, gentamicin B; Gent C, gentamicin C complex; Hyg, hygromycin; Ise, isepamicin; Kan, kanamycin; Liv, lividomycin; Neo, neomycin; Par, paromomycin; Rib, ribostamycin; Spec, spectinomycin; Strep, streptomycin; Tob, tobramycin.

Table 1.3. Continued

APH(2")-Ib	Gent C, Kan, Liv, Neo, Tob	*E. coli*	Shaw, 1997
APH(2")-Ic	Gent C, Kan, Liv, Neo, Tob	*Enterococcus gallinarum*	Chow *et al*, 1997
APH(3")-Ia (*aphE*)	Strep	*Streptomyces griseus*	Heinzel *et al*, 1988
APH(3")-Ib (*strA*)	Strep	*E. coli*	Scholz *et al*, 1989
APH(6)-Ia (*aphD*)	Strep	*S. griseus*	Distler *et al*, 1987
APH(6)-Ib (*sph*)	Strep	*Streptomyces glaucescens*	Vogtli & Hutter, 1987
APH(6)-Ic (*str*)	Strep	*E. coli*	Mazodier *et al*, 1985
APH(6)-Id (*strB*)	Strep	*E. coli*	Scholz *et al*, 1989
APH(9)-Ia	Spec	*Legionella pneumophila*	Suter *et al*, 1997
APH(9)-Ib (*spcN*)	Spec	*Streptomyces flavopersicus*	Lyutzkanova *et al*, 1997
APH(4)-Ia	Hyg	*E. coli*	Gritz & Davies, 1983
APH(4)-Ia (*glpA*)	Hyg	*Pseudomonas pseudomallei*	Penaloza-Vazquez *et al*, 1995
APH(7")-Ia	Hyg	*Streptomyces hygroscopicus*	Zalacain *et al*, 1986
APH(3')-VSr	Kan, Neo	*Streptomyces rimosus*	Akopiants & Danilenko, 1995
Hydroxyurea kinase (*hur*)	hydroxyurea	*Streptomyces aureofaciens*	Kormanec *et al*, 1992
MPH-I (*mphA, mphK*)	erythromycin	*E. coli*	Noguchi *et al*, 1995; Kim & Choi, 1996
MPH-II (*mphB*)	erythromycin	*E. coli*	Noguchi *et al*, 1996
Viomycin kinase (*vph*)	viomycin	*Streptomyces vinaceus*	Bibb *et al*, 1985
Capreomycin kinase (*cph*)	capreomycin	*Streptomyces capreolus*	Thiara & Cundliffe, 1995
MtPH-I	unknown	*Mycobacterium tuberculosis*	Cole *et al*, 1998
MtPH-II	unknown	*M. tuberculosis*	Cole *et al*, 1998
APH-LI (*orf8*)	unknown	*Lactococcus lactis subsp. lactis*	Delorme *et al*, 1992
APH-STRN (*strN*)	unknown	*S. griseus*	Pissowotzki *et al*, 1991

Within the largest single family of APHs, family A, are the APH(3'), and these enzymes can be distinguished by their AG resistance profile. Shaw *et al* (1993), using this criteria, have subdivided the APH(3') into seven smaller groupings. Of the seven classes of APH(3') enzymes, the catalytic mechanisms of APH(3')-Ia, APH(3')-IIa, APH(3')-IVa, and APH(3')-IIIa are the best-characterized. Thus for the purposes of this thesis, which deals primarily with APH(3')-IIIa, only a discussion of these APH(3)

enzymes is relevant. The bifunctional APH, AAC(6')-APH(2"), is also well characterized and because this enzyme is the predominant cause of AG resistance in MRSA (Miller *et al*, 1997), this enzyme will also be discussed.

1.4.4.3.1. AAC(6')-APH(2")

Identical genes encoding the bifunctional enzyme, AAC(6')-APH(2"), have been cloned from both *E. faecalis* and *S. aureus* (Ferretti *et al*, 1986; Rouch *et al*, 1987), where the *aac(6')-aph(2")* gene is often found on transposable elements present in chromosomes or on R plasmids (Culebras & Martinez, 1999). The sequences of the *aac(6')-aph(2")* genes from these organisms are identical, at the nucleotide level (Rouch *et al*, 1987), thereby pointing to a common origin. The *aac(6')-aph(2")* gene is thought to be the result of a fusion between genes encoding AAC and APH enzymes (Ferretti *et al*, 1986), as primary structure homology to these types of enzymes exists in the N- and C-terminal, respectively (Ferretti *et al*, 1986).

The *aac(6')-aph(2")* gene has been overexpressed in both *Bacillus subtilis* and *E. coli* and the protein product purified to homogeneity (Azucena *et al*, 1997; Daigle *et al*, 1999a). The regiospecificity of acetylation and phosphorylation by APH(6')-APH(2") has also been established (Azucena *et al*, 1997; Daigle *et al*, 1999a). For kanamycin A, a 4,6-disubstituted AG, the *in vitro* site of acetylation was determined to be the 6' amino group, whereas the site of phosphorylation was determined to be the 2" hydroxyl (Azucena *et al*, 1997).

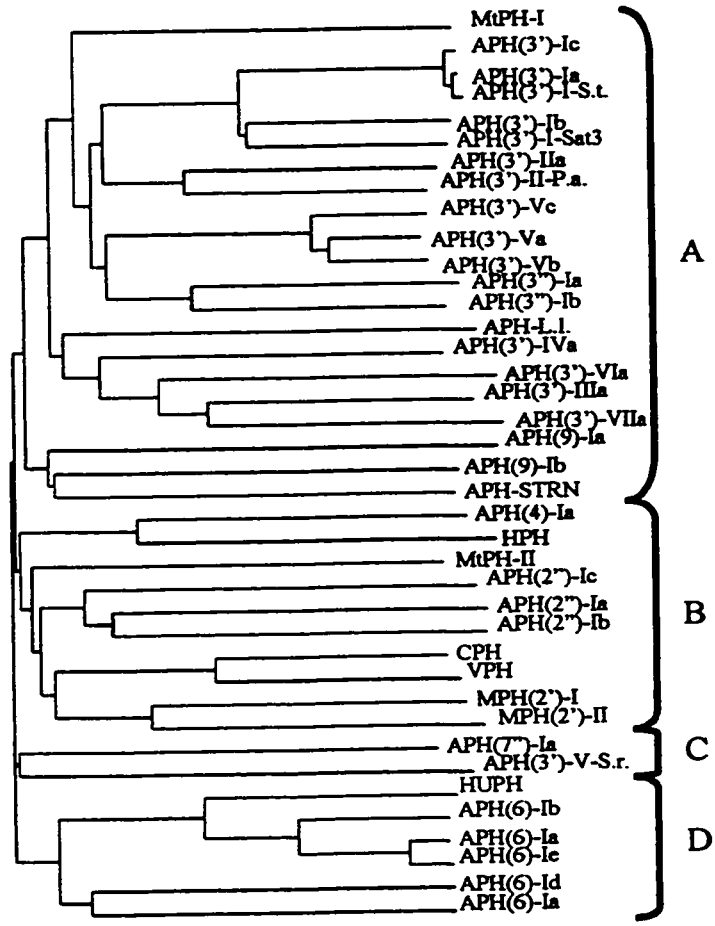

Figure 1.9. Phylogeny of APHs and related proteins. Primary sequence alignments of known APHs and related proteins were made using the Clustal W program (Thompson, *et al*, 1994). The phylogenetic tree was drawn using the program Treedraw. An alignment these sequences has previously been described (Wright & Thompson, 1999), however, it should be noted that a putative mycobacterial APH, identified, and designated as MtPH-III, by Wright & Thompson (1999), was omitted from this alignment. This protein sequence was omitted in order to remain consistent with the functional designations of the putative proteins identified during the sequencing of the *M. tuberculosis* genome (Cole, *et al*, 1998). Omission of this sequence did little to affect the 4 families of APH homologues described in Wright & Thompson (1999). The only effect was the placement of the APH(4)-Ia and HPH enzymes in the APH(2") family (Family B) instead of the APH(6) family (Family D). For the unusual APH homologues the enzyme designations are as follows: HPH, hygromycin phosphotransferase; MtPH, *M. tuberculosis* phosphotransferase; CPH, capreomycin phosphotransferase; VK, viomycin phosphotransferase; MPH, macrolide phosphotransferase; HUPH, hydroxyurea phosphotransferase.

The *in vitro* sites of kanamycin A modification, by APH(6')-APH(2"), were determined by the complete assignment of the NMR spectra of an acetylated and phosphorylated (doubly modified) derivative of this AG. However, only the O2" phosphorylated derivative of kanamycin A could be purified from *in vivo* cell cultures (Azucena *et al*, 1997). For neomycin B, a 4,5-disubstituted AG, Daigle *et al* (1999a), using NMR and mass spectral techniques, determined that the APH(6')-APH(2") enzyme catalyzed the phosphorylation of both the 3'- and 3"-hydroxyl. However, they noted that the 3'-hydroxyl was the predominant site of phosphorylation. Daigle *et* al (1999a) also established the site of phosphorylation for lividomycin A, another 4,5-disubstituted AG, which lacks a 3'-hydroxyl. This AG is phosphorylated at the 5"-hydroxyl. The fact that phosphorylation of neomycin B, and lividomycin A, did not occur at the 2"-hydroxyl is not altogether unsurprising, especially when one considers the fact that in 4,5-disubstituted AGs the double primed ring is a pentose, whereas in 4,6-disubstituted AGs this ring is a hexose. Subtle differences between the solution structures of 4,5- and 4,6-disubstituted AGs likely preclude O2" phosphorylation of the 4,5-disubstituted AGs.

Steady state kinetic analysis of AAC6')-APH(2") reveals an enzyme that has a very broad substrate specificity; k_{cat}/K_m values for the AAC activity range from 10^4-10^5, whereas k_{cat}/K_m values for the APH activity range from 10^3-10^5. It should be noted that for the APH activity some discrepancy exists between the k_{cat} values reported by Daigle *et al* (1999a) and Azucena *et al* (1997). The k_{cat}s reported by the former are ~500-fold lower than those reported by the latter. The reason for such a discrepancy is not known, although it is possible that the differences are assay dependent, as Azucena *et al* (1997)

used a fluorescence-based assay, whereas Daigle *et al* (1999a) used an absorbance based assay. Despite this discrepancy, it appears that during evolution of the AAC(6')-APH(2") enzyme, efficiency, as measured by k_{cat}/K_m, was sacrificed for a broad substrate specificity. The kinetic mechanism of the APH(2") portion of the APH(6')-APH(2") enzyme has also been described, and is a ternary complex one, where substrate binding and release occurs in a random fashion (Martel *et al*, 1983).

1.4.4.3.2. APH(3')-Ia

The APH(3')-Ia enzyme, originally cloned from the transposable element Tn*903*, present in *E. coli* (Oka *et al*, 1981), has been overexpressed in this organism, and purified in a single step using a neomycin affinity column (Siregar *et al*, 1995). The regiospecificity of kanamycin A phosphorylation by this enzyme has unambiguously been confirmed to be the 3'-hydroxyl, using NMR and mass spectral methods (Siregar *et al*, 1995). While this enzyme can efficiently phosphorylate, $k_{cat}/K_m \sim 10^6$ the aminohydroxybutyrate containing AGs, amikacin and butirosin *in vitro*, this enzyme only provides a moderate level of protection *in vivo*, minimal inhibitory concentrations (MIC) are < 10 μg/mL (Siregar *et al*, 1995). Siregar *et al* (1995) have also reported that the kinetic mechanism of APH(3')-Ia is one where a ternary complex is formed, where formation of that complex occurs in a random fashion i.e. there is no requirement for ATP to bind to the enzyme prior to AG binding, or *vice versa*.

1.4.4.3.3 APH(3')-IIa

The APH(3')-IIa enzyme has been extensively characterized by a number of groups. The gene was originally cloned from a transposable element, Tn*5*, present in

Salmonella typhimurium (Beck *et al*, 1982; Shaw *et al*, 1993). The primary structure of this enzyme revealed that this protein is evolutionarily related to APH(3')-Ia; in fact, these proteins are 55% identical (Beck *et al*, 1982). Many of the regions of sequence identity are present in the C-terminal region of the protein, and Beck *et al* (1982) have shown that the removal of the 22 amino acids at the C-terminal end of the protein abolishes the resistance that the wild type *aph(3')-IIa* gene affords *in vivo*. The APH(3')-IIa enzyme has been overexpressed in *E. coli*, and after a 4 step purification, 17 mg of pure enzyme was obtained (Siregar *et al*, 1994). Kinetic characterization of this enzyme revealed that this enzyme efficiently phosphorylates a number of AG substrates with k_{cat}/K_m values on the order of 10^6-10^7. The relatively inefficient phosphorylation of amikacin, $k_{cat}/K_m \sim 10^4$, explains why the *aph(3')-IIa* gene poorly mediates resistance to this AG *in vivo* (Kocabiyik & Perlin, 1992b; Perlin & Lerner, 1986).

Mobashery's group has examined the importance of electrostatic interactions in the binding of AGs to the APH(3')-IIa enzyme. This was accomplished by selectively deaminating the AGs kanamycin A and neamine (Roestamdji *et al*, 1995). The ability of the APH(3')-Ia enzyme to use these compounds has also been characterized (Roestamdji *et al*, 1995). For APH(3')-IIa, the N1 and N6' of kanamycin A are important for binding, as kanamycin analogues, deaminated at those positions, have a dramatically decreased affinity for this enzyme, as evidenced by the 80- and 350-fold increases in K_m, respectively. Amino groups at these positions are also important for kanamycin A binding to APH(3')-Ia. While these kanamycin A analogues were poor substrates for

both the APH(3')-Ia and APH(3')-IIa enzymes, the antimicrobial activity of these compounds was unfortunately quite poor (Roestamdji *et al*, 1995).

Site directed mutagenesis of a number of residues in APH(3')-IIa has been carried out by a number of groups (Yenofsy *et al*, 1990; Blazquez *et al*, 1991; Kocabiyik & Perlin, 1992a; Kocabiyik & Perlin, 1992b; Kocabiyik & Perlin, 1994). The side chains of Val36, Glu182, His188, Gly189, Asp190, Asp208, Gly210, Arg211, Asp216, Asp220, and Asp261 (APH(3')-IIa numbering) were suggested to be important for catalysis, as bacteria expressing an *aph(3')-IIa* gene, mutated at the corresponding positions, were dramatically more susceptible to a number of AG antibiotics (Blazquez *et al*, 1991; Kocabiyik & Perlin, 1992a; 1992b). Kocabiyik & Perlin (1992a) also used crude cell extracts from bacteria expressing His188, Asp190, Asp216, and Asp220 mutant enzymes to determine the steady state kinetic parameters for ATP. These studies suggested to Kocabiyik & Perlin that all 4 residues were important for nucleotide binding. However, the maximum effect on K_m is only 2.1 fold, and the crystal structure of APH(3')-IIIa complexed with ADP indicates that none of these residues are involved in ATP binding (Hon *et al*, 1997). Thus, these residues are unlikely to form part of the APH(3')-IIa nucleotide binding pocket. These authors rightly suggested (see Chapter 4), that the decrease in activity associated with the Asp190 and Asp208 mutants could be due to the involvement of these residues in magnesium binding. However, these authors wrongly suggested (see Chapter 3), that the 36-fold decrease in activity associated with the mutation of His188 to Gln was consistent with a role for His188 in forming a phospho-enzyme intermediate, specifically as a phosphate accepting residue (Kocabiyik & Perlin,

1992a). Gln would neither be expected to be a good phosphate acceptor nor a good phosphate donor. Based upon some limited sequence homology between APHs and other nucleotide binding proteins, Martin *et al* (1988) had previously suggested that His188 could act as a phosphate donor/acceptor. Blazquez *et al* (1991) have also generated His188 mutants of APH(3')-IIa, and they rightly suggested that the results obtained when they independently generated the Tyr, Ser and Leu mutants of His188 that the decreases in activity, which were not dramatic, were not consistent with a role for this residue as a phosphate acceptor/donor. For example, the level of AG resistance, mediated by the His188Tyr mutant, was lower (MIC $\leq$ 5 μg/mL) than the level of AG resistance mediated by the His188Leu mutant. A Tyr residue would be expected to be a much better phosphate donor/acceptor than a Leu residue.

Kocabiyik & Perlin (1994) also used site directed mutagenesis to examine the roles of Gly205, Gly210, and Arg211 in the catalytic mechanism of APH(3')-IIa. In this study the authors suggest that this region of APH(3')-IIa forms the nucleotide positioning loop (NPL) present in ATP/GTP binding proteins. While the homologous region in APH(3')-IIIa is close to the bound nucleotide, the crystal structure of APH(3')-IIIa bound to ADP (Hon *et al*, 1997) reveals that these residues do not form the NPL of APH(3')-IIIa, and presumably all other 3'-APHs. In APH(3')-IIIa, the NPL is composed of Thr22to Ser27. Nonetheless, *in vitro* antibiotic susceptibilities and enzyme assays on crude cell extracts indicated the importance of these residues to the catalytic mechanism of APH(3')-IIa. In *in vitro* antibiotic susceptibility assays, cells expressing the APH(3')-IIa mutant enzymes displayed much greater susceptibility to a broad range of 4,6- and

4,5-disubstituted AGs than the level of susceptibility observed for cells expressing the wild type APH(3')-IIa enzyme (Kocabiyik & Perlin, 1994). In enzymatic assays the relative activities of the Gly210 and Arg211 mutant enzymes were dramatically reduced (~50-100-fold), whereas the relative activity of the Gly205 mutant was less dramatically reduced (~10-fold). However, Western blot analysis indicated that expression of the Gly210 and Arg211 mutants was markedly reduced and only negligible amounts of protein were produced. Thus, the reductions in activity, observed for these mutant enzymes, is more likely associated with the reduced protein levels, rather than with a specific role for these residues in the catalytic function of APH(3')-IIa. As a partial confirmation of this hypothesis, we have shown the relative unimportance of Arg211 to the catalytic mechanism of APH(3')-IIIa, using purified mutant enzyme (Thompson *et al*, 1999; Chapter 5).

Further mutagenesis experiments, by Kocabiyik & Perlin (1992b), examined the importance of Tyr218 to the catalytic mechanism of APH(3')-IIa. Mutation of this residue to Ser resulted in an 8 fold increase in resistance to amikacin, which normally is a poor substrate for the APH(3')-IIa enzyme (Siregar *et al*, 1994). A corresponding ~3-fold decrease in K_m was observed when the steady state kinetic parameters were determined, using crude cell extracts prepared from bacteria expressing this mutant enzyme. The authors suggested that the hydroxyl group of Tyr 218 could be important for AG binding, however in the crystal structure of APH(3')-IIIa bound to ADP (Hon *et al*, 1997) the corresponding residue, which is a Trp, is located at the start of an α-helix that is far from the proposed AG binding site of this enzyme (Thompson *et al*, 1999).

Thus, in light of the position of this residue in the APH(3')-IIIa crystal structure, it is most likely that this residue is important for maintaining the tertiary structure of the enzyme. Yenofsky *et al* (1990) identified a mutation in an APH(3')-IIa bearing plasmid used to transform tobacco tissues. The mutation results in the generation of a Glu182Asp mutant enzyme with reduced catalytic activity. Siregar *et al* (1994) purified this mutant enzyme to homogeneity and determined the steady state kinetic parameters for ATP and a number of AG substrates. Results of this study indicated that affinity of this mutant enzyme for ATP is decreased 8.9-fold. Thus this residue would appear to be important for nucleotide binding. However, the crystal structure of APH(3')-IIIa bound to ADP indicates that the homologous residue, Glu182, is quite far (> 20 Å at closest approach) from the bound nucleotide. Thus, this residue may also be important for maintaining the correct tertiary structure of this enzyme.

1.4.4.3.4. APH(3')-IVa

The gene encoding the APH(3')-IVa enzyme, cloned from *Bacillus circulans* (Herbert *et al*, 1986), has also been overexpressed in *E. coli* (Sarwar & Akhtar, 1990). The enzyme has been purified, and the regiospecificity of ribostamycin phosphorylation was determined from the ^{1}H, ^{13}C, and ^{31}P NMR spectra of the phosphorylated derivative (Sarwar & Akhtar, 1990). This NMR data showed that this enzyme exclusively phosphorylates the 3'-hydroxyl of ribostamycin. When expressed in *E. coli*, APH(3')-IVa was found to be localized in the cytoplasm. Thus, it would appear that in order to successfully mediate resistance, this enzyme must detoxify AG antibiotics as soon as these compounds traverse the membrane and make their way into the cell.

1.4.4.3.5. APH(3')-IIIa

While other APHs have been well characterized, our current and past *in vitro* studies on the catalytic mechanism of APH(3')-IIIa, when combined with the crystal structure of APH(3')-IIIa bound to ADP, have provided an understanding of its catalytic mechanism that is unmatched for any other APH, or for that matter, any other AG modifying enzyme. The genes encoding the APH(3')-IIIa enzymes are plasmid borne, and were originally cloned from both *E. faecalis* and *S. aureus* (Trieu-Cuot & Courvalin, 1983; Gray & Fitch, 1983). The nucleotide sequences of the *aph(3')-IIIa* genes from these organisms are virtually identical. The only difference that exists between the two gene sequences lies in the 5' end of the *E. faecalis* gene, here there is a 3-nucleotide insertion. Thus, the *E. faecalis* gene encodes a 264 amino acid protein whereas the *S. aureus* gene encodes a 263 amino acid protein. The additional amino acid in the *E. faecalis* enzyme corresponds to Val35.

The enterococcal enzyme has been overexpressed in *E. coli* and purified in high yield (30-40 mg/L of cell culture) (McKay *et al*, 1994a). The regiospecificity of APH(3')-IIIa, for a number of AG substrates, has been established through the use of NMR and mass spectral methods (McKay *et al*, 1994a; Thompson *et al*, 1996; Chapter 2) and the steady state kinetic parameters have been determined for the APH(3')-IIIa catalyzed phosphorylation of a number of AG substrates (McKay *et al*, 1994a). These studies indicate that this enzyme has extremely broad substrate specificity, and can phosphorylate members of both the 4,5- and 4,6-disubstituted classes of AG antibiotics, including: kanamycin A, kanamycin B, amikacin, neomycin B, paromomycin, ribostamycin, and butirosin. This enzyme can also catalyze the phosphorylation of

lividomycin, a 4,5-disubstituted AG, which lacks a 3' hydroxyl (McKay *et al*, 1994a). All these substrates are fairly efficiently phosphorylated with k_{cat}/K_m values ranging from 10^4-10^5. However, other 3'-APHs with a more limited substrate range, for example APH(3')-Ia and APH(3')-IIa, are generally much more efficient APHs; k_{cat}/K_m values for these enzymes are at least 10 fold higher (Siregar *et al*, 1994; Siregar *et al*, 1995). Thus, it appears, for APH(3')-IIIa, that the catalytic power of this enzyme has been sacrificed in order to compensate for an expanded substrate specificity.

Through the use of specifically deaminated derivatives of neamine and kanamycin A, McKay *et al* (1996a) have determined the importance of particular amino groups for binding of AG antibiotics to APH(3')-IIIa. The results indicate the relative importance, to substrate binding, of the amino groups at positions 1, 2' and 6' of neamine. The 6' amino group also appears to be critical for kanamycin A binding. A number of AGs have been modeled into the crystal structure of APH(3')-IIIa, including kanamycin A, and these studies have indicated that the 6' amino group interacts with the C-terminal carboxylate, which is critical for enzymatic activity (Thompson *et al*, 1999; Chapter 5).

McKay & Wright (1995) have established that the kinetic mechanism of APH(3')-IIIa, is one where a ternary complex is formed. However, for APH(3')-IIIa, ternary complex formation occurs in an ordered fashion, with ATP binding first and the AG binding second (Figure 1.10). For this enzyme, product release also occurs in an ordered fashion, with the phosphorylated AG being released prior to the release of ADP. This type of mechanism is generally termed an ordered bi bi kinetic mechanism.

However, for APH(3')-IIIa, the rates of phosphoryl transfer and phospho-AG release are fast relative to the release of ADP, thus this type of kinetic mechanism is a special case of an ordered bi bi reaction, which is termed Theorell-Chance (McKay & Wright, 1995).

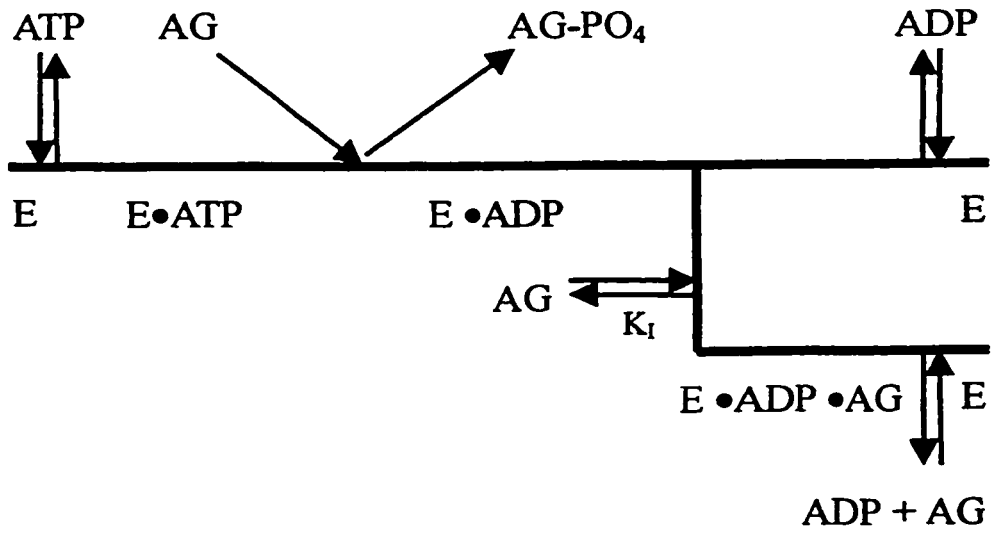

Figure 1.10. Kinetic mechanism of APH(3')-IIIa. This mechanism is a special case of an ordered bi bi reaction termed Theorell-Chance (McKay & Wright, 1995).

Solvent isotope and solvent viscosity effects have also been determined for APH(3')-IIIa (McKay & Wright, 1996b). For this enzyme, the solvent isotope effect is small, which indicates that the rate of substrate deprotonation, *vis a vis* the rate of phosphoryl transfer is fast relative to the measured rate of reaction, the k_{cat}. Conversely, the effect of solvent viscosity on the rate of the APH(3')-IIIa catalyzed reaction, the k_{cat}, is large, thereby indicating that the rate of the reaction catalyzed by APH(3')-IIIa is limited by a diffusion controlled step, i.e. the release of ADP. These studies, therefore, help confirm the kinetic mechanism because they show that second product release is

completely rate limiting, which is consistent with a Theorell-Chance mechanism. Knowledge of the kinetic mechanism (McKay & Wright, 1995) helps to explain why the rate of the APH(3')-IIIa catalyzed reaction decreases at high concentrations of an AG substrate (McKay *et al*, 1994). At high concentrations of AG, non-productive binding of AGs to the ADP bound form of the enzyme occurs at a significant rate. Effectively this results in a decrease in the amount of enzyme in a catalytically competent state.

Amino acid residues in APH(3')-IIIa, required to promote catalysis, have also been identified. Using an electrophilic ATP analogue, 5'-[*p*-(fluorosulfonyl)benzoyl] adenosine (FSBA) McKay *et al* (1994b) were able to identify a region of APH(3')-IIIa that forms part of the nucleotide binding pocket. FSBA was shown to covalently modify both Lys33 and Lys44, although the predominant site of modification was Lys44 (McKay *et al*, 1994b). The fact that Lys44 is highly conserved among the APHs led McKay *et al* (1994b) to suggest that this residue could be involved in binding the triphosphate moiety of ATP. To confirm that hypothesis, the Lys33Ala and Lys44Ala mutants were generated, produced, and purified. The steady state kinetic parameters for both these mutants were determined (Hon *et al*, 1997), and while the Lys33Ala mutant displays near wild type kinetics, the affinity of the Lys44Ala mutant for ATP is significantly reduced. The K_m for ATP is increased 26.4-fold. Thus Lys44, and not Lys33, is important for nucleotide binding. The determination of the structure of APH(3')-IIIa bound to ADP confirmed the importance of Lys44 in nucleotide binding (Hon *et al*, 1997).

The determination of the crystal structure of APH(3')-IIIa bound to ADP (Hon *et al*, 1997) revealed that this enzyme crystallized as a disulfide-linked head-to-tail dimer,

with two independent active sites readily apparent. An earlier study, which had determined the steady state kinetic parameters of an APH(3')-IIIa monomer, and found them to be indistinguishable from those obtained with an APH(3')-IIIa dimer, helped to confirm the independence of the active sites (McKay *et al*, 1994a). The amino terminal end of the APH(3')-IIIa monomer is primarily composed of a 5 stranded β-sheet, which is connected to the C-terminal portion of the enzyme by a 12 residue linker (Hon *et al*, 1997). The carboxyl terminal end of the APH(3')-IIIa monomer is primarily composed of α-helices. The site of nucleotide binding, and by inference the active site of an APH(3')-IIIa monomer, lies between the N- and C-terminal regions. Representative figures of the active site, and the structure of the APH(3')-IIIa monomer, can be found in Chapter 4 (Figures 4.3 and 4.4, respectively). Overall the structure of the APH(3')-IIIa monomer resembles the structures determined for a number of eukaryotic protein kinases (ePKs), and for example, in several regions the position of main chain atoms of APH(3')-IIIa can easily be superimposed onto the positions of the main chain atoms of cyclic AMP dependent protein kinase A (PKA) (Hon *et al*, 1997). The determination of the crystal structure of APH(3')-IIIa bound to ADP (Hon *et al*, 1997) confirmed the prediction that the tertiary structure of the APHs would resemble the tertiary structure of the ePKs (Thompson *et al* (1996b). Research, described in this thesis, has gone on to confirm that the catalytic mechanism of APH(3')-IIIa is also similar to the catalytic mechanism of ePKs (Thompson *et al*, 1996b; Daigle *et al*, 1999b; Chapter 3; Chapter 4).

1.4.5. Effect of Covalent Modifications on Aminoglycoside Binding to 16 S rRNA

The covalent modification of a number of structurally distinct amino and hydroxyl groups, present on AGs, mediates resistance to this class of antibiotics. The effects of these modifications are discussed below, however, it is first appropriate to briefly discuss the region of the A^- site implicated in AG binding. Moazed and Noller (1987) first described the location of the region in 16S rRNA that is required for binding the 4,5- and 4,6-disubstituted AGs. This region is located in the 3' end of the 16 S rRNA sequence, specifically those nucleotides between 1400 and 1500 (*E. coli* numbering). A minimal AG binding domain has been defined by chemical footprinting methods. This domain encompasses nucleotides 1404-1412, 1450-1453,1497 and nucleotides 1488-1497 (*E. coli* numbering), and a 27 mer oligonucleotide (A^{-27}) incorporating these elements can bind AG antibiotics (Miyaguchi *et al*, 1996). The three dimensional structure of this same oligonucleotide bound to paromomycin, a 4,5-disubstituted AG, has been determined using multidimensional NMR techniques (Fourmy *et al*, 1996; PDB code 1PBR).

A hydroxyl group is present at the 6' position of paromomycin, whereas in many other AGs, for example neomycin, an amino group is present at this position (see Figure 1.2C), and modification of N6'is a major cause of AG resistance (Miller *et al*, 1997). Thus, there are difficulties in using the paromomycin-A^{-27} site rRNA structure to explain why the modification of this site is a cause of resistance. However, these drugs are thought to bind similarly to A^- site rRNA, as they have similar chemical footprinting patterns, and the N6' of gentamicin is bound in a similar fashion to A^{-27} site rRNA

(Moazed and Noller, 1987; Myaguchi *et al*, 1996; Yoshizawa *et al*, 1998). Therefore, interactions observed between the O6' of paromomycin and A site rRNA, should be generally applicable.

The solution structure of paromomycin bound to A^{-27} site RNA reveals that the O6' of paromomycin is not involved in any significant interactions with the rRNA, although it should be noted that this residue is close to the ring structure of both adenine 1492 and 1493 (3.7-5.0 Å). Thus, binding of a 6' N-acetylated AG would likely be hindered for steric reasons. The amino group at the 2' position, another site of acetylation, does not appear to be involved in any specific interactions with the A^{-27} site RNA. Thus, it is not entirely clear why the acetylation of this position would result in AG resistance. However, this group does appear to form a hydrogen bond with O4", present on the pentose ring of paromomycin, and the disruption of this hydrogen bond could conceivably alter the conformation of the drug in such a way that its affinity for A^- site RNA is decreased (Fourmy *et al*, 1996). Acetylation of N3, present on the aminocyclitol ring, would disrupt a hydrogen bond between the N7 of guanine 1494 and this amino group (3.4 Å), thereby decreasing the affinity of the modified AG for A site RNA (Fourmy *et al*, 1996). Steric hindrance would also prevent the binding of AGs adenylated at O4' and O2", as both of these hydroxyl groups are in close proximity to the phosphate backbone. The hydroxyl at O4' is close to the 5' phosphate of adenine 1493 (3.8 Å), whereas the hydroxyl at O2" is close to the 5' phosphate of guanine 1405 (4.6 Å).

Most of the clinically relevant sites of modification by the APHs (Figure 1.8) appear to interact with the phosphate backbone of the rRNA. The 3' hydroxyl, O3', is close to the 5' phosphates of guanine 1491 (3.2 Å) and adenine 1492 (3.2 Å), whereas O2" appears to interact with the 5' phosphate of guanine 1405 (4.6 Å). The 5" hydroxyl, O5", appears to interact with the 5' phosphates of both uracil 1490 (4.3 Å) and guanine 1491 (3.2 Å). Thus, the close proximity of these AG functional groups to the phosphate backbone, suggests that electrostatic repulsions would prevent binding of AGs phosphorylated at these positions.

1.5. Reversing aminoglycoside resistance.

The covalent modification of the current arsenal of AGs, such that they are less susceptible to the AG resistance mechanisms described above, as well as the design of inhibitors to those resistance mechanisms, are the two possible methods to 'rehabilitate' the usefulness of the AG antibiotics. The first method has been extensively employed (reviewed in Mingeot-Leclercq *et al*, 1999), and has for example led to the development of the clinically important drug amikacin (Kawaguchi *et al*, 1972). Amikacin is a semi-synthetic derivative of kanamycin A, which possesses an aminohydroxybutyrate substituent at the N1 position of the aminocyclitol ring (Figure 1.11). In an effort to avoid the resistance to amikacin, which is afforded by O3' phosphorylation or O4' adenylation, Kondo *et al* (1973) synthesized arbekacin. Arbekacin is equivalent to 3',4'-deoxy-amikacin (Figure 1.11). However, in the early 1990s the bifunctional enzyme (AAC(6')-APH(2")) was determined to be the cause of arbekacin resistance in MRSA

clinical isolates (Kondo *et al*, 1993a). Therefore, in an effort to avoid the resistance afforded by this enzyme, Kondo *et al* (1993b) developed derivatives of arbekacin.

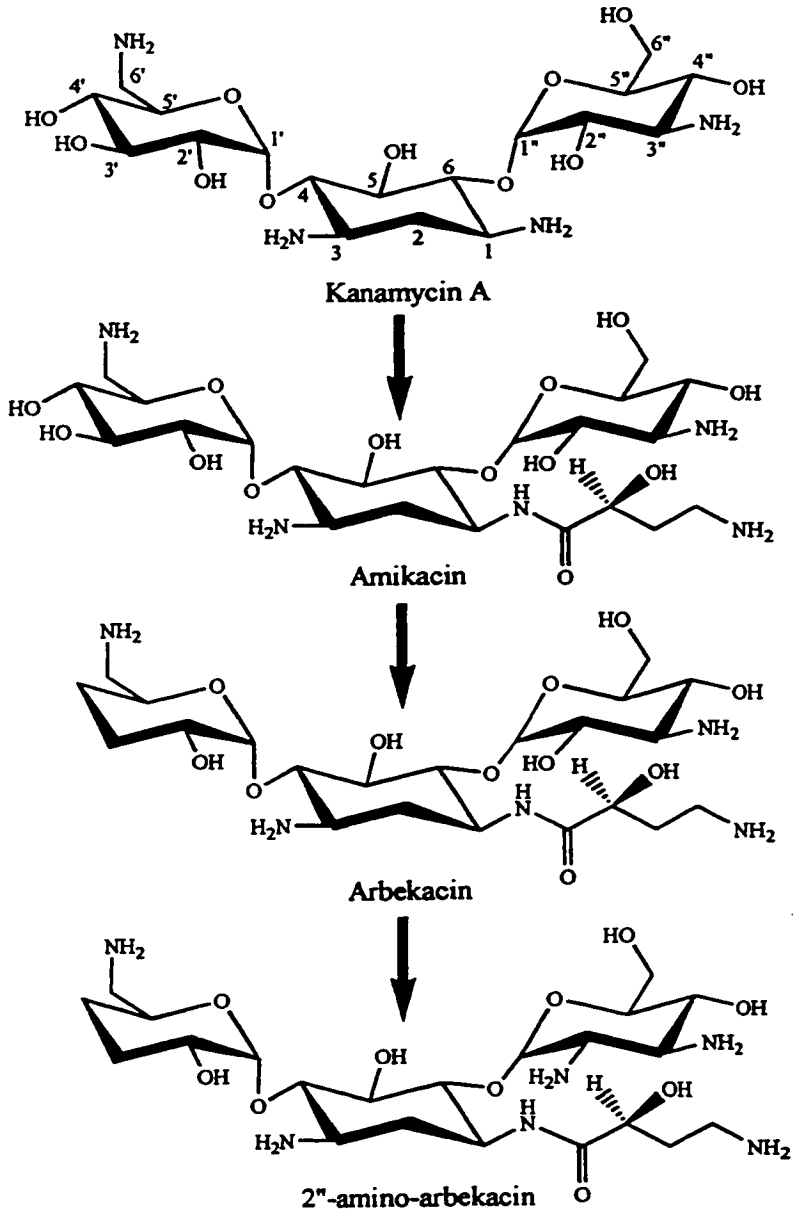

Figure 1.11. Redesigning AG antibiotics to avoid resistance. The generation of amikacin, arbekacin, and 2"-amino-arbekacin from kanamycin A.

In these arbekacin derivatives the 2"-hydroxyl group was replaced with an amino functionality. This modification substantially reduces, but does not diminish, the ability of the bifunctional enzyme to mediate resistance in clinical MRSA isolates, presumably because these drugs still possess a 6' amino group. The development of other AG derivatives has not met with such great success for reasons of either toxicity or because of a lack of antimicrobial activity (Mingeot-Leclercq *et al*, 1999). After more than 30 years of research into the development of AG derivatives, this method of antibiotic development may have run its course. Although it should be noted that Tok and Rando (1998) have identified two aminol compounds (Figure 1.12) that interact with A site rRNA in a manner that is competitive with paromomycin binding, which suggests that these molecules could form the structural backbone of synthetic AG-like compounds.

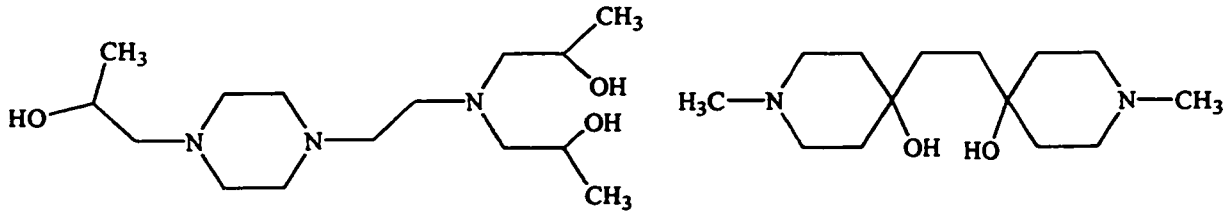

Figure 1.12. Aminols that bind A-site rRNA (Tok & Rando, 1998). Potential 'lead compounds' for the synthesis of novel AG-like antibiotics.

While structure based design methods have yet to successfully yield any *in vivo* inhibitors to the various AG-modifying enzymes, this methodology has led to the successful development of inhibitors to the β-lactamases. Thus, our enhanced understanding of the structures and catalytic mechanisms of a number of AG resistance enzymes will undoubtedly aid the discovery of inhibitors to enzymes of these types. A

thorough understanding of the catalytic mechanism of such enzymes is important to the design of inhibitors because it provides clues to the types of compounds that are likely to be successful lead compounds. For example, by determining that both the APH(3')-Ia and APH(3')-IIa enzymes catalyze the modification of the 3' hydroxyl (see above), Mobashery's group was able to design specific mechanism-based inactivators of these enzymes. These inactivators are derivatives of neamine and kanamycin B that incorporate a nitro group at the 2' position (Figure 1.13A) (Roestamadji *et al*, 1995).

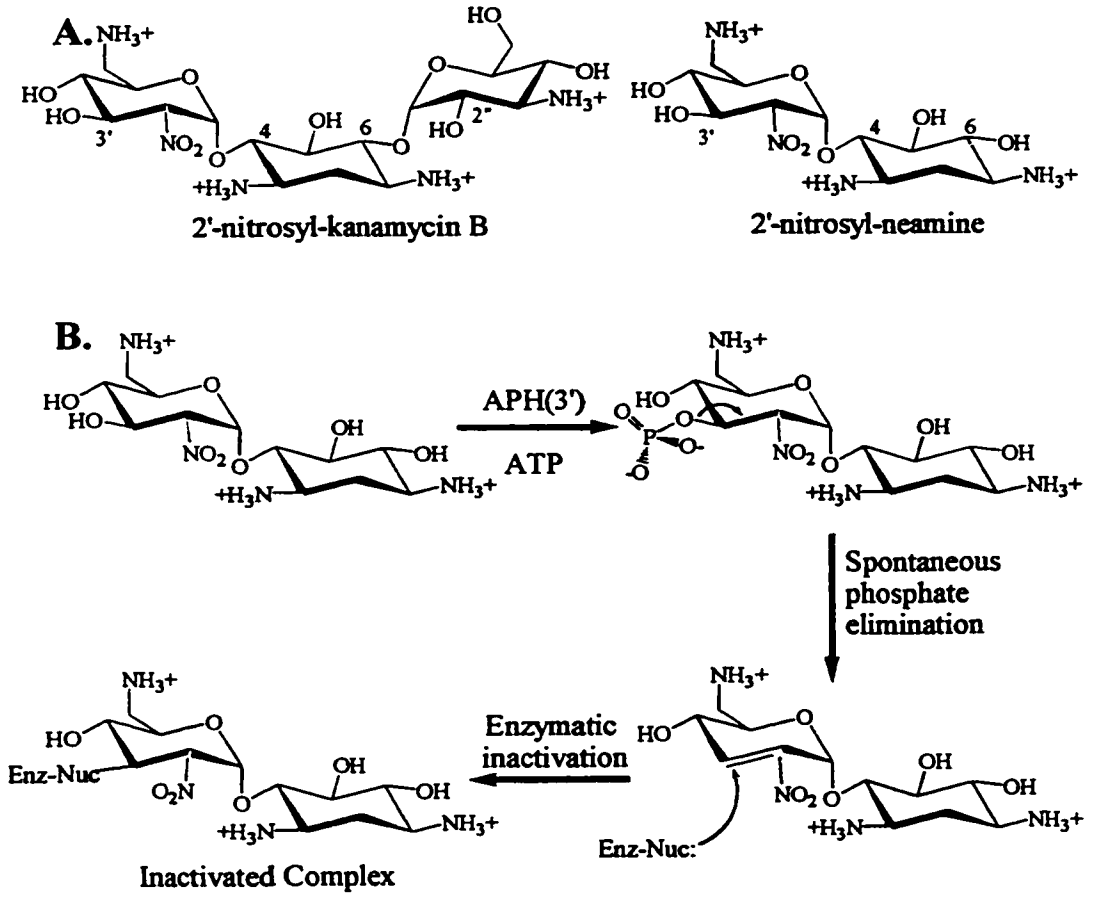

Figure 1.13. Mechanism-based inactivation of APH(3') enzymes. A. Structures of nitro derivatives of kanamycin B and neamine. **B.** Proposed mechanism of APH(3') inactivation by the nitrosylated neamine derivative.

Phosphorylation of either the neamine or kanamycin B derivative is thought to lead to the spontaneous elimination of the added phosphate, which results in the formation of an electrophilic intermediate (Figure 1.13B) that is susceptible to covalent modification. Enzyme inactivation occurs when the side chain of an amino acid, likely present in the active site of the enzyme, acts as a nucleophile to form a covalent enzyme-AG adduct. Despite the fact that the neamine and kanamycin B derivatives are particularly potent inactivators of the APH(3')-Ia and APH(3')-IIa enzymes, respectively[2] (Roestamadji *et al*, 1995), these compounds are said to lack any *in vivo* utility (Wright *et al*, 1999). While these specific inactivators may lack the ability to inhibit the AG resistance mediated by these enzymes, other compounds, using similar design principles, may be able to potentiate that resistance.

Another example of how an understanding of the catalytic mechanism of an APH(3') enzyme contributed to the identification of lead compounds was the finding that the catalytic mechanism of APH(3')-IIIa resembles that of eukaryotic protein kinases (Thompson *et al*, 1996; Chapters 3 and 4 of this thesis). This finding in combination with the determination of the three dimensional structure (Hon *et al*, 1997) led to the identification of a number of protein kinase inhibitors that could also be used to inhibit both APH(3')-IIIa and AAC(6')-APH(2") (Daigle *et al*, 1997). These compounds include the isoquinoline sulfonamides: H-9, H-1004, H-7, CKI-7, and CKI-8. These compounds are μM competitive inhibitors of ATP binding to both the APH(3')-IIIa and

---

[2] The partition ratios (k_{cat}/k_{inact}) of these inactivators for both of the 3'-APHs examined was low (< 2). The partition ratio is a measure of the number of catalytic events, which occur per molecule of enzyme inactivated. A low partition ratio indicates an effective mechanism based inactivator.

AAC(6')-APH(2") enzymes. While none of these compounds could reverse the AG resistance phenotype mediated by either of the *aph(3')-IIIa* or *aac(6')-aph(2")* genes, the core structure of these compounds, the isoquinoline sulfonamide ring, should be an excellent framework for the design and synthesis of newer and more specific inhibitors of both of these enzymes.

A thorough understanding of the catalytic mechanism can also aid drug design because it can provide an idea as to what the transition state (TS) of the enzyme resembles. From TS theory, we know that for an enzyme to afford rate accelerations on the order of 10^{10}-10^{15}-fold, the enzyme must bind to the TS with higher affinity than it binds the substrates or products of the reaction, 10^{-14}-10^{-15} M versus 10^{-3}-10^{-6} M (Schramm, 1998). Thus, if one can take advantage of even 1% of the energy imparted for binding the TS state, then one would have developed a very effective inhibitor, as only small quantities would be required to exert a biological effect. While a TS is transient by nature (ca. 10^{-13} sec), TS analogues are stable compounds that constantly mimic the TS, thereby explaining why only small quantities of these analogues are needed to inhibit a reaction. Thus, in theory the successful design of such inhibitors should lead to the continued usefulness of a variety of AG antibiotics.

1.6. Summary.

The increasing incidence of antibiotic resistant clinical isolates is a disturbing phenomenon. If left unchecked, infections that today are considered routine, could soon become life threatening. Thus, a search for new and better ways to kill these deadly microbes is urgently needed. Along those lines, our lab has been interested in

'rehabilitating' the usefulness of the AG class of antibiotics. Since the primary mechanism of AG resistance is their covalent modification, we have sought to identify inhibitors of the enzymes that modify these drugs. The approach we are taking is a rational one, which requires a thorough understanding of the catalytic mechanisms of these enzymes.

Therefore, I have extensively examined the catalytic mechanism of one of these resistance enzymes, APH(3')-IIIa, in the hope that these studies would help identify inhibitors to this enzyme. It was also hoped that our understanding of the catalytic mechanism of this enzyme would lead to the identification of inhibitors for AAC(6')-APH(2"). In this thesis, I describe my work to: i) identify the regiospecific sites of APH(3')-IIIa catalyzed AG phosphorylation (Chapter 2); ii) to determine the route of phosphoryl transfer (Chapter 3); iii) the catalytic mechanism of this enzyme (Chapter 4); iv) describe how a part of the C-terminal domain of this enzyme is critical for both AG recognition and catalysis (Chapter 5); v) describe my characterization of a novel APH, APH(9)-Ia, from *Legionella pneumophila* (Chapter 6). Finally, in Chapter 7, I attempt to briefly summarize my contributions to our understanding of the catalytic mechanism of the APHs. In this chapter, I will also attempt to discuss our prospects for the future design of APH inhibitors.

1.7. References.

Akopiants, K.E., & Danilenko, V.N. (1995). Instability of the genome and 'silent' genes in Actinomycetes. *Direct Submission* (GenBank accession number U24442).

Anand, N, & Davis, B.D. (1960). Effect of streptomycin on *Escherichia coli. Nature* **185**, 22-23.

Anderson, P., Davies, J., & Davis, B.D. (1967). Effect of spectinomycin on polypeptide synthesis in extracts of *Escherichia coli. J. Mol. Biol.* **29**, 203-215.

Azucena, E., Graspas, I., &Mobashery, S. (1997). Properties of a bifunctional bacterial antibiotic resistance enzyme that catalyzes ATP-dependent 2"-phosphorylation and acetyl-CoA-dependent 6'-acetylation of aminoglycosides. *J. Am. Chem. Soc.* **119**, 2317-2318.

Bakker, E.P. (1992). Aminoglycoside and aminocyclitol antibiotics: hygromycin B is an atypical bactericidal compound that exerts effects on cells of *Escherichia coli* characteristic for bacteriostatic aminocyclitols. *J. Gen. Microbiol.***138**, 563-569.

Beauclerk , A.A.D., & Cundliffe, E. (1987). Sites of action of two ribosomal RNA methylases responsible for resistance to aminoglycosides. *J. Mol. Biol.* **193**, 661-671.

Beck, E., Ludwig, G., Auerswald, E.A., Reiss, B., & Schaller, H. (1982). Nucleotide sequence and exact localization of the neomycin phosphotransferase gene from transposon Tn*5*. *Gene* **19**, 327-336.

Benveniste, R., & Davies, J. (1973a). Mechanisms of antibiotic resistance in bacteria. *Annu. Rev. Biochem.* **42**, 471-506.

Benveniste, R., & Davies, J. (1973b). Aminoglycoside antibiotic-inactivating enzymes in actinomycetes similar to those present in clinical isolates of antibiotic resistant bacteria. *Proc. Natl. Acad. Sci. USA* **70**, 2276-2280.

Bibb, M.J., Bibb, M.J., Ward, J.M., & Cohen, S.N. (1985). Nucleotide sequences encoding and promoting expression of three antibiotic resistance genes indigenous to Streptomyces. *Mol. Gen. Genet.* **199**, 26-36.

Blazquez, J., Davies, J., & Moreno, F. (1991). Mutations in the *aphA-2* gene of transposon Tn*5* mapping within the regions highly conserved in aminoglycoside-phosphotransferases strongly reduce aminoglycoside resistance. *Mol. Microbiol.* **5**, 1511-1518.

Brighty, K.E., Kohlbrenner, W., McGuirk, P.R. (1993). Recent developments in antbacterial resistance mechanisms. *Ann. Rep. Med. Chem.* **28**, 141-147.

Bryan, L.E., & Van Den Elzen, H.M. (1976). Streptomycin accumulation in susceptible and resistant stains of *Escherichia coli* and *Pseudomonas aeruginosa*. *Antimicrob. Agents Chemother.* **9**, 928-938.

Bryan, L.E., & Van Den Elzen, H.M. (1977). Effects of membrane-energy mutations and cations on streptomycin and gentamicin accumulation by bacteria: a model for entry of streptomycin and gentamicin in susceptible and resistant bacteria. *Antimicrob. Agents Chemother.* **12**, 163-177.

Bryan, L.E., & Kwan, S. (1983). Roles of ribosomal binding, membrane potential, and electron transport in bacterial uptake of streptomycin and gentamicin. *Antimicrob. Agents Chemother.* **23**, 835-845.

Cabanas, M.J., Vazquez, D., Modolell, J. (1978). Dual interference of hygromycin B with ribosomal translocation and with aminoacyl-tRNA recognition. *Eur. J. Biochem.* **87**, 21-27.

Chow, J.W., Zervos, M.J., Lerner, S.A., Thal, L.A., Donabedian, S.M., Jaworski, D.D., Tsai, S., Shaw, K.J., & Clewell, D.B. (1997). A novel gentamicin resistance gene in enterococcus. *Antimicrob. Agents Chemother.* **41**, 511-514.

Cohen, M.L. (1992). Epidemiology of drug resistance: implications for a post-antimicrobial era. *Science* **257**, 1050-1055.

Cole, S.T. *et al*, & Barrell, B.G. (1998). Deciphering the biology of *Mycobacterium tuberculosis* from the complete genome sequence. *Nature* **393**, 537-544.

Costa, Y., Galimand, M., Leclercq, R., Duval, J., & Courvalin, P. (1993). Characterization of the chromosomal *aac(6')-Ii* gene specific for *Enterococcus faecium*. *Antimicrob. Agents Chemother.* **37**, 1896-1903.

Culebras, E., & Martinez, J.L. (1999). Aminoglycoside resistance mediated by the bifunctional enzyme 6'-N-aminoglycoside acetyltransferase-2"-O-aminoglycoside phosphotransferase. *Front. Biosci.* **4**, d1-8.

Cundliffe, E. (1987). On the nature of antibiotic binding sites in ribosomes. *Biochimie* **69**, 863-869.

Cundliffe, E. (1989). How antibiotic producing organisms avoid suicide. *Annu. Rev. Microbiol.* **43**, 207-233.

Cundliffe, E. (1992). Resistance to macrolides and lincosamides in *Streptomyces lividans* and to amonoglycosides in *Micromonospora purpae*. *Gene* **115**, 75-84.

Daigle, D.M., McKay, G.A., Wright, G.D. (1997). Inhibition of aminoglycoside resistance enzymes by protein kinase inhibitors. *J. Biol. Chem.***272**, 24755-24758.

Daigle, D.M., Hughes, D.W., Wright, G.D. (1999a). Prodigious substrate specificity of AAC(6')-APH(2"), an aminoglycoside antibiotic resistance determinant in enterococci and staphylococci. *Chem. Biol.* **6**, 99-110.

Daigle, D.M., McKay, G.A., Thompson, P.R. & Wright, G.D. (1999b). Aminoglycoside antibiotic phosphotransferases are also serine protein kinases. *Chem. Biol.* **6**, 11-18.

Davies, J., Gilbert, W., & Gorini, L. (1964). Streptomycin, suppression, and the code. *Proc. Natl. Acad. Sci. USA* **51**, 883-890.

Davies, J. (1994). Inactivation of antibiotics and the dissemination of resistance genes. *Science* **264**, 375-382.

Davis, B.D. (1987). Mechanism of bactericidal action of aminoglycosides. *Microbiological Rev.* **51**, 341-350.

Delorme, C., Ehrlich, S.D., & Renault, P. (1992). Histidine biosynthesis genes in *Lactococcus lactis subsp. lactis*. *J. Bacteriol.* **174**, 6571-6579.

Dickie, P., Bryan, L.E., & Pickard, M.A. (1978). Effect of enzymatic adenylation on dihydrostreptomycin accumulation in *Escherichia coli* carrying an R-factor: Model explaining aminoglycoside resistance by inactivating mechanisms. *Antimicrob. Agents Chemother.* **14**, 569-580.

Distler, J., Braun, C., Ebert, A., & Piepersberg, W. (1987). Gene cluster for streptomycin biosynthesis in *Streptomyces griseus*: analysis of a central region including the major resistance gene. *Mol. Gen. Genet.* **208**, 204-210.

Dubin, D.T., & Davis, B.D. (1961). The effect of streptomycin on potassium flux in *Escherichia coli*. *Biochim. Biophys. Acta.* **52**, 400-402.

Dutnall, R.N., Tafrov, S.T., Sternglanz, R., Ramakrishnan, V. (1998). Structure of the histone acetyltransferase Hat1: a paradigm for the GCN5-related *N*-acetyltransferase superfamily. *Cell* **94**, 427-438.

Eisenberg, E.S., Mandel, L.J., Kaback, H.R., & Miller, M.H. (1984). Quantitative association between electrical potential across the cytoplasmic membrane and early gentamicin uptake and killing in *Staphylococcus aureus*. *J. Bacteriol.* **157**, 863-867.

Ferretti, J.J., Gilmore, K.S., & Courvalin, P. (1986). Nucleotide sequence analysis of the gene specifying the bifunctional 6'-aminoglycoside acetyltransferase 2"-aminoglycoside phosphotransferase enzyme in *Streptococcus faecalis* and identification and cloning of gene regions specifying the two activities. *J. Bacteriol.* **167**, 631-638.

Fleming, A. (1929). On the antibacterial action of cultures of a penicillium, with special reference to their use in the isolation of *B. influenzae. Brit. J. Exp. Path.* **10**, 226-236.

Fourmy, D., Recht, M.I. Blanchard, S.C., & Puglisi, J.D. (1996). Structure of the A site of *Escherichicia coli* 16S ribosomal RNA complexed with an aminoglycoside antibiotic. *Science* **274**, 1367-1371.

Gale, E.F., Cundliffe, E., Reynolds, P.E., Richmond, M.H., & Waring, M.J. (1981). In *The molecular basis of antibiotic action.* (Second Edition). John Wiley & Sons, London, pp. 418-439.

Gates, C.A., & Northrop, D.B. (1988). Alternative substrate and inhibition kinetics of aminoglycoside nucleotidyltransferase 2"-I in support of a Theorell-Chance kinetic mechanism. *Biochemistry* **27**, 3826-3833.

Gorini, L., & Kataja, E. (1964). Phenotypic repair by streptomycin of defective genotypes in *E. coli. Proc. Natl. Acad. Sci. USA* **51**, 487-493.

Gray, G.S., & Fitch, W.M. (1983). Evolution of antibiotic resistance genes: the DNA sequence of a kanamycin resistance gene from *Staphylococcus aureus. Mol Biol Evol* **1**, 57-66.

Gritz, L., & Davies, J. (1983). Plasmid-encoded hygromycin B resistance: the sequence of hygromycin B phosphotransferase gene and its expression in *Escherichia coli* and *Saccharomyces cerevisiae. Gene* **25**, 179-188.

Hachler, H., Santarnam, P., & Kayser, F.H. (1996). Sequence and characterization of a novel chromosomal aminoglycoside phosphotransferase gene, *aph(3')-IIb*, in *Pseudomonas aeruginosa. Antimicrob. Agents Chemother.* **40**, 1254-1256.

Heinzel,P., Werbitzky,O., Distler,J. & Piepersberg,W. (1988). A second streptomycin resistance gene from *Streptomyces griseus* codes for streptomycin-3'-phosphotransferase. Relationships between antibiotic and protein kinases. *Arch. Microbiol.* **150**, 184-192.

Herbert, C.J., Sarwar, M., Ner, S.S., Giles, I.G., & Akhtar, M. (1986). Sequence and interspecies transfer of an aminoglycoside phosphotransferase gene *(APH)* of *Bacillus circulans. Biochem. J.* **233**, 383-393.

Hiramatsu, K., Hanaki, H., Ino, T., Yabuta, K., Oguri, T., & Tenover, F.C. (1997). Methicillin-resistant *Staphylococcus aureus* clinical strain with reduced vancomycin susceptibility. *J. Antimicrob. Chemother.* **40**, 135-136.

Hon, W-C., McKay, G.A., Thompson, P.R., Sweet, R.M. Yang, D.S.C., Wright, G.D., & Berghuis, A.M. (1997). Structure of an enzyme required for aminoglycoside antibiotic resistance reveals homology to eukaryotic protein kinases. *Cell* **89**, 887-895.

Honore, N., & Cole, S.T. (1994). Streptomycin resistance in Mycobacteria. *Antimicrob. Agents Chemother.* **38,** 238-242.

Hooper, D.C. (1998). Bacterial topoisomerases, anti-topoisomerases, and anti-topoisomerase resistance. *Clin.Infect.Dis.* **27 (Suppl 1),** S54-S63.

Hoshiko, S., Nojiri, C., Matsunaga, K., Katsumata, K., Satoh, E., & Nagaoka, K. (1988). Nucleotide sequence of the ribostamycin phosphotransferase gene and of its control region in *Streptomyces ribosidificus*. *Gene* **68**, 285-296.

Howe, R.A., Brown, N.M., & Spencer, R.C. (1996). The new threats of Gram positive pathogens: re-emergence of things past. *J. Clin. Pathol.* **49**, 444-449.

Humbert, R., & Altendorf, K. (1989). Defective γ subunit of ATP synthase (F_1F_o) from *Escherichia coli* leads to resistance to aminoglycoside antibiotics. *J. Bact.* **171**, 1435-1444.

Kadurugamuwa, J.L., Clarke, A.J., & Beveridge, T.J. (1993). Surface action of gentamicin on *Pseudomonas aeruginosa*. *J. Bacter.* **175,** 5798-5805.

Kashiwagi, K., Tsuhako, M.H., Sakata, K., Saisho, T., Igarashi, A., Pinto Da Costa, S.O., & Igarashi, K. (1998). Relationship between spontaneous aminoglycoside resistance in *Escherichia coli* and a decrease in oligopeptide binding protien. *J. Bacteriol.* **180**, 5484-5488.

Kawaguchi, H., Naito, T., Nakagawa, S., & Fujisawa, K.I. (1972). BB-K 8, a new semisynthetic aminoglycoside antibiotic. *J. Antibiot.* **25**, 695-708.

Kim,S. & Choi,E. (1996). Nucleotide sequence, expression and transcriptional analysis of the *Escherichia coli mphK* gene, encoding a macrolide phosphotransferase K. *Mol. Cells* **6**, 153-160.

Kocabiyik, S., & Perlin, M.H. (1992a). Site-specific mutations of conserved C-terminal residues in aminoglycoside 3'-phosphotransferase II: phenotypic and structural analysis of mutant enzymes. *Biochem. Biophys. Res. Comm.* **185**, 925-931.

Kocabiyik, S., & Perlin, M.H. (1992b). Altered substrate specificity by substitutions at Tyr218 in bacterial aminoglycoside 3'-phosphotransferase-II. *FEMS Microbiol. Lett.* **93**, 199-202.

Kocabiyik, S., & Perlin, M.H. (1994). Amino acid substitutions within the analogous nucleotide binding loop (P loop) of aminoglycoside 3'-phosphotransferase. *Int. J. Biochem.* **26**, 61-66.

Kondo, S., Iinuma, K., Yamamoto, H., Maeda, K., Umezawa, H. (1973). Syntheses of 1-*N*-(S)-4-amino-2-hydroxybutyryl)-kanamycin B and -3', 4'-dideoxykanamycin B active against kanamycin-resistant bacteria. *J. Antibiot.* **26**, 412-415.

Kondo, S., Tamura, A., Gomi, S., Ikeda, Y., Takeuchi, T., & Mitsuhashi, S. (1993a). Structures of enzymatically modified products of arbekacin by methicillin-resistant *Staphylococcus aureus*. *J. Antibiot.* **46**, 310-315.

Kondo, S., Shibahara, S., Usui, T., Kudo, T., Tamura, A., Gomi, S., Ikeda, Y., Ikeda, D., & Takeuchi, T. (1993b). New 2"-amino derivatives of arbekacin, potent aminoglycoside antibiotics agains methicillin-resistant *Staphylococcus aureus*. *J. Antibiot.* **46**, 531-534.

Kormanec, J., Farkasovsky, M., Potuckova, L., & Godar, S. (1992). A gene (*hur*) from *Streptomyces aureofaciens*, conferring resistance to hydroxyurea, is related to genes encoding streptomycin phosphotransferase. *Gene* **114**, 133-137.

Lando, D., Cousin, M.A., & de Garilhe, M.P. (1973). Misreading, a fundamental aspect of the mechanism of action of several aminoglycosides. *Biochemistry* **12**, 4528-4533.

Leclercq, R., & Courvalin, P. (1991). Bacterial resistance to macrolide, lincosamide, and streptogramin antibiotics by target modification. *Antimicrob. Agents Chemother.* **35**, 1267-1272.

Leclercq, R., Dutka-Malen, S., Brisson-Noël, A., Molinas, C., Derlot, E., Arthur, M., Duval, J., & Courvalin, P. (1992). Resistance of enterococci to aminoglycosides and glycopeptides. *Clin. Infect. Dis.* **15**, 495-501.

Leclercq, R., & Courvalin, P. (1997). Resistance to glycopeptides in enterococci. *Clin. Infect. Dis.* **24**, 545-556.

Lee, K.Y., Hopkins, J.D., & Syvanen, M. (1991). Evolved neomycin phosphotransferase from an isolate of *Klebsiella pneumoniae*. *Mol. Microbiol.* **5**, 2039-2046.

Lyutzkanova, D., Distler, J., & Altenbuchner, J. (1997). A spectinomycin resistance determinant from the spectinomycin producer *Streptomyces flavopersicus*. *Microbiology* **143**, 2135-2143.

Marquardt, M. (1949). In *Paul Ehrlich.* William Heinemann Medical Books, Ltd., London, pp 84-92.

Martel, A., Masson, M., Moreau, N., & Le Goffic, F. (1983). Kinetic studies of aminoglycoside acetyltransferase and phosphotransferase from *Staphylococcus aureus* RPAL. Relationship between the two activities. *Eur. J. Biochem.* **133**, 515-521.

Martin, P., Jullien, E., & Courvalin, P. (1988). Nucleotide sequence of *Acinetobacter baumannii aphA-6* gene: evolutionary and functional implications of sequence homologies with nucleotide-binding proteins, kinases and other aminoglycoside-modifying enzymes. *Mol. Microbiol.* **2**, 615-625.

Mates, S.M., Eisenberg, E.S., Mandel, L.J., Patel, L. Kaback, H.R., & Miller, M.H. (1982). Membrane potential and gentamicin uptake in *Staphylococcus aureus*. *Proc. Natl. Acad. Sci. USA* **79**, 6693-6697.

Matsunaga, K., Yamaki, H., Nishimura, T., & Tanaka, N. (1986). Inhibition of DNA replication initiation by aminoglycoside antibiotics. *Antimicrob. Agents Chemother.* **30**, 468-474.

Mazodier, P., Cossart, P., Giraud, E., & Gasser, F. (1985). Completion of the nucleotide sequence of the central region of Tn5 confirms the presence of three resistance genes. *Nucl. Acids Res.* **13**, 195-205.

McKay, G.A., Thompson, P.R., & Wright, G.D. (1994a). Broad spectrum aminoglycoside phosphotransferase type III from *Enterococcus*: overexpression, purification, and substrate specificity. *Biochemistry* **33**, 6936-6944.

McKay, G.A., Robinson, R.A., Lane, W.S., & Wright, G.D. (1994b). Active-site labeling of an aminoglycoside antibiotic phosphotransferase (APH(3')-IIIa). *Biochemistry* **33**, 14115-14120.

McKay, G.A., & Wright, G.D. (1995). Kinetic mechanism of aminoglycoside phosphotransferase type IIIa. Evidence for a Theorell-Chance mechansim. *J. Biol. Chem.* **270**, 24686-24692.

McKay, G.A., Roestamadji, J., Mobashery, S., & Wright, G.D. (1996a). Recognition of aminoglycoside antibiotics by Enterococcal-Staphylococcal aminoglycoside 3'-phosphotransferase type IIIa: role of substrate amino groups. *Antimicrob. Agents Chemother.* **40**, 2648-2650.

McKay, G.A., & Wright, G.D. (1996b). Catalytic mechanism of Enterococcal kanamycin kinase (APH(3')-IIIa): viscosity, thio, and solvent isotope effects support a Theorell-Chance mechanism. *Biochemistry* **36**, 8680-8685.

Meier, A., Kirschner, P., Bange, F-C., Vogel, U., & Bottger, E.C. (1994). Genetic alterations in streptomycin-resistant *Mycobacterium tuberculosis*: mapping of mutations conferring resistance. *Antimicrob. Agents Chemother.* **38**, 228-233.

Miller, M.H., Edberg, S.C., Mandel, L.J., Behar, C.F., & Steigbigel, N.H. (1980). Gentamicin uptake in wild type and aminoglycoside resistant small colony mutants in *Staphylococcus aureus*. *Antimicrob. Agents Chemother.* **18**, 722-729.

Miller, G.H., Sabatelli, F.J., Hare, R.S., Glupczynski, Y., Mackey, P., Schlaes, D., Shimizu, K., Shaw, K.J., & the Aminoglycoside Study Groups (1997). The most frequent aminoglycoside resistance mechanisms-changes with time and geographic area: a reflection of aminoglycoside usage patterns? *Clin. Infect. Dis.* **24(Suppl 1)**, S46-S62.

Mingeot-Leclercq, M-P., Glupczynski, Y., & Tulkens., P.M. (1999). Aminoglycosides: activity and resistance. *Antimicrob. Agents Chemother.* **43**, 727-737.

Misumi, M., Nishimura, T., Komai, T., & Tanaka, N. (1978). Interaction of kanamycin and related antibiotics with the large subunit of ribosomes and the inhibition of translocation. *Biochem. Biophys. Res. Comm.* **84**, 358-365.

Moazed, D., & Noller, H.F. (1987). Interaction of antibiotics with functional sites in 16S ribosomal RNA. *Nature* **327**, 389-394.

Moellering Jr., R.C., Korzeniowski, O.M., Sande, M.A., & Wennersten, C.B. (1979). Species-specific resistance to antimicrobial synergism in *Streptococcus faecium* and *Streptococcus faecalis*. *J. Infect. Dis.* **140**, 203-208.

Moellering Jr., R.C. (1991). The enterococcus: a classic example of the impact of antimicrobial resistance on therapeutic options. *J. Antimicrob. Chemother.* **28**, 1-12.

Moore, R.A. & Hancock, R.E.W. (1986). Involvement of outer membrane of *Pseudomonas cepacia* in aminoglycoside and polymyxin resistance. *Antimicrob. Agents Chemother.* **30**, 923-926.

Moore, R.A., DeShazer, D., Reckseidler, S., Weissman, A., & Woods, D.E. (1999). Efflux-mediated aminoglycoside and macrolide resistance in *Burkholderia pseudomallei*. *Antimicrob. Agents Chemother.* **43**, 465-470.

Muir, M.E., Hanwell, D.R., & Wallace, B.J. (1981). Characterization of a respiratory mutant of *Escherichia coli* with reduced uptake of aminoglycoside antibiotics. *Biochim. Biophys. Acta* **638**, 234-241.

Muir, M.E., Ballesteros, M., & Wallace, B.J. (1985). Respiration rate, growth rate and the accumulation of streptomycin in *Escherichia coli. J. Gen. Microbiol.* **131**, 2573-2579.

Murray, B.E. (1990). The life and times of the enterococcus. *Clin. Microbiol. Rev.* **3**, 46-65.

Musser, J.M. (1995). Antimicrobial agent resistance in mycobacteria: Molecular genetic insights. *Clin. Microb. Revs.* **8**, 496-514.

Myaguchi, H., Narita, H., Sakamoto, K., & Yokoyama, S. (1996). An antibiotic-binding motif from the A-site-related region of *Escherichia coli* 16S rRNA. *Nucl. Acids Res.* **24**, 3700-3706.

Nakano, M.M., Mashiko, H., & Ogawara, H. (1984). Cloning of the kanamycin resistance gene from a kanamycin-producing *Streptomyces* species. *J. Bacteriol.* **157**, 79-83.

Neu, H.C. (1992). The crisis in antibiotic resistance. *Science* **257**, 1064-1073.

Nikaido, H. (1994). Prevention of drug access to bacterial targets: permeability barriers and active efflux. *Science* **264**, 382-388.

Noguchi, N., Emura, A., Matsuyama, H., O'Hara, K., Sasatsu, M., & Kono, M. (1995). Nucleotide sequence and characterization of erythromycin resistance determinant that encodes macrolide 2'-phosphotransferase I in *Escherichia coli. Antimicrob. Agents Chemother.* **39**, 2359-2363.

Noguchi, N., Katayama, J., & O'Hara, K. (1996). Cloning and nucleotide sequence of the *mphB* gene for macrolide 2'-phosphotransferase II in *Escherichia coli. FEMS Microbiol. Lett.* **144**, 197-202.

Oka, A., Sugisaki, H., & Takanami, M. (1981). Nucleotide sequence of the kanamycin resistance transposon Tn*903*. *J. Mol. Biol.* **147**, 217-226.

Okamoto, S., & Suzuki, Y. (1965). Chloramphenicol-, dihydrostreptomycin-, and kanamycin inactivating enzymes from multiple drug-resistant *Escherichia coli* carrying episome '*R*'. *Nature* **208**, 1301-1303.

Pansegrau, W., Miele, L., Lurz, R., & Lanka, E. (1987). Nucleotide sequence of the kanamycin resistance determinant of plasmid RP4: homology to other aminoglycoside

3'-phosphotransferases. *Plasmid* **18**, 193-204.

Pedersen, L.C., Benning, M.M., & Holden, H.M. (1995). Structural investigation of the antibiotic and ATP-binding sites in kanamycin nucleotidyltransferase. *Biochemistry* **34**, 13305-13311.

Penaloza-Vazquez, A., Mena, G.L., Herrera-Estrella, L., & Bailey, A.M. (1995). Cloning and sequencing of the genes involved in glyphosate utilization by *Pseudomonas pseudomallei. Appl. Environ. Microbiol.* **61**, 538-543.

Perlin, M.H., & Lerner, S.A. (1986). High-level resistance in *Escherichia coli* due to phosphorylation and impaired aminoglycoside uptake. *Antimicrob. Agents Chemother.* **29**, 216-224.

Pissowotzki, K., Mansouri, K., & Piepersberg, W. Genetics of streptomycin production in *Streptomyces griseus*:molecular structure and putative function of genes *strELMB2N.* (1991). *Mol. Gen. Genet.* **231**, 113-123.

Radika, K., & Northrop, D.B. (1984). The kinetic mechanism of kanamycin acetyltransferase derived from the use of alternative antibiotics and coenzymes. *J. Biol. Chem.* **259**, 12543-12546.

Rather, P.N., Orosz, E., Shaw, K.J., Hare, R., & Miller, G. (1993). Characterization and transcriptional regulation of the 2'-N-acetyltransferase gene from *Providencia stuartii. J. Bacteriol.* **175**, 6492-6498.

Recht, M.I., Douthwaite, S., Dahlquist, K.D., & Puglisi, J.D. (1999a). Effect of mutations in the A site of 16 S rRNA on aminoglycoside antibiotic-ribosome interaction. *J. Mol. Biol.* **286**, 33-43.

Recht, M.I., Douthwaite, S., & Puglisi, J.D. (1999b). Basis for prokaryotic specificity of action of aminoglycoside antibiotics. *EMBO J.* **18**, 3133-3138.

Roestamadji, J., Grapsas, I., & Mobashery, S. (1995). Loss of individual electrostatic interactions between aminoglycoside antibiotics and resistance enzymes as an effective means to overcoming bacterial drug resistance. *J. Am. Chem. Soc.* **117**, 11060-11069.

Roth, H., Amos, H., & Davis, B.D. (1960). Purine nucleotide excretion by *Escherichia coli* in the presence of streptomycin. *Biochim. Biophys. Acta* **37**, 398-405.

Rouch, D.A., Byrne, M.E., Kong, Y.C., & Skurry, R.A. (1987). The *aacA-aphD* gentamicin and kanamycin resistance determinant of Tn*4001* from *Staphylococcus aureus:* expression and nucleotide sequence analysis. *J. Gen. Microbiol.* **133**, 3039-3052.

Sakon, J., Liao, H.H., Kanikula, A.M., Benning, M.M., Rayment, I., & Holden, H.M. (1993). Molecular structure of kanamycin nucleotidyltransferase determined to 3.0-Å resolution. *Biochemistry* **32**, 11977-11984.

Salauze, D., & Davies, J. (1991). Isolation and characterisation of an aminoglycoside phosphotransferase from neomycin-producing *Micromonospora chalcea*; comparison with that of *Streptomyces fradiae* and other producers of 4,6-disubstituted 2-deoxystreptamine antibiotics. *J. Antibiot.* **44**, 1432-1443.

Sarwar, M., & Akhtar, M. (1990). Cloning of aminoglycoside phosphotransferase (*APH*) gene from antibiotic-producing strain of *Bacillus circulans* into a high-expression vector, pKK223-3®. *Biochem. J.* **268**, 671-677.

Schatz, A., Bugie, E., & Waksman, S.A. (1944). Streptomycin, a substance exhibiting antibiotic activity against Gram-positive and Gram-ngative bacteria. *Proc. Soc. Exp. Biol. Med.* **55**, 66-69.

Schlaes, D.M., Binczewski, B., & Rice, L.B. (1993). Emerging antimicrobial resistance and the immunocompromised host. *Clin. Infect. Dis.* **17(Suppl 2)**, S527-S536.

Schlessinger, D. (1988). Failure of aminoglycoside antibiotics to kill anaerobic, low-pH, and resistant cultures. *Clin. Microbiol. Revs.* **1**, 54-59.

Schramm, V.L. (1998). Enzymatic transition states and transition state analog design. *Ann. Rev. Biochem.* **67**, 693-720.

Service, R.E. (1995). Antibiotics that resist resistance. *Science* **270**, 724-727.

Schlaes, D.M., Binczewski, B., & Rice, L.B. (1993). Emerging antimicrobial resistance and the immunocompromised host. *Clin. Infect. Dis.* **7 (Suppl. 2)**, S527-S536.

Scholz, P., Haring, V., Wittmann-Liebold, B., Ashman, K., Bagdasarian, M., & Scherzinger, E. (1989). Complete nucleotide sequence and gene organization of the broad-host-range plasmid RSF1010. *Gene* **75**, 271-288.

Shaw, K.J., Rather, P.N., Hare, R.S., & Miller, G.H. (1993). Molecular genetics of aminoglycoside resistance genes and familial relationships of the aminoglycoside-modifying enzymes. *Microbiol. Rev.* **57**, 138-163.

Shaw, K.J. (1997). Personal communication.

Siregar, J.J., Lerner, S.A., & Mobashery, S. (1994). Purification and characterization of aminoglycoside 3'-phosphotransferase type IIa and kinetic comparison with a new mutant enzyme. *Antimicrob. Agents Chemother.* **38**, 641-647.

Siregar, J.J., Miroshnikov, K., & Mobashery, S. (1995). Purification, characterization, and investigation of the mechanism of aminoglycoside 3'-phosphotransferase type Ia. *Biochemistry* **34**, 12681-12688.

Spratt, B.G. (1994). Resistance to antibiotics mediated by target alterations. *Science* **264**, 388-393.

Suter, T.M., Viswanathan, V.K., & Cianciotto, N.P. (1997). Isolation of a gene encoding a novel spectinomycin phosphotransferase from *Legionella pneumophila. Antimicrob. Agents Chemother.* **41**, 2135-2143.

Sutherland, R. (1991). Beta-lactamase inhibitors and reversal of antibiotic resistance. *Trends Pharmacol. Sci.* **12**, 227-232.

Taber, H.W., Mueller, J.F., Miller, P.F., & Arrow, A.S. (1987). Bacterial uptake of aminoglycoside antibiotics. *Micorbiol. Rev.* **51**, 439-457.

Tai, P-C., Wallace, B.J., & Davis, B.D. (1978). Streptomycin causes misreading of natural messenger by interacting with ribosomes after initiation. *Proc. Natl. Acad. Sci. USA* **75**, 275-279.

Tanaka, N., Masukawa, H., & Umezawa, H. (1967). Structural basis of kanamycin for miscoding activity. *Biochem. Biophys. Res. Comm.* **26**, 544-549.

Tanaka, N., Matsunaga, K., Yamaki, H., & Nishimura, T. (1984). Inhibition of DNA synthesis by aminoglycoside antibiotics. *Biochem. Biophys. Res. Comm.* **122**, 460-465.

Tenover, F.C., Gilbert, T., & O'Hara, P. (1989). Nucleotide sequence of a novel kanamycin resistance gene, *aphA-7*, from *Campylobacter jejuni* and comparison to other kanamycin phosphotransferase genes. *Plasmid* **22**, 52-58.

Thiara, A.S., & Cundliffe, E. (1995). Analysis of two capreomycin-resistance determinants from *Streptomyces capreolus* and characterization of the action of their products. *Gene* **167**, 121-126.

Thompson, C.J., & Gray, G.S. (1983). Nucleotide sequence of a streptomycete aminoglycoside phosphotransferase gene and its relationship to phosphotransferases encoded by resistance plasmids. *Proc. Natl. Acad. Sci. USA* **80**, 5190-5194.

Thompson, J., Skeggs, P.A., & Cundliffe., E. (1985). Methylation of 16S ribosomal RNA and resistance to the aminoglycoside antibiotics gentamicin and kanamycin determined by DNA from the gentamicin-producer, *Micromonospora purpae. Mol. Gen. Genet.* **201**, 168-173.

Thompson, J.D., Higgins, D.G., & Gibson, T.J. (1994). CLUSTAL W: improving the sensitivity of progressive multiple sequence alignment through sequence weighting, position-specific gap penalties and weight matrix choice. *Nucl. Acids Res.* **22**, 4673-4680.

Thompson, P.R., Hughes, D.W., & Wright, G.D. (1996). Regiospecificity of aminoglycoside phosphotransferase from *Enterococci* and *Staphylococci* (APH(3')-IIIa). *Biochemistry* **35**, 8686-8695.

Thompson, P.R., Hughes, D.W., Cianciotto, N.P., & Wright, G.D. (1998). Spectinomycin kinase from *Legionella pneumophila*. Characterization of substrate specificity and identification of catalytically important residues. *J. Biol. Chem.* **273**, 14788-14795.

Thompson, P.R., Schwartzenhaur, J., Hughes, D.W., Berghuis, A.M., & Wright, G.D. (1999). The C-terminus of aminoglycoside phosphotransferase (3')-IIIa is critical for antibiotic recognition and resistance. *J. Biol. Chem.* **In press.**

Tok, J.B.-H., & Rando, R.R. (1998). Simple aminols as aminoglycoside surrogates. *J. Am. Chem. Soc.* **120**, 8279-8280.

Trieu-Cuot, P., & Courvalin, P. (1983). Nucleotide sequence of the *Streptococcus faecalis* plasmid gene encoding the 3'5"-aminoglycoside phosphotransferase type III. *Gene* **23**, 331-341.

Trieval, R.C., Rojas, J.R., Sterner, D.E., Venkataramani, R.N., Wang, L., Zhou, J., Allis, C.D., Berger, S.L., & Marmorstein, R. (1999). Crystal structure and mechanism of histone acetylation of the yeast GCN5 transcriptional coactivator. *Proc. Natl. Acad. Sci. USA* **96**, 8931-8936.

Umezawa, H., Okanishi, M., Kondo, S., Hamana, K., Utahara, R., Maeda, K., & Mitsihashi, S. (1967). Phosphorylative inactivation of aminoglycosidic antibiotics by *Escherichia coli* carrying R factor. *Science* **157**, 1559-1561.

Umezawa, H., & Kondo, S. (1982). Mechanism of resistance to aminoglycoside antibiotics. *In* Aminoglycoside Antibiotics. Umezawa, H., & Hooper, I.R., *eds.* Springer-Verlag, Berlin, pp. 267-292.

Van Pelt, J.E., Iyengar, R., Frey, P.A. (1986). Gentamicin nucleotidyltransferase – stereochemical inversion at phosphorous in enzymatic 2'deoxyladenylyl transfer to tobramycin. *J. Biol. Chem.* **261**, 15995-15999.

Vogtli, M., & Hutter, R. (1987). Characterisation of the hydroxystreptomycin phosphotransferase gene (sph) of *Streptomyces glaucescens*: nucleotide sequence and promoter analysis. *Mol. Gen. Genet.* **208**, 195-203.

Weinstein, R.E. (1998). Nosocomial infection update. *Emerg. Infect. Dis* **4**, 416-420.

Williams, J.W., & Northrop, D.B. (1978). Kinetic mechanism of gentamicin acetyltransferase I. *J. Biol. Chem.* **253**, 5902-5907.

Woodcock, J., Moazed, D., Cannon, M., Davies, J., & Noller, H.F. (1991). Interaction of antibiotics with A- and P-site-specific bases in 16S ribosomal RNA. *EMBO J.* **10**, 3099-3103.

Wolf, E., Vassilev, A., Makino, Y., Sali, A., Nakatani, Y., & Burley, S.K. (1998). Crystal structure of a GCN5-related *N*-acetyltransferase: *Serratia marcescens* aminoglycoside 3-*N*-acetyltransferase. *Cell* **94**, 439-449.

Wright, G.D., & Thompson, P.R. (1999). Aminoglycoside phosphotransferases: proteins, structure, and mechanism. *Frontiers in BioSci.* **4**, d9-21.

Wright, G.D., Berghuis, A.M., & Mobashery, S. (1999). Aminoglycoside antibiotics: structures, function and resistance. In *Resolving the antibiotic paradox: progress in drug design and resistance.* (Rosen, B.P., & Mobashery, S., eds), pp. 27-69, Plenum Publishing Corporation, New York, NY.

Wybenga-Groot, L.E., Draker, K.A., Wright, G.D., & Berghuis, A.M. (1999). Crystal structure of an aminoglycoside 6'-*N*-acetyltransferase: defining the GCN5-related *N*-acetyltransferase superfamily fold. *Structure* **7**, 497-507.

Yenofsky, R.L., Fine, M., & Pellow, J.W. (1990). A mutant neomycin phosphotransferase II gene reduces the resistance of transformants to antibiotic selection pressure. *Proc. Natl. Acad. Sci. USA* **87**, 3435-3439.

Yoshizawa, S., Fourmy, D., & Puglisi, J.D. (1998). Structural origins of gentamicin antbiotic action. *EMBO J.* **17**, 6437-6448.

Zalacain, M., Gonzalez, A., Guerrero, M.C., Mattaliano, R.J., Malpartida, F., & Jimenez, A. (1986). Nucleotide sequence of the hygromycin B phosphotransferase gene from *Streptomyces hygroscopicus*. *Nucl. Acids Res.* **14**, 1565-1581.

Chapter 2

Regiospecificity of APH(3')-IIIa

Adapted from

McKay, G.A., Thompson, P.R., & Wright, G.D.
Biochemistry, 1994, vol. 33. pp 6936-6944.
&
Thompson, P.R., Hughes, D.W., & Wright, G.D.
Biochemistry, 1996, vol 35, pp. 8686-8695.

The work described in this chapter entails my characterization of the regiospecificity of the APH(3')-IIIa enzyme. All NMR spectra, save for phospho-kanamycin, were recorded and analyzed by D.W. Hughes, in the Department of Chemistry, McMaster University. For phospho-kanamycin the NMR spectra were recorded by D.W. Hughes, but analyzed by G.D. Wright. All of the remaining data presented in this chapter was obtained by myself.

Chapter 2: Regiospecificity of APH(3')-IIIa

2.1. Introduction

Since we ultimately are interested in developing inhibitors to the AG-modifying enzymes, we have explored the molecular mechanisms of a number of these enzymes, hoping that these studies will aid the development of specific inhibitors to these enzymes. One such enzyme that we are studying is APH(3')-IIIa. We chose this enzyme as a model for our study of the APH class of AG-modifying enzymes because APH(3')-IIIa confers resistance to the broadest range of AG antibiotics (Shaw *et al*, 1993), which suggested that this enzyme represented a highly evolved APH. Thus, we began a characterization of the molecular mechanism of APH(3')-IIIa.

When one begins a study into the molecular mechanism of an enzyme, it is key that one first identifies the reaction catalyzed, as well as the products of the reaction. Since APH(3')-IIIa catalyzes the transfer of the γ-phosphate of ATP to an AG hydroxyl, the products of the reaction are ADP and phospho-AGs. However, for a complete understanding of the molecular mechanism of an enzyme, it is not sufficient to simply know what the products are; one must also know the specific site(s) on the substrate that are covalently modified. This site(s) of modification defines the regiospecificity of the enzyme. Since the regiospecificity of APH(3')-IIIa had not been definitively established, one of our first steps in the characterization of this enzyme was to identify the site of phosphorylation, using a number of 4,5- and 4,6-disubstituted AGs as model compounds.

Since this enzyme shares significant sequence identity with other APH(3') (Shaw *et al*, 1993), it was expected that it would also catalyze the phosphorylation of an AG at the 3'-hydroxyl. However, the regiospecificity of APH(3')-IIIa was not entirely clear, as APH(3')-IIIa also catalyzes the phosphorylation of lividomycin A, a 4,5-disubstituted AG, which does not possess a 3' hydroxyl (see Figure 1.2 in Chapter 1).

While the regiospecificity of phosphoryl transfer to lividomycin A, had not been established, clues to the site of phosphorylation came from earlier experiments that used an APH enzyme, purified from a lividomycin A resistant strain of *Pseudomonas aueruginosa*, (Kondo *et al*, 1972), to generate, and purify, sufficient quantities of lividomycin-phosphate for regiospecific analyses. By hydrolyzing the lividomycin-phosphate, obtained in this manner, and comparing the relative mobilities of the products to known standards, it was possible to identify ring C of lividomycin as the site of modification (Kondo *et al*, 1972). Further analysis of the lividomycin product, with a number of one-dimensional ^{1}H NMR techniques, including proton-decoupling experiments, enabled the determination that the 5"-hydroxyl was the site of phosphorylation (Kondo *et al*, 1972). Thus, it has been assumed that lividomycin A resistance, generally, is due the modification of this site. As a consequence of this assumption, APH(3')-IIIa was also presumed to mediate phosphorylation of the 5"-hydroxyl.

If APH(3')-IIIa does indeed catalyze the phosphorylation of the 5" hydroxyl on lividomycin A, then number of questions can be raised, including whether or not APH(3')-IIIa is a highly regiospecific enzyme i.e. are structurally related AGs

phosphorylated at the same hydroxyl? If this is the case, then the next question that one must ask, is whether or not the 4,5- and 4,6-disubstituted AGs are phosphorylated at distinct sites, as members of both these classes of AGs are substrates for APH(3')-IIIa. Experiments with an APH from a lividomycin A resistant strain of *E. coli* have indicated that this is possible, as this enzyme can phosphorylate the 3' hydroxyl of kanamycin and the 5" hydroxyl of lividomycin A (Umezawa *et al*, 1973; Umezawa *et al*, 1975). However, a number of 4,5-disubstituted AGs possess both a 3'- and a 5"-hydroxyl, and since rings A and B (Figure 1.2) are present in both the 4,5- and 4,6-disubstituted AGs, the question of what happens when APH(3')-IIIa is presented with such an AG, naturally follows.

Therefore, in an effort to answer these questions, a number of AGs, that are representative of both the 4,5- and 4,6-disubstituted AG antibiotics (Figure 1.2), were *in vitro* phosphorylated. Purification of the phosphorylated products enabled a determination of the stoichiometry and regiospecificity of phosphate transfer through the use of mass spectral and NMR techniques. These studies indicate that APH(3')-IIIa is a highly regiospecific enzyme that phosphorylates the 4,5-disubstituted and 4,6 disubstituted AGs at the 3' hydroxyl. While these results also confirmed our suspicion that lividomycin A was phosphorylated at the 5" hydroxyl, they further demonstrated that 4,5-disubstituted AGs, that possess both a 3'- and 5"-hydroxyl, can be bis-phosphorylated at both these positions. This work has previously been described in McKay *et al* (1994) and Thompson *et al* (1996).

2.2. Materials and Methods.

2.2.1. Chemicals.

Kanamycin A, neomycin B, lividomycin A, butirosin A, amikacin, and ribostamycin were obtained from Sigma (St. Louis, MO). ATP was from Boehringer-Mannheim (Laval, Quebec) and sodium hydroxide (50% w/v) was from Fisher (Unionville, Ontario). D_2O (99.9%) was obtained from Isotec (Miamisburg, OH). Enzymes used for DNA manipulations were obtained from New England Biolabs, unless otherwise noted.

2.2.2. Preparation of an aph(3')-IIIa protein expression construct.

An *aph(3')-IIIa* construct, incorporating a unique *Sac*I restriction site, at position 547, was originally generated to perform independent random mutagenesis experiments on either the 5' or the 3' ends of this gene. The *aph(3')-IIIa* overexpression construct, pETPCRG6, described in McKay *et al* (1994), was used as the template to introduce this restriction site, by the method of Kunkel (1985). Briefly, pETPCRG6 plasmid DNA was used to transform *E. coli* CJ236 (*dut ung*$^-$), and one of the colonies obtained from this procedure was used to inoculate a 1 mL overnight culture. The following day half of this culture was used to inoculate 50 mL of LB-ampicillin-chloramphenicol. Ampicillin was added to 100 μg/mL, whereas chloramphenicol was added to 30 μg/mL. The culture was grown to an $O.D._{600}$ of 0.1, at which point 50 μL of a helper phage (R408) solution, with a titre of 5×10^{11} plaque forming units/mL, was added. Cells were grown for an additional 4.5 hours at 37° C and the single stranded DNA recovered. Polynucleotide kinase (10 units), in the presence of 2 mM ATP, was

used to phosphorylate the oligonucleotide, 5'-CGTGGGAAAAGAC**GAGCTC**CTCTT-CGGGC-3', which incorporates the silent *Sac*I site (in bold). The phosphorylated oligonucleotide (10 pmoles) was dissolved in 10 μL of 20 mM Tris-HCl pH 7.5, 10 mM $MgCl_2$, 50 mM NaCl, 1 mM dithiothreitol (DTT), and subsequently annealed to the single stranded template DNA (0.25 pmoles) in a total volume of 10 μL. The annealing reaction was heated to 70° C for 10 minutes, and then allowed to slowly cool to room temperature over at least 30 minutes. At this point, T_4 DNA ligase (5 units), the Klenow fragment of DNA polymerase (2.5 units), and 2 μL of a 10 x extension buffer solution (100 mM Tris-HCl pH 7.5, 50 mM $MgCl_2$, 20 mM DTT, 5 mM dNTPs, 10 mM ATP) was added, and the volume adjusted to 20 μL with sterile ddH_2O. Extension reactions were incubated for 15 minutes at room temperature, and then incubated for a further 2 hours at 37° C. After which 30 μL of TE (10 mM Tris-HCl pH 8.0, 0.1 mM EDTA) was added and a portion used to transform $CaCl_2$ competent *E. coli* BL 21 (DE3).

Sequencing of one of the resultant positive clones, pETSAC, revealed the insertion of an extra AT base pair at position 730 of the *aph(3')-IIIa* gene. However, since no other mutations were detected, the *Nde*I to *Sac*I fragment from pETSAC was cloned into similarly cut pETSACSel1, a second positive clone, with no mutations in the *Sac*I to *Hin*dIII fragment of the *aph(3')-IIIa* gene. The resultant clone, pETSACG1, was sequenced in its entirety to ensure that no other mutations had been incorporated during the mutagenesis procedure. All sequencing reactions were carried out using the T7 DNA Polymerase Sequencing kit (Amersham Pharmacia Biotech, Montreal).

2.2.3. Purification of APH(3')-IIIa.

The purification of wild type APH(3')-IIIa has previously been described (McKay *et* al, 1994). A single colony of pETSACG1/*E. coli* BL 21(DE3) was used to inoculate 25 mL of LB (10 g Tryptone, 5 g yeast extract, 10 g NaCl per L ddH_2O)-ampicillin (100μg/mL). The next day 10 mL of this culture was used to inoculate 1 L of LB-ampicillin (100μg/mL). The cells were then grown at 37° C in an orbital shaker set for 250 r.p.m. to an $O.D._{600}$ of ~0.6, at which time 10 mL of 100 mM β-D-thiogalactopyranoside (IPTG) was added. The cells were then grown for an additional 3 hours and harvested by centrifugation at 5000 x g. The cells were resuspended in approximately 50 mL of 0.85% NaCl, after which, the cells were re-centrifuged at 5000 x g. The cell pellet was then frozen at –20° C, overnight. The next day the frozen pellet was thawed on ice and re-suspended in 10 mL of 50 mM Tris-HCl pH 8.0, 5 mM EDTA, 200 mM NaCl, 1 mM dithiothreitol (DTT), 1 mM phenylmethanesulfonyl fluoride (PMSF). The cells were then lysed by 2 passages through a French Pressure cell (20000 psi). The resultant lysate, ~12 mL, was cleared by centrifugation (20000 x g for 20 minutes). The cleared lysate was diluted to ~50 mL with Buffer A (50 mM Tris-HCl pH 8.0, 1 mM EDTA) and applied directly to a Q-Sepharose (Amersham Pharmacia Biotech, Montreal, Quebec, Canada) column (2.6 x 11.5 cm). Bound proteins were eluted from the column, pre-equilibrated in Buffer A, at a rate of 3 mL/min using a 30-50% linear gradient of Buffer B (Buffer A plus 1 M NaCl) over 2 column volumes. 6 mL fractions were collected. The presence of APH(3')-IIIa, in fractions corresponding to the major

peaks in the 280 nm trace, was determined by enzyme assay, and by denaturing electrophoresis using a 15% sodium dodecyl sulfate-polyacrylamide gel electrophoresis (SDS-PAGE). SDS-PAGE gels were stained with 0.1% Coomassie Brilliant Blue to assess the purity of individual fractions. The purest fractions were pooled, concentrated, dialyzed against Buffer A and then reapplied to the same Q-Sepharose column. This time, however, bound proteins were eluted at 3 mL/min using a 30-50% linear gradient of Buffer B over at least 4 column volumes. The presence and purity of APH(3')-IIIa was similarly assessed, and the purest fractions pooled.

2.2.4. Preparation and purification of phosphorylated aminoglycosides.

Purified APH(3')-IIIa was used to phosphorylate a number of AGs that represent both the 4,5-disubstituted and 4,6-disubstituted class of 2-deoxystreptamine AGs. The phosphorylation and purification of these AGs followed one of two protocols.

Method A. Phosphorylation of 100 mg of kanamycin A was carried out in 50 mM Tris-HCL pH 7.5, 40 mM KCl, and 10 mM $MgCl_2$. A 2-fold molar excess of ATP was also present. Since high concentrations of kanamycin A can inhibit its phosphorylation by APH(3')-IIIa, the final concentration of kanamycin A was approximately an order of magnitude below the substrate inhibition K_i of APH(3')-IIIa for this drug. The phosphorylation reaction was initiated by the addition of 1 mg of pure enzyme, and allowed to proceed for approximately 20 hours. A further 1 mg of pure enzyme was then added and the reaction allowed to proceed for a further 24 hours. Phosphorylation reactions were carried out at 37° C in an orbital shaker set for 250 r.p.m.

Phosphorylation reactions were allowed to proceed until the point at which kanamycin A was completely inactivated. This end-point was determined through the use of a *Bacillus subtilis* disk susceptibility assay. In such an assay, a LB-agar plate is overlaid with a small volume (200 μL) of an overnight culture of *B. subtilis*, in order to generate a lawn of bacteria. Filter paper disks (6.4 mm) are then overlaid onto the solid media, and the test samples (15 μL) applied. The plate is then incubated, upright, overnight at 37° C. The presence of active antibiotic is readily assessed by the size of the area surrounding the filter disk that does not support the growth of a lawn of *B. subtilis*. The lack of a zone of inhibition indicates that the drug has been inactivated. *B. subtilis* is susceptible to kanamycin A, with a minimal inhibitory concentration (MIC) of 1 μg/mL.

Once kanamycin A was completely inactivated, the entire phosphorylation reaction was applied to an AG50W-X8 (Bio-Rad) cation exchange column (10 x 3 cm), pre-equilibrated in ddH_2O. Prior to sample loading the cation exchange resin had been washed with 1% ammonium hydroxide to generate the NH_4^+ form. 4 mL fractions were collected. Separation of the components of the reaction was achieved by first washing the column with 200 mL of ddH_2O. This step eluted the negatively charged components of the reaction i.e. ATP and APH(3')-IIIa. Positively charged components, including the phosphorylated aminoglycoside, were then eluted with 0.1% NH_4OH. The presence of AG antibiotics in individual fractions was assessed by thin layer chromatography on silica-60 plates (Merck). Chromatographic separation of kanamycin and kanamycin-

phosphate was achieved by using either Solvent A (n-butyl alcohol/ethanol/chloroform/ammonium hydroxide (4:5:2:8)) or Solvent B (methanol/ammonium hydroxide (5:2)), as the mobile phase. The presence of 4 primary amines on kanamycin A permits the use of 0.1% ninhydrin, in ethanol, as a method to detect this drug and its phosphorylated derivative on TLC plates. The R_fs for the AGs and phospho-AGs described in this study can be found in Table 2.1. Fractions testing positive for the presence of kanamycin-phosphate were pooled and lyophilized. The lyophilized powder was resuspended in 2 mL of ddH_2O.

Table 2.1 R_fs of AGs and phospho-AGs described in this study.

	R_f	Solvent
Kanamycin	0.31	A
Kanamycin-phosphate	0.26	A
Amikacin	0.34	B
Amikacin-phosphate	0.07	B
Butirosin	0.16	A
Butirosin-phosphate	0.08	A
Ribostamycin	0.08	B
Ribostamycin-phosphate	0.03	B
Neomycin	0.13	B
Neomycin-phosphate	0.06	B
Lividomycin	0.23	A
Lividomycin-phosphate	0.20	A

Further purification was obtained by the application of kanamycin-phosphate to a BioRex 70 (Bio-Rad) column (11 x 3 cm). The column had been washed with 1% (v/v) ammonium hydroxide to generate the NH_4^+ form and then pre-equilibrated with 200 mL of ddH_2O. The entire sample, obtained from the first purification step, was applied to the column and the column was then washed with 200 mL of ddH_2O. A linear gradient of 0-

1 M NH_4OH was used to separate kanamycin-phosphate from any contaminating species, and the presence of the product, in the fractions collected, was analyzed by TLC as described above. Fractions testing positive for the presence of kanamycin-phosphate were pooled and lyophilized. The dried powder was dissolved in 500 µL of ddH_2O, and desalted by application to a Sephadex G-25 (Pharmacia) column (82 x 2 cm). The mobile phase was ddH_2O and the flow rate was 1.5 mL/min. TLC was again used to detect the presence of kanamycin-phosphate and positive fractions were pooled and lyophilized.

Method B. The reactions to generate the phosphorylated derivatives of amikacin, butirosin A, lividomycin A, neomycin B and ribostamycin, were carried out under similar conditions. However, it should be noted that for these AGs, the phosphorylation reactions were carried out in 50 mM HEPES pH 7.5, and 10 mM $MgCl_2$, and not the buffer described above. HEPES was used instead of Tris-HCl because it was noted during an initial attempt to purify lividomycin-phosphate that Tris co-elutes with phospho-AGs from both the AG50W-X8 and Mono S resins. In this buffer system, phosphorylation reactions were initiated by the addition of 1 mg of APH(3')-IIIa and they were typically allowed to proceed for 45-48 hours at 37°C at 250 rpm. An additional 1 mg of enzyme was added after the first ~24 hours.

The phosphorylated derivatives were purified by the batchwise application of the reaction mixture to a 50 mL slurry of AG 50W-X8 resin (NH_4^+ form). This mixture was allowed to equilibrate for 1 hour with stirring. The resin was then applied to a sintered glass funnel and washed with 1 L of H_2O. Phosphorylated AGs were eluted with

500 mL of 1% ammonium hydroxide and 50 mL fractions collected. These fractions were analyzed by silica TLC and the presence of phospho-AGs determined using the ninhydrin reaction. Those fractions containing phospho-AGs were pooled and lyophilized. The lyophilized product was taken up in 1 mL of ddH_2O and applied to a Sephadex G-10 (Amersham Pharmacia Biotech, Montreal) column (81x 2 cm), and the phosphorylated AGs were desalted at a flow rate of 1.5 mL/min. Fractions were analyzed by TLC, and the peak fractions were pooled and applied directly to a Mono S column (HR 5/5) (Amersham Pharmacia Biotech), equilibrated with ddH_2O. Generally, phospho-AGs were eluted using linear gradients of 0-15% 300 mM ammonium hydroxide. This purification step was carried out at 4 °C. The elution profiles were monitored at 210 nm, and the presence of phospho-AGs in peak fractions was confirmed using the TLC system described above. Fractions containing phospho-AGs were pooled and lyophilized.

Further purification of butirosin A-bis-phosphate and neomycin B-bis-phosphate, for NMR analysis, was achieved by isocratic chromatography, on a CSC-Spherisorb-ODS2 C-18 reverse phase column (5 μM 25 x 0.46 cm), using 8% CH_3CN with 0.016 M heptafluorobutyric acid as the mobile phase (McLaughlin and Henion, 1992). Elution of AGs was carried out at 0.5 mL/min, and eluting compounds were detected at 220 nm. TLC was then used to test the absorbance peaks for the presence of phospho-AGs. Positive fractions were pooled and lyophilized.

Generally speaking, method B was superior to method A for two reasons. Firstly, by substituting the AG50-WX8 column, in Method A, with a batchwise purification step the time required to purify each phospho-AG was reduced by

approximately 1 day. Secondly, the yield of kanamycin A, using Method A, was 12.6 mg, whereas the yields using Method B were typically higher, and averaged ~20 mg.

2.2.5. HPLC analysis of neomycin bis-phosphorylation.

A smaller scale neomycin phosphorylation reaction was prepared (5 mL), under the following conditions: 50 mM HEPES pH 7.5, 40 mM KCl, 10 mM $MgCl_2$, 250 μM ATP, 150 μM neomycin B, and 0.5 nmoles APH(3')-IIIa. The experiment was performed in duplicate, at 37° C, and at specific time points (0, 1.5, 5.3, 15, 30.6, 45.2, 53, 74.7, and 120 minutes) 500 μL aliquots were taken and immediately frozen in liquid nitrogen. Prior to injection the samples were heated to 65° C for 10 minutes to inactivate the enzyme. A portion of each aliquot (100 μL) was then applied to a Dionex CarboPac PA1 carbohydrate analysis column (4 x 250 mm) equilibrated with 0.5 mM NaOH. Separation of the reaction components was achieved, after an initial 5 minute wash with 0.5 mM NaOH, by a series of linear gradients where the concentration of NaOH was increased. The first gradient raised the concentration of NaOH from 0.5 to 15 mM over 10 minutes and resulted in the elution of any unreacted neomycin B. The second gradient raised the concentration of NaOH from 70 to 100 mM over 4 minutes and resulted in the elution of the HEPES buffer. The final gradient raised the concentration of NaOH from 100 to 2000 mM over 15 minutes, and this gradient was used to separate the phosphorylated neomycin derivatives from ADP and ATP. Elution profiles were monitored with Dionex ED40 pulsed amperometric detector. The detector settings were essentially as previously described (Statler, 1990). The potential was set at 0.10 V for

1.50 ms, whereupon integration began, and continued for a further 1.5 ms. At this point the voltage was increased to 0.6 V for 120 ms after which the voltage was stepped down to -0.80 V for 300 ms before returning to 0.10 V. In order to minimize background signals a 500 mM NaOH solution was added post column. During data analysis, using the Dionex PeakNet software package, the baseline, a water-only injection, was subtracted from the elution profiles obtained.

2.2.6. Mass Spectrometry of Phosphorylated Aminoglycosides.

The mass to charge ratio of purified phosphorylated AGs were determined using electrospray ionization mass spectrometry (ESI-MS) in both positive and negative ion modes at the McMaster Regional Centre for Mass Spectrometry. The spectra were acquired using a Fison platform quadrupole spectrometer, with the AGs typically being dissolved in a solution of 50:50 acetonitrile:water with either trifluoroacetic acid or ammonium hydroxide as the organic modifier to enhance ion formation.

2.2.7. Enzyme Assay.

The enzymatic activity of APH(3')-IIIa was monitored by coupling the production of ADP phosphorylation to NADH oxidation through a pyruvate kinase and lactate dehydrogenase system, as is described in (McKay *et al*, 1994; see also Chapter 4).

2.2.8. Sample Preparation for NMR Analysis.

The purified phosphorylated AG derivatives were exchanged in 1 mL of D_2O (99%), lyophilized, and then dissolved in 99.9% D_2O such that the final concentration was approximately 7 mg/mL. Where a microprobe was employed, approximately 1 mg of the phosphorylated AG was exchanged in 1 mL of D_2O (99%), lyophilized, and then

dissolved in 150 μL of 99.9% D_2O. The pD values for the phospho-AGs were between 8 and 9.

2.3. Results

2.3.1. Stoichiometry of aminoglycoside phosphorylation.

The preparation and purification of the phosphorylated derivatives of kanamycin A, amikacin, butirosin, ribostamycin, neomycin B, and lividomycin A enabled a determination of the stoichiometry of AG phosphorylation by electrospray mass spectrometry. For the phosphorylated derivatives of kanamycin A and amikacin, both 4,6-disubstitued AGs, the observed mass to charge ratios are consistent with the production of a mono-phosphorylated species (Table 2.2). For the 4,5-disubstituted AGs examined, the situation was more complex. For lividomycin A, a 4,5-disubstituted AG that lacks a 3' hydroxyl, only a mono-phosphorylated derivative could be identified, whereas for both butirosin and ribostamycin bis-phosphorylated derivatives were readily identified. While mono-phosphorylated derivatives of both butirosin and ribostamycin could readily be purified, it was only possible to purify a mono-phosphorylated derivative of neomycin B by decreasing the incubation length of the *in vitro* phosphorylation reaction, otherwise this AG purifies exclusively as the bis-phosphorylated derivative. The fact that the mono and bis-phosphorylated derivatives of butirosin and ribostamycin are purified as a mixture suggests that the addition of the second phosphate, to these AGs, is kinetically slow.

Table 2.2. Stoichiometry of aminoglycoside phosphorylation by APH(3')-IIIa

Antibiotic	Expected (g/mole)	Observed m/z (Da/e)	Stoichiometry of phosphorylation
4,6-disubstituted aminoglycosides			
kanamycin A	566.2	565.3	mono
amikacin	666.3	666.3	mono
4,5-disubstituted aminoglycosides			
lividomycin A	842.8	842.4	mono
butirosin A	635.6	636.1	mono
	715.6	714.1	di
neomycin B	694.7	695.2	mono
	774.7	774.5	di
ribostamycin	534.5	535.3	mono
	614.5	615.2	di

2.3.2. Aminoglycoside phosphorylation in the steady state.

The finding that the 4,5-disubstituted AGs are bis-phosphorylated offered an explanation for a phenomenon that is observed during the kinetic analysis of specific 4,5-disubstituted AGs. Our kinetic assay is a continuous one, and monitors the production of ADP by coupling it to the oxidation of NADH. As a result, AG phosphorylation causes a decrease in the absorbance at 340 nm. For the 4,6-disubstituted AGs, and for lividomycin A and butirosin, both 4,5-disubstituted AGs, the progress of the reaction is a rapid one, and reaches a plateau at the point where all of the AG substrate in the assay solution is phosphorylated (Figure 2.1). For these AGs, the change in absorbance, between the initial absorbance (A_o) and the plateau, is consistent with the transfer of a single phosphoryl group to a single AG. However, the progress curves for neomycin and

ribostamycin phosphorylation are dramatically biphasic (Figure 2.1), and possess a distinct inflection point.

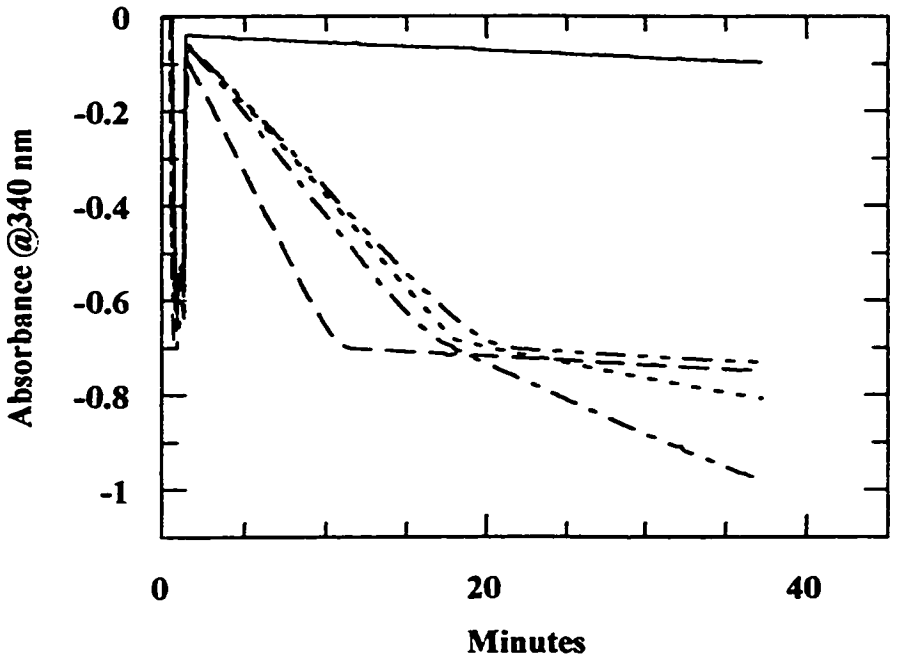

Figure 2.1. Progress curves for the phosphorylation of the 4,5-disubstituted AGs lividomycin A (liv) (- - - - - -), butirosin (but) (— · · —), ribostamycin (rib) (.....), and neomycin B (neo) (— · — ·). Progress curves were obtained by coupling the production of ADP to the oxidation of NADH (see Materials and Methods), and monitoring the consequent decrease in absorbance at 340 nm. In all cases, ATP was added to 1 mM, and the concentration of the AGs examined was 100 μM.

For these AGs, the change in absorbance during the first phase, A_o to the inflection point, is consistent with the transfer of a single phosphoryl group to a single AG. The second phase of neomycin B and ribostamycin phosphorylation is slower than the first, and eventually reaches a plateau at a point where the change in absorbance, between A_o and the plateau, is consistent with the addition of two phosphates per AG.

Thereby suggesting that the biphasic nature of these progress curves represents the consecutive addition of the first and second phosphates.

2.3.3. HPLC analysis of aminoglycoside bis-phosphorylation.

The fact that the inflection point and the plateau occur at positions that correspond to the addition, to a 4,5-disubstituted AG, of the first and second phosphate, suggested that the second phase be due to the addition of the second phosphate. The results from the stoichiometry studies further suggested that this was indeed likely. Therefore, in order to confirm that each phase represents the addition of a single phosphate, I devised an HPLC assay that monitors the production of phosphorylated neomycin B derivatives. From this analysis (Figure 2.2), it is readily apparent that the peak corresponding to neomycin B (retention time 10 minutes) is significantly diminished after 15 minutes, and completely absent after 53 minutes. This decrease in the size of the neomycin peak occurs concomitantly with the appearance of a peak corresponding to neomycin mono-phosphate (retention time 25 minutes). However, a peak corresponding to neomycin bis-phosphate is not apparent (retention time 28 minutes), until after the complete disappearance of the neomycin peak. These results thereby indicate that the addition of the first phosphate precedes the addition of the second phosphate.

Further confirmation of the existence of two phosphorylation phases comes from a plot of the area under each peak versus time (Figure 2.3). What is readily apparent from this analysis is the intermediary nature of neomycin mono-phosphate. Also apparent is the fact that neomycin B is completely converted to the mono-

phosphorylated derivative, prior to the addition of the second phosphate. Thus confirming that the biphasic nature of the progress curves is due to the addition of the first phosphate in the first phase, and the addition of the second phosphate in the second phase.

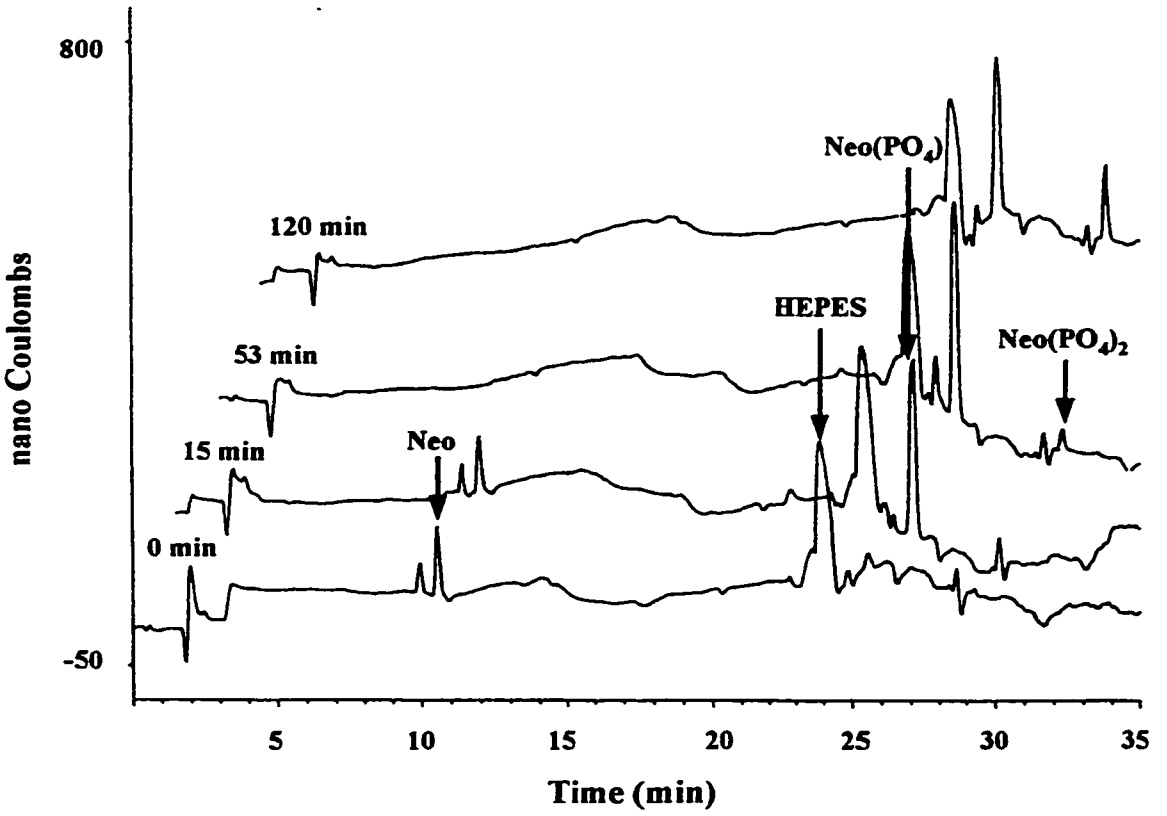

Figure 2.2. HPLC chromatograms monitoring the progress of the neomycin B bis-phosphorylation reaction. Representative chromatograms from 0, 15, 53 and 120 minutes are shown, and the peaks corresponding to reaction components labeled in the first chromatogram in which they appear. The retention times of neomycin B (Neo), neomycin B mono-phosphate ($Neo(PO_4)$), and neomycin B bis-phosphate ($Neo(PO_4)_2$) are 10.5, 23.5, and 29.5 minutes, respectively. Note that each of the chromatograms shown is offset by 1.5 minutes. Also note that the presence of one of the buffering components of the reaction, HEPES, was detected, and has a retention time of 23.5 minutes.

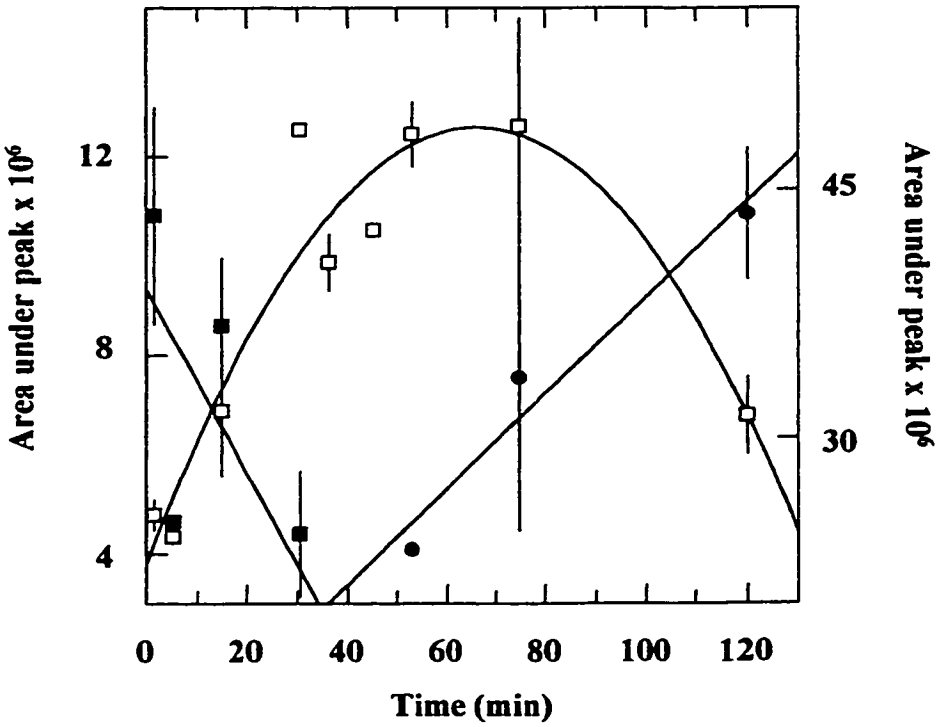

Figure 2.3. Analysis of HPLC chromatograms. The area under the peaks corresponding to neomycin (■) and neomycin mono-phosphate (□) are plotted versus time, using the Y-axis (left), whereas the area under the peak corresponding to neomycin bis-phosphate (●) is plotted versus time, using the Y2-axis (right). See Section 2.2.5 for experimental methods.

2.4. Discussion.

For a complete understanding of the catalytic mechanism of an enzyme one must know the products of the reaction. Based upon the homology of APH(3')-IIIa to other known APH(3') (Shaw *et al*, 1993), it was expected that this enzyme would catalyze the transfer of the γ-phosphate of ATP to the 3'-hydroxyl, which is present on most 4,5- and 4,6-disubstituted AGs. However, the fact that lividomycin, which lacks a 3'-hydroxyl, is also an excellent substrate for this enzyme (McKay *et al*, 1994), suggested

that the situation might be more complex. Past precedents with APH(3') enzymes from *P. aueruginosa* and *E. coli* had suggested that the 5" hydroxyl was the likely site of phosphorylation (Kondo *et al*, 1972; Umezawa *et al*, 1973; Umezawa *et al*, 1975), but the presence of 9 other equally reactive hydroxyls indicated that a rigorous analysis of the regiospecificity of APH(3')-IIIa was required. We were also interested in determining the regiospecificity of APH(3')-IIIa, because if we were to assume that the 5" hydroxyl was the site of lividomycin A phosphorylation, then we wondered what site, on other 4,5-disubstituted AGs, would be phosphorylated, as many of these AGs possess both a 3'- and a 5"-hydroxyl. Thus, in an effort to clarify the regiospecificity of APH(3')-IIIa, a number of 4,5- and 4,6-disubstituted AGs, which are representative of both these classes of AG antibiotics, were phosphorylated, using pure APH(3')-IIIa as the catalyst, and the phosphorylated derivatives purified.

Purification of the phosphorylated derivatives enabled the subsequent determination of the stoichiometry of phosphorylation, using the technique of electrospray ionization mass spectrometry. Kanamycin A and amikacin, both 4,6-disubstituted AGs, are mono-phosphorylated, as is the 4,5-disubstituted AG lividomycin A. However, bis-phosphorylated species were detected for all of the other 4,5-disubstituted AGs examined in this study. While bis-phosphorylated derivatives of butirosin and ribostamycin were detected, these AGs purified as a mixture of the mono- and bis-phosphorylated species, suggesting that the addition of the second phosphate is not favorable. This is in marked contrast to the results obtained for the phosphorylation of neomycin B, as the mono-phosphorylated derivative of neomycin B can only be

purified if the incubation time, for the *in vitro* phosphorylation reaction, is decreased substantially. Thus, the rate of the addition of the second phosphate is AG-dependent.

Since we were interested in determining the processivity of phosphorylation, I developed an HPLC assay to monitor the production of the mono- and bis-phosphorylated neomycin B derivatives. Since the AGs are UV transparent, the elution of neomycin, and the phospho-neomycin derivatives, was monitored through the use of a pulsed amperometric detector, which measures changes in the electrochemical potential of a solution. This HPLC analysis revealed that the addition of the second phosphate is preceded by the complete mono-phosphorylation of this AG. These results parallel the biphasic progress curves obtained for the phosphorylation of neomycin B, and thereby confirm that the first phase, that we observe in our progress curves, is associated with the addition of the first phosphate, while the second phase is associated with the addition of the second phosphate. This pattern of phosphorylation likely holds true for other 4,5-disubstituted AGs, which possess both a 3' and a 5" hydroxyl, for example ribostamycin, as these AGs are bis-phosphorylated, and exhibit the same characteristic biphasic progress curves. While APH(3')-IIIa is capable of catalyzing the bis-phosphorylation of a number of 4,5-disubstituted AGs, the addition of the second phosphate is AG-dependent, as the rate of the second phase varies greatly. For example, the addition of the second phosphate to neomycin B occurs at a much higher rate than that which is observed for the addition of the second phosphate to either ribostamycin or butirosin. In fact, the progress curves for butirosin phosphorylation do not even appear to be biphasic.

In addition to the studies described above, the preparation and purification of the phosphorylated derivatives of kanamycin A, amikacin, butirosin, neomycin B, and lividomycin enabled a determination of the sites of modification by NMR. For kanamycin A and amikacin, both 4,6-disubstituted AGs, the site of phosphorylation is the 3' hydroxyl. For butirosin and neomycin B, both 4,5-disubstituted AGs that are bis-phosphorylated, the sites of phosphorylation are the 3'- and the 5"-hydroxyls. However, for lividomycin A, a mono-phosphorylated 4,5-disubstituted AG, the site of phosphorylation is exclusively the 5"-hydroxyl. These results suggest a paradigm for the reactions catalyzed by APH(3')-IIIa; 4,6-disubstituted AGs are phosphorylated exclusively at the 3'-hydroxyl, and 4,5-disubstituted AGs are phosphorylated at both the 3'-and 5"-hydroxyl, as long as both these groups are present (Figure 2.4).

The preparation and purification of the mono-phosphorylated derivatives of butirosin and neomycin B permitted a more definitive evaluation of the processivity of phosphorylation. For neomycin B, the addition of the first phosphate occurs predominantly (77% of the time) at the 5"-position, whereas for butirosin there is a strong preference (70%) for first phosphate addition to occur at the 3'-hydroxyl. Although butirosin and neomycin share the same core three ring structure, butirosin is substituted at the N1 position with an aminohydroxybutyrate group, whereas neomycin is substituted at the O4" position with an amino sugar moiety. Thus, this difference in the processivity of phosphorylation likely reflects the structural differences that exist between these AGs.

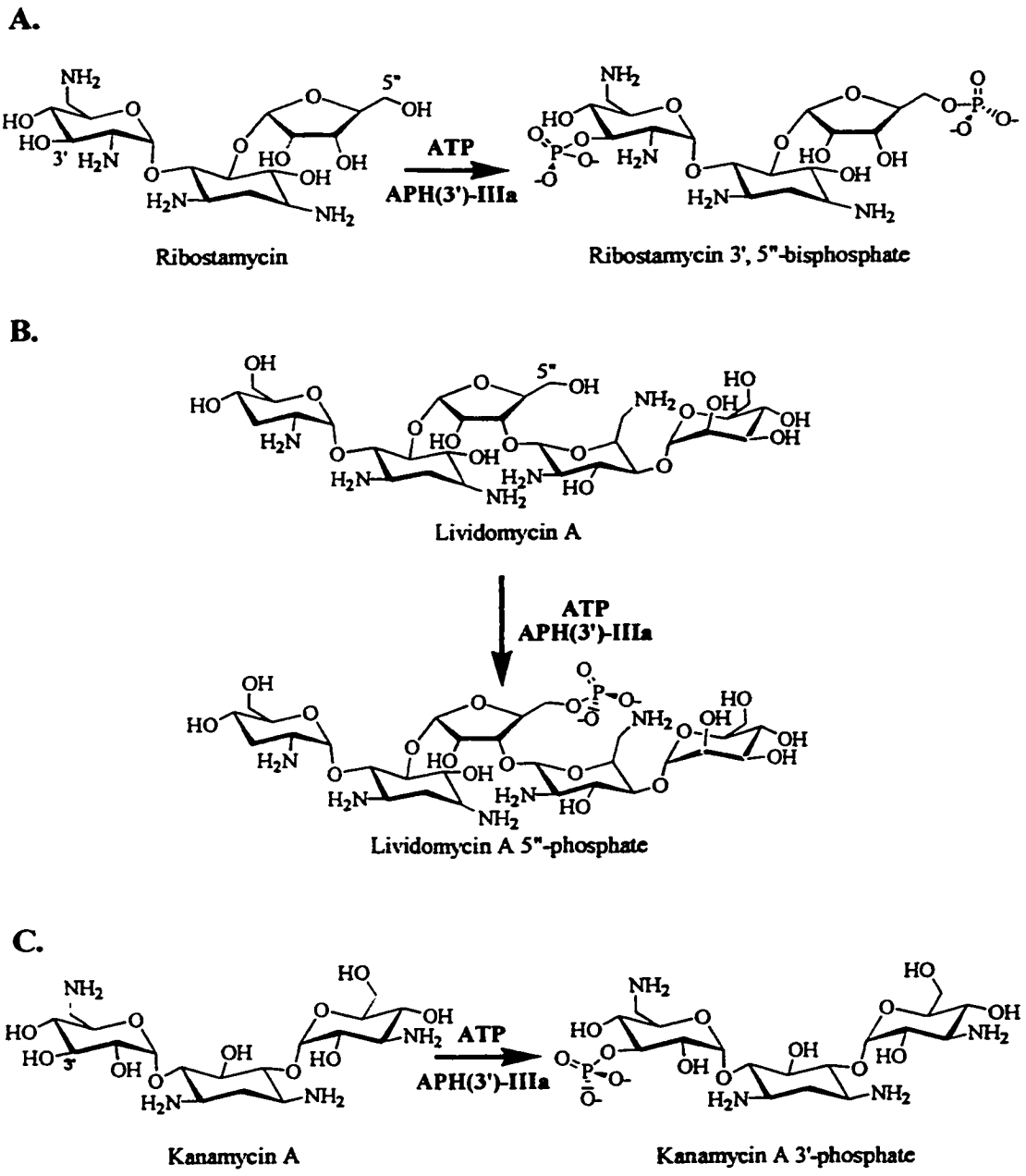

Figure 2.4. Regiospecificity of APH(3')-IIIa, a paradigm. A. Phosphorylation of 4,5-disubstituted AGs at both the 3' and 5" hydroxyls. **B.** Phosphorylation of 4,6-disubstituted AGs at the 3' hydroxyl.

2.5. Conclusions.

The finding that the 4,5-disubstituted AGs are multiply phosphorylated in a regiospecific manner, suggests that the APH(3')IIIa enzyme possesses at least two AG binding modes. Whether these binding modes are only subtly or grossly different is not known. However, Umezawa *et al* (1973) has pointed out that it is possible to generate a molecular model of ribostamycin where the 3'- and 5"-hydroxyls are close in space, suggesting that only a subtle change is required. Further support for only a subtle change, in the binding mode, comes from the determination of the solution structure of butirosin bound to APH(3')-IIIa (Cox *et al*, 1996). Cox *et al*, (1996), using paramagnetic resonances between Cr^{3+}ATP and butirosin, when bound to the enzyme, found that the 3'- and 5"-hydroxyls are close in space. Thus, it would appear likely that only a subtle change in the binding mode would be required to position either the 3'- or the 5"-hydroxyl close to the γ-phosphate of ATP. However, three caveats must be noted. Firstly, the structure of butirosin bound to APH(3')-IIIa is a time averaged picture of this AG bound to the enzyme, and since productive phosphate transfer to the 3'-hydroxyl only occurs 70% of the time, the close positioning of the 5"-hydroxyl, observed in this structure, to the γ-phosphate of ATP, may be the result of the 30% of the time that this residue is positioned for phosphate transfer. Thus it is not entirely clear that an AG would bind with both hydroxyls poised for phosphate transfer. Secondly, it is not known how the addition of the first phosphate would affect the solution structures of the AGs that are bis-phosphorylated. Finally, it is not known how APH(3')-IIIa would bind a

mono-phosphorylated AG, as charge repulsions, between the γ-phosphate of ATP and the mono-phosphorylated AG would be expected to inhibit drug binding. Thus these caveats would argue against a mono-phosphorylated AG binding to APH(3')-IIIa in a subtly different manner, and would suggest that multiple modes of AG binding are possible. The ability to bind structurally related AGs in different conformations would likely explain the broad substrate specificity of this enzyme.

2.6. References.

Cox, J.R., McKay, G.A., Wright, G.D., & Serpersu, E.H. (1996). Arrangement of substrates at the active site of an aminoglycoside 3'-phosphotransferase (APH(3')-IIIa) as determined by NMR. *J. Am. Chem. Soc.* **118**, 1295-1301.

Gray, G.S., & Fitch, W.M. (1983). Evolution of antibiotic resistance genes: the DNA sequence of a kanamycin resistance gene from *Staphylococcus aureus*. *Mol Biol Evol* **1**, 57-66.

Kondo, *S.*, Yamamoto, H., Naganawa, H., Umezawa H., & Mitsuhashi, H. (1972). Isolation and characterization of lividomycin A inactivated by *Pseudomonas aueruginosa* and *Escherichia coli* carrying R factor. *J. Antibiot.* **25**, 483-484.

Kunkel, T.A. (1985). Rapid and efficient site specific mutagenesis without phenotypic selection. *Proc. Natl. Acad. Sci. USA* **82**, 488-492.

McKay, G.A., Thompson, P.R., & Wright, G.D. (1994). Broad spectrum aminoglycoside phosphotransferase type III from *Enterococcus*: overexpression, purification, and substrate specificity. *Biochemistry* **33**, 6936-6944.

McLaughlin, L.G., & Henion, J.D. (1992). Determination of aminoglycoside antibiotics by reversed-phase ion-pair high-performance liquid chromatography coupled with pulsed amperometry and ion spray mass spectrometry. *J. Chromatogr.* **591**, 195-206.

Shaw, K.J., Rather, P.N., Hare, R.S., & Miller, G.H. (1993). Molecular genetics of aminoglycoside resistance genes and familial relationships of the aminoglycoside-modifying enzymes. *Microbiol. Rev.* **57**, 138-163.

Statler, J.A. (1990). Determination of tobramycin using high-performance liquid chromatography with pulsed amperometric detection. *J. Chromatogr.* **527**, 244-246.

Thompson, P.R., Hughes, D.W., & Wright, G.D. (1996). Regiospecificity of aminoglycoside phosphotransferase from *Enterococci* and *Staphylococci*. *Biochemistry* **35**, 8686-8695.

Trieu-Cuot, P., & Courvalin, P. (1983). Nucleotide sequence of the *Streptococcus faecalis* plasmid gene encoding the 3'5"-aminoglycoside phosphotransferase type III. *Gene* **23**, 331-341.

Umezawa, H., Yamamoto, H., Yagisawa, M., Kondo, S., Takeuchi, T., & Chabbert, Y-A. (1973). Kanamycin phosphotransferase I: mechanism of cross resistance between kanamycin and lividomycin. *J. Antibiot.* **26**, 407-411.

Umezawa, H., Yagisawa, M., Sawa, T., Takeuchi, T., Umezawa, H., Matsumoto, H., & Tazaki, T. (1975). Aminoglycoside 3'-phosphotransferase III, a new phosphotransferase. *J. Antibiot.* **28**, 845-853.

Chapter 3

APH(3')-IIIa employs a direct in-line phosphate transfer mechanism.

Adapted from

Thompson, P.R., Hughes, D.W., & Wright, G.D.
Chemistry & Biology, 1996, vol 3, pp. 747-755.

The work described in this chapter entails my characterization of the phosphate transfer mechanism of the APH(3')-IIIa enzyme. NMR spectra, for the positional isotope exchange experiments, were recorded and analyzed by D.W. Hughes, in the Department of Chemistry, McMaster University. The author of this thesis obtained the remainder of the data presented in this chapter.

CHAPTER 3: APH(3')-IIIa employs a direct in-line phosphate transfer mechanism.

3.1. Introduction

Prior to 1996, little was known about the catalytic mechanism of APH(3')-IIIa, or for that matter any other APH(3') isozyme. This is despite the fact that mutagenesis studies had putatively identified a number of catalytically important residues (see Section 1.4.4.3.3 in Chapter 1). Many of the residues identified in these studies are conserved among the APH(3'), and Martin *et al*, (1988) noted that of these conserved residues most are found in the C-termini of APH(3') isozymes, present in one of three motifs (Figure 3.1).

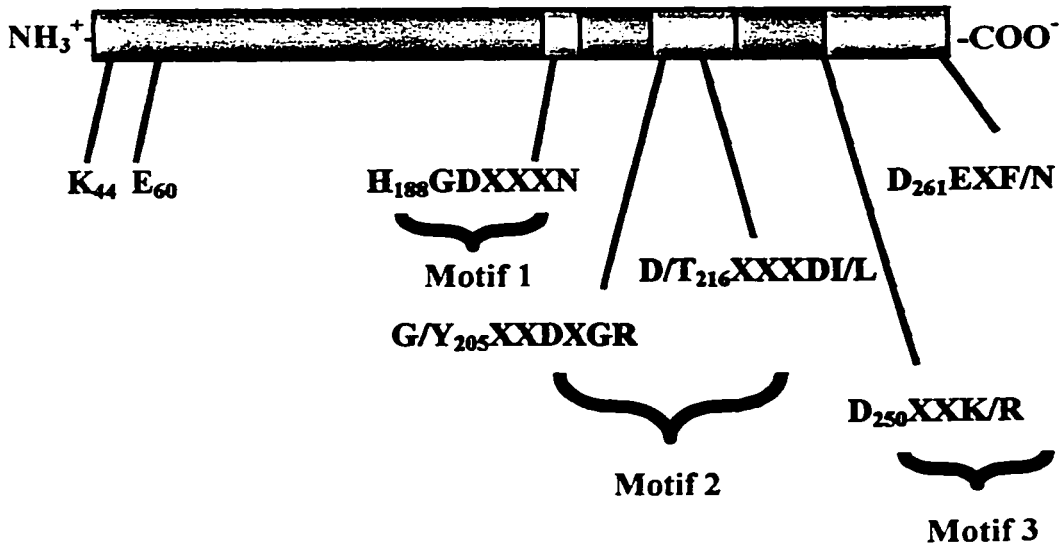

Figure 3.1. Regions of APH(3') homology. Residues conserved among the APH(3') family of enzymes are identified, as are the three motifs defined by Martin *et al* (1988). These motifs are highlighted in yellow.

While the functional significance of each of these motifs was not known, Martin *et al* (1988), by comparing the primary structures of the APH(3') to other known phosphotransferases, speculated that: motif 2 forms a part of the nucleotide binding site; motif 3 is required for AG binding; and motif 1 is required for catalysis. With regard to motif 1, these authors specifically postulated that an absolutely conserved His residue, His188 in APH(3')-IIIa, could act as a phosphate accepting residue, mediating the transfer of the γ-phosphate of ATP to an AG hydroxyl through the formation of a phospho-enzyme intermediate (Figure 3.2A). While we had found no evidence to support such a mechanism of phosphate transfer, it could not be ruled out because the kinetic mechanism of APH(3')-IIIa is a special case of an ordered bi bi reaction that is termed a Theorell-Chance (McKay & Wright, 1995). In a Theorell-Chance kinetic mechanism the chemical step of phosphate transfer is fast relative to the rate of the enzyme catalyzed reaction, k_{cat}, which for APH(3')-IIIa is ADP release. Thus, the phosphate transfer step is transparent in the steady state, which we postulated would make the detection of a phospho-enzyme intermediate difficult to observe. Thus, a double displacement mechanism, with initial phosphate-transfer to the enzyme, was a distinct possibility. Nevertheless, the fact that we could not identify a phospho-enzyme intermediate suggested that the direct in-line transfer of the γ-phosphate of ATP, to an AG hydroxyl (Figure 3.2B), was an equally plausible phosphate transfer mechanism.

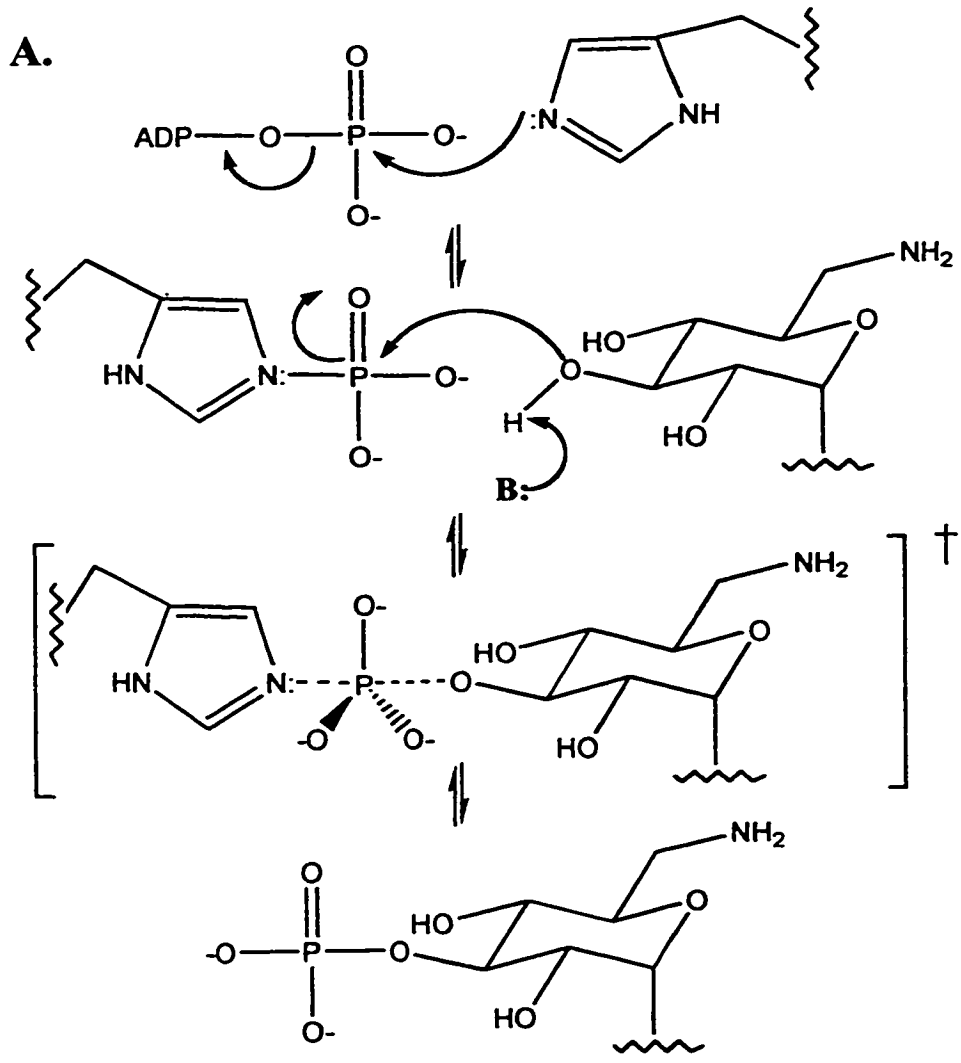

Figure 3.2. The two possible phosphate transfer mechanisms employed by APH(3')-IIIa. A. A double displacement mechanism with a phospho-histidine intermediate. **B.** A direct in-line transfer mechanism (overleaf).

Therefore, in order to decide between these two possibilities I employed the positional isotope exchange (PIX) method, originally pioneered by Midelfort & Rose (1976). The PIX technique has been successfully used to provide evidence for the existence of phosphorylated intermediates in the reaction pathways of a number of enzymes, including the reactions catalyzed by glutamine synthetase, carbamoyl-

phosphate synthetase and CTP synthetase (Midelfort & Rose, 1976; Wimmer *et al*, 1979; Raushel & Villafranca, 1980; von der Saal *et al*, 1985). In general, the PIX methodology employs phosphate analogues that are isotopically labeled with ^{18}O, and monitors the exchange of this isotope with ^{16}O (reviewed in Raushel & Villafranca, 1988). This exchange is easily monitored using ^{31}P NMR, as a P-^{18}O bond causes, approximately, a 0.02 ppm upfield shift in ^{31}P NMR spectra (Villafranca, 1989).

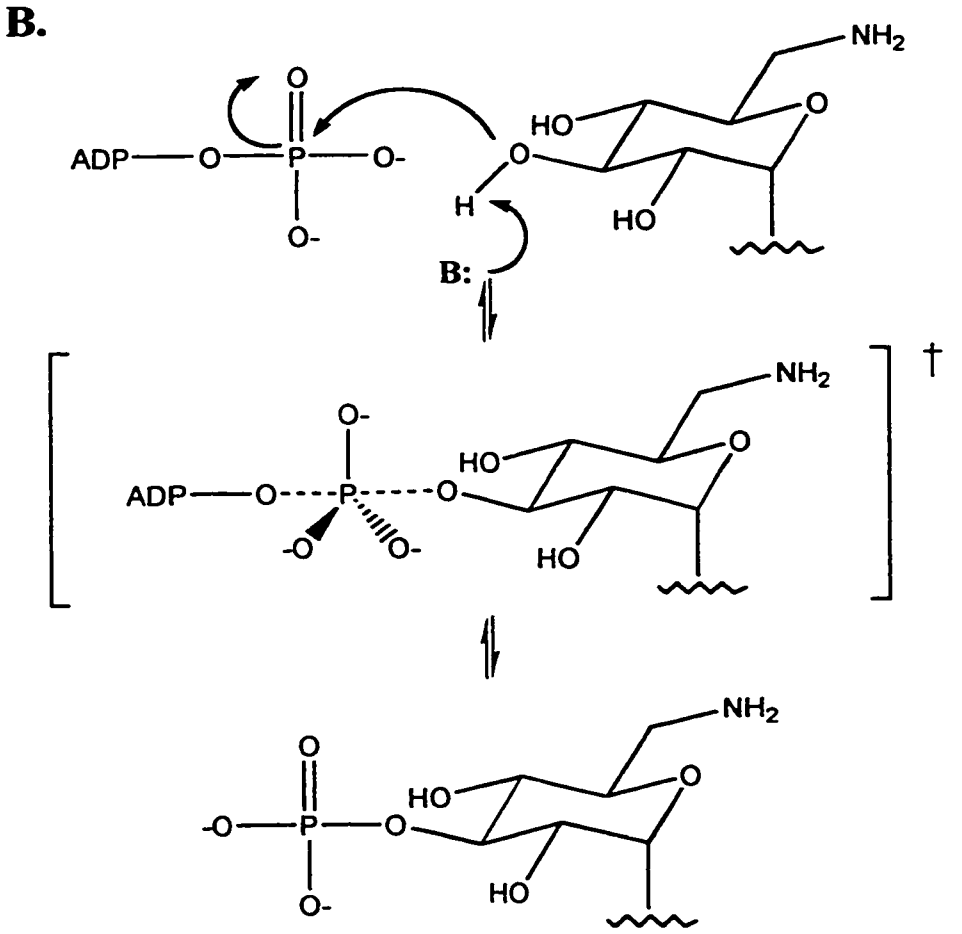

Figure 3.2. Continued.

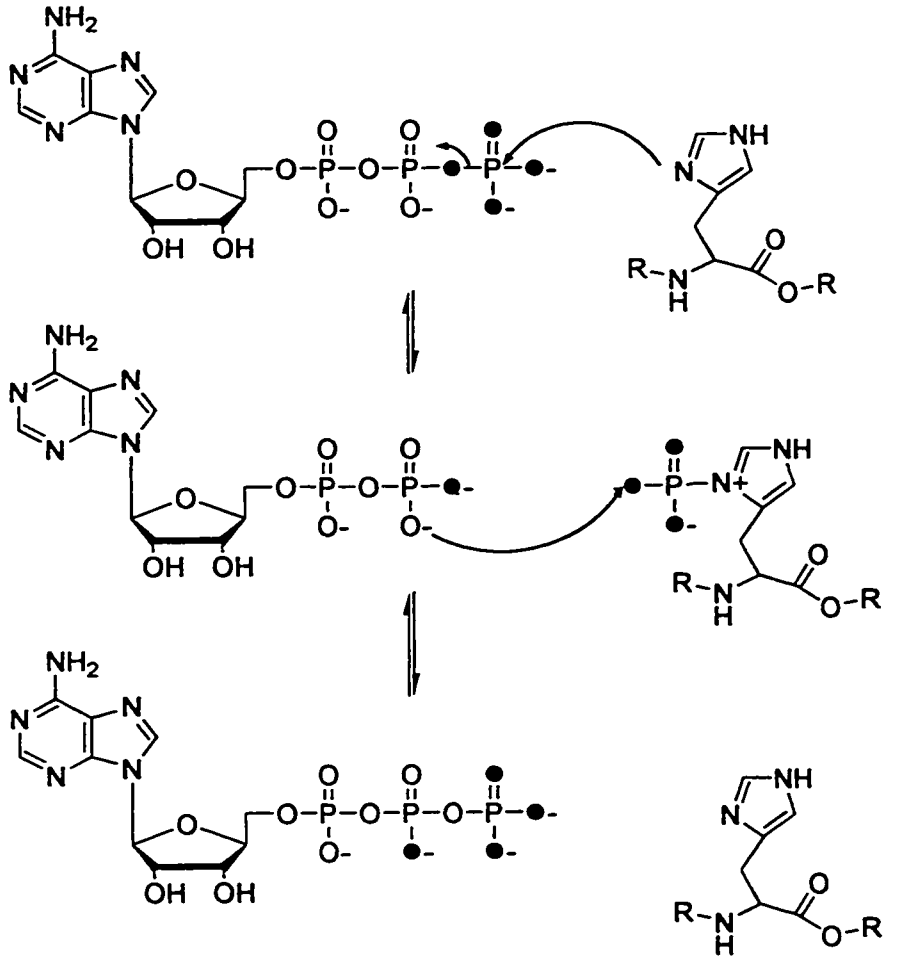

Figure 3.3. Positional isotope exchange in a double displacement phosphate transfer mechanism. Phosphate transfer to an enzyme nucleophile results in oxygen scrambling at the β-phosphoryl group and as a result, ^{18}O (shown in solid black circle) moves from the βγ-bridge position to a β-non-bridge position, during the reverse reaction.

In order to apply the PIX methodology to APH(3')-IIIa, and thereby assess the existence of a phospho-enzyme intermediate, an ATP analogue that is isotopically labeled with ^{18}O at the γ-phosphate non-bridge oxygens, and at the β-γ-phosphate bridge oxygen, was used (Figure 3.3). If a phospho-enzyme intermediate does exist in the

APH(3')-IIIa catalyzed reaction, then the incubation of γ-[^{18}O]-ATP with this enzyme should result in a readily observable PIX. This is due to the fact that the γ-phosphate of ATP would be reversibly transferred to the enzyme nucleophile, as a result of the concept of microscopic reversibility. During the reverse reaction, the PIX is the result of the movement of the β-γ-bridging ^{18}O to one of the two β-phosphate non-bridging positions, which in a double displacement mechanism will occur two thirds of the time. This movement of course assumes that the β-phosphoryl group is free to rotate in the enzyme active site. The absence of a PIX could suggest that either the β-phosphoryl group is not free to rotate in the enzyme active site, or more likely, a phospho-enzyme intermediate does not exist. If the latter is the case, then the direct in-line transfer of the γ-phosphate of ATP to an AG hydroxyl is the most likely phosphate transfer mechanism employed (Figure 3.2B). While it should be noted that the presence of a PIX could also signify the existence of a metaphosphate intermediate (see Section 4.1 in Chapter 4), such a finding would be unprecedented, as a metaphosphate intermediate is not thought to exist in solution (Herschlag & Jencks, 1989).

While it was hoped that the PIX studies would give insight into the phosphate transfer mechanism employed by APH(3')-IIIa, I was also interested in beginning a determination of the amino acid residues that are required for catalysis. Therefore, in addition to our PIX experiments with APH(3')-IIIa we also used amino acid specific chemical modifiers to identify the classes of amino acids that are required for catalysis i.e. do they possess a thiol, a carboxylate, an amino, or an imidazole functionality.

While these studies indicated that a number of different types of amino acid residues are required for catalysis, I was most interested in further exploring the finding that a His modifier, diethylpyrocarbonate (DEPC), could inactivate APH(3')-IIIa due to the fact that His188 had previously been suggested to act as a phosphate acceptor, in a double displacement mechanism (Martin *et al*, 1988). Therefore, in an effort to describe the contribution of His residues to the catalytic mechanism of APH(3')-IIIa, I have determined the stoichiometry and rate of APH(3')-IIIa inactivation by DEPC, as well as the effect of mutating His78, His82, His123, and His188 to Ala. The data, from these analyses, indicates that phosphate transfer occurs by the direct in-line phosphate transfer mechanism, and that His188 is not a phosphate-accepting residue. Portions of this work have previously been published in Thompson *et al* (1996).

3.2. Materials and Methods.

3.2.1 Chemicals.

Kanamycin A, neomycin B, amikacin, tobramycin, pyruvate kinase/lactate dehydrogenase, anhydrous pyridine, and anhydrous dimethyl sulfoxide were obtained from Sigma (St. Louis, MO). ATP was obtained from Boehringer Mannheim (Laval, Quebec, Canada). $H_2{}^{18}O$ (97.8 atom%) was obtained from Isotec (Miamisburg, OH). $KH_2P^{18}O_4$ was synthesized by the method of Risley and Van Etten (1978). Briefly, 0.5 mL of $H_2{}^{18}O$ was placed at the bottom of a 28 x 150 mm test tube connected to an aspirator and a $CaCl_2$ drying tube. The tube was placed in dry ice, and 1.45 g of PCl_5 was quickly added to the frozen water, and the drying tube replaced, in order to minimize any exchange of the $H_2{}^{18}O$ with unlabelled atmospheric moisture. This reaction was

performed at freezing temperatures because it is highly exothermic. Since the reaction is virtually complete upon addition of PCl_5, the reaction was almost immediately brought to room temperature, and subsequently warmed to 80° C, in a waterbath, over 90 minutes. The latter step removes HCl, a byproduct of the reaction. The pH of the viscous liquid product was then adjusted, with 2M KOH, to 4.66, and $KH_2P^{18}O_4$ precipitated by the addition of 4 volumes of 66% ethanol. $KH_2P^{18}O_4$ was obtained in 54.3% yield.

ADP-morpholidate (compound 1). Compound 1 was prepared as previously described (Wehrli *et al*, 1965) (Figure 3.4). To a refluxing solution of 50% aqueous t-butylalcohol (16 mL), containing 0.8 mmoles ADP (free acid) and 5 mmoles morpholine, a solution of dicyclohexylcarbodiimide (DCC) (4.8 mmoles), dissolved in 35 mL of t-butylalcohol, was added dropwise over 3 hours. After all of the DCC had been added, the reaction was refluxed for a further 3 hours. The solution was then allowed to cool and evaporated to ~25 mL. The mixture was then extracted with 50 mL of ether, and the dicyclohexylurea by-product, which partitions in the organic phase, removed by filtration. The aqueous portion of the reaction mixture was then applied to a 2 x 25 cm AG1-X2 column (HCO_3^- form), and the column washed first with 483 mL of ddH_2O, and then with 462 mL of 0.1 M aqueous triethylammonium bicarbonate buffer (TEAB) pH 7.5. Separation of the reaction components was achieved, using a 0.1–0.5 M linear gradient of TEAB pH 7.5, over 2.1 L. Final elution of compound 1, from the column, was achieved by stepping the gradient up to 1 M and washing the column with 896 mL of TEAB this solution. The peak corresponding to compound 1 was dried, *in vacuo*, at 30° C, and residual buffer removed by repeatedly dissolving the compound in methanol, and

drying *in vacuo*. Compound 1 was obtained in 86.7% yield, and electrospray mass spectra (observed 495.1 ,m/z; expected 496.3), and TLC, on polyethylimine cellulose (R_f 0.76), using 1 M LiCl as the mobile phase, confirmed the identity of the compound.

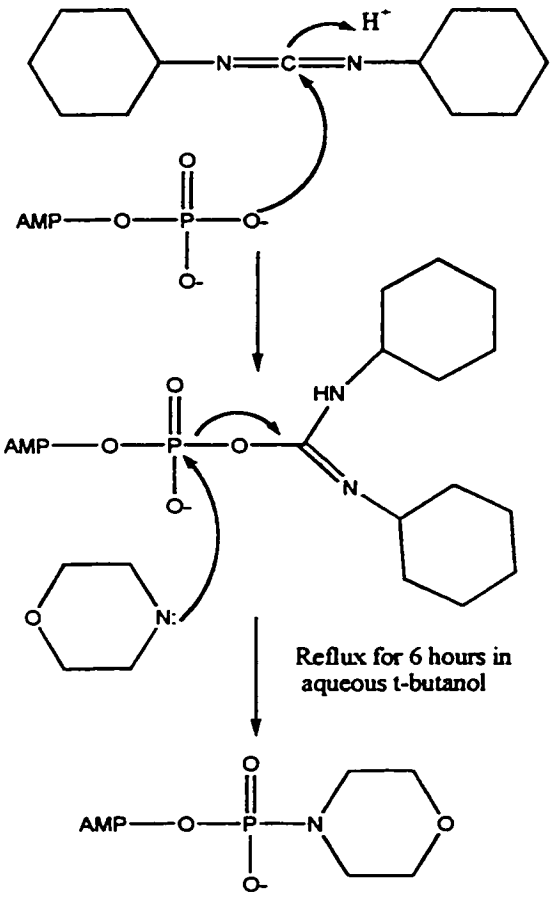

Figure 3.4. Synthesis of ADP-morpholidate.

[γ-^{18}O]-ATP (compound 2): Compound 2 was prepared by the reaction of $KH_2P^{18}O_4$ with compound 1, as previously described (Wehrli *et al*, 1965) (Figure 3.5). In order to render the reaction mixture completely anhydrous, 0.2 mmoles of compound 1 was

dissolved in 3 mL of anhydrous pyridine and the pyridine removed, *in vacuo*, at 30° C. These steps were repeated 3 times with 2 mL aliquots of anhydrous pyridine, in order to remove any remaining contaminating water. Subsequently, the dried material was dissolved in 2 mL of freshly redistilled anhydrous benzene, and the benzene removed, *in vacuo*, thereby removing the pyridine. This step was repeated a second time. The reaction vessel was then sealed under a stream of dry N_2.

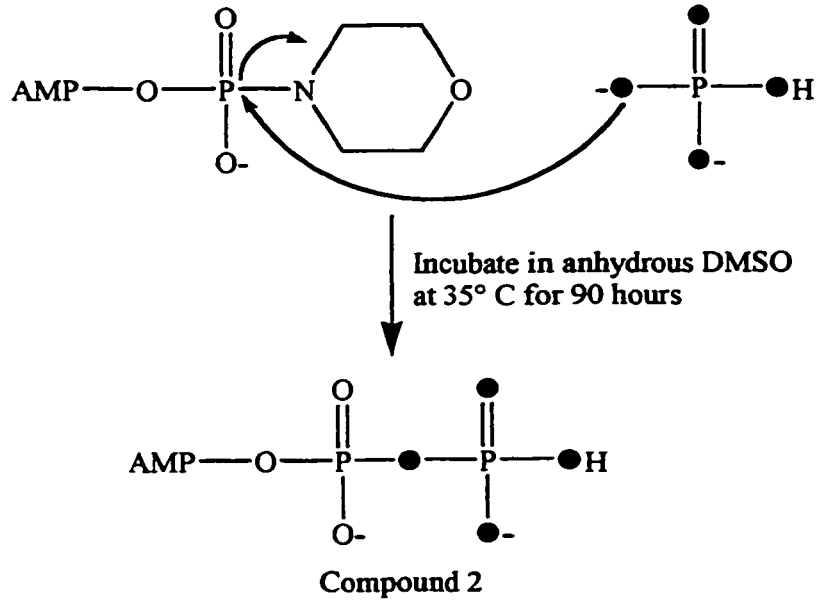

Figure 3.5. Coupling of ADP-morpholidate to $P^{18}O_4$. ^{16}O are depicted as open circles, whereas ^{18}O are depicted as solid black circles.

In a **second** reaction vessel, 300 µL of a 1 M $KH_2P^{18}O_4$ solution was diluted to 1.5 mL with 1.2 mL of anhydrous pyridine. To this solution was added 72 µL (0.3 mmoles) of tri-n-butylamine, and the solution evaporated to dryness *in vacuo* at 30° C. In order to render this material anhydrous, the dried material was dissolved in 2 mL

anhydrous pyridine, and dried *in vacuo*. This step was repeated 2 more times. The anhydrous material was then dissolved in 2 mL of freshly redistilled anhydrous benzene and dried *in vacuo*, at 30° C, in order to remove any remaining pyridine. This step was repeated a second time. The dried material from this step was then dissolved in 2 mL of anhydrous dimethyl sulfoxide, and this solution was added to the anhydrous form of compound 1, as prepared above. The solution was sealed under a stream of dry N_2, and stored at 35° C for 190 hours with stirring. To minimize the contamination of solutions with atmospheric moisture, sample handling up to this point had been performed in a glove bag under a stream of dry N_2. The coupling mixture was then diluted to 20 mL, with ddH_2O, and 5 mL aliquots repeatedly applied to an Mono Q HR 5/5 (Amersham Pharmacia Biotech) column. Purification of compound 2 was achieved, using a linear gradient of 0-40% TEAB buffer pH 7.5 over 21 column volumes. Compound 2 eluted with a retention time corresponding to unlabelled ATP. The purified product was dried, *in vacuo*, and contaminating buffer removed by repeatedly dissolving the compound in methanol, and evaporating *in vacuo*. Compound 2 was precipitated by the addition of 0.5 mL of a 1M NaI solution, in acetone, to the labeled analogue, dissolved in 2 mL of methanol, and the subsequent addition of ~10 mL of acetone. The yield was approximately 14.6 % and ^{31}P NMR was used to confirm that the labeled phosphate was correctly incorporated at the γ-position.

3.2.2. Survey of Chemical Modifying Agents.

The effect on aminoglycoside kinase activity after treatment of APH(3')-IIIa with N-ethylmaleimide (500 μM), *p*-chloromercuribenzoic acid (500 μM), phenylglyoxal (2.5 mM), DEPC (10 mM), and tetranitromethane (2.5 mM) was determined as follows. Typically, an inactivation reaction was performed in 50 mM HEPES pH 7.5, 10 mM $MgCl_2$ and allowed to proceed for 1 hour at 37° C, after which the chemical modifier was removed by passage through a Sephadex G-10 spin column (0.4 mL) and aliquots assayed for enzymatic activity. Treatment of APH(3')-IIIa with phenylglyoxal was performed in 100 mM sodium bicarbonate pH 8.0. The inactivation with tetranitromethane was performed at room temperature.

The rate of APH(3')-IIIa inactivation by DEPC, as well as the stoichiometry of inactivation, was studied in greater detail. Activity remaining was plotted against time and analyzed by nonlinear least squares fitting to equation 1, which describes a double exponential decay,

$$A = A_{o1}e^{-k1t} + A_{o2}e^{-k2t} \qquad \text{(Eq. 1)}$$

where A is enzyme activity, A_o is initial activity, k_1 and k_2 are rate constants and t is time. The stoichiometry of inactivation was determined using a final DEPC concentration of 5 mM. Wavelength scans were obtained after a 1 hour incubation with DEPC at room temperature and the change in absorbance at 242 nm was determined. The stoichiometry of inactivation was determined using an extinction coefficient of 3200 M^{-1} cm^{-1} (Miles, 1977).

3.2.3. Site Directed Mutagenesis.

The *aph(3')-IIIa* gene, from pETSACG1 (see Chapter 2, Section 2.2.2), was cloned into M13mp18, using the restriction sites *Xba*I and *Hind*III. Single stranded phage DNA from the resulting construct was used to generate the APH(3')-IIIa^{H188A} mutant by the Kunkel methodology (Kunkel, 1985) using the oligonucleotide 5'-CTCCCAGGTCGCCGGCGGAAAAAGA CGAGCTC-3'. The mutated gene was subcloned into pET-22b(+) (NovaGen, Madison, WI) using the restriction enzymes *Nde*I and *Hind*III, in order to generate the expression construct, pAPHH188A.

Mutagenic oligonucleotides 5'-CATGCCGTTCAAAGGCCAGGACCTTTGG-3', 5'-GCTCCAGCCATCAGCCCGTTCAAAGTGC-3', and 5'-CGATATGTCGATC-GAGGCAAAGAGCCTGATGC-3' were used to generate the APH(3')-IIIa^{H78A}, the APH(3')-IIIa^{H82A}, and the APH(3')-IIIa^{H123A} mutants, respectively, by the megaprimer polymerase chain reaction (PCR) mutagenesis method (Sarkar & Sommer, 1990). In all cases, a megaprimer was amplified by PCR using the mutagenic oligonucleotide and the 5' PCR primer, 5'-GCTCTAGACATATGGCTAAAATGAGA-3' (McKay *et al*, 1994). In order to re-generate the full length gene, the mutagenic megaprimers were first isolated, after electrophoresis in a 1% agarose gel, using the Qiaex II: Gel Extraction Kit (Qiagen, Mississauga, ON), and then used in a PCR reaction in combination with the 3' PCR primer, 5'-CGAAGCTTGGACTAAAACAATTCATCCAG-3' (McKay *et al*, 1994). In both PCR reactions, Vent DNA polymerase (New England Biolabs) was used to minimize the incorporation of undesired mutations, and pETSACG1 was used as the template. The isolated, full length, fragments were digested with *Nde*I and *Hind*III and

ligated into similarly cut pET-22b(+). The presence of the desired mutations, in the pETH78A and pETH82A constructs, were confirmed by sequencing at The Central Facility of the Institute for Molecular Biology and Biotechnology, McMaster University. The presence of the desired mutation in the pETH123A construct was confirmed by the incorporation of a silent *Pvu*I site in the mutagenic oligonucleotide. All confirmed mutant constructs were subsequently sequenced, in their entirety, to ensure that no undesired mutations had occurred during the two PCR amplifications.

3.2.4. Purification of mutant APH(3')-IIIa proteins.

The His to Ala mutant APH(3')-IIIa proteins were purified using the method described for the purification of the wild type enzyme (Chapter 2, Section 2.2.3). However, further purification was required for the APH(3')-IIIa^{H82A} and the APH(3')-IIIa^{H188A} mutants. For these mutant enzymes, pure protein could be obtained by the application of fractions from the second Q Sepharose step to a Superdex 200 (HR 10/30) column, at a flow rate of 0.4 mL/min in 50 mM Tris-HCl pH 8.0, 1 mM EDTA and 200 mM NaCl. Enzyme activity was analyzed by coupling the release of ADP to a pyruvate kinase/lactate dehydrogenase reaction, and the initial rates were used to determine the steady state kinetic parameters, as has been previously described (McKay *et al*, 1994). This assay is described in greater detail in Chapter 4, Section 4.2.5.

3.2.5. Western Analysis.

A single colony of *E. coli* BL 21 (DE3)/pETSACG1 and *E. coli* BL 21 (DE3)/ pAPHH188A were used to inoculate 2 mL of LB-ampicillin (100 μg/mL). The following

day these cultures were used to inoculate 200 mL of LB-ampicillin (100 μg/mL), which were grown at 37° C (250 r.p.m.), and induced as previously described (McKay *et al*, 1994; Chapter 2, Section 2.2.3.). Cells were harvested by centrifugation, lysed in a French pressure cell (20000 psi), and the lysate cleared by centrifugation (12 000 x g for 20 minutes). The insoluble pellet, P1, was resuspended in 5 mL of lysis buffer (50 mM Tris-HCl pH 7.5, 5 mM EDTA, 200 mM NaCl, 1 mM PMSF, and 0.1 mM DTT) plus 0.1% SDS. The protein concentration of both the supernatant (S1) and P1 fractions was determined by the Bradford method, and identical amounts of total protein (2 μg) were applied to the top of a 15% SDS-polyacrylamide gel. The gel was then subjected to electrophoresis for ~45 minutes at 200 volts, at which point the proteins, embedded in the gel, were electroblotted onto nitrocellulose, and the blots obtained were then probed with rabbit anti-APH(3')-IIIa polyclonal antibody (McKay and Wright, unpublished data). Blots were then incubated with an alkaline phosphatase-conjugated donkey-anti-rabbit (IgG) antibody (Jackson Immuno Research), and developed using 5-bromo-4-chloro-3-indoylphosphate-*p*-toluidine salt/nitroblue tetrazolium chloride (GIBCO/BRL).

3.2.6. Positional Isotope Exchange.

[γ-^{18}O]-ATP (400 μM) was incubated for 15 minutes, at 37° C, in 50 mM HEPES pH 7.5, 15 mM $MgCl_2$, and 13% D_2O, either alone, or with APH(3')-IIIa (0.1 nmoles), or with enzyme and 20 μM tobramycin. APH(3')-IIIa activity was quenched by the addition of EDTA to a final concentration of 40 mM and 100 μL of CCl_4. The pH was then adjusted to 9.2.

3.3. Results.

3.3.1. Survey of chemical modifying agents.

Since we were interested in defining the catalytic mechanism of APH(3')-IIIa, I employed a number of amino acid specific chemical modifying agents, to identify the types of amino acid residues that are required to promote catalysis. These studies were initiated prior to the determination of a crystal structure of APH(3')-IIIa, and it was hoped that an analysis of this type would give clues as to the identity of catalytically important residues. For this analysis, I employed agents that modify cysteines, histidines, tyrosines, arginines, and carboxylate containing residues (Table 3.1). After treatment of the wild type APH(3')-IIIa enzyme with these agents the percent activity remaining was determined (Table 3.1). From this analysis, it would appear that histidines, tyrosines, arginines and carboxylate containing amino acid residues are important to the catalytic mechanism of APH(3')-IIIa.

Table 3.1: Survey of chemical modifying agents.

Chemical modifying agent	Concentration of chemical modifier (mM)	Amino acid modified	% Activity Remaining
Control, pH 7.5	-	-	100
N-Ethylmaleimide	0.5	Cys	47
p-Chloromercuribenzoic acid	0.5	Cys	3
DEPC	10	His, Tyr, Cys, Lys	2
1-Ethyl-3-(3-dimethylaminopropyl) carbodiimide	2.5	C-term COO^- Asp, Glu	23
Tetranitromethane	2.5	Tyr	1.8
Control, pH 8.0	-	-	100
Phenylglyoxal	2.5	Arg	10

3.3.2. Analysis of the inactivation of APH(3')-IIIa by DEPC.

The fact that the His modifier DEPC inactivated APH(3')-IIIa, in combination with the purported importance of His188 to the catalytic mechanism of APH(3') (see introduction), suggested that further analysis, of the mechanism by which DEPC inactivates APH(3')-IIIa, was required. Therefore, for the wild type enzyme, I examined the stoichiometry and the rate of the inactivation of this enzyme by DEPC. As DEPC can also modify Tyr, Lys and Cys residues, I first determined whether or not this agent was modifying these two types of amino acid residues. To detect Tyr modification, wavelength scans were obtained in the absence, and presence of DEPC. Modification of even a single Tyr residue, by DEPC, is readily detected because O-carboxyethylation of a Tyr residue results in a decrease in absorbance at 278 nm ($\varepsilon = 1310\ cm^{-1}M^{-1}$) (Miles, 1977). Since these scans show no change in the absorbance at 278 nm (Figure 3.6), the inactivation of APH(3')-IIIa is not due to the modification of a Tyr residue.

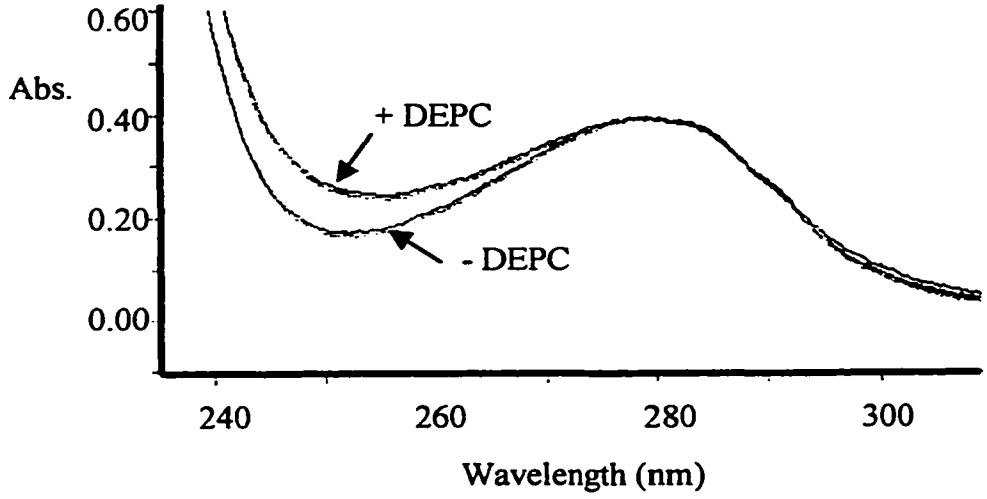

Figure 3.6. Wavelength scans of wild type APH(3')-IIIa, after either treatment with DEPC in ethanol, or ethanol alone. DEPC inactivation reactions were performed in duplicate at room temperature.

To confirm that the modification of Cys or Lys residues was not the cause of inactivation, I also examined the ability of neutralized hydroxylamine (pH 7.5), to reactivate the enzyme. Modest reactivation was observed (not shown), thereby indicating that the inactivation of APH(3')-IIIa is not due to the modification of sulfydryl or lysyl residues (Miles, 1977). Therefore, the inactivation of APH(3')-IIIa by DEPC is most likely due to the modification of one or more His residues.

In order to determine the number of His residues modified, I examined wavelength scans that were obtained in the absence, or after treatment of the wild type protein with DEPC (Figure 3.6). The change in the absorbance at 242 nm was determined and used with the molar extinction coefficient for carboxyethylated histidines ($\varepsilon = 3200\ cm^{-1}M^{-1}$) to determine the stoichiometry of modification. For wild type APH(3')-IIIa, 3.4 His residues, per monomer, are modified (Table 3.2), suggesting that three of the 4 His residues are readily modified, and the fourth is only partially susceptible to N-carboxyethylation.

Table 3.2: Stoichiometry and rate of APH(3')-IIIa inactivation by DEPC.

His Mutant	Stoichiometry	Rates of Inactivation	
		Rate 1	Rate 2
Wild Type	3.4	0.17±0.054	0.010±0.011
His78Ala	2.3	0.49±0.156	-0.003±0.006
His82Ala	2.9	2.12±1.75	0.032±0.026
His123Ala	3.3	0.36±0.12	0.009±0.009
His188Ala	2.0	0.75±0.047	0.009±0.009

I have also determined the rate of APH(3')-IIIa inactivation by DEPC. The progress of the inactivation reaction fit best to a double exponential decay model, where

the initial inactivation phase is fast, relative to the second phase (Table 3.2). These results are consistent with my stoichiometry studies, as the presence of two inactivation phases suggests that multiple His modifications are required to fully inactivate APH(3')-IIIa.

3.3.3. Kinetic analysis of APH(3')-IIIa His mutants.

The finding that the modification of multiple His residues results in the inactivation of APH(3')-IIIa, combined with the absolute conservation of His188 among the APH(3') family of enzymes, suggested that a more thorough analysis of the role of His residues, in the catalytic mechanism of APH(3')-IIIa was required. This was simplified by the fact that only four His residues are present in the primary structure of APH(3')-IIIa. Therefore, I generated the APH(3')-IIIa^{H78A}, the APH(3')-IIIa^{H82A}, the APH(3')-IIIa^{H123A}, and the APH(3')-IIIa^{H188A} mutants, in order to determine the contribution of each one of these residues to catalysis. The mutant enzymes were overexpressed, purified, and the steady state kinetic parameters determined with pure mutant enzyme. In order to confirm that enzyme preparations contained the desired His to Ala mutants, and thereby determine if any of the enzyme preparations were contaminated by native APH(3')-IIIa, the molecular weights of all the His to Ala mutants were determined by electrospray ionization mass spectrometry at the Department of Chemistry, University of Waterloo. In all cases the molecular weight observed, 30778 Da, was consistent with the molecular weight expected 30779 for a His to Ala APH(3')-IIIa mutant, lacking the N-terminal methionine . Therefore, enzyme preparations were not contaminated by any of the wild type enzyme.

3.3.3.1 Histidine 78.

His78 is not conserved among the APH(3') family of enzymes, and the reason for this lack of conservation is readily apparent from the steady state kinetic parameters determined for the APH(3')-IIIa^{H78A} mutant (Table 3.3), as only small changes in the K_ms and k_{cat}s are detected, for a number of different substrates. Furthermore, the effect on V/K is small, a decrease of 1- to 2.8-fold. The K_m of ATP and kanamycin A is only increased 0.4-fold, whereas the K_m for neomycin B is increased 3.5-fold. Thus, this residue is not critical for either AG or nucleotide binding. Similarly, the imidazole ring of His78 is not required for catalysis, as the maximum decrease in k_{cat} is only 2.7 fold, which is observed for both ATP and kanamycin A.

3.3.3.2. Histidine 82.

His82 is also not conserved among the APH(3') family of enzymes, and the steady state kinetic parameters determined, for a number of substrates, with the APH(3')-IIIa^{H82A} mutant, indicate that this residue is also not critical for either nucleotide or AG binding. The K_ms for all of the substrates examined are increased 0.2- to 0.4-fold. However, the imidazole ring of His82 appears to play a role in catalysis, as a decrease in the k_{cat}s of a variety of substrates is apparent, and ranges between 3.0- and 5.1- fold. The molecular basis for this effect on the rate of reaction is not known (see below). While this residue may play a role in catalysis, it is undoubtedly an indirect one, as there is only a small decrease in the V/K of this mutant enzyme (0.6- to 2.0-fold).

3.3.3.3. Histidine 123.

His123 is partially conserved among the APH(3') family of enzymes, however, the steady state kinetic parameters, determined for the APH(3')-IIIa^{H123A} mutant, reveal

that this residue is also not critical for catalysis, as the second order rate constant (V/K) of this mutant does not vary significantly from the value observed for the wild type enzyme. Although, it should be noted that the K_ms for ATP, and the AGs tested, are increased 0.04- to 0.4-fold, and the k_{cat}s are decreased 2.5- to 3.1-fold. Nevertheless, the functional group of His123 is not critical to catalysis, and it is unclear how the removal of this imidazole ring could affect substrate binding (see below).

Table 3.3: Steady state kinetic parameters for APH(3')-IIIa and APH(3')-IIIa^{H78A}, APH(3')-IIIa^{H82A}, APH(3')-IIIa^{H123A}, and APH(3')-IIIa^{H188A} mutant proteins.

	Wild Type[1]	
Substrate	K_m (μM)	k_{cat} (s^{-1})
ATP	27.7±3.7	1.76±0.08
Kanamycin A	12.6±2.6	1.79±0.09
Neomycin B	7.72±0.9	2.08±0.07
Amikacin	245±27	2.46±0.11

	APH(3')-IIIa^{H78A} [2]				
Substrate	K_m (μM)	$K_{m(mut)}/K_{m(WT)}$	k_{cat} (s^{-1})	$k_{cat(WT)}/k_{cat(mut)}$	$V/K_{WT}/V/K_{mut}$
ATP	10.9±1.8	0.4	0.66±0.01	2.7	1.1
Kanamycin A	5.1±1.6	0.4	0.67±0.04	2.7	1.1
Neomycin B	27.0±5.1	3.5	2.46±0.18	0.8	2.8
Amikacin	206±13	0.8	1.74±0.04	1.4	1.1

[1] Steady state kinetic parameters for the aminoglycoside substrates are taken from McKay *et al* (1994). The steady state kinetic parameters for ATP are taken from Hon *et al* (1997).
[2] For the His78Ala mutant, substrate inhibition was noted for kanamycin A and neomycin B. The substrate inhibition constants for these AGs are 1.68±0.86 mM and 1.84±0.58 mM, respectively.

Table 3.3. Continued.

	APH(3')-IIIa^{H82A} [3]				
Substrate	K_m (μM)	$K_{m(mut)}/K_{m(WT)}$	k_{cat} (s^{-1})	$k_{cat(WT)}/k_{cat(mut)}$	$V/K_{WT}/V/K_{mut}$
ATP	12.17±2.5	0.4	0.35±0.01	5.0	2.0
Kanamycin A	2.44±0.52	0.2	0.35±0.01	5.1	1.0
Neomycin B	1.31±0.20	0.2	0.69±0.01	3.0	0.6
Amikacin	93.1±10	0.4	0.50±0.01	4.9	2.0

	APH(3')-IIIa^{H123A} [4]				
Substrate	K_m (μM)	$K_{m(mut)}/K_{m(WT)}$	k_{cat} (s^{-1})	$k_{cat(WT)}/k_{cat(mut)}$	$V/K_{WT}/V/K_{mut}$
ATP	11.6±1.8	0.4	0.571±0.02	3.1	1.2
Kanamycin A	0.92±0.2	0.1	0.49±0.01	3.7	0.4
Neomycin B	0.29±0.13	0.04	0.83±0.01	2.5	0.1
Amikacin	110±13	0.4	0.87±0.03	2.8	1.1

	APH(3')-IIIa^{H188A} [5]				
Substrate	K_m (μM)	$K_{m(mut)}/K_{m(WT)}$	k_{cat} (s^{-1})	$k_{cat(WT)}/k_{cat(mut)}$	$V/K_{WT}/V/K_{mut}$
ATP	33.5±5.9	1.2	3.75±0.16	0.5	0.6
Kanamycin A	17.4±1.7	1.4	3.36±0.07	0.5	0.7
Neomycin B	3.2±0.7	0.4	1.20±0.05	1.7	0.7
Amikacin	184±30	0.8	2.04±0.09	1.2	1.0

[3] For the His82Ala mutant, substrate inhibition was only noted for kanamycin A. The substrate inhibition constant for this AG is 6.7±2.8 mM.

[4] For the His123Ala mutant, substrate inhibition was noted for kanamycin A and neomycin B. The substrate inhibition constants for these AGs are 5.03±2.82 mM and 6.95±3.13 mM, respectively.

[5] For the His188Ala mutant, substrate inhibition was only noted for neomycin B. The substrate inhibition constant for this AG is 2.74±0.88 mM.

3.3.3.4. Histidine 188.

If this residue did act as a phosphate-accepting residue, as has been suggested (see introduction), then I hypothesized that it would be critical for the activity of the wild type enzyme, and that a APH(3')-IIIa^{H188A} mutant would have little or no detectable activity. The steady state kinetic parameters of the APH(3')-IIIa^{H188A} mutant, for ATP, and a variety of AG substrates (Table 3.3) indicate that this residue is not critical for catalysis, as the k_{cat} is decreased a maximum of 1.7-fold, and as well, the K_ms, and the *V/K*s, for a variety of substrates are similar to those values observed with APH(3')-IIIa. Thus, His188 is unlikely to act as a phosphate-accepting residue in a double displacement mechanism. While His188 is not important for catalysis, I noted, during the purification of the APH(3')-IIIa^{H188A} mutant that the amount of soluble protein produced is low, relative to APH(3')-IIIa. For this enzyme, 30-50 mg of pure enzyme is obtained from a 1 L *E. coli* culture, whereas for the APH(3')-IIIa^{H188A} mutant approximately 1 mg of pure protein was obtained. To determine the cause of this poor yield, I examined the protein expression patterns of cells expressing either the APH(3')-IIIa enzyme or the APH(3')-IIIa^{H188A} mutant by Western blotting (Figure 3.7).

For the wild type enzyme there is an approximately equal distribution of enzyme between the insoluble and soluble fractions, whereas for the APH(3')-IIIa^{H188A} mutant the distribution is unequal and greater than 95% of the protein detected, in this manner, is present in the insoluble fraction. This occurs, despite the fact that this mutant enzyme is expressed at least as well as the wild type enzyme. These results suggest that His188 is required for the proper folding of the wild type APH(3')-IIIa enzyme.

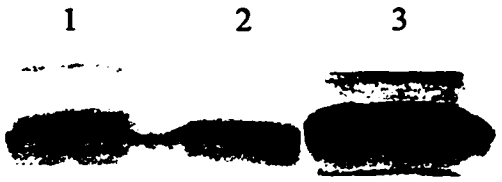

Figure 3.7. Overexpression of APH(3')-IIIa and the APH(3')-IIIa^{H188A} mutant. Cells overexpressing APH(3')-IIIa and the APH(3')-IIIa^{H188A} mutant were fractionated, by centrifugation, and proteins present in the P1 and S1 fractions separated by 15% SDS-PAGE. The presence of wild type and mutant proteins was detected by Western blotting (see Section 3.2.5. for experimental details). Lanes 1 and 2 correspond to the P1 and S1 fractions, respectively, obtained, after cell lysis, from cells overexpressing wild type APH(3')-IIIa. Lanes 3 and 4 correspond to the P1 and S1 fractions, respectively, obtained from cells overexpressing the APH(3')-IIIa^{H188A} mutant.

3.3.4. DEPC inactivation of the four His mutants.

As the modification of His residues appears to result in the inactivation of APH(3')-IIIa, I examined the ability of DEPC to inactivate the APH(3')-IIIa^{H78A}, the APH(3')-IIIa^{H82A}, the APH(3')-IIIa^{H123A}, and the APH(3')-IIIa^{H188A} mutants. All of these mutants were inactivated upon incubation with DEPC (Table 3.2). The stoichiometry of the inactivation reactions, indicates that 2 to 3 of the remaining 3 His residues are modified by this agent, which parallels the results obtained with the wild type enzyme, where greater than three His residues were modified. Using the stoichiometry studies as a guide, the ease of modifying a particular His residue increases, on the order of His123, His82, His78, to His188, where His188 is the most easily modified His residue. The results of this analysis clearly indicates that the modification of multiple His residues causes the inactivation of APH(3')-IIIa, and the inactivation of this enzyme cannot be ascribed to the modification of a single His residue.

3.3.5. Analysis of positional isotope exchange experiments.

In an effort to probe the existence of a phospho-enzyme intermediate, I employed the PIX technique of Midelfort & Rose (1976). In this experiment, [γ-^{18}O]-ATP was incubated alone, in the presence of APH(3')-IIIa, or in the presence of the enzyme and tobramycin, a non-phosphorylatable derivative of kanamycin B, which lacks a 3' hydroxyl and acts as a competitive inhibitor of APH(3')-IIIa (McKay *et al*, 1995). Assuming that a phosphoenzyme intermediate exists, and the β-phosphoryl group is free to rotate in the active site of APH(3')-IIIa, then 40% of the labeled compound should have undergone a PIX reaction. This would have resulted in the appearance of new signals either ~0.02 ppm downfield from the signal corresponding to the γ-phosphate of ATP or ~0.02 ppm upfield from the signal corresponding to the β-phosphate of ATP. The NMR spectra corresponding to the β- and γ-phosphates of ATP are shown in Figure 3.8. Since no new signals in the ^{31}P NMR spectra are apparent, we conclude that a PIX **has not** occurred. Therefore, the existence of a phospho-enzyme intermediate is **highly** unlikely.

3.4. Discussion.

In my first attempts to delineate the catalytic mechanism of APH(3')-IIIa, I relied upon past literature precedents, which had suggested the importance of histidines. One such study that compared the primary structure of the APH(3') with the primary structures of a number of phosphotransferases, including adenylate kinase and specific eukaryotic protein kinases, had suggested that motif 1 (see Figure 3.1) could act directly in the phosphate transfer mechanism, and more specifically suggested that the His

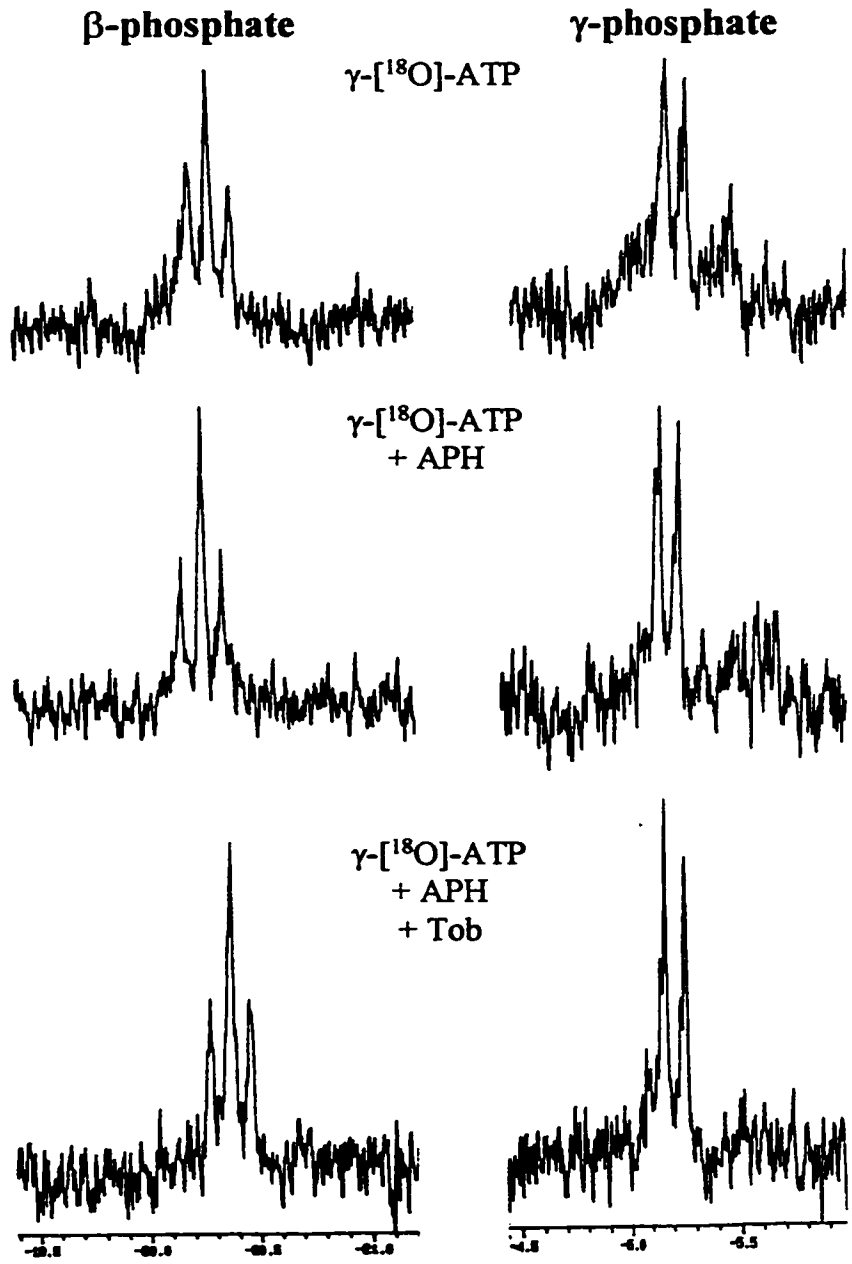

Figure 3.8. PIX experiments. The ^{31}P NMR spectra, corresponding to β- and γ-phosphates of ATP, are shown for [γ-^{18}O]-ATP, incubated alone (**Top**), in the presence of APH(3')-IIIa (APH) (**Middle**), or in the presence of enzyme and tobramycin (Tob) (**Bottom**). Tobramycin is a non-phosphorylatable analogue of kanamycin B, which acts as a competitive inhibitor of APH(3')-IIIa.

residue present in that motif (His 188 in APH(3')-IIIa) could act as a phosphate-accepting residue, in a double displacement phosphate transfer mechanism. Support for this hypothesis came from Kocabiyik & Perlin (1992), who found that cells expressing an APH(3')-IIa^{H188Q} mutant enzyme exhibited an increased *in vivo* susceptibility to AG antibiotics, and when crude cell extracts of bacteria expressing this mutant enzyme were assayed, a dramatic decrease in AG phosphotransferase activity was noted.

Thus, based on this literature, my initial experiments were guided by the expectation that His188, in APH(3')-IIIa, would play a similar role in the catalytic mechanism of this enzyme. While there was such an expectation, we were not convinced about the existence of a phospho-enzyme intermediate, as we had found no evidence to support the existence of such an intermediate (McKay & Wright, unpublished results). Nevertheless, the existence of a phospho-enzyme intermediate could not be ruled out because the ternary complex cannot be detected in the steady state, due to the fact that product release is fully rate limiting for the wild type enzyme (McKay & Wright, 1995; 1996). Therefore, I have employed a His modifying agent, steady state kinetic analyses of His site specific mutants, and PIX experiments, in an effort to determine the importance of His residues to the catalytic mechanism of APH(3')-IIIa, as well as to confirm or refute the existence of a phospho-enzyme intermediate.

3.4.1. Role of histidines in the catalytic mechanism of APH(3')-IIIa.

In a survey of chemical agents, that target specific amino acid residues, the finding that DEPC has the ability to inactivate APH(3')-IIIa, when combined with the precedents cited above, suggested that a more thorough understanding of the mechanism

by which this agent inactivates APH(3')-IIIa was in order. I, therefore, determined the stoichiometry, and the rate of APH(3')-IIIa inactivation by DEPC. For the wild type enzyme, the fact that multiple His residues are modified, combined with the fact that the curve for the rate of inactivation is best fit to a double exponential decay model, suggested that the modification of multiple His residues is required for the inactivation of APH(3')-IIIa.

Since the DEPC studies had suggested that the modification of more than one His residue was required for the inactivation of the wild type enzyme, and since there are only 4 His residue in APH(3')-IIIa, I used site directed mutagenesis, on the *aph(3')-IIIa* gene, to convert His78, His82, His123, and His188 to Ala. Overexpression and purification of these mutant enzymes permitted the determination of their steady state kinetic parameters. While small changes, to both k_{cat} and K_m, are observed, no single His residue, including His188, is critical to the catalytic mechanism of APH(3')-IIIa. Thus, His188 is unlikely to act as a phosphate-accepting residue in a double displacement mechanism. This fact, was initially somewhat surprising, given the literature precedents cited above, combined with the fact that the modification of multiple His residues, by DEPC, inactivates APH(3')-IIIa, therefore, in an effort to probe the role of His residues further, I examined the susceptibility of the His mutants to DEPC. All of the His mutants remain susceptible to DEPC, despite the fact that the stoichiometry of modification is decreased, thereby confirming that the modification of multiple His residues, by this agent, is required for the inactivation of APH(3')-IIIa. This further suggests that

inactivation is the result of modifications that destabilize the tertiary structure of this enzyme.

3.4.2. Role of His188.

Steady state kinetic analysis of the APH(3')-IIIa^{H188A} mutant had indicated the relative unimportance of this residue to the catalytic mechanism of APH(3')-IIIa, but it was not clear why this residue is absolutely conserved among the APH family of enzymes. However, I had noted, during the purification of the APH(3')-IIIa^{H188A}, that this enzyme purified in much poorer yield, relative to APH(3')-IIIa. While we expected that the poor yield could be due to the poor expression of this mutant protein, an alternative possibility was that the APH(3')-IIIa^{H188A} mutant was being overexpressed, but was not able to adopt the correct tertiary structure, resulting in the formation of insoluble inclusion bodies. Western blots of the P1 and S1 fractions, obtained from cells overexpressing, either the wild type enzyme or APH(3')-IIIa^{H188A}, clearly indicate that the mutant enzyme is overexpressed, but is found predominantly in the insoluble fraction. These results, therefore, offer an explanation for the discrepancy that exists between the results obtained with the APH(3')-IIa^{H188Q} (Kocabiyik & Perlin, 1992) and the APH(3')-IIIa^{H188A} mutants. For APH(3')-IIIa^{H188A}, the steady state kinetic parameters were essentially wild type, whereas for the APH(3')-IIa^{H188Q} mutant the phosphotransferase activity is decreased 36-fold. The discrepancy likely arises from the manner in which Kocabiyik & Perlin (1992) determined the relative activity of the APH(3')-IIa^{H188Q} mutant. They used crude cell extracts obtained from cells expressing this mutant

enzyme, and did not correct for changes in protein expression levels. Thus, His188 is important for protein folding, and **not** required for catalysis.

3.4.3. The mechanism of APH(3')-IIIa catalyzed phosphate transfer.

While His188 is not a phosphate-accepting residue in a double displacement mechanism, it was not possible to definitively rule out the occurrence of a phospho-enzyme intermediate, for the reasons cited above. However, the results obtained during the study of APH(3')-IIIa were also consistent with a direct in-line phosphate transfer mechanism, therefore, in an effort to distinguish between these two mechanistic possibilities, I employed the PIX technique of Midelfort & Rose (1976).

In a double displacement mechanism, transfer of the γ-phosphate, to an enzyme nucleophile, which when followed by rotation of the β-phosphoryl group, results in the movement of the ^{18}O in the βγ-bridge position to a β-non-bridge position, during the reverse reaction (Figure 3.3). [γ-^{18}O]-ATP was incubated alone, in the presence of APH(3')-IIIa (APH), or in the presence of enzyme and tobramycin. Since tobramycin is a 4,6-disubstituted AG that lacks a 3'-hydroxyl, and can therefore act as a competitive inhibitor of APH(3')-IIIa, I tested for the presence of a PIX reaction in the presence of tobramycin because it was hypothesized that phosphate transfer to an enzyme nucleophile might not occur unless an AG was also bound to the enzyme. If a PIX reaction had occurred, new signals, shifted downfield (to your left), from those corresponding to the γ-phosphate, would have been expected, due to the movement of ^{16}O from the β non-bridge position to the βγ-bridge position. Similarly, new signals

shifted upfield from those corresponding to the β-phosphate would have been expected as ^{18}O moves from the βγ-bridge position to a β non-bridge position. The fact that no PIX was detected is inconsistent with the existence of a phospho-enzyme intermediate. The lack of a PIX is consistent with results obtained for hexokinase and pyruvate kinase, two phosphotransferases that catalyze the direct transfer of the γ-phosphate of ATP to a substrate hydroxyl, and that lack a PIX (Rose, 1980; Hassett *et al*, 1982). Thus, the most likely route of phosphoryl transfer is the direct transfer of the γ-phosphate of ATP to an AG hydroxyl (Figure 3.2B).

3.5. Conclusions.

While the modification of His residues, by DEPC, can inactivate APH(3')-IIIa, my initial analysis of the catalytic mechanism of this enzyme, facilitated by the generation of His to Ala mutants, clearly indicates that His78, His82, and His123 are not required for the catalytic activity of this enzyme. Also, this analysis suggests that while His188 is absolutely conserved among the APH family of enzymes it is also not required for catalysis, but is instead required to direct optimal protein folding. My initial analysis of the catalytic mechanism of APH(3')-IIIa also included the use of PIX experiments to define the mechanism of phosphate transfer, and the results described herein, are only consistent with the direct in-line transfer of the γ-phosphate of ATP, to an AG hydroxyl. The PIX experiments also rule out the generation of a dissociative intermediate (see Chapter 4), along the reaction coordinate of this enzyme.

Since it was known that APH(3')-IIIa did not to employ a double displacement mechanism, the primary structure identities, originally noted between the APHs and other phosphotransferases (Brenner, 1987; Heinzl *et al*, 1988; Martin *et al*, 1988), began to take on new meaning, and suggested that other conserved residues are likely to be important for catalysis. The homology to eukaryotic protein kinases (ePKs) led to the suggestion that the catalytic mechanism of APH(3')-IIIa would resemble the catalytic mechanism of these enzymes, and it was specifically postulated that Asp190, in APH(3')-IIIa, could have a role that is similar to the corresponding residue, Asp166, in cyclic AMP dependent protein kinase (PKA) (Thompson *et al*, 1996). Asp166 is thought to act as a catalytic base (Taylor *et al*, 1995). Such a hypothesis is supported by the finding that a PKA Asp166Ala mutant is markedly impaired in its ability to phosphorylate peptide substrates (Gibbs & Zoller, 1991). This hypothesis is also supported by crystal structures of a number of protein kinases, including the ternary complex crystal structure of PKA, wherein, this residue is positioned close to both the γ-phosphate of ATP, and the peptide substrate (Zheng *et al*, 1993). Experiments describing the actual role of Asp190 in the catalytic mechanism of APH(3')-IIIa are discussed in Chapter 4.

Subsequent to this work, the crystal structure of APH(3')-IIIa bound to ADP was determined (Hon *et al*, 1997), and the structural homology to eukaryotic protein kinases that was observed, validated the hypothesis predicted by the primary structure homology to the ePKs. The crystal structure of this enzyme also validated the work described herein. With the determination of the APH(3')-IIIa•ADP crystal structure, the roles of

the four His residues, present in APH(3')-IIIa, can now be more clearly defined (Figure 3.9). His78 and His82 are present in the N-terminal lobe of the enzyme, far from the site of ADP binding, which presumably is representative of the active site of the enzyme. This finding validates my analysis of the steady state kinetic parameters determined for the APH(3')-IIIa^{H78A} and APH(3')-IIIa^{H82A}, which indicated that these residues were not important for catalysis. His123 is present in the C-terminal lobe, and is also far from the active site of the enzyme, again validating the near wild type steady state kinetic parameters determined for the APH(3')-IIIa^{H123A} mutant. In comparison to these residues, His188 is relatively close to the nucleotide binding site, but as the APH(3')-IIIa•ADP crystal structure reveals, the functional group of this residue is likely too far (7-10 Å), from the site of phosphate transfer, to participate in the catalytic mechanism of this enzyme. These results thereby confirm that His188 is neither a phosphate-accepting residue nor is it involved in substrate binding and rate enhancement in the catalytic mechanism of APH(3')-IIIa. The structural homology to PKA (Hon *et al*, 1997), also helps to validate the phosphate transfer mechanism proposed herein, as PKA is known to transfer the γ-phosphate of ATP with inversion of configuration (Ho *et al*, 1988). Such a finding is most consistent with a direct in-line phosphate transfer mechanism.

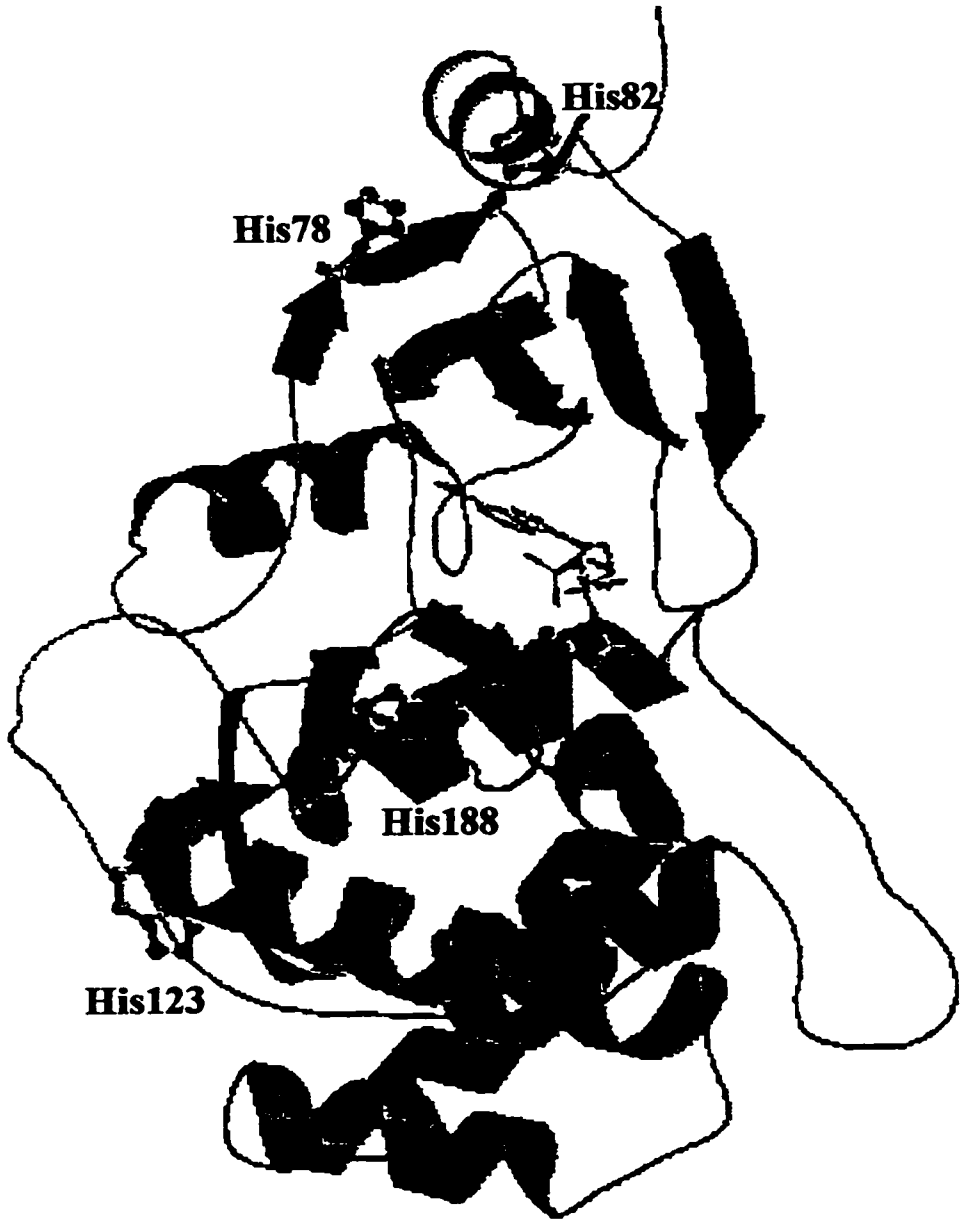

Figure 3.9. Structure of the APH(3')-IIIa monomer, bound to ATP. This structure is described in Thompson, *et al* (1999). The positions of the four histidines in this protein are highlighted. This figure was prepared using the MOLSCRIPT and RASTER3D programs (Kraulis, 1991; Merritt and Murphy, 1994).

3.6. References.

Brenner, S. (1987). Phosphotransferase sequence homology. *Nature* **329**, 21.

Blazquez, J., Davies, J., & Moreno, F. (1991). Mutations in the *aphA-2* gene of transposon Tn*5* mapping within the regions highly conserved in aminoglycoside-phosphotransferases strongly reduce aminoglycoside resistance. *Mol. Microbiol.* **5**, 1511-1518.

Gibbs, C.S. & Zoller, M.J. (1991). Rational scanning mutagenesis of a protein kinase identifies functional regions involved in catalysis and substrate interactions. *J. Biol. Chem.* **266**, 8923-8931.

Hassett, A., Blattler, W., & Knowles, J.R. (1982). Pyruvate kinase: is the mechanism of phospho transfer associative or dissociative? *Biochemistry* **21**, 6335-6340.

Herschlag, D., & Jencks, W.P. (1989b). Evidence that metaphosphate monoanion is not an intermediate in solvolysis reactions in aqueous solution. *J. Am. Chem. Soc.* **111**, 7579-7586.

Ho, M.F., Bramson, H.N., Hansen, D.E., Knowles, J.R., & Kaiser, E.T. (1988). Stereochemical course of the phospho group transfer catalyzed by cAMP-dependent protein kinase. *J. Am. Chem Soc.* **110**, 2680-2681.

Hon, W-C., McKay, G.A., Thompson, P.R., Sweet, R.M., Yang, D.S.C., Wright, G.D. & Berghuis, A.M. (1997). Structure of an enzyme required for aminoglycoside resistance reveals homology to eukaryotic protein kinases. *Cell* **89**, 887-895.

Kocabiyik, S., & Perlin, M.H. (1992). Site-specific mutations of conserved C-terminal residues in aminoglycoside 3'-phosphotransferase II: phenotypic and structural analysis of mutant enzymes. *Biochem. Biophys. Res. Comm.* **185**, 925-931.

Kraulis, P.J. (1991). MOLSCRIPT: a program to produce both detailed and schematic plots of protein structures. *J. Appl. Cryst.* **24**, 946-950.

Kunkel, T.A. (1985). Rapid and efficient site specific mutagenesis without phenotypic selection. *Proc. Natl. Acad. Sci. USA* **82**, 488-492.

Martin, P., Jullien, E., & Courvalin, P. (1988). Nucleotide sequence of *Acinetobacter baumannii aphA-6* gene: evolutionary and functional implications of sequence homologies with nucleotide-binding proteins, kinases and other aminoglycoside-modifying enzymes. *Mol. Microbiol.* **2**, 615-625.

McKay, G.A., Thompson, P.R. & Wright, G.D. (1994). Broad spectrum aminoglycoside phosphotransferase type III from *Enterococcus*: Overexpression, purification, and substrate specificity. *Biochemistry* **33**, 6936-6944.

McKay, G.A. & Wright, G.D. (1995). Kinetic mechanism of aminoglycoside phosphotransferase Type IIIa: Evidence for a Theorell-Chance kinetic mechanism. *J. Biol. Chem.* **270**, 24686-24692.

McKay, G.A. & Wright, G.D. (1996). Catalytic mechanism of enterococcal kanamycin kinase (APH(3')-IIIa): Viscosity, thio, and solvent isotope effects support a Theorell-Chance mechanism. *Biochemistry*, **35**, 8680-8685.

Merritt, E.A., & Murphy, M.E.P. (1994). RASTER3D version 2.0: a program for photorealistic molecular graphics. *Acta Cryst.* **D50**, 869-873.

Midelfort, C.F., & Rose, I.A. (1976). A stereochemical method for the detection of ATP terminal phosphate transfer in enzymatic reactions. *J. Biol. Chem.* **251**, 5881-5887.

Miles, E.W. (1977). Modification of histidyl residues in proteins by diethylpyrocarbonate. *Methods Enzymol.* **47**, 431-442.

Heinzl, P., Werbitzky, O., Distler, J., & Piepersberg, W. (1988). A second streptomycin-resistance gene from *Streptomyces griseus* codes for streptomycin-3"-phosphotransferase. *Arch. Microbiol.* **150**, 184-192.

Raushel, F.M., & Villafranca, J.J. (1980). Phosphorous-31 nuclear magnetic resonance application to positional isotope exchange reactions catalyzed by *Escherichia coli* carbamoyl-phosphate synthetase: analysis of forward and reverse enzymatic reactions. *Biochemistry* **19**, 3170-3174.

Raushel, F.M., & Villafranca, J.J. (1988). Positional isotope exchange. *CRC Crit. Rev, Biochem.* **23**, 1-26.

Risley, J.M., & Van Etten, R.L. (1978). A convenient synthesis of crystalline potassium phosphate-$^{18}O_4$ (monobasic) of high isotopic purity. *J. Label. Compounds Radiopharm.* **15**, 533-538.

Rose, I.A. (1980). Mechanism of phosphoryl transfer by hexokinase. *Biochem. Biophys. Res. Comm.* **94**, 573-578.

Sarkar, G., & Sommer, S.S. (1990). The 'megaprimer' method of site-directed mutagenesis. *Biotechniques* **8**, 404-407.

Schramm, V.L. (1998). Enzymatic transition states and transition state analog design. *Ann. Rev. Biochem.* **67**, 693-720.

Taylor, S.S., Radzio-Andzelm, E., & Hunter, T. (1995). How do protein kinases discriminate between serine/threonine and tyrosine? Structural insights from the insulin receptor protein-tyrosine kinase. *FASEB J.* **9**, 1255-1266.

Thompson, P.R., Hughes, D.W., & Wright, G.D. (1996). Mechanism of aminoglycoside 3'-phosphotransferase type IIIa: His188 is not a phosphate-accepting residue. *Chem. Biol.* **3**, 747-755.

Villafranca, J.J. (1989). Positional isotope exchange using phosphorus-31 nuclear magnetic resonance. *Methods Enzymol.* **177**, 390-403.

von der Saal, W., Anderson, P.M., & Villafranca, J.J. (1985). Mechanistic investigations of *Escherichia coli* cytidine-5'-triphosphate synthetase. Detection of an intermediate by positional isotope exchange experiments. *J. Biol. Chem.* **260**, 14933-14997.

Wehrli, W.E., Verheyden, D.L.M., & Moffatt, J.G. (1965). Dismutation reactions of nucleoside polyphosphates. II. Specific chemical synthesis of α-, β-, and γ-^{32}P-nucleoside 5'triphosphates. *J. Am. Chem. Soc.* **87**, 2265-2277.

Wimmer, M.J., Rose, I.A., Powers, S.G., & Meister, A. (1979). Evidence that carboxyphosphate is a kinetically competent intermediate in the carbamyl phosphate synthetase reaction. *J. Biol. Chem.* **254**, 1854-1859.

Zheng, J., Knighton, D.R., Eyck, L.F.T., Karlsson, R., Xuong, N-h., Taylor, S.S., Sowadski, J.M. (1993). Crystal structure of the catalytic subunit of cAMP-dependent protein kinase complexed with MgATP and peptide inhibitor. *Biochemistry* **32**, 2154-2161.

Chapter 4

Structure/Function Analysis of APH(3')-IIIa

Parts of this chapter have been adapted from

Hon, W-C., McKay, G.A., Thompson, P.R., Sweet, R.M.,
Yang, D.S.C., Wright, G.D. & Berghuis, A.M.
Cell, 1997, vol. 89, pp. 887-895.

&

Daigle, D.M., McKay, G.A., Thompson, P.R. & Wright, G.D.
Chemistry & Biology, 1999, vol. 6, pp. 11-18.

The author of this thesis obtained all of the results, presented in this chapter, unless otherwise noted.

CHAPTER 4: Structure/Function Analysis of APH(3')-IIIa

4.1: Introduction

As discussed in Chapters 1 and 3, a thorough understanding of the catalytic mechanism of an enzyme-catalyzed reaction is important for the design of transition state (TS) analogues. Therefore, our lab has engaged in an effort to thoroughly understand the catalytic mechanism of APH(3')-IIIa. I have previously shown that APH(3')-IIIa transfers the γ-phosphate of ATP to an AG hydroxyl through a mechanism that is most consistent with a direct in-line transfer (Thompson *et al*, 1996a; Chapter 3). This result, combined with the limited amount of amino acid sequence homology that exists between ePKs and APHs (Figure 4.1), suggested that the catalytic mechanism of this enzyme would likely resemble the catalytic mechanism of the ePKs. Similarities in the primary structures of these two classes of proteins had been previously noted (Brenner, 1987; Heinzl *et al*, 1988). This homology, combined with the eventual determination of the structure of APH(3')-IIIa, bound to ADP (Hon *et al*, 1997), aided the identification of potential catalytically important residues. These include Lys44 and Asp190, which have roles in ATP binding and phosphate transfer, respectively (Hon *et al*, 1997). Residues, corresponding to Asp190 in ePKs, have been described as putative catalytic bases (Taylor *et al*, 1995).

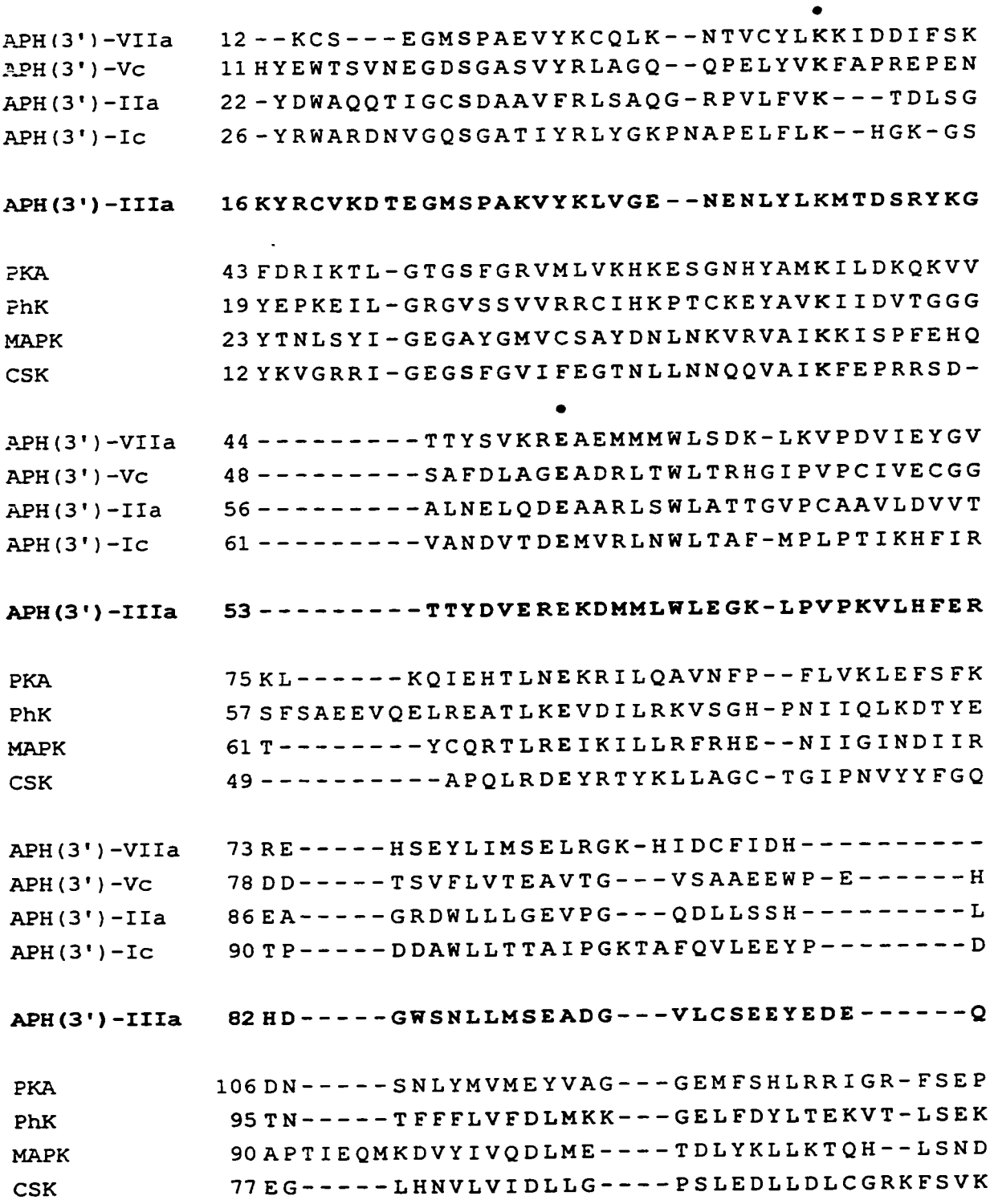

Figure 4.1. See below for alignment details.

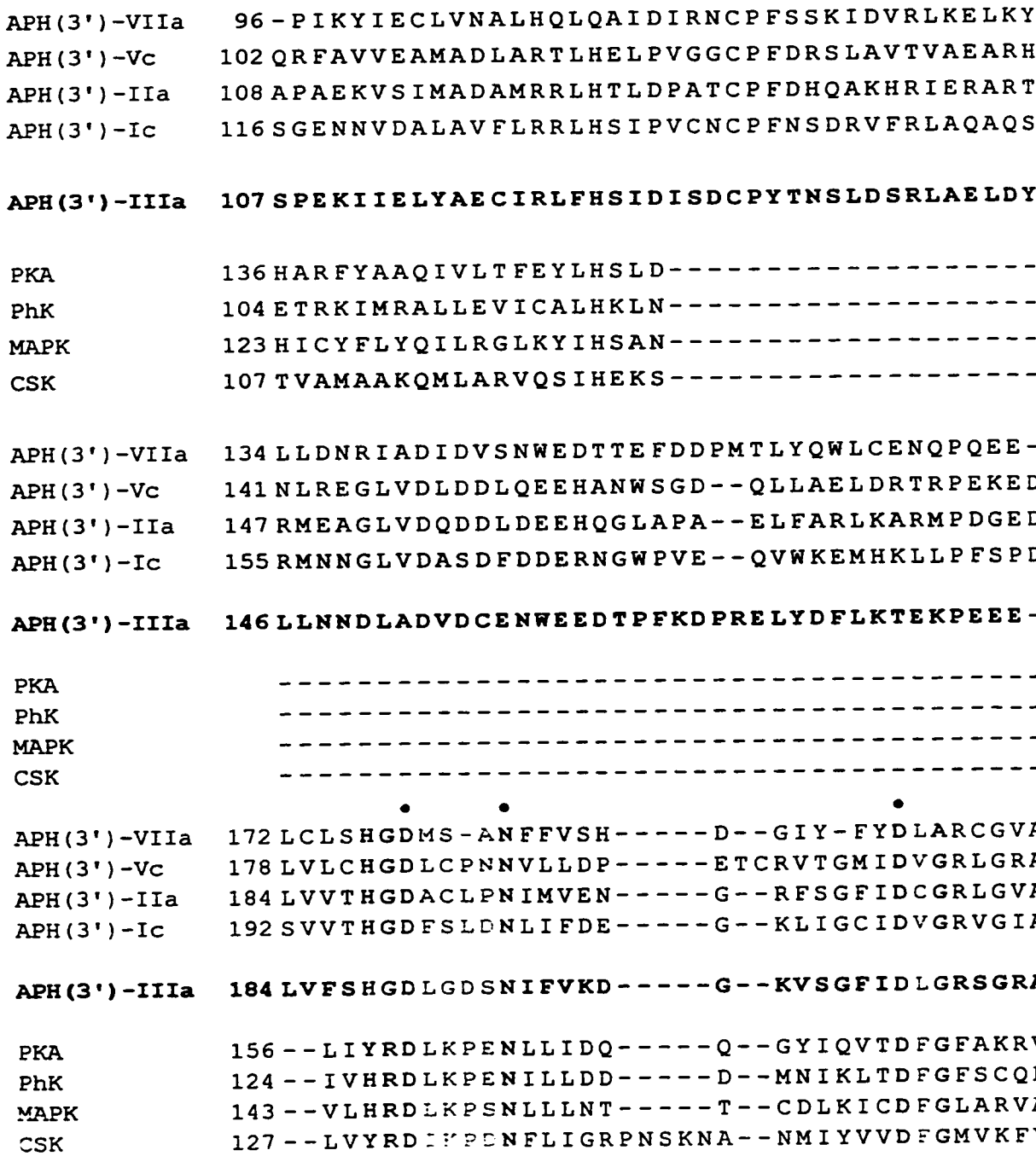

Figure 4.1. Continued.

```
APH(3')-VIIa   201 ------------------
APH(3')-Vc     211 ------------------
APH(3')-IIa    247 ------------------
APH(3')-Ic     223 ------------------

APH(3')-IIIa   215 ------------------

PKA            186 -KG------RTWT---LC
PhK            154 -DPGE----KLRE---VC
MAPK           173 -DPDHDHTGFLTE---YV
CSK            162 RDPVTKQHIPYREKKNLS
```

Figure 4.1. Sequence homology between 3'-aminoglycoside phosphotransferases and eukaryotic protein kinases. Absolutely conserved residues are shown in red (•), highly conserved residues are shown in blue (o), and partially conserved residues are shown in dark yellow(□). The APH(3') were aligned using Clustal W (Thompson *et al*, 1994). The primary structures of the ePKs have previously been aligned to APH(3')-IIIa, using a structure based method, and that alignment is adapted here (Hon *et al*, 1997). Going from top to bottom the amino acid sequences for the APH(3') proteins are from: Lee *et al*, 1991; Beck *et al*, 1982; Salauze *et al*, 1991; Tenover *et al*, 1988; Gray & Fitch, 1983 and Trieu-Cuot & Courvalin, 1983. The primary structure for PKA is that of the *Mus musculus* isoform (Knighton *et al*, 1991). The primary structure for casein kinase (CSK) is that of *Schizosaccharomyces pombe* (Xu *et al*, 1995). The primary structure for mitogen activated protein kinase (MAPK) is that of *Rattus norvegicus* (Her, *et al*, 1991). The primary structure of phosphorylase kinase (PhK) is from *Oryctolagus cuniculus* (Owen, *et al*, 1995b).

Site directed mutagenesis work, research that showed that APH(3')-IIIa has a protein kinase activity (Daigle *et al*, 1999), and the fact that this enzyme is inhibited by protein kinase inhibitors (Daigle *et al*, 1997), validated our prediction about the catalytic mechanism employed by APHs (Thompson *et al*, 1996). Thus, the catalytic mechanism of the APHs and ePKs are likely similar.

Phosphoryl transfer is thought to occur through one of two possible routes (reviewed in Knowles, 1980). One route is an associative reaction mechanism, whereas the second route is a dissociative reaction mechanism. In an associative mechanism,

there is considerable bond formation from the incoming nucleophile to the phosphoryl center, and little bond breakage between the phosphoryl center and the leaving group. The TS intermediate is thus trigonal bipyrimidal and has a formal charge of –3 (Figure 4.2A).

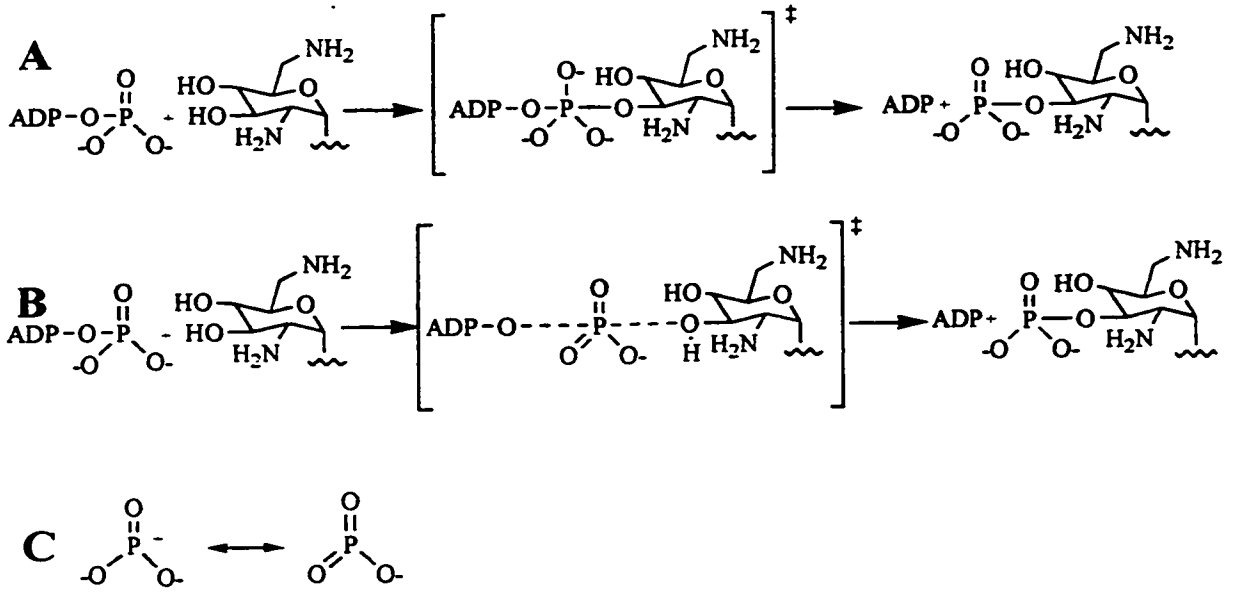

Figure 4.2: Potential mechanisms of phosphoryl transfer. A. An associative reaction. **B.** A dissociative reaction. **C.** The different resonance forms of a metaphosphate intermediate.

The TS of this reaction is analogous to a Sn2 reaction to a carbon center and is thus a compact one. Thus, phosphate transfer occurs with inversion of configuration of the pro-pro-chiral phosphorous. Substrate deprotonation is thought to be important for an associative mechanism, and this type of reaction mechanism is favored for phosphate transfer reactions involving phosphodiesters and phosphotriesters (reviewed in Khan & Kirby, 1970; Knowles, 1980; Mildvan & Fry, 1987; Cleland & Hengge, 1995). In a dissociative mechanism, there is complete bond breakage between the leaving group and

the phosphoryl center, and no bond formation with the incoming nucleophile (Figure 4.2B). In such a mechanism, a trigonal planar monoanionic metaphosphate intermediate is formed (Figure 4.2C).

A metaphosphate intermediate is highly electrophilic, and hence aids the transfer of the phosphate group to a nucleophile. Metaphosphate monoanion transfer can occur with either retention or inversion of configuration. In this type of reaction mechanism, substrate deprotonation would not be required until after phosphate transfer has occurred (Mildvan & Fry, 1987; Herschlag & Jencks, 1989a; Maegley *et al*, 1996). However, in solution phosphoryl transfer of phosphate monoesters occurs with inversion of configuration (Buchwald & Knowles, 1982; Buchwald *et al*, 1984), which would suggest that a metaphosphate is not the route of phosphoryl transfer for phosphate monoesters. Furthermore, a completely dissociative transition state is unlikely, as evidence to date indicates that a metaphosphate monoanion does not exist in solution (Herschlag & Jencks, 1989b).

While on the face of it, these results appear to argue in favor of an associative mechanism for phosphate monoesters, they do not, in fact, rule out a dissociative-like mechanism[1] where there is considerable, but not complete bond breakage, and little, but not zero, bond formation in the TS. In a dissociative-like mechanism, phosphate

[1] For the purposes of this thesis a dissociative-like transition state is one where the bond to the leaving group is considerably broken prior to nucleophilic attack and there is also little bond formation to the incoming nucleophile. For a classical Sn2 type reaction there is 50% bond cleavage and 50% bond formation in the transition state. Thus a reaction with more than 50% bond breakage and less than 50% bond formation is beginning to become more dissociative-like than associative like. Thus a dissociative-like transition state is one where the percentage of bond breakage begins to approach 100 and the percentage of bond formation approaches 0 (Mildvan, 1997).

monoester transfer would be expected to occur with inversion of configuration. Furthermore, in solution, this type of reaction mechanism appears to be favored by phosphate monoesters (Kirby & Vargolis, 1967; Herschlag & Jencks, 1989a; Cleland & Hengge, 1995). Thus, based on the behaviour of small molecules in solution, the ePKs and the APHs would be expected to transfer the γ-phosphate of ATP through a dissociative-like mechanism. However, there is great debate about the validity of such a claim.

The crystal structures of a number of proteins involved in phosphate monoester cleavage, crystallized in the presence of the TS mimics BeF_3 or AlF_3/AlF_4, suggest that the reaction coordinate distance is too small to be consistent with a dissociative reaction mechanism (reviewed in Matte *et al*, 1998). For a fully dissociative reaction, the reaction coordinate distance should be greater than 6.3 Å, the sum of the Van der Waals radii of the incoming and departing atoms involved in the reaction (Mildvan, 1997). Values relating the reaction coordinate distance to the percent associativity of a reaction can be determined. These values are obtained by halving the ground-state reaction coordinate distance and applying that value to Equation 1 (the ground-state reaction coordinate distance is halved because one assumes a symmetrical TS),

$$D_{(n)} = D_{(1)} - 0.60 \log_{(n)}, \quad \text{(Equation 4.1)}$$

where (n) is the fractional bond number, $D_{(n)}$ is the bond distance and $D_{(1)}$ is the single bond distance, which in this case is 1.73 Å, the P-O bond distance. Using this methodology, it was possible to estimate that the cAMP dependent protein kinase (PKA) catalyzed reaction is ~24% associative. Distances were obtained from Zheng *et al*

(1993), as determined from a crystal structure of this enzyme bound to MgATP and a peptide inhibitor. Thus, this reaction is more associative-like than dissociative-like. However, Mildvan (1997), using an alternate set of coordinates, showed that the reaction catalyzed by PKA is only 8.4% associative, which indicates the reaction is 91.6% dissociative. Thus it appears, using this methodology, that PKA employs a dissociative-like mechanism. Thus, because of the inconsistencies observed using this type of methodology we regard measurements of this type to be fairly speculative. The argument that these types of measurements are speculative is especially compelling if one considers that it is unclear how well BeF_3, AlF_4, and AlF_3 truly reflect the TS of a phosphate transfer reaction. BeF_3 is tetrahedral, AlF_4 is octahedral and AlF_3 is trigonal bipyrimidal. While AlF_3 likely most closely resembles the TS for an associative reaction, it is not clear why enzymes show a preference for either AlF_3 or AlF_4 (Wittinghofer, 1997). Although recently it has been suggested that the pH of the solution could play a role in selecting for either of these two species (Schlichting & Reinstein, 1999). Nevertheless, these TS "mimics" may in fact induce the enzyme to structurally reorganize, albeit in a subtle manner, in order to bind these specific compounds, thereby making the reaction coordinate distance estimates suspect at best. If these TS "mimics" induce the enzyme to adopt such a conformation, then these compounds are not likely to accurately reflect the TS of phosphoryl transfer. The adoption of a conformation that does not accurately reflect the TS is not unreasonable, as the time scale of data collection for X-ray structure determination is long (minutes to days), whereas the lifetime of a TS is extremely short (ca. 10^{-13}s).

While the crystallographic evidence for kinases may point to an associative mechanism, studies of enzymatic phosphate monoester transfer reactions in solution point to a dissociative-like reaction mechanism. These studies have involved the determination of kinetic isotope effects and linear free energy relationships (Weiss & Cleland, 1989; Cleland & Hengge, 1995; Hollfelder & Herschlag, 1995; Hengge *et al*, 1995; Kim & Cole, 1997; Kim & Cole, 1998; Admiraal *et al*, 1999). Therefore, with the overwhelming evidence from solution studies, one would expect that APH(3')-IIIa employs a dissociative-like TS. For APH(3')-IIIa, a fully dissociative transition state is unlikely as PIX was not observed when this enzyme was incubated with γ-^{18}O-ATP alone or γ-^{18}O-ATP in combination with a non-phosphorylatable AG substrate analogue (Thompson *et al*, 1996a). However, a metaphosphate-like intermediate would not be expected to undergo PIX. Thus, a dissociative-like TS cannot completely be ruled out.

There is also great debate about the importance of a catalytic base to the reaction mechanism of these enzymes. For the reasons cited above, this debate has an impact on whether the TS is more likely to be an associative or a dissociative one. Presteady state kinetic studies on PKA indicate a pH independence on the 'burst' kinetics between pH 6 and pH 9 (Zhou & Adams, 1997). If a catalytic base were important to the catalytic mechanism of this enzyme, then one would expect a significant rate enhancement, up to 1000-fold. Such an increase would reflect the increased proportion of the peptide substrate in the anionic form, which increases as the pH is increased. Since this was not observed, the rate of reaction is unlikely to be promoted by general base catalysis. The 'burst' rate was also unaffected by the addition of D_2O (Zhou & Adams,

1997). The lack of a solvent isotope effect is also inconsistent with a role for a general base catalyst. The Zhou & Adams (1997) suggest, but do not favor, that the lack of a pH effect could be obscured if the 'burst' rate measured was not the phosphoryl transfer step, but a metal ion dependent conformational change.

There is also debate about the relative importance of the 'putative' catalytic base, Asp314 (equivalent to Asp190 in APH(3')-IIIa), in the protein tyrosine kinase C-terminal sarc kinase (CSK). The importance of general base catalysis to the reaction mechanism of this enzyme was examined, using a trifluorotyrosine containing peptide (Cole *et al*, 1995). The pKa of the trifluorotyrosine hydroxyl present in this peptide analogue was measured to be 6.2. Therefore, if general base catalysis were important to the catalytic mechanism of this enzyme, one would expect a rate enhancement of up to 10^4. This estimate of the rate enhancement reflects the difference in pKas of the tyrosine hydroxyl and the trifluorotyrosine hydroxyl. The rate of reaction was only 1.3-fold higher when this peptide analogue was examined as a substrate, suggesting that tyrosine deprotonation is not required to promote catalysis (Cole *et al*, 1995). However, the actual rate enhancement offered by the trifluorotyrosine analogue may be obscured by the fact that ADP release is partially rate limiting with CSK, when Mn^{2+} is used as the divalent cation (Cole *et al*, 1994). Nevertheless, the true role of the catalytic base is questionable especially when one considers the fact that the solvent isotope effect of the CSK^{D314E} mutant is near unity and actually slightly inverse. Since the k_{cat} of the CSK^{D314E} is ~10^5-fold lower than the wild type enzyme, phosphate transfer should be fully rate limiting, and if substrate deprotonation was important for phosphoryl transfer then the solvent

isotope effect should be greater than 2 (Cole *et al*, 1995). A tetrafluorotyrosine analogue has also been used to probe the mechanism of CSK(Kim & Cole, 1997). The pKa of this peptide substrate analogue is 5.2, which indicates that the phenoxide anion should predominate (> 99%) at the pH used for kinetic assays. The tetrafluorotyrosine analogue is phosphorylated at least 10 times less efficiently than a tyrosine containing peptide. However, by decreasing the pH, which decreases the amount of this analogue in the phenoxide form, it is possible to restore the activity of CSK towards this compound (Kim & Cole, 1997). These assays were performed in the presence of magnesium, where phosphate transfer chemistry is presumed to be largely rate limiting (Kim & Cole, 1997; Grace *et al*, 1997). Thus, the substrate of CSK is a protonated phenol. These results argue in favor of a dissociative-like TS, where substrate deprotonation is not expected to be important for catalysis until after phosphate transfer has occurred, and when product deprotonation should be relatively easy. These data, combined with the determination of the Brønsted nucleophile (β_{nuc}) and leaving group (β_{lg}) coefficients, suggest that CSK employs a dissociative-like TS. For CSK the β_{nuc} is small (<0.1) and the β_{lg} is slightly negative (-0.33). Both of these values are consistent with those observed in solution for phosphate monoester hydrolysis (Kim & Cole, 1997; Kim & Cole, 1998). Thus, by inference, the rate enhancement afforded by Asp190, the putative catalytic base of APH(3')-IIIa, would not be expected to be large and indeed it is not (Hon *et al*, 1997; and see below).

Since the AG substrates of the APHs are not easily amenable to chemical substitution, the fluorine substitution studies described for CSK are not readily possible

for APH(3')-IIIa. Similarly, the lack of ready access to the equipment to examine the pre-steady state kinetics of this enzyme has precluded my ability to extend the studies described above for PKA to APH(3')-IIIa. However, given the available precedents I have assumed that the TS of APH(3')-IIIa would resemble a dissociative-like TS. If this is indeed the case then a number of questions arise. These include 1) what are the requirements for the generation of a dissociative-like TS; 2) how does APH(3')-IIIa stabilize such a TS; and 3) how does the enzyme promote a dissociative-like TS? One requirement for a metaphosphate-like intermediate is the lengthening of the Pγ-O bond. Hydrogen bonding and electrostatic interactions are also required to stabilize a metaphosphate-like TS; although the presence of too much positive charge around a metaphosphate is thought to be inhibitory and would render the TS more associative in character (Herschlag & Jencks, 1989a; Maegley *et al*, 1996; and references cited therein). With those requirements in mind, I examined the contribution of the residues lining the catalytic core of APH(3')-IIIa to rate enhancement, with the ultimate goals being a better understanding of how the enzyme stabilizes the TS, and, as well, how the enzyme promotes the formation of that TS. Since the residues I examined in this study are also conserved among the ePKs, an understanding of the contribution of those residues to catalysis should also have an impact on the understanding of the catalytic mechanism of ePKs. Herein I describe the effect mutating 4 out of the 5 residues, Glu60, Asp190, Asn195 and Asp208, which are absolutely conserved between ePKs and the APHs (Figure 4.1; the position of these residues in the active site of APH(3')-IIIa can be seen in Figure 4.3).

The effect of mutating the fifth absolutely conserved residue, Lys44, has been previously described (Hon *et al*, 1997). Herein, I also describe the effect of mutating Ser27, a residue that is absolutely conserved among the APH(3'), but only partially conserved among the ePKs (Figure 4.1). I further describe the divalent metal dependence of APH(3')-IIIa and the effect of using a sulfur substituted ATP analogue on the activity of this enzyme. These data, taken together with partial proteolysis studies point to a biomechanical model for phosphate transfer. This model for phosphate transfer is not necessarily restricted to the APHs, and likely also holds for the ePKs.

4.2 Materials and Methods

4.2.1 Chemicals

Ribostamycin, lividomycin, neomycin B, butirosin, amikacin, β-NADH, phosphoenol pyruvate, and PK/LDH enzymes were from Sigma (St. Louis, MO). ATPγ-S was from Boehringer-Mannheim and kanamycin A was from Bioshop (Burlington, ON, Canada). All oligonucleotide primers were synthesized at the Central Facility of the Institute for Molecular Biology and Biotechnology, McMaster University.

4.2.2 Site Directed Mutagenesis.

The generation of the APH(3')-IIIa^{S27A} and APH(3')-IIIa^{S27P} mutants was undertaken using the Quik-Change mutagenesis method (Stratagene, La Jolla, CA). The degenerate oligonucleotide, 5'-GATACGGAAGGAATGC(A,G)CTCCTGCTAAGG-3', and its reverse complement were designed to generate both the alanine and proline mutants from a single set of mutagenic primers. These primers in combination with 10, 15, or 25 ng of template DNA, i.e. pETSACG1 (Chapter 2), were used in *Pfu* DNA

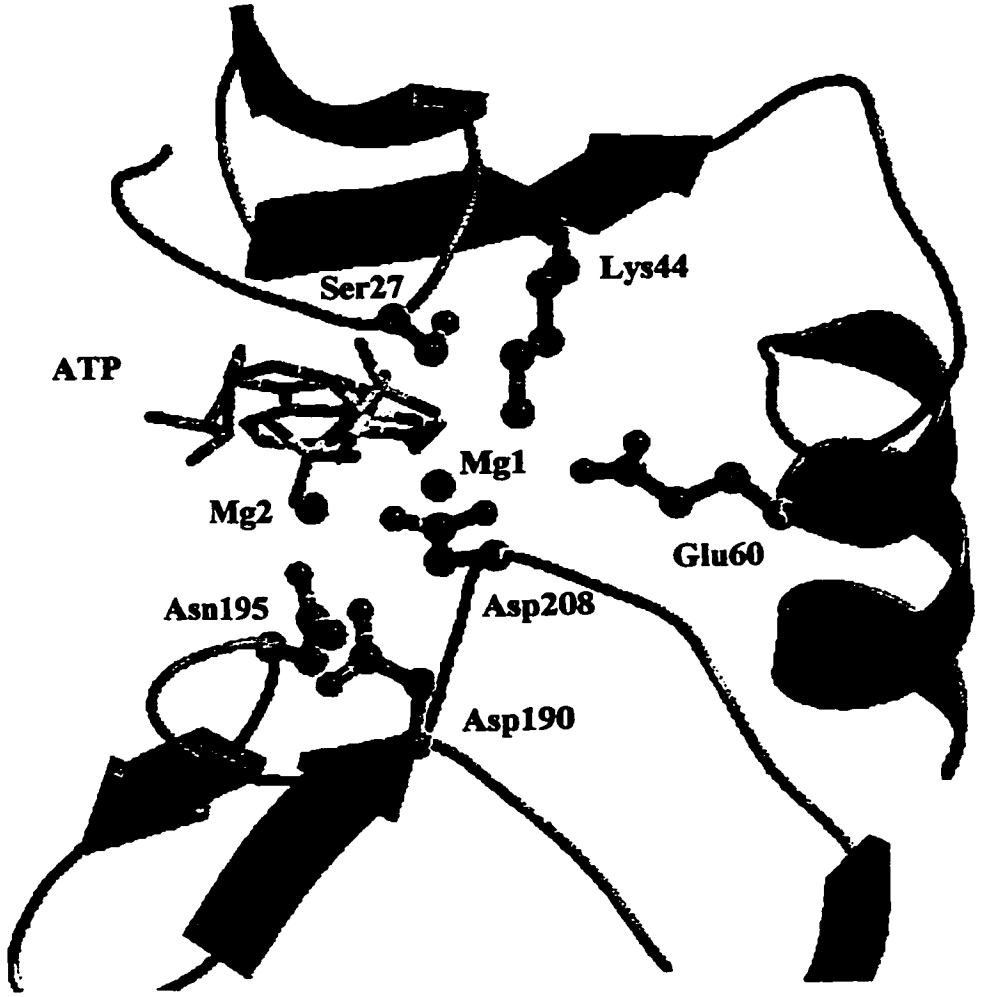

Figure 4.3: The Active Site of APH(3')-IIIa. The view depicted in Figure 4.4 is the one depicted here except in closeup. All the residues that are absolutely conserved among APHs and ePKs are shown: Lys44, Glu60, Asp190, Asn195, and Asp208. Also shown are the highly conserved residue Ser27 and Mg1 and Mg2. This Figure was prepared using the MOLSCRIPT and RASTER3D programs (Kraulis, 1991; Merritt and Murphy, 1994).

polymerase (Stratagene, La Jolla, CA) catalyzed PCR reactions. Mutant plasmid DNA was transformed into $CaCl_2$ competent *E. coli* MV1190 (BioRad) that were freshly prepared.

The Quik-Change mutagenesis protocol was also used to generate the APH(3')-IIIa^{N195A} and the APH(3')-IIIa^{D208A} mutants. A mutagenic oligonucleotide. 5'-ATCTT TCACAAAGATGGCGCTGTCTCCCAG-3' and its reverse complement, were used as primers to generate the former, whereas the latter mutant construct was generated using the mutagenic oligonucleotide, 5'-CTTCTCCCAAGAGCAATAAAGC-CAC-3', and its reverse complement.

The APH(3')-IIIa^{E60A} mutant was generated using the 'Megaprimer' methodology (Sarkar and Sommer, 1990). The mutagenic oligonucleotide, 5'-GTGGA ACGGGCAAAGGACATGATG-3', was used in PCR reactions in combination with the reverse primer, described in (McKay *et al*, 1994a; Chapter 3), to generate the megaprimer. The megaprimer was prepared as previously described (Chapter 3) and then used in combination with the forward primer (McKay *et al*, 1994a; Chapter 3), to regenerate the full length gene. In order to minimize the incorporation of undesired mutations during PCR reactions Vent DNA polymerase (New England BioLabs) was used. In both cases, plasmid pETSACG1 was used as the template for PCR reactions. The full length PCR product was then digested with *Nde*I and *Hind*III and ligated into similarly cut pET22b(+) (Novagen, Madison, WI).

The generation of the APH(3')-IIIa^{D190A}, APH(3')-IIIa^{D190N}, and the APH(3')-IIIa^{D190E} mutants was undertaken in a manner similar to that described for the generation

of the APH(3')-IIIa^{E60A}. In this case the forward primer was used in combination with the mutagenic oligonucleotides 5'-GCTGTCTCCCAGGGCGCCGTGGGAAAAGAC-3', 5'-GCTGTCTCCCAGGTT-GCCGTGGGAAAAGAC-3', and 5'-GCTGTCTCCCA GTTCGCCGTGGAAAAGAC-3', to generate the megaprimers for the APH(3')-IIIa^{D190A}, APH(3')-IIIa^{D190N}, and the APH(3')-IIIa^{D190E} mutants, respectively. Purified megaprimer and the reverse primer were then used to PCR amplify the full length genes. The APH(3')-IIIa^{D190A}, APH(3')-IIIa^{D190N}, and the APH(3')-IIIa^{D190E} PCR products were cloned into pET22b(+) from *Nde*I to *Hind*III. The resultant positive clones were then subcloned into M13mp18 from *Xba*I to *Hind*III and single stranded DNA obtained for nucleotide sequencing reactions. The sequencing reactions were carried out using the T7 DNA Polymerase Sequencing kit (Amersham Pharmacia Biotech, Montreal).

In all cases, nucleotide sequencing assessed the presence of the desired mutations, and all of the mutant constructs described, herein, were sequenced in their entirety to ensure that no other mutations had been incorporated during the PCR reaction. Unless otherwise noted, sequencing of mutant DNA was performed at the Central Facility of the Institute for Molecular Biology and Biotechnology, McMaster University. All of the plasmids described above were transformed into *E. coli* BL 21(DE3) to enable protein overexpression.

4.2.3 Purification of Mutant APH(3')-IIIa Proteins.

The purification of APH(3')-IIIa is described in Chapter 2, Section 2.2.3. The purification of mutant APH(3')-IIIa proteins followed essentially the same procedure and any deviations from that procedure are noted below.

For the purification of the APH(3')-IIIa^{S27A} mutant, proteins bound to the first Q Sepharose column were eluted, using a linear gradient of 30-50% Buffer B (50 mM Tris-HCl pH 8.0, 1 mM EDTA, 1 M NaCl), over at least 3 column volumes. In the second Q Sepharose purification step, the linear gradient was lowered to 20-40% Buffer B, over 4.5 column volumes. The protein was then concentrated using a Millipore 15 mL Ultrafree concentrator (10,000 molecular weight cutoff), for kinetic assays. To purify the APH(3')-IIIa^{S27P} mutant, the linear gradient of the first column was extended to at least 7 column volumes. The linear gradient of the second step was lowered to 20-40% Buffer B, but this time the gradient was extended to at least 7.5 column volumes. Similarly to the purification of the APH(3')-IIIa^{S27A} mutant, the APH(3')-IIIa^{S27P} mutant was concentrated for kinetic analysis.

For the purification of the APH(3')-IIIa^{E60A} mutant, the culture volume was increased from 1 L of LB-Amp (100μg/mL) to 4 L because it was expected, based upon the position of this residue in the crystal structure of the APH(3')-IIIa enzyme, that this residue might be important for protein folding. However, this was not the case. After cell lysis, the cleared lysate was applied to the first Q Sepharose column, and eluted over at least 2.5 column volumes. In order to further purify this mutant protein, the second Q Sepharose step was omitted, and the dialyzed protein fraction split into two and applied to a 1 x 10 cm Macro Prep Q (BioRad, Mississauga, ON, Canada) column, equilibrated in Buffer A. Bound proteins were eluted at a flow rate of 2 mL/min, using a linear gradient of 10-40% Buffer B, over at least 8.5 column volumes. The same approach was taken to

purify the APH(3')-IIIa^{D190A} mutant, except that the culture volume was only 1 L, and the Macro Prep Q step utilized a 20-50% linear gradient.

The APH(3')-IIIa^{D190N} mutant was purified similarly to wild type APH(3')-IIIa, except that the 30-50% linear gradient, used in the first Q Sepharose step, was allowed to proceed over 3 column volumes. For the second step, bound proteins were eluted using the same gradient as that described for the first step. Pure protein was obtained by applying concentrated protein from the second Q Sepharose step to a Superdex 200 (HR 10/30) (Amersham Pharmacia Biotech), equilibrated with 50 mM Tris-HCl pH 8.0, 1 mM EDTA, 200 mM NaCl, and 0.1 mM dithiothreitol. The flow rate was 0.4 mL/min and 1 minute fractions were collected. The APH(3')-IIIa^{D190E} mutant was purified in the same manner as that described for the purification of the APH(3')-IIIa^{D190N} mutant.

In order to obtain the APH(3')-IIIa^{N195A} mutant in pure form, the cleared lysate was applied to the first Q Sepharose column, and bound proteins eluted, in the manner described for the purification of the APH(3')-IIIa^{D190N} mutant. For the second Q Sepharose step, bound proteins were eluted using a 30-50% gradient over 6 column volumes. The APH(3')-IIIa^{D208A} mutant was purified similarly to the wild type enzyme, except that the linear gradient for the first Q sepharose column was 20-50%, over approximately 4 column volumes. Bound proteins were eluted from the second Q Sepharose column using a 30-50% linear gradient over 4 column volumes.

4.2.4 Kinetic Assay

The kinetic assay employed measures the production of ADP, generated upon AG phosphorylation (Reaction 1).

$$\text{Aminoglycoside} + \text{ATP} \longrightarrow \text{Aminoglycoside-PO}_4^{2-} + \text{ADP} \qquad \text{(Reaction 1)}$$

The production of ADP is coupled to the oxidation of β-NADH through the enzymes pyruvate kinase and lactate dehydrogenase (Reactions 2 and 3).

$$\text{ADP} + \text{Phosphoenolpyruvate} \longrightarrow \text{Pyruvate} + \text{ATP} \qquad \text{(Reaction 2)}$$

$$\text{Pyruvate} + \beta\text{-NADH} \longrightarrow \text{lactate} + \text{NAD}^+ \qquad \text{(Reaction 3)}$$

The rate of ADP production was determined by monitoring the decrease in absorbance at 340 nm. The change in absorbance over time was converted to nmole/min using the molar extinction coefficient of β-NADH (6300 $M^{-1}cm^{-1}$). Initial rates were fitted by nonlinear least fit squares to Equation 2,

$$v = (k_{cat}/E_t)[S]/(K_m + [S]) \qquad \text{(Eq. 2)},$$

or Equation 3,

$$v = (k_{cat}/E_t)[S]/(K_m + [S])(1 + [S]/K_i)) \qquad \text{(Eq. 3)},$$

if substrate inhibition was detected using the Grafit software suite (version 3.0) (Leatherbarrow, 1992). Kinetic assays were performed in duplicate at 37° C in 50 mM HEPES pH 7.5, 40 mM KCl, 10 mM $MgCl_2$, 0.2 mg/mL β-NADH, 0.6 mg/mL phosphoenol pyruvate (PEP), 3.7 U/mL pyruvate kinase (PK), and 5.2 U/mL lactate dehydrogenase (LDH). Both the fixed and variable substrates were pre-incubated in the assay solution and then enzyme was added to initiate the reaction. ATP was fixed at 1

mM and kanamycin A was fixed at 100 μM when measuring the steady state kinetic parameters for AGs substrates and ATP, respectively.

4.2.5 Metal Ion Dependence

The magnesium ion dependence, of wild type and mutant APH(3')-IIIa enzymes, was determined by varying the concentration of $MgCl_2$ from 0.1 to 10 mM. To ensure that the coupled assay system was active at such low concentrations of Mg^{2+}, ADP was added and the rate of reaction determined. At all concentrations of $MgCl_2$ tested, the rate of ADP turnover, by pyruvate kinase, was faster than the rate of AG phosphorylation. The initial rates determined were fit to either Equation 1 or Equation 2 by non-linear least squares, depending on whether or not magnesium inhibition was noted. The best fits of the data were obtained when the initial rates were plotted against the concentration of free Mg^{2+} and not when plotted against the concentration of total Mg^{2+}. The concentration of free Mg^{2+} was calculated using the parameters described in Fabiato & Fabiato (1979). The manganese dependencies of both the wild type and APH(3')-IIIa^{N195A} enzymes were determined by varying the total concentration of $MnCl_2$ from 0.05-10 mM and 0.05-15 mM, respectively. At all concentrations of $MnCl_2$ tested, the rate of ADP turnover, by pyruvate kinase, was faster than the rate of AG phosphorylation.

4.2.6 Measurement of Solvent Isotope, Solvent Viscosity and Thio effects for APH(3')-IIIa

The measurement of the solvent isotope and solvent viscosity effects for the wild type APH(3')-IIIa enzyme has previously been described (McKay & Wright, 1996). For the APH(3')-IIIa^{N195A} mutant, the solvent isotope effect was determined by preparing

the coupled assay buffer in D_2O and setting the pD 0.4 units above the pH. The H_2O content was ≤3.5% (v/v). For the APH(3')-IIIa^{N195A} mutant, the effect of solvent viscosity was studied using glycerol as the microviscogen. Briefly, glycerol was added to the coupled enzyme assay buffer to concentrations from 0 to 30% (w/v) and the steady state kinetic parameters were determined at the different concentrations of glycerol. ATP was examined as the variable substrate and kanamycin A was held constant at 125 μM. Assays were carried out in duplicate at 37 °C. The relative viscosity of the glycerol containing assay buffer was determined in quadruplicate using an Ostwald viscometer, as described in McKay *et al* (1996).

The effect of substituting a sulfur atom, for a non-bridge γ-phosphate oxygen atom, was determined by measuring the rate of ADP production from ATPγS. ATPγS is contaminated with up to 10% ADP, and in the coupled assay described above ADP is regenerated to ATP. So in order measure the true rate of ADP production phosphoenolpyruvate was omitted from the coupled assay buffer. All other components of the buffer were the same, except that the concentration of $MgCl_2$ was decreased to 1 mM. Variable concentrations, 50, 100, 250, 500 and 1000 μM, of ATPγS were incubated in the presence or absence of 100 μM kanamycin A. The wild type enzyme (0.4 nmoles) was added to initiate AG phosphorylation. The reaction was allowed to proceed at 37° C for 5 minutes, at which time $MnCl_2$ was added to a final concentration of 10 mM, in order to quench the activity of APH(3')-IIIa. Under similar conditions, using ATP as the substrate, the reaction is linear to 5 minutes. The wild type APH(3')-IIIa enzyme is potently inhibited by high concentrations of $MnCl_2$ (see below) whereas the PK/LDH

enzymes are not. Thirty seconds after the addition of the $MnCl_2$, 10 μL of a 60 mg/mL solution of PEP was added and the change in absorbance at 340 nm determined. Reactions were performed in duplicate as were kanamycin A null controls. The average amount of ADP present in the kanamycin null controls was subtracted from the amount present in kanamycin containing assays. The change in absorbance was divided by 5 minutes, converted to nmoles/min as described above and then fitted by nonlinear least fit squares to Equation 1.

4.2.7 Partial Proteolysis of Wild Type APH(3')-IIIa.

The susceptibilities of APH(3')-IIIa to either subtilisin or trypsin proteolysis were examined in a similar fashion. Proteolysis reactions consisted of 48 μg pure protein in 50 mM HEPES pH 7.5, 40 mM KCl, and 10 mM $MgCl_2$. The proteases were added to a final concentration of 2 μg/mL. The final volume was 120 μL. Proteolysis reactions were incubated on ice, and 10 μL aliquots removed after 0, 15, 30, 45, and 60 minutes. The remainder of the proteolysis reaction was then warmed to room temperature and incubated for an additional hour, with 10 μL aliquots being removed 15, 30, 45 and 60 minutes after the transfer to the higher temperature. The proteolysis reaction was quenched by the addition of 1 μL of a 10 mM PMSF solution, and 10 μL of 2 x SDS PAGE loading buffer. The samples were placed in a boiling water bath for 15 min, and then analyzed by 15% SDS PAGE.

Substrate protection experiments were carried out under the conditions described above except that 12 μg of pure protein was tested in a final volume of 30 μL. ATP and tobramycin were added, alone or in combination, to a final concentration of 1

mM and 500 μM respectively. Proteolysis reactions were carried out for 60 minutes on ice and processed for SDS-PAGE analysis as described above.

4.2.8 Amino Terminal Sequencing of Peptide Fragments.

Approximately 1 mg of pure APH(3')-IIIa was used in a scaled up version of the proteolysis reactions described above. The total volume was 1 mL. This proteolysis reaction was incubated for 2 hours on ice. The reaction was stopped by the addition of 25 μL of 100 mM PMSF. The reaction was then dried to <100 μL using a Speed Vac. An equivalent amount of 2 x SDS-PAGE loading buffer was added, the samples boiled for 10 minutes, and 20 μL added to the lanes of a 20% SDS-PAGE gel. One third of the gel was electroblotted onto polyvinylidene difluoride (PVDF) membranes (BioRad) for 30 minutes at 80 volts. Protein bands on the electroblot were visualized with Ponceau S (0.1% in 1% Acetic acid), excised, and N-terminal sequenced at the Alberta Peptide Institute, University of Alberta, Edmonton.

4.3 Results

The determination of the crystal structure of APH(3')-IIIa bound to ADP immensely aided my understanding of the catalytic mechanism of this enzyme. The overall structure of APH(3')-IIIa is bilobal, where the nucleotide binds at the apex of the two lobes (Figure 4.4). The amino terminal portion of the enzyme is primarily composed of β-sheet, whereas the carboxyl terminal portion of the enzyme is primarily α-helical (Hon *et al*, 1997). The determination of the crystal structure of APH(3')-IIIa, complexed with ADP, indicated that the AG phosphotransferases (APHs) are structurally related to

eukaryotic protein kinases (ePK) (Hon *et al*, 1997). The primary structure homology (Figure 4.1), and structural information, helped identify a number of conserved residues lining the active site of APH(3')-IIIa, which appeared likely to be important for catalysis. Since there has not been a thorough examination of the contribution of individual residues, to the catalytic power of an AG phosphotransferase, I undertook the task of mutating the conserved residues lining the active site of this enzyme (Figure 4.3) and characterizing their contribution to catalysis.

4.3.1 Kinetic Analyses of APH(3')-IIIa Mutants.

4.3.1.1 Glutamate 60

Glutamate 60 is conserved among both the ePK and APH superfamilies of enzymes. In the APH(3')-IIIa•ADP complex, the functional group of this residue appears to coordinate with the ε-amino group of Lys44. Lys44 is involved in binding ATP through α and β position non-bridge oxygens. A role for Lys44 in ATP binding has been previously confirmed by mutagenesis and affinity labeling studies (Hon *et al*, 1997; McKay *et al*, 1994b). The ε-amino group of Lys44 and the γ-carboxylate of Glu 60 are 2.9 Å apart. Thus, an electrostatic interaction is possible. The APH(3')-IIIa^{E60A} mutant showed only slight changes in its ability to bind either ATP or AG substrates (Table 4.1). Although it should be noted that the K_m for neomycin B is increased 6.7-fold, The inconsistent changes in AG affinity are mirrored in the inconsistent changes to k_{cat}. For ATP, amikacin and kanamycin A the k_{cat} is decreased 2.8-, 2.4- and 3.5-fold, respectively, whereas the k_{cat} for neomycin B has increased only slightly (1.3-fold). A comparison of the second order rate constants ($V/K_{WT}/V/K_{mut}$) reveals that the

Figure 4.4: Crystal structure of the APH(3')-IIIa monomer bound to ADP (Hon, *et al*, 1997). The figure also shows the modeled γ-phosphate and the two magnesium ions. This Figure was prepared using the MOLSCRIPT and RASTER3D programs (Kraulis, 1991; Merritt and Murphy, 1994). The loops containing the potential sites of subtilisin cleavage are shown in gold (residues 66-76), forest green (residues 120-136), and orange-red (residues 154-162).

APH(3')-IIIa^{E60A} mutant is only slightly impaired in its ability to catalyze the phosphorylation of AG substrates. V/K_{mut} is decreased only 0.5- to 5.4-fold. Thus, these results would suggest that this residue does not make a significant contribution to the catalytic power of this enzyme.

Table 4.1: Steady State Kinetic Parameters for the Wild Type and Mutant APH(3')-IIIa Proteins.

	Wild Type[2]	
Substrate	K_m (μM)	k_{cat} (s^{-1})
ATP	27.7±3.7	1.76±0.08
Kanamycin A	12.6±2.6	1.79±0.09
Neomycin B	7.72±0.9	2.08±0.07
Amikacin	245±27	2.46±0.11
Butirosin	34.3±3.1	2.02±0.07
Ribostamycin	9.3±1.8	1.89±0.10
Lividomycin A	31.6±5.1	3.97±0.25
Isepamicin	198±28.5	1.41±0.35

	APH(3')-IIIa^{S27A}				
Substrate	K_m (μM)	$K_{m(mut)}/K_{m(WT)}$	k_{cat} (s^{-1})	$k_{cat(WT)}/k_{cat(mut)}$	$V/K_{WT}/V/K_{mut}$
ATP	54.4±6.5	2.0	0.51±0.02	3.5	7.0
Kanamycin A	15.0±3.7	1.2	0.61±0.03	2.9	3.1
Neomycin B	ND[3]	-	0.28±0.02	7.4	-
Amikacin	574±162	2.3	0.32±0.04	7.7	18
Ribostamycin	13.9±3.8	1.5	0.68±0.03	2.8	4.2

[2] Steady state kinetic parameters for the aminoglycoside substrates are taken from McKay, *et al*, 1994, whereas the steady state kinetic parameters for ATP are taken from Hon, *et al*, 1997.

[3] The K_m for neomycin B could not be reliably determined, but we can estimate an upper limit of 3.5 μM.

Table 4.1. Continued.

	APH(3')-IIIa^{S27P}				
Substrate	K_m (μM)	$K_{m(mut)}/K_{m(WT)}$	k_{cat} (s^{-1})	$k_{cat(WT)}/k_{cat(mut)}$	$V/K_{WT}/V/K_{mut}$
ATP[4]	32.3±3.9	1.2	0.056±0.001	31.4	37
Kanamycin A	11.9±1.7	0.94	0.038±0.001	47.1	44
Neomycin B[5]	ND	-	0.0518±0.0004	40.2	-
Amikacin[6]	ND	-	≤0.009±0.0004	273	-
Butirosin	122±33	2.6	0.021±0.002	96.2	250
Ribostamycin	5.0±0.7	0.54	0.047±0.001	40.2	22

	APH(3')-IIIa^{E60A}				
Substrate	K_m (μM)	$K_{m(mut)}/K_{m(WT)}$	k_{cat} (s^{-1})	$k_{cat(WT)}/k_{cat(mut)}$	$V/K_{WT}/V/K_{mut}$
ATP	12.5±2.3	0.6	0.62±0.02	3.3	2.0
Kanamycin A	7.8±2.7	0.6	0.51±0.02	3.3	2.0
Neomycin B	51.8±11.5	6.7	2.6±0.15	0.8	5.4
Amikacin	57.6±6.0	0.2	1.02±0.03	2.5	0.5

	APH(3')-IIIa^{D190A}				
Substrate	K_m (μM)	$K_{m(mut)}/K_{m(WT)}$	k_{cat} (s^{-1})	$k_{cat(WT)}/k_{cat(mut)}$	$V/K_{WT}/V/K_{mut}$
Kanamycin A	ND	-	≤0.0033±0.0003[7]	550	-

[4] Neomycin B was fixed at 100 μM.
[5] V_{max} occurred at the lowest substrate concentration tested. The k_{cat} reported is an estimation using the data corresponding to 100 μM neomycin B and 1 mM ATP.
[6] Amikacin was an exceptionally poor substrate for the Ser27Pro mutant. Thus an estimation of the k_{cat} was made using the rate of reaction observed at 1.5 mM amikacin and 1 mM ATP.
[7] The relative inactivity of this mutant precluded a determination of K_m for the nucleotide or aminoglycoside substrates. Therefore a lower estimate of the activity of this enzyme in 1 mM ATP and 0.1 mM kanamycin A is reported.

Table 4.1. Continued.

	APH(3')-IIIa^{D190N}				
Substrate	K_m (μM)	$K_{m(mut)}/K_{m(WT)}$	k_{cat} (s^{-1})	$k_{cat(WT)}/k_{cat(mut)}$	$V/K_{WT}/V/K_{mut}$
Kanamycin A	ND	-	0.013±0.001[5]	140	-

	APH(3')-IIIa^{D190E}				
Substrate	K_m (μM)	$K_{m(mut)}/K_{m(WT)}$	k_{cat} (s^{-1})	$k_{cat(WT)}/k_{cat(mut)}$	$V/K_{WT}/V/K_{mut}$
ATP	108±11	5.1	0.047±0.001	39	200
Kanamycin A	334±37	26.5	0.043±0.001	42	1100
Neomycin B	ND	-	≤0.011±0.0003[8]	190	-
Amikacin	ND	-	≤0.011±0.0004	220	-

	APH(3')-IIIa^{N195A}				
Substrate	K_m (μM)	$K_{m(mut)}/K_{m(WT)}$	k_{cat} (s^{-1})	$k_{cat(WT)}/k_{cat(mut)}$	$V/K_{WT}/V/K_{mut}$
ATP	113±10	5.3	1.70±0.06	1.1	5.8
Kanamycin A	15.6±2.7	1.2	2.03±0.07	0.9	1.1
Neomycin B	4.1±1.0	0.5	1.34±0.05	1.6	0.8
Amikacin	1020±260	4.2	0.83±0.09	3.0	12.6
Butirosin	59.0±17.0	1.7	0.53±0.04	3.8	6.5
Ribostamycin	5.8±1.0	0.6	1.86±0.05	1.02	0.6
Lividomycin A	13.4±3.2	0.4	3.05±0.14	1.3	0.5
Isepamicin	624±149	3.2	0.86±.09	1.6	5.1

[8] The rates for the phosphorylation of amikacin and neomycin B were too slow to accurately measure the steady state kinetic parameters. Approximations for the k_{cat}s are given.

Table 4.1. Continued.

	APH(3')-IIIa^{D208A}				
Substrate	K_m (μM)	$K_{m(mut)}/K_{m(WT)}$	k_{cat} (s^{-1})	$k_{cat(WT)}/k_{cat(mut)}$	$V/K_{WT}/V/K_{mut}$
Kanamycin A	ND	-	<0.0010±0.0004[9]	1800	-

4.3.1.2 Serine 27

Ser27 is at the apex of the nucleotide positioning loop (NPL) (Figure 4.3), and while this residue is highly conserved in the N-terminus of the APHs, it is only partially conserved among the ePKs (Figure 4.1). The role of this residue is not obvious from the APH(3')-IIIa•ADP crystal structure (Hon *et al*, 1997). The hydroxyl group of Ser27 is pointing away from the site of phosphoryl transfer, and does not appear to make any interactions with the bound nucleotide. Furthermore, this hydroxyl is likely too far away to interact with an AG substrate. However, the thermal factors for the functional groups of a number of residues in the NPL are high, suggesting that this region of APH(3')-IIIa is conformationally flexible. Since a crystal structure of APH(3')-IIIa bound to ATP is as yet unavailable, a γ-phosphate has been modeled into the APH(3')-IIIa•ADP crystal structure, using the available structures of several ePKs as guides, (Thompson *et al*, 1999). This model agrees fairly well with the preliminary crystal structure of this enzyme bound to AMPPNP (A.M. Berghuis, personal communication). Therefore, this structure was used to enable a better understanding of the interactions that the enzyme makes with the nucleotide substrate. It should be noted that both magnesium ions are

[9] The level of activity detected with this mutant was not above assay background at 1 mM ATP, 0.1 mM kanamycin A.

present in the APH(3')-IIIa•ADP crystal structure. Thus, based on the APH(3')-IIIa crystal structure, with the modeled γ-phosphate of ATP, it does appear that the backbone amide proton of Ser27 is within hydrogen bonding distance (3.7 Å) of a γ-phosphate non-bridge oxygen. However, the orientation of the potential hydrogen bond does not appear to be ideal in the current conformation of the NPL. Nevertheless, I was interested in determining the importance of this residue to the promotion of catalysis. Therefore, mutant versions of the *aph(3')-IIIa* gene were generated, such that Ser27 was converted to either an Ala or a Pro. The APH(3')-IIIa^{S27A} mutant is only moderately impaired in its ability to phosphorylate AG antibiotics. Using the apparent dissociation constant, K_m, as a measure of substrate affinity, there appears to be little change, 1.2- to 2.3-fold, in the affinity of various substrates for this mutant enzyme. However, there is a somewhat more substantial effect on the rate of phosphate transfer. The k_{cat}s for ATP, kanamycin A, and ribostamycin are decreased ~3-fold. The most dramatic effects on k_{cat}, approximately a 10-fold decrease, are seen with neomycin B and amikacin. The reason for these rather dramatic decreases in k_{cat} is not readily apparent from the crystal structure of the wild type enzyme and were at first somewhat surprising. However, a comparison of V/K_{WT} and V/K_{mut} clearly indicates that the interaction between enzyme and substrate is significantly impaired. Thereby indicating an important role for the functional group of this residue in phosphate transfer. The role of this functional group is discussed below.

The effects of a Ser27 to Pro change should reflect both the loss of any interaction with the amide proton, as well as any interaction with the hydroxyl group of Ser27.

Steady state kinetic analyses of the APH(3')-IIIa^{S27P} mutant indicate that the K_m for ATP is largely unaffected by the APH(3')-IIIa^{S27P} change (Table 4.1). Since the K_m of ATP represents the dissociation constant for this substrate, at least for the wild type enzyme (McKay and Wright, 1995), the small change indicates the relative unimportance of this residue to nucleotide recognition in the ground state. However, this mutant is significantly impaired in its ability to phosphorylate AG substrates. The k_{cat}s are decreased 31-fold for ATP to 270-fold for amikacin. The likely reasons for this dramatic decrease in activity are discussed below.

4.3.1.3 Asparagine 195

This residue is completely conserved among both the APHs and the ePKs (Figure 4.1). In the APH(3')-IIIa•ADP crystal structure, the β-amide group of this residue is involved in coordinating Mg2 (see Figure 4.3 for metal site nomenclature). The amide oxygen is the metal ligand, whereas the amine is within hydrogen bonding distance (3.4-3.7 Å) of both Asp208 and Asp190. While Asn195 appears to be a simple metal ligand, I was curious to determine whether the magnesium ion coordinated by Asn195 is simply involved in ATP binding or whether Mg2 is involved in promoting catalysis. To begin to answer those questions I mutated this residue to alanine, and determined the steady state kinetic parameters.

The results reported in Table 4.1, for the APH(3')-IIIa^{N195A} mutant, are consistent with a role for Asn195 in nucleotide binding, as there was a 5.3-fold increase in the dissociation constant, K_m, for ATP (see above). This result, together with the fact that this residue is a ligand for Mg2, suggests that the Asn-Mg2-Nuc interaction is

important for ATP binding. This residue does not appear to be important for AG binding, as most of the effects on the K_ms of AG substrates are small. The K_ms are increased 0.4- to 1.2 fold. There is a more significant effect on the K_ms of AGs that are substituted at the N1 position of the aminocyclitol ring. For example, the K_m for amikacin is increased 4.2-fold. These small effects on K_m are generally mirrored by the small changes in the second order rate constants obtained for a number of AG substrates, further indicating the relative unimportance of this residue for substrate binding. The k_{cat}s are also largely unaffected, and the decreases range from a 0.9-fold decrease for kanamycin A to a 1.6-fold decrease for neomycin B. Although, it should be noted that for AGs substituted at the N1 position the decrease in k_{cat} is more substantial.

4.3.1.4 Aspartate 190

Aspartate 190 is also absolutely conserved among both APHs and ePKs (Figure 4.1). This residue is positioned 4.4 Å to the modeled γ-phosphate of ATP and 3.9 Å to Mg1, at closest approach. When the structure of the 4,6-disubstituted AG amikacin was modeled into the active site of APH(3')-IIIa the 3'O is 2.3 to 3.3 Å from the functional group of Asp190. Similarly the 4,5-disubstituted AG butirosin, when positioned for phosphorylation of the 5"-hydroxyl, is 3.5 to 3.7 Å from the carboxylate functionality of Asp190. This residue as noted above is within hydrogen bonding distance of Asn195 and while the distance is long, 3.9 Å, the carboxylate of Asp190 could take up a coordination position on the Mg1. Primary structure homology, the position of this residue in the APH(3')-IIIa•ADP crystal structure, and the precedent set when the corresponding residue, Asp210 (Asp166 using the numbering for the bovine C subunit), in yeast PKA

was mutated to alanine (Gibbs & Zoller, 1991), indicated that this residue would be important for the catalytic mechanism of APH(3')-IIIa, and perhaps be involved in general base catalysis.

In order to confirm the importance of this residue, I first generated the APH(3')-IIIa^{D190A} mutant. This mutant is markedly impaired in its ability to phosphorylate AG substrates (Table 4.1), and the steady state kinetic parameters for this mutant could not be measured reliably due to the low level of activity. An estimation of the rate of reaction was, therefore, made using the residual activity present at 100 μM kanamycin A and 1 mM ATP. These concentrations are saturating for the APH(3')-IIIa. The results of this analysis indicated that the APH(3')-IIIa^{D190A} mutant was 550-fold less active than the wild type enzyme.

To further explore the role of Asp190, the APH(3')-IIIa^{D190E} and the APH(3')-IIIa^{D190N} mutants were generated. For the APH(3')-IIIa^{D190E} mutant, there is a rather significant increase in the dissociation constant of ATP. The K_m for ATP is increased 5.1-fold. For kanamycin A the effect on substrate affinity was much more dramatic, as the V/K of the APH(3')-IIIa^{D190E} mutant for this AG is decreased 1100-fold. There is also a significant effect on k_{cat}. The k_{cat} for ATP is decreased 38.7-fold, and there is a corresponding decrease in the k_{cat} measured for kanamycin A phosphorylation (41.6-fold). The APH(3')-IIIa^{D190E} mutant is also impaired in its ability to phosphorylate a variety of AG antibiotics, as amikacin and neomycin B were also tested as substrates, but the rates of reaction were too low to accurately determine the steady state kinetic parameters. For amikacin and neomycin B, the k_{cat}s are decreased 220- and 190-fold,

respectively. The APH(3')-IIIa^{D190N} mutant was also severely impaired in its ability to phosphorylate kanamycin. An estimation of the residual activity, of the APH(3')-IIIa^{D190N} mutant, was made in the same manner as that described for the APH(3')-IIIa^{D190A} mutant. Using this methodology, the APH(3')-IIIa^{D190N} mutant was 140-fold less active than the wild type enzyme.

4.3.1.5 Aspartate 208

Aspartate 208 is also absolutely conserved among both the APHs and the ePKs. In the crystal structure of APH(3')-IIIa, bound to ADP, this residue acts as a ligand for Mg1. The two oxygens of the Asp208 carboxylate appear to take up two of the up to 6 possible magnesium coordination positions. In the APH(3')-IIIa•ADP structure, one of the oxygens also appears to interact with Mg2. Mg1 is also a ligand for the β-phosphate of ADP. In the crystal structure of AMPPNP bound to APH(3')-IIIa, Mg1 also interacts with the γ-phosphate (Hon & Berghuis, unpublished results). The positioning of this magnesium ion is consistent with that observed in the crystal structure of PKA bound to ATP and a peptide inhibitor (Zheng *et al*, 1993). The absolute conservation of this residue among APHs and ePKs motivated my original rationale to mutate this residue. The results obtained for the APH(3')-IIIa^{N195A} mutant, highlighting the importance of the metal ions to the catalytic mechanism of this enzyme (see below), further indicated the importance of understanding the role that those metal ions, and their direct ligands, play in promoting phosphoryl transfer. I therefore generated the APH(3')-IIIa^{D208A} mutant. This mutant lacked any detectable activity above the assay background. An upper limit on the rate enhancement, that this mutant enzyme affords, was therefore determined

(Table 4.1), at concentrations of both substrates that are saturating for the wild type enzyme. The results indicate that the APH(3')-IIIa^{D208A} mutant is at least 1800-fold less active than the wild type enzyme. This loss of activity is greater than 3-fold higher than the decrease in activity caused by the mutation of Asp190 to Ala.

4.3.2 Metal Ion Effects.

The role of metal ions in phosphoryl transfer reactions is unclear. In the case of APH(3')-IIIa, 2 metal ions are present in the crystal structure of this enzyme complexed with ADP. The residues that these metals interact with are shown in Figure 4.3 and have been discussed above. The presumed role of Asn195 in Mg^{2+} binding prompted further investigation into the role of metals in the catalytic mechanism of both APH(3')-IIIa and the APH(3')-IIIa^{N195A} mutant. In order to accomplish this goal, I initially examined whether this mutant could use Mn^{2+} as the divalent cation required for the phosphoryl transfer reaction. APH(3')-IIIa is strongly inhibited by high concentrations of Mn^{2+} (Figure 4.5). However, the APH(3')-IIIa^{N195A} mutant was quite active in up to 15 mM $MnCl_2$ and the steady state kinetic parameters comparing the 10 mM $MgCl_2$ catalyzed reaction to the 15 mM $MnCl_2$ catalyzed reaction can be found in Table 4.2.

The most striking feature of the Mn^{2+} catalyzed reaction is the significant decrease in the dissociation constant for ATP. The K_m for ATP is decreased to near wild type levels. The electronic nature of Mn^{2+} may permit a stronger series of interactions that are able to hold the nucleotide in the active site, or alternatively inhibit ADP release. This may be the molecular basis for the strong inhibition of APH(3')-IIIa by manganese.

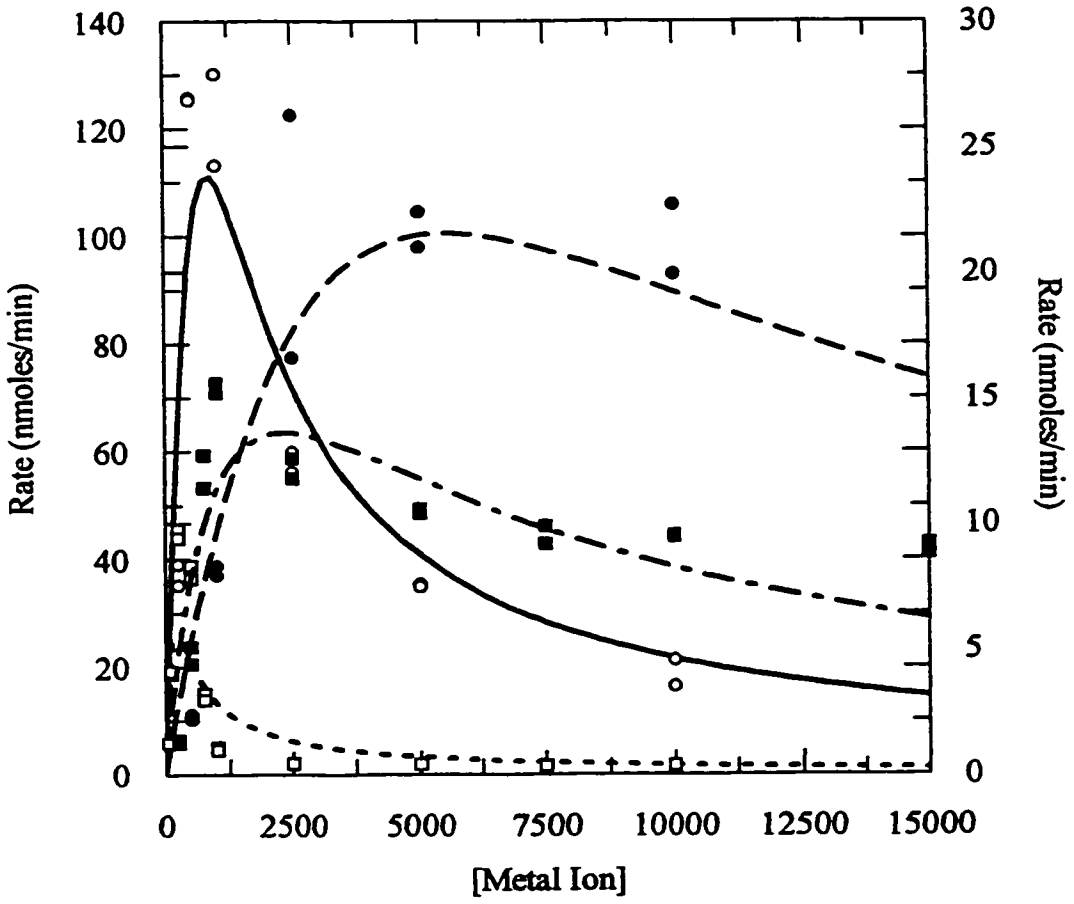

Figure 4.5: Magnesium and manganese metal ion dependencies of APH(3')-IIIa and the APH(3')-IIIa^{N195A} mutant. Initial rates were plotted against the total metal ion concentration (μM). The magnesium dependency of APH(3')-IIIa is represented by the solid line and open circle (____ ;○) and the magnesium dependency of the APH(3')-IIIa^{N195A} mutant is represented by the dashed line and closed circle (_ _ _ ;●). The manganese dependency of APH(3')-IIIa is represented by the dotted line and open square (·····; □) and the manganese dependency of the APH(3')-IIIa^{N195A} mutant is represented by the dot and dashed line and the (– · – · –; ■). The initial rates obtained for APH(3')-IIIa were plotted using the Y-axis while the initial rates obtained for the APH(3')-IIIa^{N195A} mutant were plotted using the second Y-axis.

Table 4.2: Metal and Solvent Isotope effects on APH(3')-IIIa^{N195A}.

Substrate	APH(3')-IIIa^{N195A} K_m (μM)	APH(3')-IIIa^{N195A} k_{cat} (s^{-1})
10 mM Mg^{2+}		
ATP[10]	113.7.±10.4	1.70±0.06
Kanamycin A[11]	15.6±2.7	2.03±0.07
D_2O		
ATP[1]	75.9±16.1	1.89±0.09
Kanamycin A[10]	9.8±2.7	1.98±0.05
15 mM $MnCl_2$		
ATP[9]	12.0±1.4	0.33±0.02
Kanamycin A[10]	34.3±2.4	0.44±0.01
D_2O		
ATP[9]	50.3±10.9	0.30±0.02
Kanamycin A[10,12]	34.5±8.5	0.34±0.04

If this is the case, then it should be possible to observe a 'burst' of ADP production, in the pre-steady state. Unfortunately, the lack of ready access to the equipment required for pre-steady state experiments has prevented any further exploration of this phenomenon.

The choice of divalent cation also has a significant impact on the rate of reaction. The k_{cat} measured for the Mn^{2+} catalyzed phosphorylation of kanamycin A is decreased 4.6-fold. There is a corresponding decrease in the k_{cat} determined when ATP is the variable substrate. A comparison of the rates of reaction determined at 15 mM $MnCl_2$

[10] Kanamycin A was held at 100 μM.
[11] ATP was held at 1 mM.
[12] A K_I of 2.0 mM was observed for the phosphorylation of kanamycin A in D_2O.

to those determined at 10 mM $MgCl_2$ is not unreasonable because the rate of the Mn^{2+} catalyzed reaction varies little between 5 and 15 mM $MnCl_2$ (Figure 4.5).

The rather dramatic change in the Mn^{2+} dependence of the APH(3')-IIIa^{N195A} mutant suggested that the rate-limiting step for this mutant was no longer ADP release. To test this hypothesis, I determined the steady state kinetic parameters for the APH(3')-IIIa^{N195A} mutant in D_2O, in the presence of either 10 mM $MgCl_2$ or 15 mM $MnCl_2$ (Table 4.2). When Mg^{2+} is the divalent cation, the decrease in k_{cat} is on the order of a 0.90- to 1.03-fold, for ATP and kanamycin A, respectively. Similar results were obtained when Mn^{2+} is used as the divalent cation. Here, the k_{cat}s are decreased 1.10- to 1.29-fold, for ATP and kanamycin A, respectively. These values are somewhat lower than the solvent isotope effect determined for APH(3')-IIIa (McKay & Wright, 1996). For both ATP and kanamycin A, the k_{cat}s are decreased ~1.5-fold in D_2O. Thus, regardless of the nature of the divalent cation, proton abstraction does not contribute to the rate-limiting step of the APH(3')-IIIa^{N195A} mutant. This fact, together with the observation that high concentrations of Mn^{2+} strongly inhibit the kinase reaction, suggested that ADP release remains largely rate limiting. Such a finding would also be consistent with solvent viscosity studies, which indicate that Mn^{2+} affects ADP release from PKA (Adams & Taylor, 1993). However, the decreased solvent isotope effect, observed for the APH(3')-IIIa^{N195A} mutant, also suggested that ADP release might no longer be rate-limiting for this enzyme. To test this hypothesis, I examined the effect of a microviscogen on the steady state kinetic parameters of the APH(3')-IIIa^{N195A} mutant. For APH(3')-IIIa, k_{cat} is a measure of the diffusion controlled release of ADP (McKay & Wright, 1995; McKay &

Wright, 1996), and since diffusion controlled processes are strongly affected by changes in solvent viscosity, the rate of reaction is, therefore, maximally affected by increases in solvent viscosity. A slope of approximately 1 was determined for APH(3')-IIIa (McKay & Wright, 1996). The effect of solvent viscosity on the rate of the APH(3')-IIIa^{N195A} mutant is plotted graphically in Figure 4.6. The k_{cat} of this mutant enzyme is not remarkably affected by an increase in the relative viscosity of the solution. The slope is 0.20±0.06. This result is quite different from the result obtained with APH(3')-IIIa, and indicates that ADP release is unlikely to be completely rate limiting for the APH(3')-IIIa^{N195A} mutant.

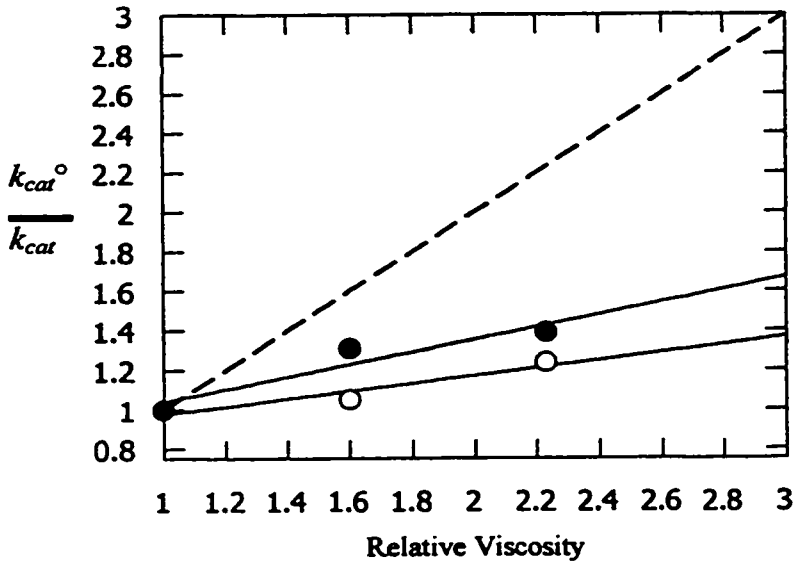

Figure 4.6: Measurement of the Solvent Viscosity Effect for the APH(3')-IIIa^{N195A} mutant. Glycerol was used as the microviscogen and k_{cat}°/k_{cat} (○) and $(k_{cat}/K_m^{\circ})/(k_{cat}/K_m)$ (●) are plotted as functions of the relative viscosity. The slope of the k_{cat}°/k_{cat} line is 0.20±0.06. The slope of the $(k_{cat}/K_m^{\circ})/(k_{cat}/K_m)$ line is 0.32±0.11. The dashed line has a slope of 1 and corresponds to the effect of solvent viscosity on the APH(3')-IIIa enzyme (McKay & Wright, 1996).

The fact that the metal ion dependence of the APH(3')-IIIa^{N195A} mutant was so different than the dependence of APH(3')-IIIa on this metal indicated that a similar study of the effects of varying the magnesium concentration on other mutant APH(3')-IIIa proteins was in order. Therefore, in an effort to better understand the metal ion dependence of APH(3')-IIIa the concentration of free Mg^{2+} was varied. Initial rates were measured at concentrations of ATP and kanamycin A that are saturating for both the wild type and mutant APH(3')-IIIa proteins. The results from this analysis are presented graphically in Figure 4.7 and the kinetic parameters for the Mg^{2+} assisted catalysis of the mutant APHs studied are presented in Table 4.3.

Table 4.3: Kinetic parameters for Mg^{2+} titrations.

Enzyme	K_m (mM)	k_{cat} (s^{-1})	K_i (mM)
APH(3')-IIIa	52.2±25.4	7.24±1.80	0.57±0.2
APH(3')-IIIa^{S27A}	266±28	0.56±0.02	ND
APH(3')-IIIa^{S27P}	577±48	0.035±0.001	ND
APH(3')-IIIa^{E60A}	304±41	0.075±0.004	21.5±5.9
APH(3')-IIIa^{D190E}	211±16	0.048±0.002	21.5±3.9
APH(3')-IIIa^{N195A}	523±252	1.71±0.32	28.7±27.3
APH(3')-IIIa^{F264A}	136±23	2.73±0.22	2.7±0.5

ND = None Detected

What is most evident from Figure 4.7, is the extent to which the wild type enzyme is inhibited by high concentrations of magnesium. As a quantitative measure of this inhibition, the K_I for magnesium was found to be 0.8±0.3 mM (Table 4.3). The detected rates of reaction were on the order of 5-fold lower at high concentrations of magnesium, than those observed at low concentrations of the divalent cation. Thus, the

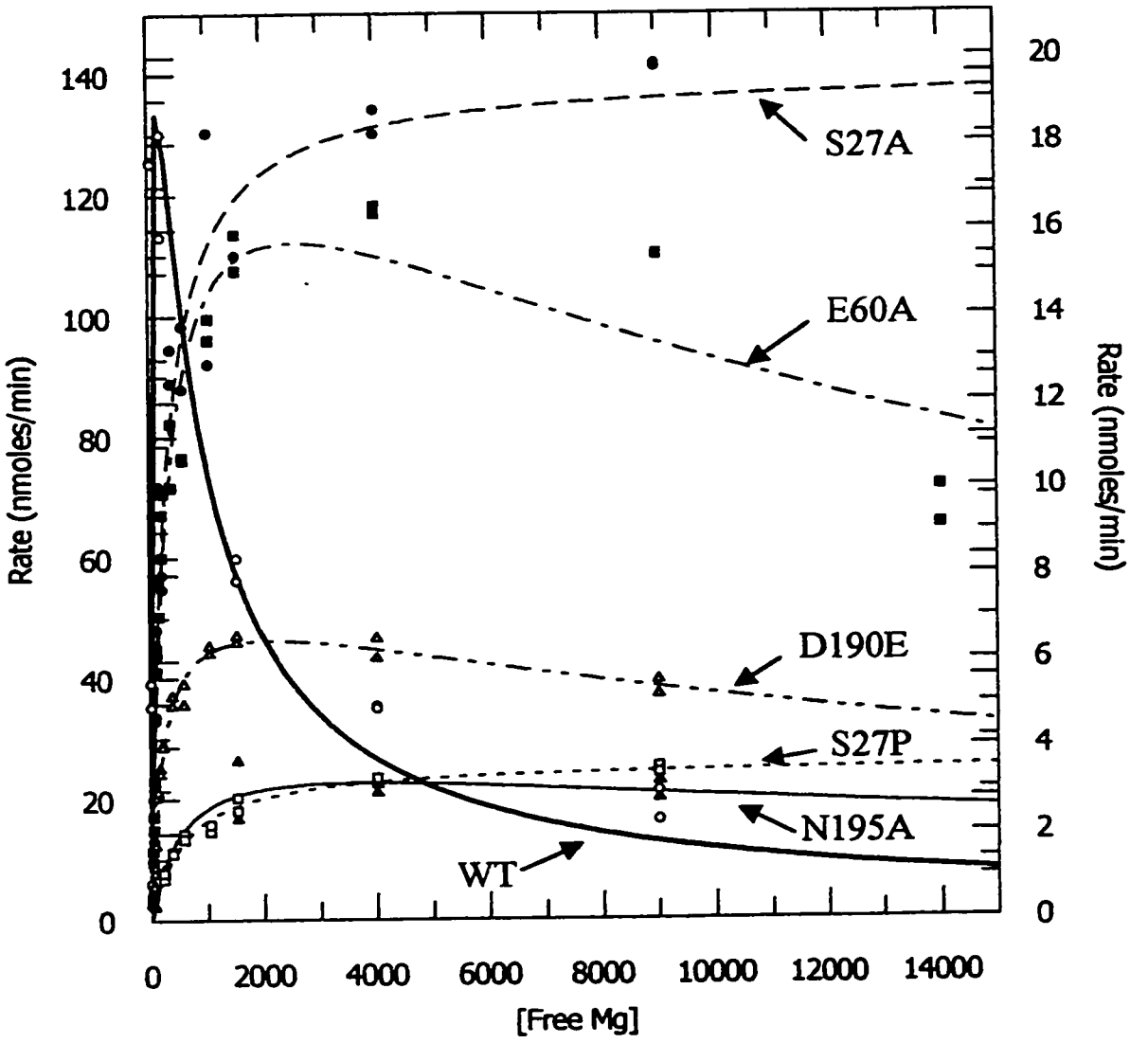

Figure 4.7: Magnesium ion dependencies of APH(3')-IIIa and Mutant APH(3')-IIIa proteins. Initial rates were plotted against the concentration of free Mg^{2+} (μM). The dependence of the initial rates on free magnesium are represented by: the thick solid line and open circles (——— ; O) for APH(3')-IIIa; the dashed line and closed circles (- - - ; ●) for the APH(3')-IIIa^{S27A} mutant; the dotted line and open squares (····· ; □) for the APH(3')-IIIa^{S27P} mutant; the dashed and dotted line and closed square (- · - · ; ■) for the APH(3')-IIIa^{E60A} mutant; the dash dot dot dash line and open triangle (— · · · ;Δ) for the APH(3')-IIIa^{D190E} mutant; and, the thin solid line and closed triangle (——— ; ▲) for the APH(3')-IIIa^{N195A} mutant. The initial rates obtained for APH(3')-IIIa, and the APH(3')-IIIa^{N195A} mutant were plotted using the Y-axis whereas the initial rates obtained for the APH(3')-IIIa^{S27A}, the APH(3')-IIIa^{S27P}, the APH(3')-IIIa^{E60A}, and the APH(3')-IIIa^{D190E} mutants were plotted using the second Y-axis.

steady state kinetic parameters for ATP and a variety of AG substrates that are representative of both the 4,5- and 4,6-disubstituted AG were determined at 1 mM $MgCl_2$ (Table 4.4).

Table 4.4: Steady state kinetic parameters determined for Wild Type APH(3')-IIIa in 1 mM $MgCl_2$.

	APH(3')-IIIa		
Substrate	K_m (μM)	k_{cat} (s^{-1})	K_I (mM)
ATP	44.9±8.4	4.29±0.22	ND
Kanamycin A	15.2±4.2	5.19±0.37	ND
Neomycin B	±[13]	1.31±0.08	1.9±0.6
Amikacin	19.4±2.3	3.14±0.06	ND
Butirosin	10.1±1.9	1.71±0.08	1.6±0.4
Ribostamycin	23.2±7.7	3.25±0.35	1.9±0.7
Lividomycin A	35.8±11.0	4.70±0.57	1.3±0.5
ATPγS	214±49	0.13±0.01	ND

ND= not detected

The k_{cat}s for ATP and kanamycin A experienced the most substantial increase when the kinetic parameters were determined at low concentrations of the divalent cation. They were increased 2.3- and 2.9-fold, respectively. The magnitude of the change in k_{cat} for the other AGs examined varies from 0.6- to 1.7-fold. The increase in the first order rate constant is likely not as significant as is apparent in Figure 4.7, as there is an extremely tight dependence of the initial rates on magnesium concentration. Generally, however, they do support the significant role that divalent ion concentration can play on enzyme kinetics. Note the substantial reduction, 12.6-fold, in the K_m for amikacin. Metal

[13] The K_m for neomycin B was quite low (≈1.5±1.3) and could therefore not be accurately determined.

ions could interact with the hydroxybutyrate group and in an unknown way inhibit amikacin binding.

The magnesium dependencies of the mutant APH(3')-IIIa proteins, described herein, are markedly different from the wild type enzyme. The magnesium dependence of the APH(3')-IIIa^{F264A} mutant was included as a negative control to show that a mutation far from the phosphoryl transfer site of APH(3')-IIIa does not have as great an impact on the magnesium dependence as do those residues that make direct or indirect contact with either Mg1 or Mg2. The effect of mutating Phe264 to alanine has previously been described (Thompson *et al*, 1999; Chapter 5). Somewhat surprisingly, the magnesium dependence of the APH(3')-IIIa^{E60A} mutant, a residue that is quite distant (approximately 6 Å) from Mg1 ion, was substantially altered. The apparent dissociation constant for Mg^{2+}, K_m, is increased 14.3-fold and the concentration of Mg^{2+} that yields half maximal activity, the K_i, was increased 26.9-fold. Not surprisingly the magnesium dependence of the APH(3')-IIIa^{N195A} mutant, which coordinates Mg2, was also quite different from that observed for the wild type enzyme. The K_m for Mg^{2+} has also increased 24.5-fold and the K_i for this cation has increased 35.9-fold. Correspondingly, a 5.3-fold increase in the dissociation constant for ATP was detected with this mutant (Table 4.1). The magnesium dependence of the APH(3')-IIIa^{D190E} mutant suggests a role for this residue in metal ion coordination. In the crystal structure of APH(3')-IIIa, complexed with ADP, Asp190 appears to be able to take up one of the coordination positions of Mg1. For the APH(3')-IIIa^{D190E} mutant, the K_m for magnesium has increased 9.9-fold whereas the K_i has increased 26.9-fold. While the hydroxyl group of Ser27 does

not appear from the APH(3')-IIIa•ADP crystal structure to be a magnesium ligand. This is despite the fact that the hydroxyl group of this residue is only 4.3 Å from Mg2. Nevertheless, the magnesium dependencies of both the APH(3')-IIIa^{S27A} and APH(3')-IIIa^{S27P} mutants were also examined. Surprisingly, the magnesium inhibition detected with APH(3')-IIIa was completely absent, when the dependence of initial rates on metal ion concentration were determined for both of these mutant enzymes. The K_ms for free magnesium have increased 12.5-fold and 27.1-fold, respectively, for the APH(3')-IIIa^{S27A} and APH(3')-IIIa^{S27P} mutants. These results, in combination with the lack of inhibition due to high concentrations of magnesium, argue in favor of a role for this residue in metal binding.

4.3.3 The Effect of ATPγS on APH(3')-IIIa Activity

In theory, the contribution of nucleophilic attack on the rate of a phosphate transfer reaction can be measured through the use of an ATP analogue that is substituted with a sulfur atom at a γ-phosphate non-bridge oxygen position. The effect of such a substitution on the rate of an enzyme-catalyzed reaction is termed the 'thio effect'. For APH(3')-IIIa a small thio effect 2.09 has been reported (McKay & Wright, 1996). This result would argue in favor of a metaphosphate like TS, or may reflect the large contribution of ADP release to k_{cat}. However, the assay employed couples the production of ADP to the oxidation of NADH, using a pyruvate kinase/lactate dehydrogenase enzyme mix. This effectively results in the regeneration of ATP from ADP. Thus, as ATPγS is consumed, ATP is produced and one runs the risk of measuring the rate of phosphate transfer from ATP and not ATPγS. This assay can be further complicated by

the presence of any contaminating ADP in commercial preparations of ATPγS. Contaminating ADP, if present in a significant amount, will be immediately converted to ATP, and again one is measuring the velocity of phosphoryl transfer from ATP. Our supply of ATPγS is contaminated with approximately 7% ADP, as determined from APH(3')-IIIa minus null controls. Therefore, to determine the validity of the thio effect reported in McKay & Wright (1996), I took advantage of the fact that APH(3')-IIIa is strongly inhibited by Mn^{2+}, whereas the coupled enzyme assay is not (not shown). These results (Table 4.4) indicate that there is indeed a significant thio effect in 1 mM $MgCl_2$, on the order of 33-fold.

4.3.4 Proteolysis Results

The susceptibility of APH(3')-IIIa to two proteases, trypsin and subtilisin was tested. While trypsin failed to result in any significant proteolysis of APH(3')-IIIa (not shown), subtilisin treatment resulted in the generation of 2 major and 1 minor proteolytic fragments (Figure 4.8A). The minor fragment is estimated to have a molecular weight of approximately 18.3 kDa whereas the two major fragments have molecular weights of approximately 14.3 and 7.9 kDa. Size estimates were made by comparing the relative mobility of the peptide fragments to a standard curve prepared by plotting the relative mobility of proteins of known molecular weight against their log(molecular weight). The identification of subtilisin as an agent that could promote the partial proteolysis of APH(3')-IIIa instigated substrate protection studies. The wild type enzyme was therefore treated with subtilisin in the absence of any substrate, in the presence of MgATP (1 mM), in the presence of tobramycin (0.5 mM), or in the presence of both tobramycin and ATP

(Figure 4.8B). Tobramycin is a 4,6-disubstituted AG that lacks a 3' hydroxyl group and thus acts as a competitive inhibitor of APH(3')-IIIa (McKay & Wright, 1995).

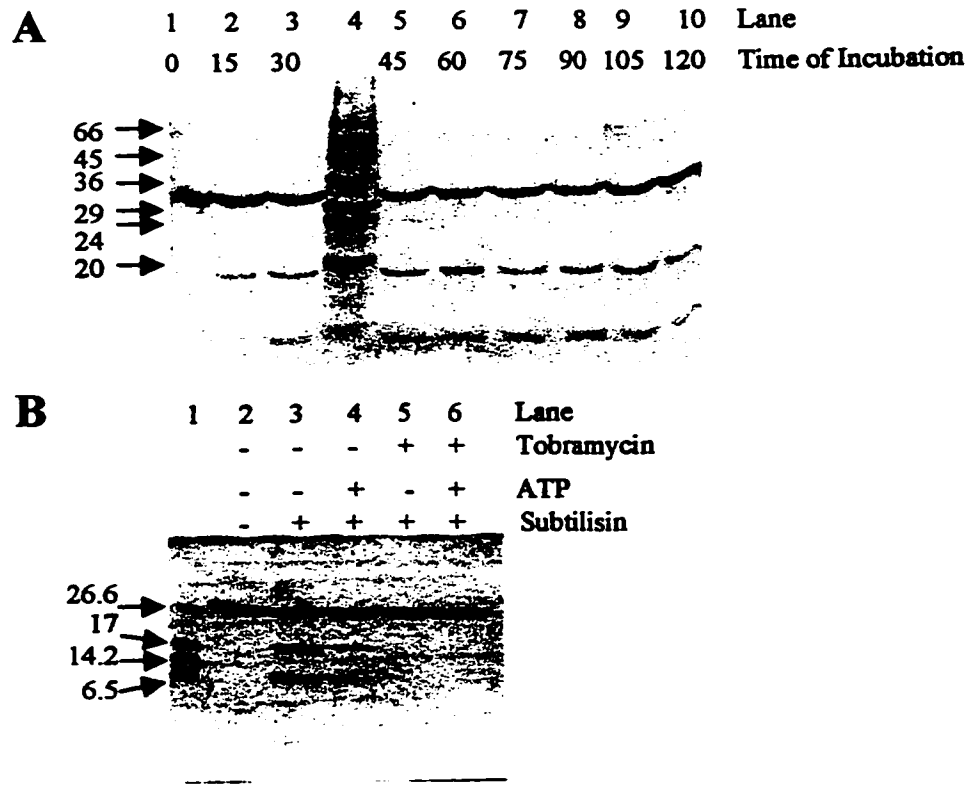

Figure 4.8: Partial Proteolysis of APH(3')-IIIa. A. Protein samples were treated with subtilisin, as described in Section 4.2, and incubated on ice (Lanes 1-3,5, and 6) and then at room temperature (Lanes 7-10) for the times indicated above each individual lane. Proteolysis reactions were stopped by the addition of PMSF and 2 x SDS-PAGE loading buffer and applied to a 15% SDS-PAGE gel. The gel was stained with 0.1% Coomassie Brilliant Blue. Lane 4 contains Low Molecular Weight markers (Sigma) and their molecular weights are listed to the left of the gel. **B.** Substrate protection experiments. Protein samples were treated, as described in Section 4.2, and incubated on ice in the presence or absence of tobramycin and ATP for the times indicated above. Lane 1 contains Ultra Low Molecular Weight markers (Sigma). Proteolysis reactions were stopped as described above and applied to a 20% SDS-PAGE gel.

The results of substrate protection experiments indicate that ATP alone cannot inhibit the partial proteolysis of APH(3')-IIIa. However, when tobramycin is present in proteolysis reactions, alone or in combination with ATP, the partial proteolysis of APH(3')-IIIa is inhibited. It should be noted that neither ATP nor tobramycin could entirely prevent the generation of the 19.5 kDa minor fragment.

The three proteolytic fragments obtained from the subtilisin proteolysis experiments, described above, were N-terminal sequenced, and the results indicate that the sites of cleavage are present in the C-terminal end of the protein, as the N-terminus is intact in all three peptides analyzed. Despite the fact that several attempts have been made to identify the precise C-terminal cleavage site, using both electrospray and MALDI-TOF mass spectrometry, none have been successful. However, using the size estimates obtained from the SDS-PAGE analysis, it is possible to speculate on the approximate sites of proteolytic attack. Thus, using this methodology Leu67, Glu122, and Asn158 have been identified as the C-terminal sites of cleavage that result in the generation of the 7.9, 14.3, and 18.3 kDa peptide fragments. The position of these residues in the crystal structure of the APH(3')-IIIa•ADP complex is discussed below.

4.4 Discussion

4.4.1 Kinetic Analyses of APH(3')-IIIa Mutants.

In an effort to understand the role of amino acid residues present in the active site of APH(3')-IIIa, the *aph(3')-IIIa* gene was mutated such that Ser27, Glu60, Asp190, Asn195, and Asp208 were converted to Ala. To further characterize the roles of particular residues in the catalytic mechanism of APH(3')-IIIa, the APH(3')-IIIa^{S27P}, APH(3')-IIIa^{D190N} and APH(3')-IIIa^{D190E} mutants were also generated. These mutant

enzymes were purified, and the steady state kinetic parameters determined. The individual effects of these mutations are described below.

For the APH(3')-IIIa^{E60A} mutant, small effects on AG affinity were observed. This was not altogether unsurprising as a number of AGs have been modeled into the active site of APH(3')-IIIa (Thompson *et al*, 1999) and Glu60 is far from the site of AG binding. For example, the functional group of Glu60 is at least 10 Å away from amikacin, at closest approach, when this AG was modeled into the active site of APH(3')-IIIa. Thus, Glu60 is unlikely to exert a direct effect upon AG binding. The lack of any significant effect on the affinity constant was somewhat surprising because mutagenesis of this residue in yeast PKA resulted in significantly higher K_ms for both ATP (2.9-fold) and the peptide substrate (50-fold) (Gibbs & Zoller, 1991). The lack of any significant effect on the first order rate constant, which is decreased a maximum of 3.5-fold, was also somewhat surprising, in light of the fact that the k_{cat} of a corresponding mutation in yeast PKA is decreased substantially, 19.4-fold. However, it is difficult to make a direct comparison of the effects of mutating these conserved Glu residues, as the kinetic data for the yeast mutant was obtained for a triple mutant (PKA$^{D134A\ E135A\ R136A}$). As a control, the authors found that the reaction catalyzed by the PKA$^{D134A\ R136A}$ double mutant was largely unperturbed. Nevertheless, one cannot disregard the potential synergistic effects of mutating all three residues. Therefore, the importance of this residue to ePK catalyzed phosphate transfer may be overstated. Alternatively, this residue may be more important for ePK mediated phosphoryl transfer, and is perhaps involved in regulating protein kinase activity. For example, in the protein kinase Hck,

this region of the protein undergoes substantial reorganization upon activation of the tyrosine kinase activity of this enzyme (Sicheri *et al*, 1997). This suggests that in the ePKs this conserved Glu is important for the correct positioning of a number of catalytic residues. Likely Glu60 has a corresponding role in the APHs, but the fact that APHs are constitutively active could explain the smaller effect seen when the kinetic parameters were determined for the APH(3')-IIIa^{E60A} mutant.

The APH(3')-IIIa^{S27A} mutant was also impaired in its ability to phosphorylate a number of AG substrates. The k_{cat} for ATP was decreased 3.5-fold, but this enzyme was more substantially impaired in its ability to phosphorylate neomycin B and amikacin. As stated above, Ser27 is at the apex of the NPL and is unlikely to interact directly with either of the two substrates of this enzyme. Nevertheless, these results suggested a more important role for this residue than was previously envisioned. Furthermore, the fact that the phosphorylation of neomycin B and amikacin is significantly impaired is suggestive of a change in the rate-limiting step i.e. ADP release is no longer rate limiting. The fact that product release is no longer rate-limiting, for this mutant, has recently been confirmed by the observation that the APH(3')-IIIa^{S27A} mutant lacks any significant solvent viscosity or solvent isotope effect (Boehr, Thompson, & Wright, unpublished results).

The APH(3')-IIIa^{S27P} mutant was also generated in order to help confirm the importance of this residue. When this residue is changed to a Pro, the effect on k_{cat} is 10-fold greater than when the same residue was mutated to alanine. The kinetic data for the APH(3')-IIIa^{S27P} and the APH(3')-IIIa^{S27A} mutants indicate the importance of the NPL

for phosphate transfer and could suggest the following: 1) The overall conformation of the NPL in these mutants is incorrect and the terminal phosphate is not correctly positioned for phosphate transfer; 2) The proline mutation prevents a conformational change within the NPL that aids phosphoryl transfer; 3) Both the hydroxyl and amide proton of Ser27 are required for TS stabilization. If the former were largely true, then one would expect an increase in the affinity constant for ATP, due to the loss of contacts between the amide protons of Gly25 and Met26, and the α-phosphate and β-phosphates, respectively. The amide nitrogen of Gly25 is 5.0 Å from the α-phosphate and the amide nitrogen of Met26 is 3.0 Å from the β-phosphate. Furthermore, if the overall conformation of the NPL were compromised, then one would expect that the effect of mutating this residue to a proline would be much more dramatic. While the first order rate constants of ATP and kanamycin A for the APH(3')-IIIa^{S27P} mutant are decreased 9.0- and 16.2-fold, respectively, relative to the APH(3')-IIIa^{S27A} mutant, there is only a small effect on the affinity of ATP. The K_ms for ATP have decreased only 2.0- and 1.2-fold for the APH(3')-IIIa^{S27A} and APH(3')-IIIa^{S27P} mutants, respectively. Thus, the conformation of the NPL is largely correct. The roles of the backbone amide and the serine hydroxyl are discussed below.

The results obtained for the APH(3')-IIIa^{N195A} mutant are consistent with a role for this residue in ATP binding, as the K_m for ATP is increased 5.3-fold. Asn195 interacts with ATP through Mg2, so the decrease in affinity likely reflects a poorly coordinated metal ion. The removal of this amide group has little effect on the binding of a variety of AG substrates. The k_{cat}s measured for both ATP and a variety of AG

substrates are decreased 0.9- to 3.8-fold and suggest that this residue is not critical for the catalytic step of phosphoryl transfer.

The APH(3')-IIIa^{D190A} mutant was significantly impaired in its ability to phosphorylate AG substrates. This mutant was approximately 550-fold less active. The corresponding mutation in yeast PKA results in a similar 340-fold decrease in the first order rate constant (Gibbs & Zoller, 1991). In both cases the effect on the rate of phosphoryl transfer is likely to be larger, especially when one considers the fact that both APH(3')-IIIa and PKA are limited by ADP release. The rate of the PKA catalyzed chemical step is approximately 24-fold greater than product release (Grant & Adams, 1996). Nevertheless, both of these results are quite surprising because if Asp190 in APH(3')-IIIa and Asp166 in PKA act as general bases, where substrate deprotonation precedes phosphoryl transfer, one would have expected that this mutation would have decreased the reaction rate to the level of the non-catalyzed reaction. The fact that this did not occur, suggests that substrate deprotonation is not critical for catalysis, consistent with a dissociative rather than an associative mechanism.

To further characterize the importance of this residue, I generated the APH(3')-IIIa^{D190E} and APH(3')-IIIa^{D190N} mutants. The Glu mutation conserves charge, but not position whereas the Asn mutation conserves position, but neutralizes charge. The APH(3')-IIIa^{D190E} mutant is markedly impaired in its ability to phosphorylate a variety of AG substrates. The finding that the second order rate constant, of this mutant, for kanamycin A is decreased 1100-fold supports a role for Asp190 in binding the AG substrate. Similarly, the fact that the K_m for ATP is also increased (5.1-fold) indicates

that this residue is important for productive ATP recognition. Asp190 could stabilize ATP binding by interacting with Mg1. Such an interaction could occur in the TS and be important for TS stabilization. The rather dramatic decrease in the k_{cat} of the APH(3')-IIIa^{D190E} mutant indicates that the positioning of the carboxylate of Asp190 is quite important for optimal rate enhancement. By comparing the catalytic rates of the APH(3')-IIIa^{D190A} mutant to the APH(3')-IIIa^{D190E} mutant it is possible to estimate the contribution that positioning makes to rate enhancement. Thus, at least two orders of magnitude can be attributed to the rate enhancement afforded by the correct positioning of this residue. A similar amount of catalytic power has been attributed to the rate enhancement afforded by the correct positioning of His122 in the catalytic mechanism of nucleoside diphosphate kinase (Admiraal *et al*, 1999).

The APH(3')-IIIa^{D190N} mutant was also impaired in its ability to phosphorylate kanamycin A. The APH(3')-IIIa^{D190N} mutant was 140-fold less active than the wild type enzyme. However, this effect is surprisingly small. The lack of a more dramatic effect is especially surprising when one considers that the pKa of an Asn residue is less than 0 and is therefore unlikely to act as a general base. Thus, the observed effect should have paralleled the results obtained for the APH(3')-IIIa^{D190A} mutant, which cannot act as a proton acceptor. These results suggest that Asp190 may be required to orient the incoming AG hydroxyl for optimal attack upon the γ-phosphate of ATP, but that phosphoryl transfer precedes substrate deprotonation i.e. a dissociative mechanism.

The fact that the APH(3')-IIIa^{D208A} mutant lacks any detectable activity indicates that this residue is critical to the catalytic mechanism of APH(3')-IIIa. This

result parallels the results obtained for the yeast PKA^{D228A} mutant (Asp184 bovine C subunit numbering). In that case, yeast cells were inviable (Gibbs & Zoller, 1991). Thus, Asp208 and Asp228 are critical to the catalytic mechanism of the APH(3') and the ePKs. By inference, these results also indicate the importance of Mg1 to the catalytic mechanisms of both these classes of enzymes. To further characterize the role of Asp208 in catalysis, I initiated studies to generate the APH(3')-$IIIa^{D208E}$ and the APH(3')-$IIIa^{D208N}$ mutants, and David Boehr completed these studies. Similarly to the APH(3')-$IIIa^{D208A}$ mutant the APH(3')-$IIIa^{D208E}$ and APH(3')-$IIIa^{D208N}$ mutants lack any detectable activity (Boehr, Thompson & Wright, unpublished results). Thus, even though the negative charge is present, the enzyme is not active. This indicates that the position of the carboxylate of Asp208, and by inference Mg1, is critical for the activity of APH(3')-IIIa. Based on the fact that Asn195 acts as a Mg^{2+} ligand, an Asn at position 208 should act as a Mg^{2+} ligand. Thus, the results obtained for the APH(3')-$IIIa^{D208N}$ mutant indicate that the charge of this residue is also critical for the proper function of APH(3')-IIIa, and that the neutralization of the charge present on Mg1 is important for generating the TS. The characterization of both the APH(3')-$IIIa^{D208E}$ and APH(3')-$IIIa^{D208N}$ mutants clearly demonstrates the important contribution that the position and charge of Mg1 make to rate enhancement.

4.4.2 Role of the Magnesium Ions in the Catalytic Mechanism of APH(3')-IIIa.

The role of the two magnesium ions in the catalytic mechanisms of kinases is unclear. Do they 1) serve only to orient substrates for nucleophilic attack; 2) act as electron withdrawing agents to generate a more electrophilic γ-phosphoryl center or; 3)

do they actively participate in the catalytic process? Clearly metal ions are required for substrate orientation, and the optimal alignment of substrates can contribute greatly to the observed rate enhancement (see above). However, it is unclear how magnesium ions could act as electron withdrawing agents. Magnesium is said to be a 'hard acid', whereas oxygen is a 'hard base'. Thus, their interactions are purely ionic with little sharing of electron density (Cowan, 1993), and they therefore would not be expected to be able to generate a more electrophilic γ-phosphoryl center through such means. When asked if the Mg^{2+} ions actively participate in the catalytic event, the answer is yes. The two Mg^{2+} ions are clearly involved in nucleotide binding, however, questions remain as to the true role of these metal ions in the phosphate transfer step i.e. do these metal ions facilitate phosphate transfer. From the crystal structure of APH(3')-IIIa, Mg2 is clearly involved in ADP binding. Interactions between this metal ion and the α- and β-phosphates are readily apparent. During phosphate transfer Mg2 likely interacts with the βγ-bridging oxygen to stabilize the developing charge on this atom. Such an interaction would help to stabilize the interactions between the enzyme and the nucleotide diphosphate portion of ATP. Therefore, the position of the α- and β-phosphates are likely to be fixed, relative to the position of the γ-phosphate. From the crystal structure of APH(3')-IIIa, Mg1 is also clearly involved in ADP binding. An interaction with the β-phosphate is readily apparent. As described above, this residue also interacts with the γ-phosphate. The interaction between the γ-phosphate and Mg1 is likely to be important for charge stabilization in the TS. In a dissociative-like phosphate transfer mechanism, the distance between Mg1 and the β-phosphate should increase in order to maintain molecular contact

with one of the non-bridging oxygens of the γ-phosphate, and possibly stabilize the charge present on that atom. The movement of Mg1 could occur spontaneously or, more likely, the movement of Mg1 could be 'directed' by the enzyme. The 'directed' movement of Mg1 away from the β-phosphate should result in a corresponding movement of the γ-phosphate away from the β-phosphate. This movement of the terminal phosphate would lengthen the βγ-PO bond, and thereby promote the generation of a metaphosphate-like intermediate. This intermediate, by its very nature, is highly electrophilic and its generation would have a significant impact on rate enhancement.

In an effort to better understand the role that metal ions play in the catalytic mechanism of APH(3')-IIIa, I examined the concentration-dependence of free magnesium on the initial rates of reaction. The dramatic change in magnesium dependence is undoubtedly a reflection of the kinetic mechanism of the wild type enzyme, where ADP release is solely rate limiting. For the APH(3')-IIIa^{E60A} mutant, the apparent dissociation constant for Mg^{2+} is increased 14.5-fold, and the inhibition constant is also increased 27-fold. In this case the change in the metal dependence likely reflects the interaction between the carboxylate of Glu60 and the ε-amino group of Lys44 (Hon *et al*, 1997). Lys44 interacts with the non-bridging oxygens of the α- and β-phosphates. This interaction is important for holding the nucleotide in place as evidenced by the 26.4-fold increase in the K_m of ATP. Thus, this interaction would clearly be important for holding ADP in place after phosphoryl transfer has occurred. Therefore, the loss of binding energy albeit indirect, would be expected to affect the inhibition caused by increasing concentrations of magnesium. The rather dramatic increase in both the

apparent dissociation and inhibition constants for Mg^{2+} was not initially expected given that the steady state kinetic parameters described above had suggested the relative unimportance of this residue to the catalytic mechanism of APH(3')-IIIa. This result, however, makes it easier to interpret the intermediate changes observed from APH(3')-$IIIa^{E60A}$ mutant and the observed changes in k_{cat} are likely a true reflection of an impaired enzyme. However, for this mutant, phosphate transfer is unlikely to be rate-limiting, as the solvent viscosity effect on the reaction catalyzed by this mutant has recently determined, and the results are inconsistent with such a conclusion (Boehr, Thompson, & Wright, unpublished results). While these results are inconsistent with phosphate transfer being rate-limiting, they are also not consistent with product release being rate-limiting, as the solvent viscosity effect, with respect to k_{cat}, is too large i.e. it is greater than 2. Simopoulous & Jencks (1994) have suggested that effects of this magnitude can be the result of an effect on the catalytic form of the enzyme, perhaps an effect on a diffusion-controlled conformational change. If this is the case, then it indicates that increases in solvent viscosity inhibit a conformational change that is required for phosphate transfer. Since the presence of Glu60 normally prevents this dramatic solvent viscosity effect, the pocket, created by the removal of this functional group, likely becomes filled with the viscogen, which prevents the diffusion controlled movement of residues lining this region of the active site. The role of Glu60 in such a conformational change is discussed below.

In the case of the APH(3')-$IIIa^{N195A}$ mutant, the inhibition due to high concentrations of magnesium is virtually non-existent. This result, in combination with the effects noted on the affinity of ATP for this mutant enzyme indicate that Mg2 is

required for the optimal binding of ATP. However, the loss of this coordination site for Mg2 did not have a severe impact on the first order rate constant of this mutant for either ATP or the various AGs examined. This is remarkable when one considers that the loss of the Asp208 carboxylate, and in effect the coordination site(s) on Mg1, results in the complete loss of any detectable activity. These results taken together suggest that Mg2 aids nucleotide triphosphate binding, but is not critical for the catalytic step of phosphoryl transfer. The loss of the inhibition induced by high concentrations of Mg^{2+} would also suggest that Asn195 plays a critical role in making ADP release the rate limiting step for APH(3')-IIIa. Solvent viscosity studies with this enzyme support such a role, as these studies indicate that V_{max} is no longer solely limited by diffusion, thereby indicating that ADP release is unlikely to be completely rate-limiting for this mutant enzyme. Thus, the fact that the APH(3')-IIIa^{N195A} mutant lacks a solvent isotope effect indicates that proton abstraction is unimportant for phosphoryl transfer, which is only consistent with a dissociative-like phosphoryl transfer reaction mechanism.

For the APH(3')-IIIa^{D190E} mutant, the less dramatic change in the apparent dissociation constant for the metal ion likely reflects the presence of the carboxylate of this mutant in a suboptimal orientation that nonetheless retains the ability to interact with Mg1. The fact that this mutant is not strongly inhibited by high concentrations of Mg^{2+} is consistent with the loss of an optimally oriented carboxylate that acts to hold Mg1 in place such that ADP release becomes rate limiting.

The position of Ser27 in the APH(3')-IIIa•ADP crystal structure appears to preclude this residue from any involvement in the catalytic mechanism of this enzyme.

However, the steady state kinetic analyses of both the APH(3')-IIIa^{S27A} and the APH(3')-IIIa^{S27P} mutants suggest otherwise. The magnesium ion dependencies of both these mutants also suggest that this residue is important for the catalytic mechanism of APH(3')-IIIa. The Mg^{2+} dependence of the Ser27 mutants further suggests that this residue can coordinate Mg1. The distance of this residue from Mg1 (3.7 Å), in the APH(3')-IIIa•ADP crystal structure, suggests that such an interaction is possible, but the interaction does not appear to be optimal. It is possible that the mutation of this residue has dramatic implications for the overall conformation of the NPL, but as I have argued above this is unlikely. Therefore, a second possibility is that a conformational change could bring the functional group of Ser27 into a position that is optimal for magnesium binding. This would more easily explain the change in the magnesium dependence. If Ser27 is a metal ligand, one might expect a decrease in affinity for ATP similar to the one detected for the APH(3')-IIIa^{N195A} mutant. However, assuming that this residue is indeed a metal ligand, then the hydroxyl group of Ser27 likely binds Mg1 in the TS, thus an effect on the K_m of the nucleotide would not necessarily be apparent, but instead should be apparent in the k_{cat}. Such a change in k_{cat} is readily detectable (Table 4.1). It should be noted that given the Mg-dependence of the Ser27 mutants I suggested that ADP release is not rate-limiting for the APH(3')-IIIa^{S27A} mutant, and indeed it is not. As such, phosphoryl transfer is likely rate limiting for these enzymes. Thus, the effect of mutating Ser27, on k_{cat}, is likely underestimated because for APH(3')-IIIa the internal rate of phosphoryl transfer is at least 10-fold higher than the k_{cat}, which is really a measure of ADP release.

4.4.3 Is the Role of Ser27 Conserved in ePKs?

While Ser27 is absolutely conserved among the APH(3'), it is not as well conserved among the ePKs (Figure 4.1). Thus, the role of this residue in the promotion of phosphate transfer may not be conserved among all ePKs. For example, in the crystal structures of HCK and CDK2 there does not appear to be a corresponding serine residue in the NPLs of these enzymes. However, in the case of the protein tyrosine kinase HCK (PDB Accession 1AD5; Sicheri *et al*, 1997) the carbonyl of Gly276 appears to be positioned such that it could fulfil a role that is similar to the role described herein for Ser27. Alternatively, the functional group of Gln278 could fulfil that role. The difficulty in interpreting a role for either of these residues comes from the fact that HCK was crystallized in the presence of Ca^{2+} and the bound AMPPNP is not in a catalytically competent state. The metal ion only coordinates to the α-phosphate, and the residue corresponding to Asp190 is 22.0 Å from the γ-phosphate. For CDK2, a Thr is present in the corresponding position at the apex of the NPL (PDB Accession 1JST; Russo *et al*, 1996). This residue could conceivably fulfil the role of Ser27, but it is difficult to ascertain the validity of this proposal because the nucleotide bound in the CDK2 structure also does not appear to be in a catalytically competent state. Only one manganese ion is bound, and this metal ion appears to only interact with the α-phosphate. Asp127, the CDK2 aspartate corresponding to Asp190 of APH(3')-IIIa is also quite far from the γ-phosphate (15.1 Å).

Serine residues in positions corresponding to Ser27 are present in the crystal structures of PKA and phosphorylase kinase γ (PHkγ) (PDB Accession 1ATP; Zheng,

1993; PDB Accession 1PHK; Owen *et al*, 1995). The catalytic sites of both of these enzymes have geometries that are similar to the catalytic site of APH(3')-IIIa. There are two serine residues in the NPL of PHKγ, Ser30 and Ser31. Structurally Ser31 appears to be the equivalent of Ser27 in APH(3')-IIIa. In PHKγ Ser31 is at the apex of the NPL and is 7.8 Å from Mg1. Thus, a large movement would be required for the functional group of this residue to take up a Mg^{2+} coordination position. It should be noted however that the NPL in this structure has very high thermal factors (67.7-76.6) thereby making such a conformational change possible. While $PHK\gamma^{S31G}$ mutant has a slightly higher k_{cat} (Lee *et al*, 1992), the affinity of this mutant for ATP is decreased by ~3-fold, and there is no corresponding change in affinity for ADP. Thus, this residue is likely the functional equivalent of Ser27 in APH(3')-IIIa. However, the lack of a k_{cat} effect, for the $PHK\gamma^{S31G}$ mutant, suggests that this residue does not play as important a role in phosphate transfer as Ser27 in APH(3')-IIIa does.

In the crystal structure of PKA bound to ATP, and a non-phosphorylatable peptide analogue, Ser53 appears to be present in a position that is structurally homologous to Ser27 in the APH(3')-IIIa•ADP crystal structure. Ser53 is 7.4 Å from Mg1. As this distance is large, a conformational change would be required to move this residue into a position, such that it could coordinate Mg1. Comparison of mouse recombinant PKA bound to adenosine with recombinant PKA bound to ATP and a non-phosphorylatable peptide analogue indicates that this loop is highly flexible (Narayana, 1997). The reduced susceptibility of this region to Fe-EDTA cleavage, upon ATP binding, indicates that this region undergoes conformational changes when PKA binds

this substrate (Cheng *et al*, 1998). Thus, this region is highly flexible and the conformational change described above is a possibility. An examination of the crystal structure of PKA bound to the inhibitor balanol indicates that Ser53 can move to approximately the position described above (Narayana *et al*, 1999). Evidence for the importance of this region to the catalytic mechanism of PKA, comes from an examination of the role of the Gly residues that are present in the NPL of this enzyme (Grant *et al*, 1998). This elegant work, that combines both steady and pre-steady state kinetic analyses, reveals the significant role that this loop plays in the catalytic event, in particular Gly50 and Gly52. The effect of a Gly52 to Ser change is most profound. The k_{cat} was decreased 12-fold from wild type, but more importantly the phosphoryl transfer step is decreased 300-fold. The authors suggest that this mutation disrupts the interaction between the Ser53 backbone amide proton and one of the γ-phosphate non-bridging oxygen, and that this is the cause of the decreased rate enhancement seen with this mutant. I concur, and using the APH(3')-IIIa structure with the modeled γ-phosphate, the Ser27 amide of APH(3')-IIIa appears to provide a similar interaction. The effect on the kinetic parameters of the PKA^{G52S} mutant is also consistent with the disruption of the proposed interaction between the hydroxyl group of Ser53 and Mg1. Thus, the role of Ser27 is likely conserved in at least one protein kinase.

The observation of an interaction between the γ-phosphate and the backbone amide of the serine residue present in the NPL is highly significant from a mechanistic point of view. In an associative mechanism, one would expect that a positive charge would be required to stabilize each of the 3 γ-phosphate oxygens as charge develops

during the TS (Figure 2A). As described above, this does not appear to be the case for either PKA or APH(3')-IIIa, and the amide in question would be unlikely to stabilize an associative TS. However, in a dissociative mechanism the presence of 3 positive charges is not required, and would in fact be inhibitory (Herschlag & Jencks, 1990; Maegley *et al*, 1996; Mildvan, 1997). Thus, based on these arguments a dissociative TS would be most consistent with the results obtained to date.

4.4.4 The effect of ATPγS on APH(3')-IIIa activity.

The effect of substituting an atom with sulfur on the rate of a reaction can generally be termed the thio effect. When ATPγS is used as a substrate for kinases, small or inverse thio effects are expected for dissociative phosphoryl transfer mechanisms because sulfur is less electronegative than oxygen (Breslow & Katz, 1968). This property aids the formation of a metaphosphate-like intermediate. For APH(3')-IIIa the rate of reaction is decreased 33-fold. While the significant effect observed would argue against a dissociative reaction mechanism in solution, there is great difficulty in quantifying the effect that metal ions exert to either stabilize or destabilize a metaphosphate-like TS when a thio-substituted ATP analogue is used. In fact, the measurement of the thio effect for CSK in the presence of a variety of different metal ions varies over a range from 136 for Mg^{2+} to 2.2 for Ni^{2+} (Grace *et al*, 1997). This change in thio effect inversely correlates with the thiophilicity of the metal ions. That is to say that the thio effect is large for atoms that prefer to bind oxygen and low for metal ions that show little or no preference for binding oxygen over sulfur. Magnesium prefers to bind oxygen on the order of 31000-fold to sulfur (Pecoraro *et al*, 1984). Similarly to

CSK a large thio effect is observed in alkaline phosphatase catalyzed reactions (Hollfelder & Herschlag, 1995) despite the fact that both enzymes, CSK and alkaline phosphatase, have been shown through other means to catalyze dissociative-like reactions. Thus, the presence of a thio effect is not a good indication of the reaction mechanism. This is especially true of enzymes, such as kinases, that employ metal ions with low thiophilicities.

4.4.5 Proteolysis Studies on APH(3')-IIIa

Proteolysis studies with subtilisin indicate that tobramycin binding can significantly prevent the partial proteolysis of APH(3')-IIIa. These results argue in favor of a tobramycin-induced conformational change that limits the accessibility of specific sites to proteolytic attack. This finding, in combination with solvent viscosity effects, indicates that a conformational change occurs first upon ATP binding (McKay & Wright, 1996) and then second when the AG binds to the enzyme.

Previous attempts to identify a conformational change had been unsuccessful even though a variety of bio-physical techniques had been employed (McKay &Wright, 1996). This suggests that the predicted conformational change that occurs upon AG binding is a subtle one, and likely moves catalytic residues into positions such that they are better able to promote the catalytic step of phosphoryl transfer. Such a subtle change is also consistent with the lack of a measurable non-specific ATPase activity associated with APH(3')-IIIa (McKay &Wright, 1996).

Identification of the products of subtilisin proteolysis has been problematic. That being the case I attempted to identify the sites N-terminal sites of cleavage by N-

terminal peptide sequencing. Sequencing of the peptide fragments revealed that the C-terminal region of APH(3')-IIIa is the site of cleavage, as the N-terminus is intact in all three peptides analyzed. Thus, the sites of cleavage are in the C-terminus. While the C-terminal sites of cleavage have yet to be definitively identified, it is possible to make an estimate of the sites of cleavage by comparing the relative mobilities of the peptide fragments to the relative mobilities of a series of proteins of known molecular weight. While highly speculative, I have used this information to identify Leu67, Glu122, and Asn158 as the potential C-terminal sites of cleavage. All three potential sites of cleavage are present on solvent exposed loops in the APH(3')-IIIa•ADP crystal structure, which is consistent with their susceptibility to proteolytic attack. Leu67 is present at the C-terminal end of an α-helix that is close to the nucleotide binding pocket. Interestingly, Glu60 is present in this α-helix. Glu122 is at the N-terminal end of a loop structure that joins two α-helices, which are on the periphery of the protein. Of these two helices, the C-terminal one is close to the C-terminal carboxylate, which has been shown to be critical for AG binding (Thompson *et al*, 1999; Chapter 5). The final site of cleavage, Asn158, is present on a loop that joins two α-helices that are present APH(3')-IIIa, but not in ePKs, and therefore these helices have been referred to as the APH αA-αB insert (Hon *et al*, 1997). This insert region is close to the site of AG binding (Thompson *et al*, 1999; Chapter 5), and as well, it is close to a number of residues that are conserved among the APH(3'), including Asp153 and Asp155. These conserved residues appear to line the AG binding pocket, and as such they are likely important for substrate binding, although their role in substrate binding has yet to be confirmed. Since Leu67, Glu122,

and Asn158 are all close to regions that are required for substrate binding, it is not unreasonable to expect that these loop regions undergo a conformational change upon AG binding, and it is likely that such a conformational change would limit their susceptibility to proteolytic cleavage.

4.4.6 Model for the Catalytic Mechanism of APH(3')-IIIa.

The data described herein, when taken in its totality, points to a reaction mechanism (Figure 4.9), wherein a metaphosphate-like intermediate is generated by the movement of Mg1 towards the AG substrate to be phosphorylated. In such a case the movement of Mg1 is likely directed by the actions of Ser27, Asp190, and Asp208. From the kinetic data obtained when these residues were mutated, it is clear that the most important amino acid residue is Asp208. The APH(3')-IIIa•ADP crystal structure reveals that Asp208 can occupy two coordination sites through its carboxylate moiety, and a similar organization is seen with the corresponding Mg^{2+} ion and aspartate residue in the crystal structures of a number of protein kinases, including PKA and glycogen phosphorylase kinase γ (PDB coordinates 1ATP and 1PHK; Zheng, 1993; Owen *et al*, 1995). In my model, Ser27, Asp190, and Asp208 act to move Mg1 towards the AG substrate while Lys44, Glu60, Asn195, and Mg2 act to hold the nucleotide in place. This effectively leads to the lengthening of the βγ-PO bond. While we have as yet no evidence to suggest whether or not the NPL of APH(3')-IIIa plays a role in holding the nucleotide diphosphate, likely it does. In PKA, Gly50 hydrogen bonds to the ribose. The K_m of the PKA^{G50S} mutant for ATP is 8.2-fold higher than the K_m of the wild type enzyme for this substrate, and most interestingly this residue no longer displays burst kinetics

(Grant *et al*, 1998). Thus phosphoryl transfer is likely rate limiting. According to my model the lack of a burst phase would reflect the failure of this mutant to hold the diphosphate portion of ATP in place, such that the βγ- PO bond is less capable of being stretched.

The lengthening of the βγ- PO bond would cause a change in the bond order of the terminal phosphate in such a way that a highly electrophilic metaphosphate-like intermediate is first generated and the γ-phosphate is then transferred to an AG hydroxyl group. For such a phosphate transfer to occur, the Asp208-containing loop must undergo a small conformational change i.e. a translation away from the bound nucleotide. However, the length of this translation need not be large (≤1 Å) (Mildvan, 1997). If the axial βγ- PO bond distance were to increase only 0.77 Å, the bond order would decrease to 0.052, indicating that the reaction is 94.8% dissociative. For a fully dissociative TS, this bond length would only have to increase 1.6 Å. Unfortunately, we have yet to obtain evidence for the conformational flexibility of this region in APH(3')-IIIa. In addition to the Asp208-containing loop, the NPL must also undergo a similar conformational change. A preliminary structure of APH(3')-IIIa, in the absence of ligand has been determined, indicates that the electron density for many of the residues in the NPL is poorly defined, suggesting that this region of the enzyme is highly flexible (Leung & Berghuis, personal communication), although we have no other biophysical data to confirm this flexibility. However, as noted above, the NPL has been identified in PKA to be conformationally flexible (Cheng *et al*, 1998). If conformational changes in the NPL and the Asp208-containing loop do result in the formation of a metaphosphate-like

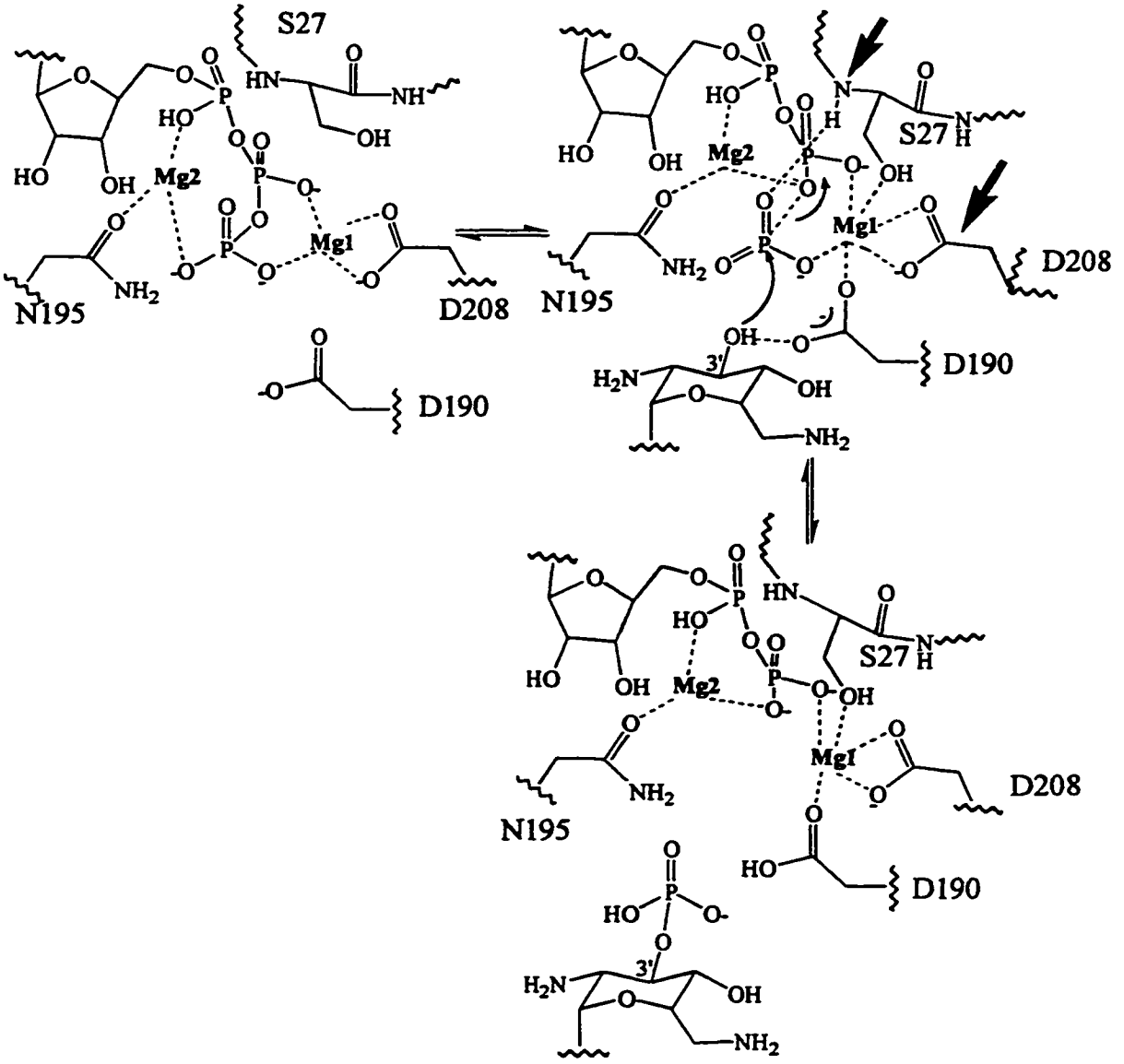

Figure 4.9: Model of the Catalytic Mechanism of APH(3')-IIIa. Left. ATP is bound to the enzyme. **Right.** An AG substrate binds and initiates the catalytic event. The NPL containing Ser27 moves in the direction indicated by the arrows. The hydroxyl group of Ser27 takes up a position coordinating Mg1, and the amide proton of this residue hydrogen bonds to a γ-phosphate non-bridge oxygen. The functional group of Asp190 also takes up a position coordinating Mg1. The loop containing Asp208 also moves in the direction indicated by the arrows. A metaphosphate-like intermediate is generated and phosphoryl transfer occurs. Thus substrate deprotonation need not occur until after phosphoryl transfer has occurred. **Bottom.** ADP is bound to the enzyme and the phosphorylated aminoglycoside leaves the enzyme active site.

intermediate, then substrate deprotonation is not required until after the phosphoryl transfer step has occurred. Such a result is consistent with my findings that substrate deprotonation does not make a significant contribution to the rate of reaction, for either the wild type enzyme or the APH(3')-IIIa^{N195A} mutant. The result with the APH(3')-IIIa^{N195A} mutant is especially significant because ADP release likely makes a much less significant contribution to the rate-limiting step. This result is also consistent with results obtained for CSK, a protein tyrosine kinase. In this case a trifluoro tyrosine analogue was examined as a substrate. The pKa of this analogue is such that it forms the phenoxide anion at neutral pH. If substrate deprotonation were required prior to phosphoryl transfer then a significant rate enhancement would be expected using this analogue. However, no significant rate enhancement was seen with the trifluorotyrosine analogue (Cole *et al*, 1995). Thus, Asp190 is unlikely to be a catalytic base, indicating that the functional group of this residue serves to orient the incoming AG hydroxyl, as well as Mg1, in order to promote phosphate transfer. Such a role is consistent with the finding that the APH(3')-IIIa^{D190N} mutant is only 140-fold less active than the wild type enzyme.

4.4.7 How Could A Conformational Change Be Transmitted to Asp208?

The catalytic mechanism described above requires that the loop containing Asp208 move 'away' from the nucleotide-binding site. There are no doubt a number of factors that could contribute to such a conformational change. Undoubtedly, the C-terminal region of APH(3')-IIIa, which is involved in AG binding (Thompson *et al*, 1999; Chapter 5), undergoes a conformational change upon AG binding that would

permit the interaction proposed above between Asp190 and Mg1. This interaction likely 'pulls' the Asp208-containing loop away from the nucleotide, and concomitantly helps lengthen the Pγ-O bond distance. However, this interaction alone is unlikely to be a sufficient driving force for the conformational change described above. Thus, the remaining driving force for a change in the conformation of the Asp208 loop is a change in the conformation of the NPL. There are two potential ways that the NPL can affect the conformation of Asp208. The first is through the interaction between Ser27 and Mg1. Similarly to Asp190 this residue could push Mg1 'away' from the nucleotide-binding site. The second is through the interactions that bridge the NPL to the Asp208-containing loop. The helix containing Glu60 bridges these two loops. The NPL could 'press' down on this helix which would force the movement of the Asp208 loop. If such a mechanism is correct it suggests that a highly conserved valine residue (Val31) be involved. The side chain of Val33 can interact with the sidechain of Lys44, and as the distance between these two residues decreases, the sidechain of Lys44 should move to compensate. Under such a circumstance, the movement of Lys44 would force the repositioning of the functional group of Glu60, which in turn forces the movement of the Asp208-containing loop. Glu60 is quite close to the backbone amide nitrogens of Asp208 (3.3 Å), Leu209 (4.1 Å), and Gly210 (3.9Å). These residues make up the DXG motif that is absolutely conserved among both the APHs and ePKs. Thus, the combination of all these forces either pushing or pulling the Asp208-containing loop results in phosphoryl transfer.

4.5 Conclusions.

The kinetic analyses of the mutant APH(3')-IIIa enzymes, described herein, help explain the contribution of each particular amino acid residue to the enhancement of phosphoryl transfer. These results also attempt to explain the roles of the two magnesium ions in the promotion of catalysis. Mg2 is required for nucleotide binding, whereas Mg1 is the catalytic magnesium ion that directs phosphoryl transfer, and thereby aids the formation of a metaphosphate-like intermediate. High concentrations of metal ions are undoubtedly the molecular basis for ADP release being fully rate limiting in the steady state. I also suggest that substrate deprotonation is not important for the catalytic activity of APH(3')-IIIa, and that Asp190 serves to orient the AG hydroxyl, and Mg1, such that phosphoryl transfer can occur. I also conclude that Asp208 is critical to the catalytic mechanism of this enzyme, and propose that this residue is required for a bio-mechanical reaction mechanism that involves the lengthening of the βγ-PO bond such that a metaphosphate-like intermediate is formed in the TS.

The results also describe the importance of a number of residues that are absolutely conserved among APHs and ePKs. The results, described herein, confirm that these residues are not only conserved at the primary and tertiary levels, but are also functionally conserved. This finding has profound implications for the evolution of enzymes when one considers that the sequence homology between APHs and PKs is less than 5%, and that only 5 absolutely conserved residues are shared between these two superfamilies of enzymes. Interestingly, these residues all make up the catalytic core of the enzyme and are involved in either nucleotide binding or in promoting phosphoryl

transfer. Thus, it appears that these two families of enzymes evolved from a common progenitor. As these enzymes evolved, the architecture of the active site was conserved while other non-catalytic residues, including the substrate binding site, were replaced in order to fulfil the specific requirements of each individual enzyme.

4.6 References.

Adams, J.A., & Taylor, S.S. (1993). Divalent metal ions influence catalysis and active-site accessibility in the cAMP-dependent protein kinase. *Prot. Sci.* **2**, 2177-2186.

Admiraal, S.J., Schneider, B., Meyer, P., Janin, J., Veron, M. Deville-Bonne, D., & Herschlag, D. (1999). Nucleophilic activation by positioning in phosphoryl transfer catalyzed by nucleoside diphosphate kinase. *Biochemistry* **38**, 4701-4711.

Beck, E., Ludwig, G., Auerswald, E.A., Reiss, B., & Schaller, H. (1982). Nucleotide sequence and exact location of the neomycin phosphotransferase gene from transposon Tn5. *Gene* **19**, 327-336.

Brenner, S. (1987). Phosphotransferase sequence homology. *Nature* **329**, 21.

Breslow, R., & Katz, I. (1968). Relative reactivities of *p*-nitrophenyl phosphate and phosphorothioate toward alkaline phosphatase and in aqueous hydrolysis. *J. Am. Chem. Soc.* **90**, 7376-7377.

Buchwald, S.L., & Knowles, J.R. (1982). Nucleophilic displacements on phosphoric monoesters: stereochemical evidence. *J. Am. Chem. Soc.* **104**, 1438-1440.

Buchwald, S.L., Friedman, J.M., & Knowles, J.R. (1984). Stereochemistry of nucleophilic displacement on two phosphoric monoesters and a phosphoguanidine. *J. Am. Chem. Soc.* **106**, 4911-4916.

Cleland, W.W., & Hengge, A.C. (1995). Mechanisms of phosphoryl and acyl transfer. *FASEB J.* **9**, 1585-1594.

Cole, P.A., Burns, P., Takacs, B., & Walsh, C.T. (1994). Evaluation of the catalytic mechanism of recombinant human Csk (C-Terminal Src Kinase) using nucleotide analogs and viscosity effects. *J. Biol. Chem.* **269**, 308801-30887.

Cole, P.A., Grace, M.R., Phillips, R.S., Burn, P. & Walsh, C.T. (1995). The role of the catalytic base in the protein tyrosine kinase Csk. *J. Biol. Chem.* **270**, 22105-22108.

Cowan, J.A. (1993). Inorganic biochemistry: an introduction. *Ed.* Cowan, J.A., VCH Publishers Inc., New York, NY, pp. 7-8.
Cheng, X., Shaltiel, S., & Taylor, S.S. (1998). Mapping substrate-induced conformational changes in cAMP-dependent protein kinase by protein footprinting. *Biochemistry* **37**. 14005-14013.

Daigle, D.M., McKay, G.A. & Wright, G.D. (1997). Inhibition of aminoglycoside antibiotic resistance enzymes by protein kinase inhibitors. *J. Biol. Chem.* **272**, 24755-24758.

Daigle, D.M., McKay, G.A., Thompson, P.R. & Wright, G.D. (1999). Aminoglycoside antibiotic phosphotransferases are also serine protein kinases. *Chem. Biol.* **6**, 11-18.

Fabiato, A., & Fabiato, F. (1979). Calculator programs for computing the composition of the solutions containing multiple metals and ligands used for experiments in skinned muscle cells. *J. Physiol. Paris* **75**. 463-505.

Gibbs, C.S. & Zoller, M.J. (1991). Rational scanning mutagenesis of a protein kinase identifies functional regions involved in catalysis and substrate interactions. *J. Biol. Chem.* **266**, 8923-8931.

Grace, M.R., Walsh, C.T. & Cole, P.A. (1997) Divalent ion effects and insights into the catalytic mechanism of protein tyrosine kinase Csk. *Biochemistry* **36**, 1874-1881.

Grant, B.D., & Adams, J.A. (1996). Pre-steady-state kinetic analysis of cAMP-dependent protein kinase using rapid quench flow techniques. *Biochemistry* **35**, 2022-2029.

Grant, B.D., Hemmer, W., Tsigelny, I., Adams, J.A., & Taylor, S.S. (1998). Kinetic analyses of mutations in the glycine-rich loop of cAMP-dependent protein kinase. *Biochemistry* **37**, 7708-7715.

Gray, G.S., & Fitch, W.M. (1983). Evolution of antibiotic resistance genes: The DNA sequence of a kanamycin resistance gene from *Staphylococcus aureus*. *Mol. Biol. Evol.* **1**. 57-66.

Heinzl, P., Werbitzky, O., Distler, J. & Piepersberg, W. (1988). A second streptomycin-resistance gene from *Streptomyces griseus* codes for streptomycin-3"-phosphotransferase. *Arch. Microbiol.* **150**. 184-192.

Hengge, A.C., Sowa, A., Wu, L., & Zhang, Z. (1995). Nature of the transition state of the protein-tyrosine phosphatase-catalyzed reaction. *Biochemistry* **34**, 13982-13987.

Her, J.H., Wu J., Rall, T.B., Sturgill, T.W., Weber, M.J. (1991). Sequence of pp42/MAP kinase, a serine/threonine kinase regulated by tyrosine phosphorylation. *Nucleic Acids Res.* **19**, 3743.

Herschlag, D., & Jencks, W.P. (1989a). Phosphoryl transfer to anionic oxygen nucleophiles. Nature of the transition state and electrostatic repulsion. *J. Am. Chem. Soc.* **111**, 7587-7596.

Herschlag, D., & Jencks, W.P. (1989b). Evidence that metaphosphate monoanion is not an intermediate in solvolysis reactions in aqueous solution. *J. Am. Chem. Soc.* **111**, 7579-7586.

Herschlag, D., & Jencks, W.P. (1990). Catalysis of the hydrolysis of phosphorylated pyridines by Mg(OH)+: A possible model for enzymatic phosphoryl transfer. *Biochemistry* **29**. 5172-5179.

Hollfelder, F., & Herschlag, D. (1995). The nature of the transition state for enzyme-catalyzed phosphoryl transfer. Hydrolysis of *O*-aryl phosphorothioates by alkaline phosphatase. *Biochemistry* **34**. 12255-12264.

Hon, W-C., McKay, G.A., Thompson, P.R., Sweet, R.M., Yang, D.S.C., Wright, G.D. & Berghuis, A.M. (1997). Structure of an enzyme required for aminoglycoside resistance reveals homology to eukaryotic protein kinases. *Cell* **89**, 887-895.

Khan, S.A., & Kirby, A.J. (1970). The reactivity of phosphate esters. Multiple structure-reactivity correlations for the reactions of triesters with nucleophiles. *J. Chem. Soc. (B)*, 1172-1182.

Kirby, A.J., & Vargolis, A.G. (1967). The reactivity of phosphate esters. Monoester hydrolysis. *J. Am. Chem. Soc.* **89**, 415-423.

Kim, K., & Cole, P.A. (1997). Measurement of a Brønsted nucleophile coefficient and insights into the transition state for a protein tyrosine kinase. *J. Am. Chem. Soc.* **119**, 11096-11097.

Kim, K., & Cole, P.A. (1998). Kinetic analysis of a protein tyrosine kinase reaction transition state in the forward and reverse directions. *J. Am. Chem. Soc.* **120**, 6851-6858.

Knighton, D.R., Zheng, J., Ten Eyck, L.F., Ashford, V.A., Xuong, N.H., Taylor, S.S., & Sowadski, J.M. (1991). Crystal structure of the catalytic subunit of cyclic adenosine monophosphate-dependent protein kinase. *Science* **253**. 407-414.

Knowles, J.R. (1980). Enzyme-catalyzed phosphoryl transfer reactions. *Ann. Rev. Biochem.* **49**, 877-919.

Kraulis, P.J. (1991). MOLSCRIPT: a program to produce both detailed and schematic plots of protein structures. *J. Appl. Cryst.* **24**, 946-950.

Leatherbarrow, R.J. (1992). *Grafit*, Ver 3.0, Erithacus Software Ltd., Staines, UK.

Lee, J-H, Maeda, S., Angelos, K.L. Kamita, S.G., Ramachandran, C., & Walsh, D.A. (1992). Analysis by mutagenesis of the ATP binding site of the γ-subunit of skeletal muscle phosphorylase kinase expressed using a baculovirus system. *Biochemistry* **31**, 10616-10625.

Lee, K.-Y., Hopkins, J.D., & Syvanen, M. (1991). Evolved neomycin phosphotransferase from an isolate of *Klebsiella pneumonia*. *Mol. Microbiol.* **5**, 2039-2046.

Maegley, K.A., Admiraal, S.J., & Herschlag, D. (1996). Ras-catalyzed hydrolysis of GTP: A new perspective from model studies. *Proc. Natl. Acad. Sci. USA* **93**, 8160-8166.

Matte, A., Tari, L.W., & Delbaere, L.T.J. (1998). How do kinases transfer phosphoryl groups? *Structure* **6**, 413-419.

McKay, G.A., Thompson, P.R. & Wright, G.D. (1994a). Broad spectrum aminoglycoside phosphotransferase type III from *Enterococcus*: Overexpression, purification, and substrate specificity. *Biochemistry* **33**, 6936-6944.

McKay, G.A., Robinson, R.A., Lane, W.S., & Wright, G.D. (1994b). Active site labeling of an aminoglycoside antibiotic phosphotransferase (APH(3')-IIIa). *Biochemistry* **33**, 14115-14120.

McKay, G.A. & Wright, G.D. (1995). Kinetic mechanism of aminoglycoside phosphotransferase Type IIIa: Evidence for a Theorell-Chance kinetic mechanism. *J. Biol. Chem.* **270**, 24686-24692.

McKay, G.A. & Wright, G.D. (1996). Catalytic mechanism of enterococcal kanamycin kinase (APH(3')-IIIa): Viscosity, thio, and solvent isotope effects support a Theorell-Chance mechanism. *Biochemistry*, **35**, 8680-8685.

Merritt, E.A., & Murphy, M.E.P. (1994). RASTER3D version 2.0: a program for photorealistic molecular graphics. *Acta Cryst.* **D50**, 869-873.

Mildvan, A.S., & Fry, D.C. (1987). NMR studies of the mechanism of enzyme action. *Adv. Enzymol.* **59**, 241-313.

Mildvan, A.S. (1997). Mechanisms of signaling and related enzymes. *Proteins: Str. Func. & Genet.* **298**, 401-416.

Narayana, N., Cox, S., Xuong, N-h., Eyck, L.F.T., & Taylor, S.S. (1997). A binary complex of the catalytic subunit of cAMP-dependent protein kinase and adenosine further defines conformational flexibility. *Structure* **5**, 921-935.
Narayana, N., Diller, T.C., Koide, K., Bunnage, M.E., Nicolaou, K.C., Brunton, L.L., Xuong, N-H, Eyck, L.F.T., & Taylor, S.S. (1999). Crystal structure of the potent natural product inhibitor balanol in complex with the catalytic subunit of cAMP-dependent protein kinase. *Biochemistry* **38**, 2367-2376.

Owen, D.J. Noble, M.E.M., Garman, E.F., Papageorgiou, A.C., & Johnson, L.N. (1995a). Two structures of phosphorylase kinase: an active protein kinase complexed with substrate analogue and product. *Structure* **3**, 467-482.

Owen, D.J. Papageorgiou, A.C., Garman, E.F., Noble, M.E. & Johnson, L.N. (1995b). Expression, purification and crystallisation of phosphorylase kinase catalytic domain. *J. Mol. Biol.* **246**, 374-381.

Pecoraro, V.L., Hermes, J.D., & Cleland, W.W. (1984). Stability constants of Mg^{2+} and Cd^{2+} complexes of adenine nucleotides and thionucleotides and rate constants for formation and dissociation of MgATP and MgADP. *Biochemistry* **23**, 5262-5271.

Russo, A.A. Jeffrey P.D., & Pavletich N.P. (1996). Structural basis of cyclin-dependent kinase activation by phosphorylation. *Nat Struct Biol* **8**, 696-700.

Salauze, D., & Davies, J. (1991). Isolation and characterisation of an aminoglycoside phosphotransferase from neomycin-producing *Micromonospora chalcea*; comparison with that of *Streptomyces fradiae* and other producers of 4,6-disubstituted 2-deoxystreptamine antibiotics. *J. Antibiot.* **44**, 1432-1443.

Sarkar, G. & Sommer, S.S. (1990). The 'megaprimer' method of site-directed mutagenesis. *Biotechniques* **8**, 404-407.

Schlichting, I., & Reinstein, J. (1997). Structures of active conformations of UMP kinase from *Dictyostelium discoideum* suggest phosphoryl transfer is associative. *Biochemistry* **36**. 9290-9296.

Schlichting, I., & Reinstein, J. (1999). pH influences fuoride coordination number of the AlF_x phosphoryl transition state analog. *Nat. Struct. Biol.* **6**, 721-723.

Sicheri, F., Moarefi, I., & Kuriyan, J. (1997). Crystal structure of the Src family tyrosine kinase Hck. *Nature* **385**, 602-609.

Simopoulos, T.T., & Jencks, W.P. (1994). Alkaline phosphatase is an almost perfect enzyme. *Biochemistry* **33**, 10375-10380.

Taylor, S.S., Radzio-Andzelm, E., & Hunter, T. (1995). How do protein kinases discriminate between serine/threonine and tyrosine? Structural insights from the insulin receptor protein-tyrosine kinase. *FASEB J.* **9**, 1255-1266.
Tenover, F.C., Gilbert, T., & O'Hara, P. (1988). Nucleotide sequence of a novel kanamycin resistance gene, *aphA-7* from *Campylobacter jejuni* and comparison to toher kanamycin phosphotransferase genes. *Plasmid* **22**, 52-58.

Thompson, P.R., Hughes, D.W. & Wright, G.D. (1996a) Mechanism of aminoglycoside 3'-phosphotransferase type IIIa: His188 is not a phosphate-accepting residue. *Chem. Biol.* **3**. 747-755.

Thompson, P.R., Schwartzenhaur, J., Hughes, D.W., Berghuis, A.M., & Wright, G.D. (1999). The C-terminus of aminoglycoside phosphotransferase (3')-IIIa is critical for antibiotic recognition and resistance. *J. Biol. Chem.* **In press.**

Thompson, J.D., Higgins, D.G., & Gibson, T.J. (1994). CLUSTAL W: improving the sensitivity of progressive multiple sequence alignment through sequence weighting, position-specific gap penalties and weight matrix choice. *Nucl. Acids Res.* **22**. 4673-4680.

Trieu-Cuot, P., & Courvalin, P. (1983). Nucleotide sequence of the *Streptococcus faecalis* plasmid gene encoding the 3'5"-aminoglycoside phosphotransferase type III. *Gene* **23**, 331-341.

Weiss, P.M., & Cleland, W.W. (1989). Alkaline phosphatase catalyzes the hydrolysis of glucose 6-phosphate via a dissociative mechanism. *J. Am. Chem. Soc.* **111**, 1928-1929.

Wittinghofer, A. (1997). Signaling mechanistics: aluminum fluoride for molecule of the year. *Curr. Biol.* **7**, R682-R685.

Xu, R.M., Carmel, G., Kuret, J., & Cheng, X. (1995). Crystal structure of casein kinase-1, a phosphate directed protein kinase. *EMBO J.* **14**, 1015-1023.

Zheng, J., Knighton, D.R., Eyck, L.F.T., Karlsson, R., Xuong, N-h., Taylor, S.S., Sowadski, J.M. (1993). Crystal structure of the catalytic subunit of cAMP-dependent protein kinase complexed with MgATP and peptide inhibitor. *Biochemistry* **32**, 2154-2161.

Zhou, J., & Adams, J.A. (1997). Is there a catalytic base in the active site of cAMP-dependent protein kinase? *Biochemistry* **36**, 2977-2984.

Chapter 5

The extreme C-terminus of APH(3')-IIIa is required for substrate binding and catalysis.

Adapted from

Thompson, P.R., Schwartzenhaur, J.,Hughes, D.W., Berghuis, A.M. & Wright, G.D. Journal of Biological Chemistry, 1999, vol. 274, pp. 30697-30706.

The work described in this chapter entails my characterization of the aminoglycoside binding pocket of APH(3')-IIIa. J. Schwartzenhaur and A.M. Berghuis, Department of Biochemistry, McMaster Univiersity, completed molecular modeling studies. D.W. Hughes, the Department of Chemistry, McMaster University, using a variety of one and two dimensional NMR techniques, determined the regiospecificity of several of the mutant APH(3')-IIIa enzymes described in this chapter. The other of this thesis obtained all other data presented in this chapter.

Chapter 5: The extreme C-terminus of APH(3')-IIIa is required for substrate binding and catalysis.

5.1. Introduction.

While the catalytic mechanism of the APH(3') and residues responsible for nucleotide binding have been firmly established, there is little information regarding the amino acid residues responsible for AG binding, as a crystal structure of an APH(3') bound to an AG has yet to be determined. Knowledge of how an APH(3')-IIIa binds to AG antibiotics is useful because it can identify potential sites of covalent modification, on the AG, that would lead to the development of drugs, which are no longer susceptible to this type of resistance mechanism. While the precise location of the AG binding pocket is not known, the C-terminal region of APH(3')-IIIa is the most likely site of AG binding, as the molecular surface of this region has a high concentration of negative charge. This negatively charged surface should provide complementary binding interactions for positively charged AGs. Support for such a location comes from the fact that the APH(3') share a significant amount primary sequence homology in the C-terminal third of the protein (see Figure 4.1 in Chapter 4).

One region of particular note in the C-terminal third of the APHs is the extreme C-terminal peptide, as this sequence is highly conserved among APH(3') proteins. Furthermore, physical mapping experiments, performed on the *aph(3')-IIa* gene, have

indicated that the 3'-end of the gene is important for mediating kanamycin resistance, as deletion of 66 nucleotides at the end of the gene obviates AG resistance (Beck *et al*, 1982). Thus, the 21 amino acids at the C-terminus of APH(3')-IIa are critical for the catalytic activity of this enzyme, and by inference APH(3')-IIIa. In APH(3')-IIIa the C-terminal peptide is composed of the amino acid sequence, Leu_{260}AspGluLeuPhe-COOH. In the crystal structure of APH(3')-IIIa, complexed with ADP, this sequence forms an α-helix that is readily observable in the electron density maps. In fact, the C-terminal carboxylate is highly defined, which is highly unusual in protein crystal structures (Hon *et al*, 1997). The C-terminal helix points back towards the nucleotide binding pocket of APH(3')-IIIa, and in the ADP complexed structure, the C-terminal phenylalanine is within 6 Å of the modeled γ-phosphate of ATP (Hon *et al*, 1997). Even with the identification of this region, it has been difficult to assign specific roles to the individual amino acids that are likely to be involved in AG binding. Nonetheless, my successful use of site directed mutagenesis to explore the catalytic mechanism of APH(3')-IIIa, suggested that this technique might be applied, to determine the roles of specific residues present in this AG binding site. Therefore, I have used this technique to examine the importance of Asp261, Glu262, and Phe264 to AG binding. These residues are highly conserved among the APH(3'), and since Phe264 is the C-terminal residue, all of these residues bear a negative charge, suggesting that they could be involved in binding the positively charged AGs. I have also examined the importance of Tyr55 and Arg211 to AG binding, as these residues also appear to line the AG binding pocket. Herein, the importance of each of these residues to substrate binding and catalysis is discussed.

5.2. Materials and Methods.

5.2.1. Chemicals.

Kanamycin A, neomycin B, butirosin, ribostamycin, lividomycin A, amikacin, phosphoenolpyruvate, and β-nicotinamide adenine dinucleotide were from Sigma. ATP and pyruvate kinase/lactate dehydrogenase were from Boehringer Mannheim. The restriction enzymes *HinD*III and *Nde*I were from MBI Fermentas (Flamborough, Ontario). Vent DNA polymerase and *Dpn*I were from New England BioLabs and *Pfu* DNA polymerase was from Stratagene. Neamine was the generous gift of S. Mobashery, Department of Chemistry, Wayne State University, Detroit, Michigan.

5.2.2. Site Directed Mutagenesis.

The APH(3')-IIIa$^{F264\Delta}$ mutant was generated by PCR amplification of the wild type gene, encoded on plasmid pETSACG1 (Chapter 3), using the mutagenic oligonucleotide, 5'-CCCGAAGCTTCTACAATTCATCCAG-3', as the reverse primer. The forward primer has been described (McKay *et al*, 1994; Chapter 3). The APH(3')-IIIa^{D261A}, the APH(3')-IIIa^{E262A}, the APH(3')-IIIa^{F264A} and the APH(3')-IIIa$^{D261A\text{-}F264\Delta}$ mutants were similarly generated, using the mutagenic oligonucleotides, 5'-CCCGAAG CTTCTAAAACAATTCAGCCAGTAAAATATAATA-3', 5'-CCCGAAGCTTCT AAAACAATGCATCCAGTAAAAT-3', 5'-CGAAGCTTGGATCCCTAAGCCAATT CATCCA-3' and 5'-CCCGAAGCTTCTACAATTCAGCCAGTAAAATATAAT ATTTTA-3', respectively, as the reverse primers. The PCR amplified products were digested with *HinD*III and *Nde*I and cloned into similarly cut pET22b(+). The mutagenic

oligonucleotides, 5'-AAAGGGACCACCGCTGATGTGGAACG-3', 5'-ATTGATCTT GGGGCAAGCGGCAGG-3', and their reverse complements were used to generate the APH(3')-IIIa^{Y55A} and the APH(3')-IIIa^{R211A} mutants by the Quik-Change mutagenesis method (Stratagene, LaJolla, CA). Plasmid pETSACG1 was also used as the template for these PCR reactions.

In all cases DNA sequencing identified the desired mutation, and the mutant gene was then completely sequenced at the Central Facility of the Institute for Molecular Biology and Biotechnology at McMaster University to ensure that no other mutations had been introduced. For the APH(3')-IIIa^{D261A}, APH(3')-IIIa^{E262A} and the APH(3')-IIIa$^{F264\Delta}$ mutants, the genes encoding these enzymes were subcloned into M13mp18, and sequenced using the T7 Polymerase Sequencing kit (Pharmacia). Mutant *aph(3')-IIIa* genes, present on plasmid pETY55A4, pETR211A6, pETF264A3 and pETFDA4, were sequenced at the Central Facility of the Institute for Molecular Biology and Biotechnology, McMaster University.

All of the constructs described above were used to transform $CaCl_2$ competent *E. coli* BL 21 (DE3), in order to facilitate protein overexpression.

5.2.3. Protein Purification.

Mutant APH(3')-IIIa proteins were overexpressed and purified essentially as described in (McKay *et al*, 1994; Chapter 2). In order to purify certain mutant APH(3')-IIIa proteins slight modifications of the purification procedure described in Chapter 2 were required and these are described below. For the purification of the APH(3')-

IIIa^{Y55A}, APH(3')-IIIa^{E262A}, and the APH(3')-IIIa^{F264A} mutant enzymes, the second column was replaced with a smaller Q Sepharose column (10 x 1 cm). Mutant proteins were eluted using a linear gradient (15-40%) of Buffer B (50 mM Tris-HCl pH 8.0, 1 mM EDTA, 1 M NaCl) over at least 8 column volumes. The APH(3')-IIIa$^{F264\Delta}$ mutant was similarly purified, but in order to obtained pure protein, fractions from the small Q Sepharose column were applied to a Superdex 200 (HR 10/30) (Pharmacia). The column was equilibrated in 50 mM Tris-HCl pH 8.0, 1 mM EDTA, 200 mM NaCl and the proteins separated at a rate of 0.4 mL/min. In the purification of the APH(3')-IIIa^{D261A} and the APH(3')-IIIa$^{D261AF264\Delta}$ mutants, the second column was again replaced with the smaller Q Sepharose column, and the mutant proteins eluted as described above. In order to obtain pure protein, fractions of the APH(3')-IIIa^{D261A} mutant were applied to a Mono Q (HR 5/5) (Pharmacia) analytical anion exchanger, and proteins were eluted using a linear gradient (10-40%) of Buffer B over 45 mL. Similarly, fractions of the APH(3')-IIIa$^{D261A\text{-}F264\Delta}$ double mutant were applied to a 1 mL Resource Q (Pharmacia), and proteins were eluted using a linear gradient (15-45%) of Buffer B over 50 mL.

5.2.4. Kinetic Analysis of Mutant APH(3')-IIIa Proteins.

The kinetic assay monitors the production of ADP by coupling it to the oxidation of NADH by a pyruvate kinase/lactate dehydrogenase system. The assay is described in greater detail elsewhere (McKay *et al*, 1994; Chapter 4). Initial rates were fitted by nonlinear least fit squares to Equation 1,

$$v = (k_{cat}/E_t)[S]/(K_m + [S]) \qquad \text{(Eq. 1)},$$

or to Equation 2,

$$v = (k_{cat}/E_t)[S]/(K_m + [S])(1 + [S]/K_i)) \quad \text{(Eq. 2)},$$

if substrate inhibition was detected, using Grafit version 3.0 (Leatherbarrow, 1992). When the kinetic parameters of the APH(3')-IIIa^{D261A} were determined for neomycin I found that the K_m was near the detection limit of the assay described above. To confirm the accuracy of the K_m reported, I took advantage of the fact that this mutant is significantly impaired in its ability to phosphorylate neomycin. Therefore, I used neomycin as an inhibitor of kanamycin A phosphorylation to determine a K_i for neomycin. The steady state parameters for kanamycin A were determined in the presence of 1.0, 10, 100, 1000 μM neomycin B and 1 mM ATP. Since some residual neomycin activity was detected, the basal rate of neomycin phosphorylation was subtracted from the kanamycin A rates of phosphorylation. These rates were fitted by non-linear least fit squares to Equation 3,

$$v = (k_{cat}/E_t)[S]/(K_m (1 + [I]/ K_{is}) + [S]) \quad \text{(Eq. 3)}.$$

5.2.5. Purification of Phosphorylated Aminoglycosides.

Phosphorylated ribostamycin was prepared and purified essentially as described in Thompson *et al* (1996), and in Chapter 2 (Method B). However, it should be noted that fractions obtained from the batchwise purification step were pooled, neutralized with 6 M HCl, and lyophilized. Typically, the lyophilized products were then dissolved in 30 mL of ddH_2O, and desalted by the application of 5 mL aliquots to an 80 x 2 cm Sephadex G-25 column. The mobile phase was water, the column run at a flow rate of 1.5 mL/min,

and 3 mL fractions were collected. Fractions were analyzed by TLC and those fractions containing the phosphorylated AG were pooled and applied to a Mono S (HR 5/5), as described (Thompson *et al*, 1996; Chapter 2). Fractions containing pure phosphorylated AG were pooled and lyophilized.

5.2.6. Sample preparation for NMR Analysis of phosphoribostamycin.

The purified phosphorylated derivatives of ribostamycin were lyophilized, dissolved in 99% D_2O, lyophilized again, and finally dissolved in 99.996% D_2O (Isotec, Inc) to a concentration of approximately 20 mg/mL.

5.2.7. Mass spectral analysis of phosphoaminoglycosides phosphorylated by mutant APH(3')-IIIa proteins.

The ability of the APH(3')-IIIa$^{F264\Delta}$ mutant to phosphorylate both ribostamycin and neomycin was examined by mass spectrometry. Electrospray mass spectra for neomycin- and ribostamycin-phosphate were determined in the positive ion mode in the presence of 0.1% formic acid and 0.2% formic acid, respectively. Electrospray mass spectral analysis of ribostamycin phosphorylated by the APH(3')-IIIa^{Y55A} and the APH(3')-IIIa^{E262A} mutants was carried out in the positive ion mode in the presence of 0.2% formic acid. All mass spectra were recorded at the McMaster Regional Center for Mass Spectrometry.

5.2.8. Determination of Minimal Inhibitory Concentrations.

Minimal inhibitory concentrations (MIC) of the various mutant APH(3')-IIIa cell strains were estimated through the use of antibiotic gradient agar plates (Cunningham *et al*, 1986). Gradient plates were prepared by the addition of drug and 25

μL of a 10% suspension of Antifoam B to 25 mL of molten Mueller Hinton agar. Kanamycin A was added to a final concentration of 150 μg/mL and neomycin was added to a concentration of 75 μg/mL. The resultant solution was then poured into a square sterile culture plate at an incline in order to create a wedge. The agar was allowed to solidify for approximately one hour at which time an overlaying wedge, made up of molten Mueller Hinton Agar (25 mL) was poured while the culture dish laid flat. The overlaying wedge was allowed to solidify for a further 2 hours. Overnight cell cultures of the wild type, and mutant plasmids, cloned into *E. coli* BL 21 (DE3) were diluted 100 fold in 2 mL of top agar (5g tryptone, 4g NaCl, 4g granulated agar). The top agar was spread across a sterile microscope slide and a uniform distribution of cells was achieved by dipping the long edge of a second sterile microscope slide into the cell suspension. The edge of the slide was then applied to the surface of the plate parallel to the gradient of drug. The plates were inverted and grown for 24 hours. The gradient was assumed to be linear, and the fraction of the total distance of the gradient, on which the mutant cell strains were able to grow was used to estimate the MICs of the APH(3')-IIIa mutants.

5.2.9. Expression of wild type and mutant enzymes.

Cells, *E. coli* BL 21 (DE3), bearing either the wild type or mutant *aph(3')-IIIa* genes were used to inoculate overnight cultures (50 mL) of LB-ampicillin (100 μg/mL) in the absence of IPTG. The overnight cultures were harvested by centrifugation at 5000 x g and resuspended in 4 mL of 50 mM Tris-HCl pH 8.0, 5 mM EDTA, and 200 mM NaCl. Cells were then lysed by 2 passages through a French pressure cell, and cleared by

centrifugation at 20000 x g. The concentration of protein was determined for each of the cleared lysates, and equivalent amounts of protein (10 μg) were diluted to 10 μL. To this was added 10 μL of 2 x SDS PAGE loading buffer, and the samples were then boiled for 30 min. These samples were then applied to a 15% SDS PAGE gel and subjected to electrophoresis. Proteins thereby separated were then electroblotted onto nitrocellulose, in preparation for western analysis, using a rabbit anti-APH(3')-IIIa antibody. The Western blot was developed using a donkey anti-rabbit IgG antibody coupled to alkaline phosphatase.

5.3 Results.

5.3.1. Kinetic analysis of APH(3')-IIIa mutants.

In an effort to examine the contribution of the aforementioned residues to the catalytic mechanism of APH(3')-IIIa, site directed mutagenesis, of the *aph(3')-IIIa* gene, was used to generate the APH(3')-IIIa^{Y55A}, APH(3')-IIIa^{R211A}, APH(3')-IIIa^{D261A}, APH(3')-IIIa^{E262A}, and APH(3')-IIIa^{F264A} mutants. In order to examine the role of Phe264 and Asp261 in greater detail, the APH(3')-IIIa$^{F264\Delta}$ and APH(3')-IIIa$^{D261A\text{-}F264\Delta}$ mutants were also generated. Once generated, the mutants were overexpressed, purified, and the purified proteins subjected to steady state kinetic analysis. For this analysis, a number of chemically related AGs were examined.

5.3.1.1. Tyrosine 55.

While Tyr55 is poorly conserved among the 3'-APHs, the decision to generate the APH(3')-IIIa^{Y55A} mutant was influenced by the observation that this residue could

form part of the presumed AG binding pocket. Additionally, the close proximity (3.9-8.5 Å) of the C-terminal phenylalanine ring to the phenolic ring of Tyr55 influenced that decision. This proximity suggested a possible stacking interaction between the two aromatic rings upon substrate binding. However, the steady state kinetic parameters of the APH(3')-IIIa^{Y55A} mutant were not substantially perturbed. Although it should be noted that the dissociation constant for ATP is increased 3.5-fold. Since the apparent dissociation constant, K_m, of APH(3')-IIIa for AG substrates includes a number of rate constants, a better measure of AG affinity is V/K, a second order rate constant that represents the interaction of the substrate with enzyme. Generally for the APH(3')-IIIa^{Y55A} mutant, the loss of the phenolic group has little effect on V/K, however, for amikacin and butirosin V/K is decreased 19.3- and 9.5-fold, respectively (Figure 5.1 and Table 5.1). Thus, the side chain of Tyr55 is important for binding AGs substituted at the N1 position. While this residue aids the binding of the semi-synthetic AGs the residue is clearly not required, generally, for the catalytic activity of this enzyme.

5.3.1.2. Arginine 211

The crystal structure of the APH(3')-IIIa•ADP complex revealed the close proximity of Arg211 to the active site. This proximity, combined with the fact that Arg211 is highly conserved among the 3'-APHs, suggested that a more thorough understanding of the role that this residue plays, in the catalytic mechanism of APH(3')-IIIa, was required. Determination of the steady state kinetic parameters for the APH(3')-

IIIa^{R211A} mutant revealed that this residue is fairly important for promoting the phosphorylation of the 4,5-disubstituted AGs (Figure 6.1 and Table 5.1), as the

Table 5.1: Steady state kinetic parameters for wild type and C-terminal mutant APH(3')-IIIa proteins.

	Wild Type[1]		
Substrate	K_m (μM)	k_{cat} (s^{-1})	K_i (mM)
ATP	27.7±3.7	1.76±0.08	NA
Kanamycin A	12.6±2.6	1.79±0.09	6.38±1.67
Neomycin B	7.72±0.9	2.08±0.07	2.65±0.59
Amikacin	245±27	2.46±0.11	NA
Butirosin	34.3±3.1	2.02±0.07	2.17±0.41
Ribostamycin	9.3±1.8	1.89±0.10	1.73±0.66
Neamine	20.0±2.8	2.00±0.15	2.00±0.4
Lividomycin A	31.6±5.1	3.97±0.25	1.53±0.42
Isepamicin	198±28	1.41±0.35	NA

	APH(3')-IIIa^{Y55A} [2]				
Substrate	K_m (μM)	$K_{m(mut)}/K_{m(WT)}$	k_{cat} (s^{-1})	$k_{cat(WT)}/k_{cat(mut)}$	$V/K_{WT}/V/K_{mut}$
ATP	97.4±14.2	3.5	2.3±0.06	0.8	2.8
Kanamycin A	9.3±2.6	0.7	1.8±0.06	1	0.7
Neomycin B	4.1±1.1	0.5	2.3±0.06.	0.9	0.5
Amikacin	1340±284	5.5	0.71±0.07	3.5	19.0
Butirosin	250±27	7.3	1.6±0.06	1.3	9.5
Ribostamycin	7.1±1.1	0.8	2.8±0.06	0.7	0.6
Neamine	46.9±14.7	2.4	2.26±0.30	0.9	2.2
Lividomycin A	16.5±2.9	0.5	2.62±0.08	1.5	0.8
Isepamicin	ND	-	ND	-	-

[1] Steady state kinetic parameters for the aminoglycoside substrates, save isepamicin, are taken from McKay, *et al* (1994). The steady state kinetic parameters for isepamicin are the unpublished results of McKay & Wright. The steady state kinetic parameters for ATP are taken from Hon, *et al*, 1997.

[2] For the APH(3')-IIIa^{Y55A} mutant substrate inhibition was only noted when neamine was examined as a substrate. The substrate inhibition constant is 2.3±1.2 mM.

Table 5.1. Continued.

	APH(3')-IIIa^{R211A} [3]				
Substrate	K_m (μM)	$K_{m(mut)}/K_{m(WT)}$	k_{cat} (s^{-1})	$k_{cat(WT)}/k_{cat(mut)}$	$V/K_{WT}/V/K_{mut}$
ATP	18.6±2.8	0.7	0.65±0.02	2.7	1.9
Kanamycin A	15.5±1.6	1.2	0.89±0.09	2.0	2.4
Neomycin B	3.3±1.1	0.4	0.33±0.01	6.3	2.5
Amikacin	588±105	2.4	0.47±0.03	5.2	12
Butirosin	138±18	4.0	0.74±0.03	2.7	11
Ribostamycin[4]	ND	-	ND	-	-
Neamine	ND	-	ND	-	-
Lividomycin A	10.7±1.6	0.3	0.30±0.01	13	4.0
Isepamicin	858±111	4.3	0.63±0.04	2.2	9.5

	APH(3')-IIIa^{D261A}				
Substrate	K_m (μM)	$K_{m(mut)}/K_{m(WT)}$	k_{cat} (s^{-1})	$k_{cat(WT)}/k_{cat(mut)}$	$V/K_{WT}/V/K_{mut}$
ATP	6.12±0.89	0.2	0.20±0.0	8.8	1.8
Kanamycin A	21.2±5.22	1.7	0.24±0.01	7.5	13
Neomycin B	2.85±0.82	0.4	0.027±0.001	77	31
Amikacin	648±111	2.6	0.21±0.02	12	30
Butirosin	121±23	3.5	0.019±0.001	100	360
Ribostamycin	22.8±4.0	2.5	0.023±0.001	82	210
Neamine	ND	-	ND	-	-
Lividomycin A	ND	-	ND	-	-
Isepamicin	ND	-	ND	-	-

[3] For the APH(3')-IIIa^{R211A} mutant substrate inhibition was only noted when kanamycin A was examined as a substrate. The substrate inhibition constant is 1.9±0.8 mM.

[4] The steady state kinetic parameters of the APH(3')-IIIa^{R211A} mutant for ribostamycin were not determined as substrate inhibition dominated at the detection limit of the enzyme assay.

Table 5.1. Continued.

	APH(3')-IIIa^{E262A} [5]				
Substrate	K_m (μM)	$K_{m(mut)}/K_{m(WT)}$	k_{cat} (s^{-1})	$k_{cat(WT)}/k_{cat(mut)}$	$V/K_{WT}/V/K_{mut}$
ATP	10.4±0.90	0.4	2.1±0.03	0.8	0.3
Kanamycin A	329±28	26	2.27±0.08	0.8	21
Neomycin B	10.4±2.1	1.4	3.39±0.0.10	0.6	0.8
Amikacin	276±50	1.1	3.26±0.23	0.8	0.9
Butirosin	18.2±1.5	0.5	0.57±0.01	3.5	1.8
Ribostamycin	78.7±4.47	8.5	0.53±0.01	3.6	31
Neamine	172±33	8.6	2.53±0.29	0.8	6.9
Lividomycin A	68.5±2.9	2.2	2.03±0.03	2.0	4.4
Isepamicin	ND	-	ND	-	-

	APH(3')-IIIa^{F264A} [6]				
Substrate	K_m (μM)	$K_{m(mut)}/K_{m(WT)}$	k_{cat} (s^{-1})	$k_{cat(WT)}/k_{cat(mut)}$	$V/K_{WT}/V/K_{mut}$
ATP	11.4±1.6	0.4	1.6±0.03	1.1	0.4
Kanamycin A	15.9±5.8	1.3	1.9±0.2	0.9	1.2
Neomycin B	23.3±2.9	3.0	5.1±.1	0.4	1.2
Amikacin	879±237	3.6	2.3±0.3	1.1	4.0
Butirosin	128±28	3.7	2.7±0.2	0.8	3.0
Ribostamycin	13.4±1.8	1.4	2.1±0.06	0.9	1.3
Neamine	ND	-	ND	-	-
Lividomycin A	ND	-	ND	-	-
Isepamicin	ND	-	ND	-	-

[5] For the APH(3')-IIIa^{E262A} mutant substrate inhibition was only noted when butirosin and neamine were examined as substrates. The substrate inhibition constants are 6.6±1.6 and 1.9±0.7 mM, respectively.
[6] For the APH(3')-IIIa^{F264A} mutant substrate inhibition was only noted when kanamycin A and ribostamycin were examined as substrates. The substrate inhibition constants are 0.66±0.29 and 10.7±4.1 mM, respectively.

Table 5.1. Continued.

APH(3')-IIIa$^{F264\Delta}$ [7]

Substrate	K_m (μM)	$K_{m(mut)}/K_{m(WT)}$	k_{cat} (s^{-1})	$k_{cat(WT)}/k_{cat(mut)}$	$V/K_{WT}/V/K_{mut}$
ATP	17.9±1.8	0.7	0.26±0.01	6.8	4.8
Kanamycin A	115±10	9.1	0.25±0.01	7.2	66
Neomycin B	18.3±2.8	2.4	0.88±0.02	2.4	5.8
Amikacin	720±261	2.9	0.10±0.02	25	71
Butirosin	435±82	13	0.14±0.01	14	180
Ribostamycin	30.5±4.3	3.3	0.23±0.01	8.2	27
Neamine	63.2±14.3	3.2	1.78±0.18	1.1	3.5
Lividomycin A	42.1±5.5	1.3	0.82±0.03	4.8	6.2
Isepamicin	ND	-	ND	-	-

APH(3')-IIIa$^{D261A-F264\Delta}$

Substrate	K_m (μM)	$K_{m(mut)}/K_{m(WT)}$	k_{cat} (s^{-1})	$k_{cat(WT)}/k_{cat(mut)}$	$V/K_{WT}/V/K_{mut}$
ATP	6.7±0.87	0.2	0.084±.0.0013	21	4.2
Kanamycin A	146±15.4	12	0.091±0.003	20	230
Neomycin B	21.1±3.5	2.7	0.081±0.003	26	69
Amikacin	436±116	1.8	0.008±0.001	320	580
Butirosin	ND[8]	-	ND	-	-
Ribostamycin	1500±210	160	0.13±0.009	15	2300
Neamine	ND	-	ND	-	-
Lividomycin A	ND	-	ND	-	-
Isepamicin	ND	-	ND	-	-

ND=not determined
NA=not applicable

[7] For the APH(3')-IIIa$^{F264\Delta}$ mutant substrate inhibition was only noted for neamine. The substrate inhibition constant for this AG, the K_i, was 4.9±3.4 mM.

[8] The steady state kinetic parameters for butirosin were not determined, as this AG was an extremely poor substrate for the APH(3')-IIIa$^{D261A-F264\Delta}$ mutant.

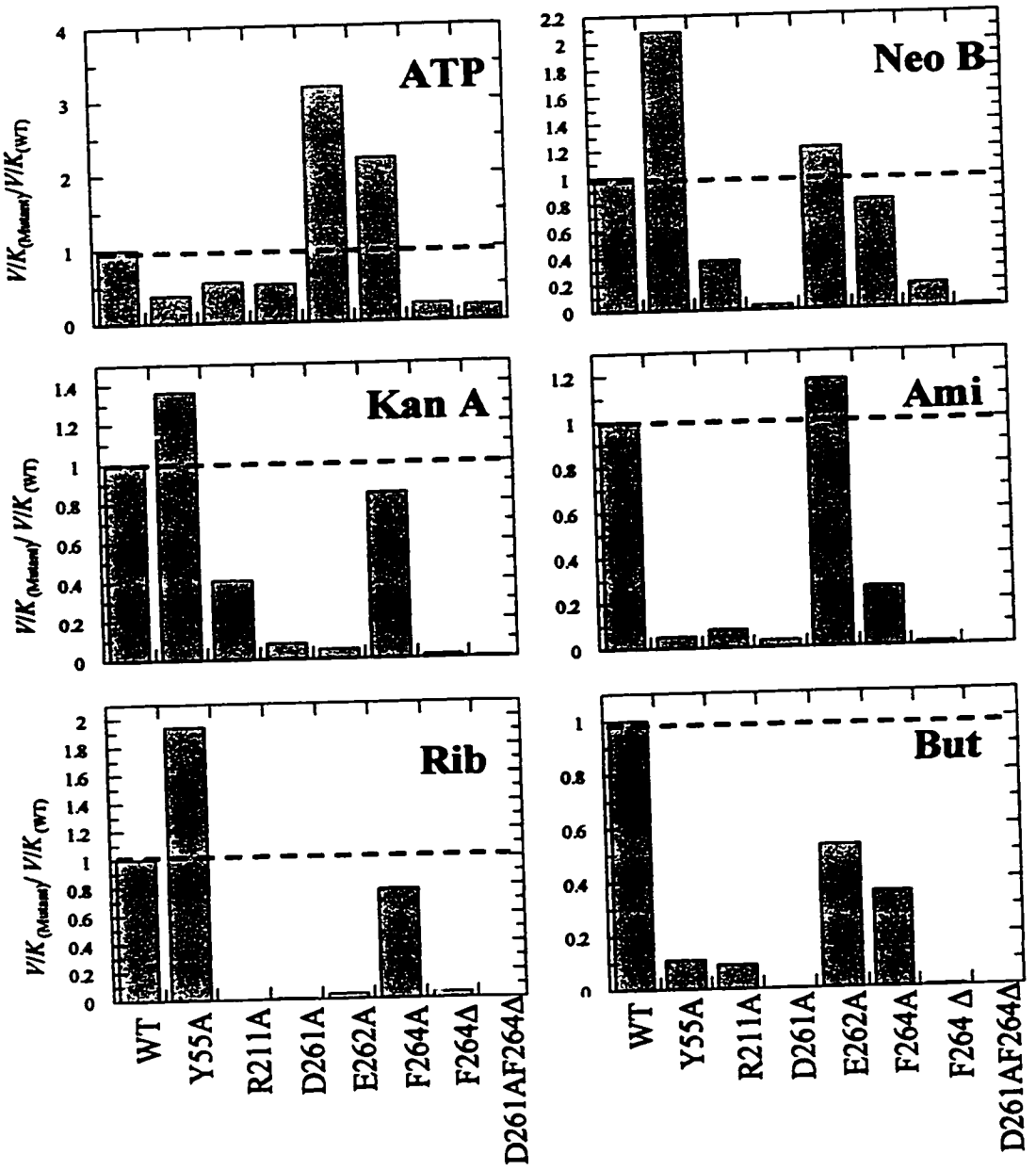

Figure 6.1. Relative specificity constants, $(V/K_{(mut)})/(V/K_{(WT)})$, of wild type and mutant APH(3')-IIIa enzymes. Note that in this figure the single letter abbreviations for amino acid residues are used to denote the mutant enzymes.

the k_{cat} for neomycin B is decreased 6.3-fold and the k_{cat} for lividomycin A is decreased 13.2-fold. However, effects on k_{cat} are not universally apparent, as the k_{cat} for kanamycin A is decreased by only 2-fold, the k_{cat} for ATP is similarly decreased by 2.7-fold, and the k_{cat} for amikacin is decreased by 5.2-fold (Table 5.1).

Generally, this residue does not appear to be important AG binding as the *V/K*s of this mutant for the majority of the AGs examined show only slight deviations from those values obtained for the wild type enzyme. However, for AGs that possess a hydroxybutyrate or hydroxypropionate group the *V/K* is decreased significantly. The *V/K*s for amikacin, isepamicin, and butirosin are decreased 12-, 9.5-, and 11-fold, respectively. These effects on *V/K* are mirrored by increases to the apparent dissociation constant, K_m.

5.3.1.3 Aspartate 261

Asp261 is absolutely conserved in the C-terminal peptide of APH(3') isozymes. For the APH(3')-IIIa^{D261A} mutant, when compared to the wild type enzyme, the most striking effect is the magnitude of the decrease in the first order rate constant (Table 5.1). There is a 7.5-fold decrease in the k_{cat} for kanamycin A and an 12-fold decrease in the k_{cat} for amikacin, both 4,6-disubstituted AGs. For such 4,5-disubstituted AGs, as butirosin, neomycin and ribostamycin, the decrease in k_{cat} is more pronounced, and on the order of 100 fold.

Consistent with the APH(3')-IIIa•ADP crystal structure Asp261 is not important for nucleotide binding as the K_m of the APH(3')-IIIa^{D261A} mutant for ATP is actually

decreased 5-fold. This residue also does not appear to be important for AG binding, as the K_ms, determined for a number of AGs, are only slightly affected (0.4-2.5-fold), although it should be noted that the V/Ks for all of the AG substrates examined are substantially lower, 13- to 360-fold, due mostly to the significant decreases in k_{cat}. To further confirm the relative unimportance of this residue to AG binding, an estimate of neomycin affinity was made, by determining the K_i for this AG. Such a determination was also necessary because the K_m, determined for neomycin, is quite low, and close to the detection limits of the assay. Since neomycin is such a poor substrate for the APH(3')-IIIa^{D261A} mutant, it was used to inhibit the phosphorylation of kanamycin A in a reaction catalyzed by this mutant enzyme. Neomycin B is a competitive inhibitor of kanamycin phosphorylation, and the K_i determined, 3.21± 0.28 μM, is in excellent agreement with the K_m reported for neomycin phosphorylation (Table 5.1). Thus, this residue is unlikely to play a significant role in AG binding.

5.3.1.4. Glutamate 262

Glu262 is also conserved in the C-termini of APH(3'), but the function of this residue is not clear from the crystal structure of APH(3')-IIIa. In this structure the Glu262 functional group is pointing away from the active site and therefore would not be expected to be involved in the binding of any AG substrate. Generally, the APH(3')-IIIa^{E262A} mutation has little effect upon the ability of this enzyme to either phosphorylate or bind AG antibiotics. The steady state kinetic parameters for ATP, neomycin B, amikacin and lividomycin A are virtually unchanged (Table 5.1). However, there is a

dramatic 21-fold decrease in the *V/K* for kanamycin A. A similar, but somewhat smaller effect is observed for neamine, an AG that is not substituted with either a pentose or hexose at the 5 or 6 positions, respectively, of the aminocyclitol ring. The *V/K* is decreased 6.9-fold. These effects on *V/K* are mirrored by changes in K_m. Thus, this would suggest, that this residue be involved in either binding the 6-aminohexose ring and/or the aminocyclitol ring.

5.3.1.5. Phenylalanine 264

The C-terminal phenylalanine ring is unlikely to be involved in AG binding, as these substrates are hydrophilic, and are therefore unlikely to interact with the hydrophobic aromatic ring. However, the position of this residue in the crystal structure and the conservation of this residue among the 3'-AG phosphotransferases indicated that the role of this residue needed to be more clearly defined.

To examine the contribution of the phenylalanine ring to the catalytic mechanism of APH(3')-IIIa, I generated the APH(3')-IIIa^{F264A} mutant. Determination of the steady state kinetic parameters for this mutant (Table 5.1) indicated that the aromatic ring was, generally, not required, as near wild type steady state kinetic parameters were observed for most AG substrates. However, it should be noted that for both amikacin and butirosin, which possess an aminohydroxybutyrate group at N1, a modest decrease in *V/K* was observed. The *V/K*s for amikacin and butirosin are decreased 4.0- and 3.0-fold, respectively. The reason for such a decrease in the affinity of this enzyme for these two substrates is not readily apparent from the crystal structure of APH(3')-IIIa complexed

with ADP. In this structure the C-terminal phenylalanine ring is pointing away from the AG binding pocket and is therefore unlikely to be involved in AG binding.

Since the aromatic ring of Phe264 is not required for either AG binding or catalysis, the role of the C-terminal carboxylate was then examined because in the APH(3')-IIIa•ADP crystal structure this carboxylate is pointing back towards the active site of this enzyme. To examine the role of this carboxylate I generated a APH(3')-$IIIa^{F264\Delta}$ mutant. Steady state kinetic analysis of this mutant indicated that the C-terminal carboxylate plays an important role in rate enhancement. The k_{cat} values for the 4,6-disubstituted AGs analyzed as substrates, kanamycin A and amikacin are dramatically lower. For kanamycin A, the k_{cat} is decreased by 7.2-fold, whereas for amikacin the k_{cat} dropped an even more dramatic 25-fold. The effect of the deletion of this residue is less clear with respect to the 4,5-disubstituted AGs. For those 4,5-disubstituted AGs that possess the quadruple primed ring, neomycin B and lividomycin A, the decrease in the k_{cat} is less dramatic than the change observed for the 4,6-disubstituted AGs examined. The k_{cat}s for neomycin B and lividomycin A are 2.4-fold and 4.8-fold lower. For butirosin and ribostamycin, 4,5-disubstituted AGs that lack the quadruple primed ring, intermediate changes to the steady state kinetic parameters are observed. For butirosin, an aminohydroxybutyrate substituted AG, there is a 14.4 fold decrease in the rate of the reaction, whereas for ribostamycin there is an 8.2 fold decrease in the rate of reaction. Thus, the C-terminal carboxylate is critical for rate enhancement, at least for a specific subset of AG substrates.

Steady state kinetic analysis of the APH(3')-IIIa$^{F264\Delta}$ mutant also indicated that the C-terminal carboxylate of APH(3')-IIIa plays an important role in substrate binding. For both of the 4,6-disubstituted AGs examined, kanamycin A and amikacin, a decrease in *V/K* is observed. The *V/K*s for kanamycin A and amikacin are decreased by 66- and 580-fold, respectively. For the 4,5-disubstituted AGs examined, the effect of deleting the C-terminal carboxylate on enzyme affinity is variable, but the results generally support a role for the C-terminus in AG binding. For neomycin B and lividomycin A, the effect of this deletion on *V/K* is significant (~6-fold), but less dramatic than its effect on either the apparent dissociation constants, or the second order rate constants obtained for butirosin and ribostamycin with the APH(3')-IIIa$^{F264\Delta}$ mutant. For ribostamycin there is a 27-fold decrease in *V/K*, whereas for butirosin there is a much more substantial 180-fold decrease in *V/K*. While it is difficult to estimate the effect of the new C-terminal carboxylate on AG binding, these variable effects likely reflect the manner in which the wild type enzyme binds these different classes of AGs.

Since the APH(3')-IIIa$^{F264\Delta}$ and the APH(3')-IIIa^{D261A} mutants poorly catalyze the phosphorylation of 4,6- and 4,5-disubstituted AGs, respectively, an APH(3')-IIIa$^{D261A-F264\Delta}$ double mutant was generated in order to see if it was possible to generate a mutant enzyme with poor activity towards both these classes of AGs. Determination of the steady state kinetic parameters for this double mutant validated this hypothesis, as both the 4,5-disubstituted and 4,6-disubstituted AGs are poor substrates (Figure 5.1 & Table 5.1). Surprisingly, the k_{cat} for neomycin B has increased 3.0 fold from that obtained for

the APH(3')-IIIa^{D261A} single mutant. The cause of such a rate enhancement is not readily apparent. Those AGs containing the aminohydroxybutyrate group are extremely poor substrates and the steady state kinetic parameters could not, therefore, be determined for butirosin. Thus, both of these C-terminal residues are required for the phosphorylation of the diverse array of AGs that are phosphorylated by APH(3')-IIIa.

5.3.2. Regiospecificity of aminoglycoside binding pocket mutants.

4,5-disubstituted AGs that possess both a 3' and 5" hydroxyl are bis-phosphorylated by APH(3')-IIIa (Thompson *et al*, 1996; Chapter 2). The second phosphorylation event is readily apparent in the steady state, as an inflection point is observed in progress curves at the point of complete monophosphorylation. I first noted that this inflection point was absent from progress curves for the phosphorylation of neomycin B by the APH(3')-IIIa$^{F264\Delta}$ mutant (Figure 5.2). I then examined the progress curves for the phosphorylation of neomycin B by all of the mutants described in this Chapter (not shown). Only the APH(3')-IIIa^{Y55A}, APH(3')-IIIa^{E262A} and the APH(3')-IIIa$^{F264\Delta}$ mutants lack the inflection point in progress curves for neomycin B phosphorylation by these mutants. To determine the significance of this observation I phosphorylated the 4,5-disubstituted AG ribostamycin, *in vitro*, using the purified APH(3')-IIIa^{Y55A}, APH(3')-IIIa^{E262A}, and APH(3')-IIIa$^{F264\Delta}$ mutant proteins. Ribostamycin was used in place of neomycin B because of the relative ease of purifying this AG once phosphorylated. Purification of the phosphorylated derivatives permitted

the analysis of these compounds by electrospray mass spectrometry and NMR. The results of these analyses are summarized in Table 5.2.

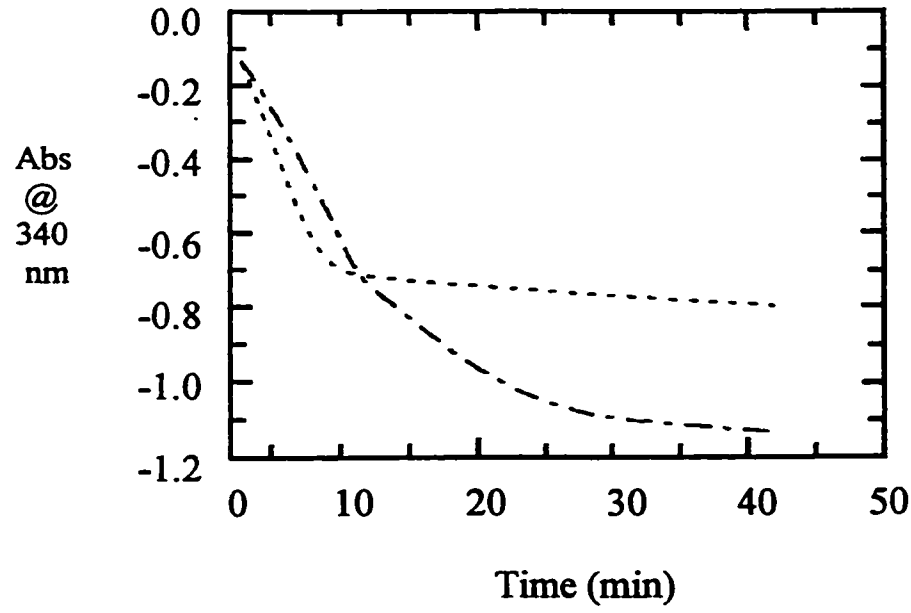

Figure 5.2. Progress curves for the phosphorylation of neomycin, by APH(3')-IIIa (— · —) and APH(3')-IIIa$^{F264\Delta}$ mutant (- - -).

Table 5.2. Regiospecificity of aminoglycoside binding pocket mutants.

Mutant Enzyme	Stoichiometry of phosphorylation	Regiospecificity of monophosphorylated derivatives
APH(3')-IIIa^{Y55A}	Di	Random
APH(3')-IIIa^{E262A}	Di	3'
APH(3')-IIIa$^{F264\Delta}$	Mono	5"

While the progress curves for the phosphorylation of neomycin B, by the APH(3')-IIIa^{Y55A} mutant did not appear to be biphasic, purification of the phosphorylated

derivatives of ribostamycin revealed that this mutant enzyme does indeed bisphosphorylate ribostamycin. However, it was only possible to purify the monophosphorylated derivative in small quantity. Nevertheless NMR analysis was possible and revealed that the first phase of phosphate addition occurs in a random fashion i.e. the phosphorylated derivative purified as a mixture of ribostamycin 3'-monophosphate and ribostamycin 5"-monophosphate. For the wild type enzyme, the addition of the first phosphate to 4,5-disubstituted AGs also occurs in a random fashion. Therefore, Tyr55 is involved in the second phosphorylation event, but is neither required for that event, nor important for directing the phosphorylation of either the 3' or 5" hydroxyls.

The APH(3')-IIIa^{E262A} mutant is also impaired in the ability to bisphosphorylate the 4,5-disubstituted class of AGs. However, purification and analysis of the phospho-ribostamycin derivatives revealed that this mutant enzyme can also bisphosphorylate 4,5-disubstituted AGs, as the reaction products contained a mixture of mono- and bisphosphorylated compounds. NMR analysis of the monophosphorylated compound revealed that this derivative is phosphorylated exclusively at the 3' hydroxyl. Thus, in the wild type enzyme this residue is likely important for directing the 5" phosphorylation of 4,5-disubstituted AGs.

The APH(3')-IIIa$^{F264\Delta}$ mutant was used to phosphorylate both neomycin B and ribostamycin. The subsequent purification, of the phosphorylated derivatives of both these AGs, enabled the determination of the stoichiometry of phosphorylation. These studies revealed that the C-terminal carboxylate is *required* for directing the addition of

the second phosphate. NMR analysis of the phospho-ribostamycin derivative indicated that the APH(3')-IIIa$^{F264\Delta}$ mutant phosphorylates this AG exclusively at the 5" hydroxyl. Thus, in the wild type enzyme the C-terminal carboxylate is important for directing the 3' phosphorylation of 4,5-disubstituted AGs. However, it should be noted that for the APH(3')-IIIa$^{F264\Delta}$ mutant, neamine displays near wild type kinetics, thereby indicating that the deletion of the C-terminal residue cannot completely abrogate the ability of this mutant enzyme to phosphorylate the 3' hydroxyl. The small size of neamine, in comparison to the other AGs examined, likely explains this result; neamine is composed of only the aminohexose and aminocyclitol rings. The smaller size of this AG also likely explains the comparatively smaller decrease in *V/K*, approximately 3.5-fold for this substrate in comparison to kanamycin A (66-fold).

5.3.3. In vivo role of aminoglycoside binding pocket mutants.

In an effort to understand the effect of mutations in the AG binding pocket I estimated, using either kanamycin A or neomycin B containing gradient agar plates, the minimal inhibitory concentrations (MICs) of cells harboring these mutant genes (Table 5.3). To ensure that the biological effect, that was observed, was not due to the poor expression of the mutant enzymes, I also examined their expression level in overnight cell cultures. The cultures were harvested, lysed, and the supernatant cleared by centrifugation. Identical amounts of total protein were subjected to denaturing polyacrylamide electrophoresis and the level of APH(3')-IIIa and mutant APH(3')-IIIa proteins determined by Western blotting. The expression of the wild type and mutant

APH(3')-IIIa proteins is similar (Figure 5.3).

Table 5.3: Minimal inhibitory concentrations of *aph(3')-IIIa* aminoglycoside binding site mutants when expressed in *E. coli* BL 21(DE3).

AG binding site mutant	MICs for kanamycin A (μg/mL)	MICs for Neomycin B (μg/mL)
Wild Type	>150	61
APH(3')-IIIa^{Y55A}	19	20
APH(3')-IIIa^{R211A}	24	13
APH(3')-IIIa^{D261A}	17	15
APH(3')-IIIa^{E262A}	DNG	<3
APH(3')-IIIa^{F264A}	38	21
APH(3')-IIIa$^{F264\Delta}$	DNG	8
APH(3')-IIIa$^{D261A-F264\Delta}$	DNG	DNG

DNG= Did not grow

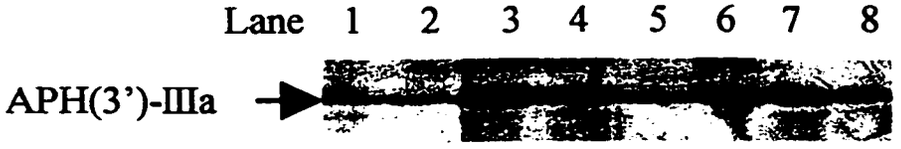

Figure 5.3. Expression of mutant APH(3')-IIIa proteins. Lanes 1-8, cleared lysates of strains expressing the wild type APH(3')-IIIa (lane 1), the Tyr55Ala mutant (lane 2), the Arg211Ala mutant (lane 3), the APH(3')-IIIa^{D261A} mutant (lane 4), the Glu262Ala mutant (lane 5), the APH(3')-IIIa^{F264A} mutant (lane 6), the APH(3')-IIIa$^{F264\Delta}$ (lane 7), and the APH(3')-IIIa$^{D261A-F264\Delta}$ double mutant (lane 8).

In general, the MICs are lower than those obtained for cells expressing the wild type APH(3')-IIIa enzyme. However in most cases, the MICs can be rationalized with the steady state kinetic parameters, determined *in vitro*. The APH(3')-IIIa^{Y55A} and APH(3')-IIIa^{D261A} mutants are the most notable exceptions. The APH(3')-IIIa^{Y55A} mutant is surprisingly susceptible to low levels of both kanamycin A and neomycin B (Table

5.3), considering that the steady state kinetic parameters of this mutant enzyme are near wild type. It is possible that the greater susceptibility of this mutant to the AGs examined is due to the decreased level of this protein in the cell, relative to wild type (Figure 5.3), but other unknown factors could be responsible for this increased susceptibility. Conversely, the APH(3')-IIIa^{D261A} mutant is resistant to higher levels of both these AGs. than was expected, as this mutant enzyme is an extremely poor catalyst (Figure 5.1), especially with regard to neomycin B, where the k_{cat} is decreased approximately 100-fold. An increase in the level of this protein in the cell, relative to wild type, could explain the greater than expected level of resistance.

While the MICs for cells expressing the APH(3')-IIIa^{Y55A} and APH(3')-IIIa^{D261A} mutant enzymes do not appear to agree with the steady state kinetic parameters determined for these enzymes, the MICs obtained for the other mutants, described in this chapter, do parallel the results determined *in vitro*. With respect to the wild type enzyme, the APH(3')-IIIa^{R211A} mutant is a modestly poorer catalyst, (Figure 5.1), as evidenced by the approximate 2-fold decrease in V/K, and there is a corresponding decrease in the MIC for both kanamycin A and neomycin B. For the APH(3')-IIIa^{E262A} mutant the K_m of kanamycin A is increased approximately 26-fold, and this decrease in kanamycin affinity is apparent in our *in vivo* assay, as this mutant does not mediate resistance to even low levels of kanamycin A. Surprisingly, cells expressing the APH(3')-IIIa^{E262A} mutant enzyme are also highly susceptible to neomycin B, this occurs despite the fact that the APH(3')-IIIa^{E262A} mutant readily phosphorylates this AG (Figure 5.1). Protein expression levels are similar to those obtained for the wild type enzyme, thus, the surprisingly poor

level of resistance to neomycin B is unlikely to be due to a decreased amount of this protein in the cell. Alternatively, the increased susceptibility to neomycin may reflect the inability of the APH(3')-IIIa^{E262A} mutant to readily phosphorylate the 5" hydroxyl, suggesting that this modification may be critical for mediating resistance to the 4,5-disubstituted AGs *in vivo*. The MICs obtained for the Phe264 mutants, described in this chapter, are also fairly consistent with the steady state kinetic parameters determined for these mutant enzymes. The APH(3')-IIIa^{F264A} mutant displays near wild type kinetics, and is resistant to moderate levels of both kanamycin A and neomycin B (Table 5.3) whereas the APH(3')-IIIa$^{F264\Delta}$ mutant is a poor catalyst (Figure 5.1), and is highly susceptible to both of the AGs examined. The MICs of the APH(3')-IIIa$^{F264\Delta}$ mutant also parallels the substrate specificity of this enzyme, as kanamycin A is a poorer substrate than neomycin B (Figure 5.1), and the APH(3')-IIIa$^{F264\Delta}$ mutant does not grow in the presence of even low levels of kanamycin A, but is resistant to low levels of neomycin B. As was to be expected, the APH(3')-IIIa$^{D261A\text{-}F264\Delta}$ mutant, which is an extremely poor catalyst, regardless of the AG, does not mediate resistance to either of the AGs examined *in vivo*.

5.4. Discussion.

Unfortunately, the determination of a structure of APH(3')-IIIa bound to an AG antibiotic has remained elusive, and it is therefore difficult to identify the specific amino acid residues that are responsible for AG binding. However, the determination of the APH(3')-IIIa•ADP crystal structure has aided the identification of a potential AG

binding pocket, as the surface potential of the identified region is highly electronegative. Such a surface would provide a complementary binding surface for the electropositive AGs. My use of site directed mutagenesis, combined with a number of biochemical techniques, has identified a number of residues in the C-terminus of APH(3')-IIIa that are important for either substrate binding or catalysis. I have also examined the role of two amino acid residues, which also appear to line the AG binding pocket, specifically Tyr55 and Arg211. The molecular modeling of several AG substrates into the putative AG binding pocket has complemented these mutagenesis studies, as they have aided a determination of the roles of these amino acid residues in substrate recognition. These modeling studies were completed by J. Schwartzenhaur and A.M. Berghuis, and involved the identification of catalytically competent conformations of amikacin, kanamycin A, butirosin, and ribostamycin bound to the APH(3')-IIIa•ATP complex, using the program DOCKVISION (Hart *et al*, 1997). The molecular models shown in Figure 5.4 were selected for their agreement with the kinetic data obtained from my site directed mutagenesis studies. Insights into the AG binding pocket of APH(3')-IIIa, gained from both modeling and site directed mutagenesis studies, are discussed below.

The steady state kinetic analysis of the APH(3')-IIIa^{Y55A} mutant revealed that this residue is not important for either substrate binding or catalysis, although this residue may be important, but not required, for the efficient bisphosphorylation of 4,5-disubstituted AGs. The lack of an important role for this residue in substrate binding is also supported by molecular modeling studies (Figure 5.4). While the hydroxyl group of Tyr55 is close (~5-8 Å) to such AGs, as kanamycin A, amikacin, neomycin B,

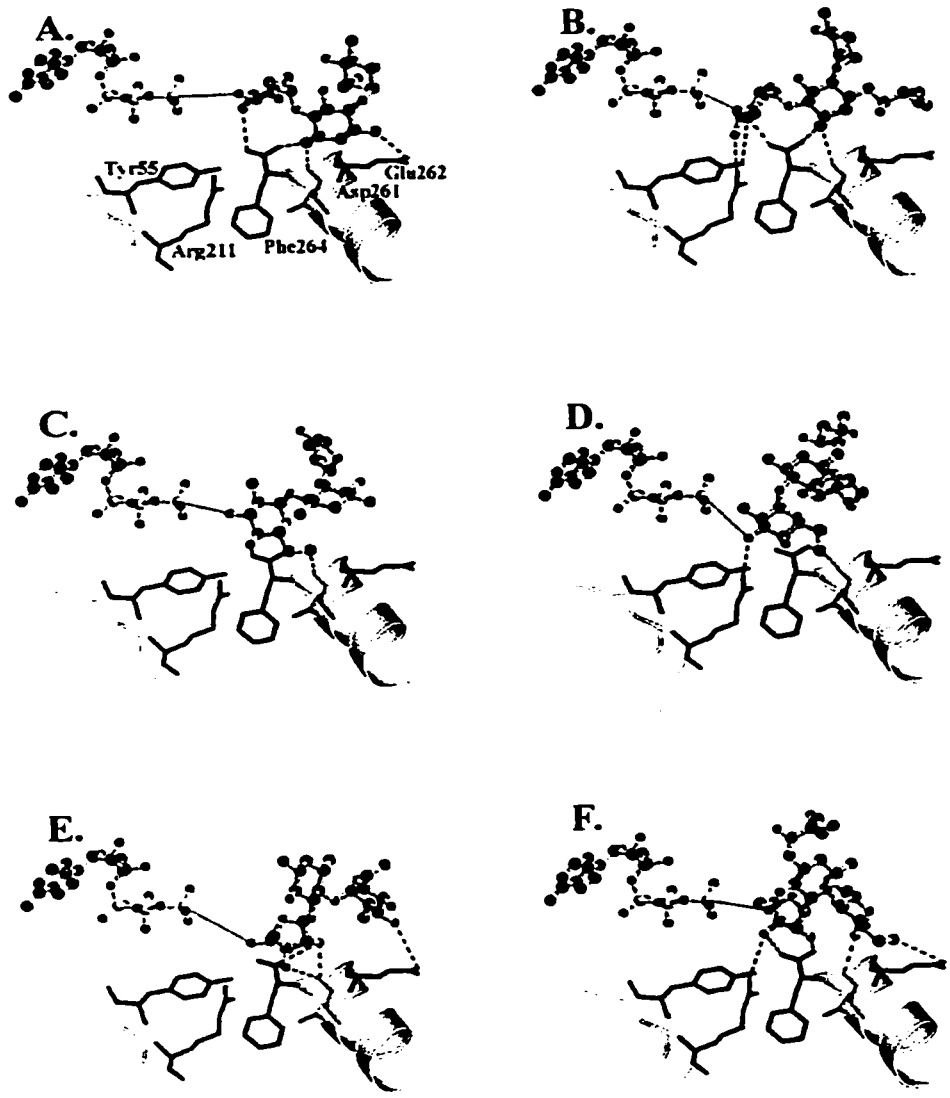

Figure 5.4. AGs modeled into the AG binding pocket of APH(3')-IIIa. Tyr55, Arg211, Asp261, Glu262, and Phe264 are shown in red, green, yellow, purple, and blue, respectively. **A.** Kanamycin A; **B.** Amikacin; **C.** Ribostamycin positioned for 3'-phosphorylation; **D.** Butirosin positioned for 3'-phosphorylation; **E.** Ribostamycin positioned for 5"-phosphorylation; **F.** Butirosin positioned for 5"-phosphorylation. This figure was prepared using the MOLSCRIPT and RASTER3D programs, and was the generous gift of J. Schwartzenhaur (Kraulis, 1991; Merritt and Murphy, 1994). Molecular modeling studies were completed by J. Schwartzenhaur and A.M. Berghuis.

ribostamycin, and butirosin, when these AGs are modeled into the active site of APH(3')-IIIa, there do not appear to be any specific interactions of note.

Despite the close proximity of the guanadinium group of Arg211 to the γ-phosphate of ATP, the steady state kinetic parameters of the APH(3')-IIIa^{R211A} mutant indicate that the side chain of this residue is relatively unimportant for catalysis. Furthermore, the fact that significant decreases in k_{cat} are not generally observed, they range from 2- to 13-fold, disputes the suggestion of Kocabivik & Perlin (1994) that this residue is involved in TS stabilization. In general, this residue is not critical for substrate binding, as the K_ms of the APH(3')-IIIa^{R211A} mutant for kanamycin A, neomycin B. ribostamycin, and lividomycin A are comparable to the K_ms and V/Ks of the wild type enzyme for these substrates. However, the effect on the K_ms and V/Ks for those AGs that are substituted at N1, amikacin, butirosin, and isepamicin, are more significant. When amikacin was modeled into the AG binding pocket a potential interaction between the O4' of amikacin (3.6 Å) and the functional group of Arg211 was noted (Figure 5.4). The loss of such an interaction could explain the decrease in affinity observed in the steady state. For butirosin, an explanation for the apparent decrease in affinity is complicated by the fact that APH(3')-IIIa catalyzes the bisphosphorylation of this AG. However, potential interactions between the O3' (3.5 Å) and the O3" (3.9 Å) of butirosin have been noted when this AG is positioned for phosphate transfer to the 3' and 5" hydroxyl groups, respectively.

The steady state kinetic parameters obtained for the APH(3')-IIIa^{D261A} mutant indicate that the functional group of this residue is critical for the catalytic activity of APH(3')-IIIa. The k_{cat}s of this mutant are decreased approximately 10-fold for 4,6-disubstitued AGs, and approximately 100-fold for 4,5-disubstituted AGs. While this residue is clearly critical for the catalytic activity of APH(3')-IIIa, the role of the Asp261 sidechain, a carboxylate, is not readily apparent from the crystal structure of APH(3')-IIIa•ADP. In this crystal structure, the Asp261 sidechain is pointing in towards the active site, but down and away from the AG binding pocket. Modeling studies suggest that, in its current position, the carboxylate of this residue could not form any significant interactions with an enzyme bound AG. The Asp261 sidechain could conceivably move as part of a conformational change, and act as a hydrogen bond acceptor, or be involved in electrostatic interactions, both of which could be important for substrate binding. However, in such a case one would expect an increase in the apparent affinity constant, K_m, which is not observed with this mutant enzyme.

An alternative explanation, and the one I favor, is where the sidechain of Asp261 is important for maintaining the stability of the C-terminal helix. In the APH(3')-IIIa•ADP crystal structure, Asp261 appears to interact with Arg226, another conserved residue, on an opposing helix. This interaction could serve to orient and stabilize the C-terminal helix and thereby orient the main chain carbonyl group of Asp261. Modeling studies suggest the importance of this carbonyl group. In docking studies with kanamycin A and amikacin, the Asp261 main chain carbonyl oxygen is

within hydrogen bonding distance (2.24-3.1 Å) of N3 (Figure 5.4). This carbonyl oxygen is also predicted to interact with N6' of butirosin and ribostamycin (3.04 and 2.37 Å, respectively) when these AGs are positioned for 3'-O-phosphorylation. Similarly, this group appears to interact with the O4" of butirosin and ribostamycin (2.87 and 2.37 Å, respectively) when the 5" hydroxyl is positioned as the phosphate accepting moiety. In addition to this potential role in AG binding, the main chain carbonyl of Asp261 appears to hydrogen bond with the main chain amide hydrogen of Phe264. The importance of this interaction likely reflects the requirement for a properly orientated C-terminal carboxylate in order to afford a significant level of rate enhancement. The importance of the C-terminal carboxylate will be discussed below.

While the sidechain of Glu262 is not generally required for either substrate binding or catalysis, it is important for kanamycin A binding, as large effects on both K_m and V/K are observed, 26- and 21-fold respectively. Modeling studies suggest a possible interaction between the Glu262 carboxylate and the N1 of kanamycin A (3.30 Å). The loss of such an interaction likely explains the decreased affinity of the APH(3')-IIIa^{E262A} mutant for this substrate. Support for such a conclusion comes from the fact that the affinity of amikacin is unaffected by this mutation. Amikacin, which is a semi-synthetic derivative of kanamycin A, is structurally identical to kanamycin A except for the substitution of an aminohydroxybutyrate group at the N1 position. Thus, an interaction between the N1 of amikacin and the carboxylate of Glu262 is already precluded, and therefore no change in the affinity of the APH(3')-IIIa^{E262A} mutant for this drug would be

expected. The lack of this interaction may also partially explain the poor affinity of amikacin for the wild type APH(3')-IIIa enzyme.

The sidechain of Glu262 is also important for directing the efficient bisphosphorylation of 4,5-disubstituted AGs, as the rate of the addition of the second phosphate is slow, relative to the wild type enzyme. The sidechain of this residue is also important for directing the specific site of phosphorylation, as the APH(3')-IIIa^{E262A} mutant exclusively phosphorylates the 3' hydroxyl group of ribostamycin, prior to the addition of the second phosphate. Normally, phosphate transfer occurs in a random fashion. The results from modeling studies, suggest that the loss of the potential interaction between the O3' of ribostamycin and the carboxylate of Glu262 (Figure 6.4) is the cause of the altered pattern of the initial phosphorylation event. An electrostatic interaction between this functional group and the N6' of butirosin is possible when this AG is positioned for 5"-O-phosphorylation (Figure 6.4). Thus, this residue is likely involved in properly orienting the 4,5-disubstituted AGs for O5" phosphorylation.

While the sidechain of Phe264 is not required for either substrate binding or catalysis, the steady state kinetic parameters of the APH(3')-IIIa$^{F264\Delta}$ mutant indicate that the C-terminal carboxylate is critical for the proper functioning of APH(3')-IIIa. Molecular modeling studies suggest that the carboxylate of this residue participate in multiple interactions with the modeled AGs. When the 3' hydroxyl of either kanamycin A, amikacin, butirosin, or ribostamycin, is positioned for phosphate transfer, a number of similar interactions are observed. For example, the C-terminal carboxylate interacts with all of these AGs at the O4' and N6' positions. However, it should be noted that for

kanamycin A, the interaction between the N6' position and the C-terminal carboxylate is long (5.3 Å), suggesting that this interaction may not make a significant contribution to kanamycin A binding. For kanamycin A and amikacin, an additional interaction between this carboxylate and the N3 position is also possible. While three interactions are apparent, the importance of each individual interaction is likely to be AG-dependent, as the magnitude of the increase in the K_ms of the APH(3')-IIIa$^{F264\Delta}$ mutant for amikacin and kanamycin A varies considerably. The K_m for kanamycin A is increased 9.1-fold, whereas the K_m for amikacin is increased only 2.9-fold. The specific reason for this difference in AG affinity is not readily apparent. The interactions between the C-terminal carboxylate and the O4' and N6' positions of both butirosin and ribostamycin are likely critical for directing the phosphorylation of the 3'-hydroxyl, as the APH(3')-IIIa$^{F264\Delta}$ mutant exclusively phosphorylates the O5" position of ribostamycin.

Modeling studies, wherein the O5"-hydroxyls of butirosin and ribostamycin are positioned for phosphate transfer, indicate the importance of interactions between the O3" and O2" positions of both these AGs, and the C-terminal carboxylate. However, it should be noted that for ribostamycin, this interaction with the O2" position is long (4.2 Å), compared to the interaction between the O2" position of butirosin and the C-terminal carboxylate, suggesting that for ribostamycin, this interaction may not be significant. The differences in the strength of the O2"-C-terminal carboxylate interaction could explain the more dramatic changes in K_m and V/K that are observed for the phosphorylation butirosin (Table 5.1). Alternatively, the more dramatic effect on the K_m

and *V/K* values observed for this AG may be due to the preference of the APH(3')-IIIa$^{F264\Delta}$ mutant to direct phosphorylation to the 5"-hydroxyl. For the wild type enzyme, phosphorylation of butirosin occurs in a random manner, but there is a strong preference for directing the initial phosphorylation to the 3'-hydroxyl. Thus the increased K_m could simply be a reflection of the lack of affinity for this AG when the 5"-hydroxyl is positioned for phosphorylation. Interestingly, there is little change in the affinity for neomycin, which is preferentially phosphorylated at the 5"-hydroxyl, by the wild type enzyme.

5.5. Conclusions.

The kinetic analyses of the APH(3')-IIIa mutants, described herein, has attempted to define the role of specific amino acid residues that line the presumed AG binding pocket, and thereby highlights the importance of the extreme C-terminus to both rate enhancement and substrate binding. *In vitro*, three C-terminal amino acid residues, Asp261, Glu262, and Phe264 are critical for catalysis. Since functional group of Asp261 does not appear to be involved in substrate binding, this residue is likely required for orienting and stabilizing the C-terminal helix. Glu262 is required for the efficient phosphorylation of the 4,5-disubstituted AGs at the 5"-hydroxyl, whereas Phe264, more specifically the C-terminal carboxylate, is required for the phosphorylation of this class of AGs at the 3'-hydroxyl. The C-terminal carboxylate is also critical for substrate recognition and rate enhancement. While in a few cases it is difficult to rationalize the results obtained *in vivo* with those results obtained *in vitro*, the results obtained from my *in vivo* studies make it clear that the C-terminal region of APH(3')-IIIa is critical for the

level of resistance afforded by this AG-modifying enzyme.

While it has been possible to identify a number of residues that are important for substrate binding, it has been difficult to definitively assign specific roles to these residues, as the effects on either K_m or V/K are not universally apparent, even for AGs that are structurally similar. Thus, I believe that the APH(3')-IIIa enzyme binds structurally related AGs in different, catalytically competent, modes. Therefore, this enzyme is a highly evolved catalyst that possesses a number of functional groups that contribute to AG binding, in an AG-dependent fashion. While the idea that an enzyme could bind similar substrates in different modes and yet still achieve a significant level of rate enhancement is novel, one should consider the following. First, for the 4,5-disubstituted AGs, we know that there are **at least** two binding modes, as these AGs are efficiently phosphorylated at both the 3'- and 5"-hydroxyls (Thompson *et al*, 1996; Chapter 2). Secondly, the NMR structures of amikacin and butirosin, bound to the APH(3')-IIIa •Cr^{2+}ATP complex, have been determined, and are significantly different. The three rings of amikacin are aligned in a 'straight line', whereas the three rings of butirosin resemble a 'V-like' structure (Cox *et al*, 1996). Finally, the binding of AGs to the hammerhead ribozyme is dependent on the electrostatic charge of the AG; the greater the positive charge, the greater the affinity (Tor *et al*, 1998). The ability to maximize electrostatic interactions is thought to result from rotations about the inter-ring glycosyl bonds, which enable the AGs to adopt subtly different conformations (Tor *et al*, 1998). For APH(3')-IIIa, the judicious placement of amino acid residues, during evolution, which carry a net negative charge, likely resulted in the formation of a 'scaffold', to

which a number of different AG antibiotics can bind, and do so in a manner that maximizes charge complementarity.

5.6. References:

Beck, E., Ludwig, G., Auerswald, E.A., Reiss, B., & Schaller, H. (1982). Nucleotide sequence and exact localization of the neomycin phosphotransferase gene from transposon Tn*5*. *Gene* **19**, 327-336.

Cox, J.R., McKay, G.A., Wright, G.D., & Serpersu, E.H. (1996). Arrangement of substrates at the active site of an aminoglycoside 3'-phosphotransferase (APH(3')-IIIa) as determined by NMR. *J. Am. Chem. Soc.* **118**, 1295-1301.

Hart, T.N., Ness, S.R., & Read, R.J. (1997). Critical evaluation of the research docking program for the CASP2 challenge. *Prot. Str. Func. Genet.* **Suppl 1**, 205-209.

Hon, W-C., McKay, G.A., Thompson, P.R., Sweet, R.M., Yang, D.S.C., Wright, G.D. & Berghuis, A.M. (1997). Structure of an enzyme required for aminoglycoside resistance reveals homology to eukaryotic protein kinases. *Cell* **89**, 887-895.

Kocabivik, S., & Perlin, M.H. (1994). Amino acid substitutions within the analogous nucleotide binding loop (P-loop) of aminoglycoside 3'-phosphotransferase. *Int. J. Biochem.* **26**, 61-66.

Kraulis, P.J. (1991). MOLSCRIPT: a program to produce both detailed and schematic plots of protein structures. *J. Appl. Cryst.* **24**, 946-950.

McKay, G.A. & Wright, G.D. (1995). Kinetic mechanism of aminoglycoside phosphotransferase Type IIIa: Evidence for a Theorell-Chance kinetic mechanism. *J. Biol. Chem.* **270**, 24686-24692.

McKay, G.A. & Wright, G.D. (1996). Catalytic mechanism of enterococcal kanamycin kinase (APH(3')-IIIa): Viscosity, thio, and solvent isotope effects support a Theorell-Chance mechanism. *Biochemistry* **35**, 8680-8685.

Merritt, E.A., & Murphy, M.E.P. (1994). RASTER3D version 2.0: a program for photorealistic molecular graphics. *Acta Cryst.* **D50**, 869-873.

Thompson, P.R., Hughes, D.W., Wright, G.D. (1996). Regiospecificity of aminoglycoside phosphotransferase from *Enterococci* and *Staphylococci*. *Biochemistry* **35**, 8686-8695.

Thompson, P.R., Schwartzenhaur, J., Hughes, D.W., Berghuis, A.M., & Wright, G.D. (1999). The C-terminus of aminoglycoside phosphotransferase (3')-IIIa is critical for antibiotic recognition and resistance. *J. Biol. Chem.* **274**, 30697-30706.

Tor, Y., Hermann, T., & Westhof, E. (1998). Deciphering RNA recognition: aminoglycoside binding to the hammerhead ribozyme. *Chem. Biol.* **5**, R277-R283.

Chapter 6

Characterization of the catalytic mechanism of APH(9)-Ia. A novel spectinomycin kinase from Legionella pneumophila.

Adapted from

Thompson, P.R., Hughes, D.W., Cianciotto, N.P., Wright, G.D.
Journal of Biological Chemistry, 1998, vol. 273, pp. 14788-14795.

The work described in this chapter entails my characterization of the catalytic mechanism of a novel APH from *Legionella pneumophila*, APH(9)-Ia. Enzymatic synthesis and purification of spectinomycin-phosphate permitted a determination of the regiospecificity of this enzyme by D.W. Hughes, in the Department of Chemistry, McMaster University, using a variety of one and two dimensional NMR techniques. All other work described in this chapter was obtained by the author of this thesis.

CHAPTER 6: Characterization of the catalytic mechanism of APH(9)-Ia. A novel spectinomycin kinase from *Legionella pneumophila.*

6.1. Introduction.

Since the catalytic mechanism of APH(3')-IIIa was similar to the catalytic mechanism employed by the ePKs, I was interested in determining if the phosphate transfer mechanism of this enzyme represented a paradigm for the catalytic mechanisms of other APHs. In order to test this possibility, a novel APH homologue was chosen, as this enzyme is distantly related to APH(3')-IIIa and as well has a much more restricted substrate range. The gene encoding this novel APH is present in the genome of *Legionella pneumophila.*

L. pneumophila, the etiological agent of Legionnaire's disease, was first identified as a human pathogen 6 months after a 1976 epidemic at a convention of the Pennsylvania American Legion (Winn, 1988). *L. pneumophila* is a Gram negative bacillus that in nature lives as an aquatic protozoan parasite (reviewed in Murray *et al*, 1994). Since *L. pneumophila* can be cultured from cooling towers, hot water tanks, and showers, the route of infection is thought to be the inhalation of the aerosols formed by these devices (Winn, 1988). Upon human infection of the lung, this bacterium colonizes macrophages and monocytes, as a facultative intracellular parasite, and causes an acute respiratory illness, for example, pneumonia (Murray *et al*, 1994). While *L. pneumophila*

can cause acute respiratory illness; endocarditis and bacteremias are also possible, although these can be caused by other *Legionella sp.* as well (Winn, 1988).

While resistance to current antimicrobial chemotherapies, which include combinations of erythromycin, rifampicin, and ciprofloxacin, are not generally observed in *L. pneumophila* clinical isolates (Onody *et al*, 1997; Barker & Farrell; Winn, 1988), this organism is resistant to the aminocyclitol antibiotic spectinomycin (Figure 6.1).

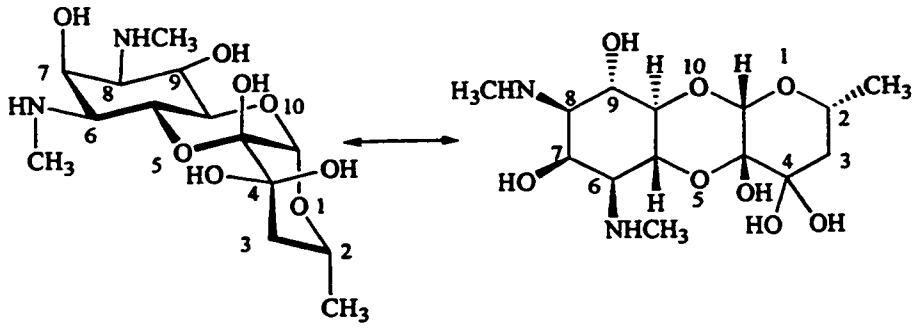

Figure 6.1. Structures of spectinomycin.

Spectinomycin resistance in this organism is due to the synthesis of spectinomycin kinase (SK), an APH homologue, which retains the same core catalytic residues that are present in APH(3')-IIIa. (Suter *et al*, 1997). The SK enzyme is a 331 amino acid, 38.5 kDa protein, which when expressed in *E. coli* mediates resistance to spectinomycin, but not kanamycin A, hygromycin, or streptomycin. This pattern of resistance is reflected *in vitro*, as SK, present in crude cell extracts, was unable to catalyze the phosphorylation of these AGs, but was able to phosphorylate spectinomycin (Suter *et al*, 1997). Thus, SK was expected to be an unusually specific APH.

Since APHs typically display a broad substrate specificity, for example APH(3')-IIIa (McKay *et al*, 1994a), the high degree of substrate specificity displayed by the SK enzyme was intriguing. It was therefore felt that this enzyme would be an ideal candidate for a study, comparing the catalytic mechanisms of known APHs. The low level of amino acid sequence identity (~10%) that exists between SK and APH(3')-IIIa, provided further support for the use of this enzyme in such a study, as I felt that if two distantly related APHs employed similar catalytic mechanisms, I could more conclusively say that the catalytic mechanism of APH(3')-IIIa represents the paradigm for AG phosphorylation. Therefore, I began an initial characterization of the catalytic mechanism of the SK from *L. pneumophila*.

Herein, I report, in this the penultimate chapter of this thesis, the overexpression, purification, and regiospecificity of the SK from *L. pneumophila*, as well as the steady state kinetic parameters for ATP and spectinomycin. I have also employed affinity-labeling techniques; site directed mutagenesis, and metal and solvent isotope effects, in an effort to characterize the catalytic mechanism of this enzyme more fully. The results, of these studies, indicate that the catalytic mechanism employed by SK is virtually identical to the one employed by APH(3')-IIIa, thereby indicating that the APH(3')-IIIa phosphate transfer mechanism is the paradigm for AG phosphorylation.

6.2. Materials and Methods.

6.2.1. Chemicals.

Spectinomycin, streptomycin, kanamycin A, neomycin B, butirosin, amikacin, and 5'-[*p*-(fluorosulfonyl)benzoyl]adenosine (FSBA) were obtained from Sigma (St.

Louis, MO). Restriction enzymes employed in this study were from MBI Fermentas (Flamborough, Ontario, Canada). Apramycin was the generous gift of Dr. A. Petric, St. Joseph's Hospital, Hamilton, Ontario, Canada. Plasmid pJLJ4 was the generous gift of Dr. N. Cianciotto, Department of Microbiology-Immunology, Northwestern University, Chicago, Illinois. This plasmid encodes the SK gene, and has previously been described (Suter *et al*, 1997).

6.2.2. Preparation of the spectinomycin kinase overproducing construct.

Construction of an APH expression plasmid was achieved by PCR amplification of the corresponding gene found on plasmid pJLJ4, using Vent DNA polymerase (New England Biolabs, Beverly, MA). The 5'-PCR primer incorporated a unique *Nde*I site (in bold), 5'-GCTCTAGA**CATATG**CTAAAACAACCA-3', and the 3'-PCR primer incorporated a unique *Hin*dIII site (in bold), 5'-CG**AAGCTT**GGATC CTTAC TGCTCTGTAGCAAAAG-3'. The amplified gene was digested with *Nde*I and *Hin*dIII, and cloned into similarly cleaved pET-22b(+) (Novagen, Madison, WI) to give plasmid pETLP7. The SK gene was completely sequenced to ensure that no undesired mutations had occurred during PCR amplification.

6.2.3. Site directed mutagenesis.

The mutagenic oligonucleotides 5'-GCCCGCATGTATAGCAGAATG ACATAGTAC-3' and 5'-CAAGTCTTATTTCATAGCGCTAAAATACGGC-3', and their reverse complements, were used to generate the SK^{D212A} and the SK^{K52A} mutants, respectively, using the Quikchange mutagenesis system (Stratagene, La Jolla, CA). The presence of the desired mutations was confirmed by DNA sequencing, and the entire

gene was then sequenced to ensure that no additional mutations had occurred during PCR amplification. The resulting constructs, pETLPD212A4 and pETLPK52A4, were subsequently used to transform *E. coli* BL 21 (DE3), in order to facilitate protein overexpression.

6.2.4. Overexpression and purification of wild type and mutant spectinomycin kinase proteins.

For overexpression of the wild type SK enzyme, four 1 L solutions of LB were each separately inoculated with 10 mL of an overnight cell culture of *E. coli* BL 21 (DE3)/pETLP7. This cell culture was then incubated at 37° C and 250 rpm in the presence of 100 μg/mL ampicillin, until the culture reached an absorbance of 0.6 at 600 nm. A solution of boiling sterile media (150 mL) was then added to raise the culture temperature to ~ 42° C, in an effort to induce the expression of chaperonins. The cultures were then incubated at room temperature for 10 minutes, and IPTG was then added to a final concentration of 0.5 mM. The cells were grown for an additional 3 hours at 30° C (250 rpm) to an absorbance of ~1.5, at 600 nm, at which time intact cells were pelleted by centrifugation at 4000 x g. The cell paste was resuspended in 0.85% NaCl, to wash the cells, after which the cells were re-pelleted by centrifugation at 4000 x g. At this point, cells were resuspended in 15 mL of lysis buffer (50 mM CHES pH 9.0, 100 mM NaCl, 1 mM EDTA, 1 mM PMSF, 1 mM DTT), and lysed by three passages through a French pressure cell (20000 p.s.i.), pre-chilled to 4° C. The lysate was cleared of cellular debris by centrifugation at 20000 x g, after which, the pellet fraction was resuspended in an additional 10 mL of lysis buffer, and this extract was then centrifuged at 20000 x g. The two supernatants were then combined and diluted to 45 mL with buffer A (50 mM CHES

pH 9.0, 1 mM EDTA) and applied to a Q-Sepharose (Amersham Pharmacia Biotech, Montreal, Quebec, Canada) column (2.6 x 11.5 cm). SK was eluted from the column using a fast linear gradient of buffer B (buffer A plus 1 M NaCl), from 0 to 30%, over 2.5 column volumes, at a flow rate of 3 mL/minute. The fractions (6 mL) were then analyzed by a combination of enzyme activity assay, and SDS-PAGE, in order to assess both enzyme activity and protein purity. Peak fractions were pooled, concentrated, dialyzed overnight against buffer A, and applied to a smaller Q Sepharose column (1 x 10 cm). SK was then eluted, using a 0 to 30% gradient of buffer B over 5 column volumes. Peak fractions were similarly analyzed, and the purest fractions were pooled, dialyzed against 25 mM KH_2PO_4 pH 7.5, and applied to a Macro-Prep Ceramic Hydroxyapatite column (10 x 64 mm) (BioRad). SK was then eluted from this column using a linear gradient of KH_2PO_4 pH 7.5 from 25 to 1000 mM. Pure fractions of SK were pooled and stored at 4° C in 50 mM Tris-HCL pH 8.0. All purification steps were carried out at 4° C.

The SK^{D212A} and the SK^{K52A} mutants were purified similarly to the manner described for the purification of the wild type enzyme. However, it should be noted that for the SK^{K52A} mutant the hydroxyapatite step was omitted, and the pooled fractions from the second Q Sepharose column were pooled, dialyzed against buffer A, and applied to a Resource Q (Amersham Pharmacia Biotech) column (1 mL). This mutant protein was eluted from the Resource Q column using a linear gradient of 0 to 30 % buffer B.

6.2.5. Spectinomycin kinase assay.

The enzyme assay employed couples the production of ADP to the oxidation of NADH using a pyruvate kinase/lactate dehydrogenase coupled assay system. The assay

has previously been described for APH(3')-IIIa (McKay *et al*, 1994a; Chapter 4). Initial rates were fitted, using Grafit version 3.0 (Leatherbarrow, 1992), by nonlinear least fit squares to either Equation 1,

$$v = (k_{cat}/E_t)[S]/(K_m + [S]) \qquad \text{(Eq. 1)},$$

or Equation 2,

$$v = (k_{cat}/E_t)[S]/(K_m + [S])(1 + [S]/K_i)) \qquad \text{(Eq. 2)},$$

when substrate inhibition was present. AGs (1 mM) were incubated with SK and ATP (930 μM), in the assay described above, in order to assess the ability of these AGs to act as substrates of SK. The ability of these AGs to act as inhibitors of SK activity was assessed by incubating ATP (930 μM), the potential AG inhibitor (100 μM), spectinomycin (100 μM) and SK in the enzyme assay described above. The protein kinase inhibitor H9 (Research Biochemicals International, Natick, MA) was similarly tested as an inhibitor at concentrations of 10, 100, and 1000 μM, in the presence of 50 μM spectinomycin and 25 μM ATP.

Solvent isotope effects were determined by evaluating the kinetic parameters in D_2O. Buffers were prepared in D_2O, and the pD was set 0.4 above the pH (pD= pH + 0.4). The final concentration of H_2O was ≤3.5% (v/v).

6.2.6. Inactivation of spectinomycin kinase with FSBA.

The ability of FSBA to inactivate SK was examined as previously described for APH(3')-IIIa (McKay *et al*, 1994a). Briefly, FSBA inactivation experiments were carried out in 50 mM Tris-HCl, 10 mM $MgCl_2$, and 0.1 mM FSBA dissolved in DMSO (1% v/v final concentration). Inactivation reactions were allowed to proceed for various

lengths of time at 37° C, and any unreacted FSBA was removed by passage through a Sephadex G-10 spin column (0.4 mL) and aliquots assayed for enzymatic activity at room temperature. The linear fits of the relative enzyme activity ($\log[(E_t - E_\infty)/(E_o - E_\infty)]$) to time were determined using the Grafit version 3.0 software (Leatherbarrow, 1992).

6.2.7. Preparation and purification of phosphorylated spectinomycin.

Phosphorylated spectinomycin was synthesized *in vitro* by the incubation of 200 mg of spectinomycin and a 3-fold molar excess of ATP (896 mg) in 50 mM Tris-HCl pH 7.5, and 10 mM $MgCl_2$. The reaction was initiated by the addition of 300 µg of purified SK, and then incubated at 37° C for 16 hours, at which time an additional 300 µg of purified enzyme was added, and the reaction allowed to proceed for a further 16 hours.

The reaction mixture was applied batchwise to a slurry of AG 50W-X8 (BioRad) (NH_4^+ form), and incubated, with stirring, for 30 minutes. The slurry was then applied to a sintered glass funnel, and the flow through saved. The slurry was then washed with 250 mL of H_2O. Fractions resulting from this step were pooled with the original flow through, and lyophilized. The dried residue was dissolved in 40 mL of H_2O and acidified by the addition of 3 drops of 6 M HCl. The sample was then applied to an AG-50W-X8 column (NH_4^+ form) (1 x 10 cm), which had been pre-equilibrated with 0.5 mM HCl. Phosphorylated spectinomycin was eluted with a linear gradient of 0 to 300 mM NH_4OH. Fractions were collected and analyzed, as previously described (McKay *et al*, 1994a and Chapter 2). The R_fs for spectinomycin and spectinomycin-phosphate are 0.30 and 0.24, respectively. Fractions deemed to contain phosphorylated spectinomycin were pooled and lyophilized. The white solid was taken up in 3 mL of H_2O and 500 µL

aliquots were applied, in separate runs, to a Mono Q HR 5/5 (Amersham Pharmacia Biotech) column, equilibrated in H_2O. Since the phosphorylated spectinomycin did not bind the column, the flow throughs were pooled and lyophilized.

6.2.8. Sample preparation for NMR analysis of phosphorylated spectinomycin.

Purified phosphorylated spectinomycin was exchanged in 1 mL of D_2O (99%), lyophilized, and then dissolved in 99.996% D_2O (Isotec, Inc), such that the final concentration was approximately 5 mg/mL. Spectinomycin samples were similarly prepared for NMR analysis, except the final concentration of this compound was approximately 25 mg/mL.

6.2.9. Miscellaneous methods.

DNA sequencing was performed at the Central facility of the Institute for Molecular Biology and Biotechnology, McMaster University. Protein concentrations were determined by the method of Bradford (1976). Electrospray ionization mass spectra were determined in the presence of trifluoroacetic acid or NH_4OH, as the organic modifiers, using a Fison platform quadrapole spectrometer at the McMaster Regional Center for Mass Spectrometry.

6.3. Results.

6.3.1. Overexpression and purification of spectinomycin kinase.

The cloning of the SK gene into the pET22b(+) *E. coli* expression vector facilitated the overexpression of the SK enzyme, thereby aiding its purification. While the enzyme overexpressed well, much of the protein was present in the insoluble pellet. Therefore, in an effort to increase the amount of protein present in the soluble fraction, I

increased the temperature of media to 42° C, prior to induction with IPTG, in an effort to induce chaperonin proteins, which were expected to facilitate the folding of soluble enzyme. Inclusion of this step eased protein purification and 5 mg of pure enzyme was obtained from 4 L of cell culture (Table 6.1 & Figure 6.2). The approximate molecular weight of this protein was examined by gel exclusion chromatography, and the size, observed (~50 kDa), was most consistent with the presence of a monomer in solution.

Table 6.1. Purification of spectinomycin kinase.

Step	Total Protein (mg)	Activity (μmoles/min)	Specific Activity (units/mg)	*n*-fold purification	% Recovery
S1	266	-			100
Q-Sepharose, (steep gradient)	40.3	565	14.0		15
Q-Sepharose, (shallow gradient)	24.2	413	17.1	0.82	9.1
Hydroxyapatite	4.7	127	27.0	1.93	1.8

6.3.2. Characterization of spectinomycin phosphate.

With pure SK in hand, it was now possible to characterize the stoichiometry of spectinomycin phosphorylation, as pure protein facilitated the purification of *in vitro* phosphorylated spectinomycin phosphate. The stoichiometry of phosphorylation was determined through the use of electrospray ionization mass spectrometry. In both the positive and negative ion modes the mass to charge ratios observed, 431.1 and 429.0, respectively, were consistent with the mass expected (430.4) for a monophosphorylated derivative of spectinomycin phosphate.

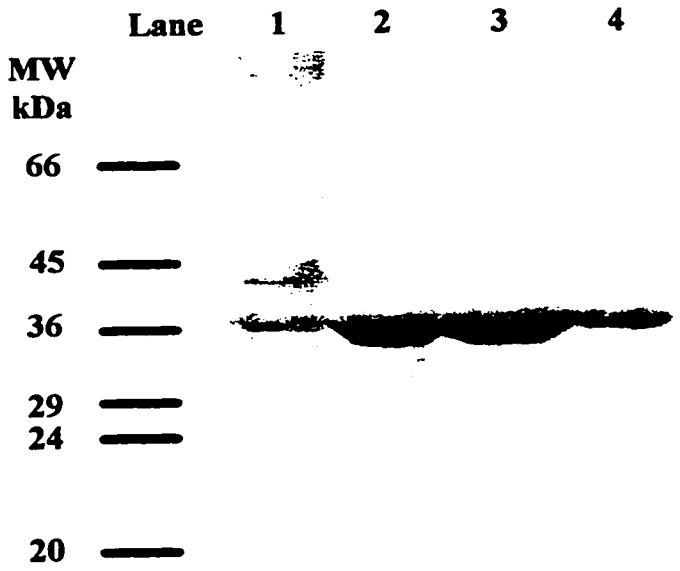

Figure 6.2. Purification of spectinomycin kinase. Aliquots, 10 μL, from each purification step, were applied to an 11% SDS-PAGE gel. Lane 1 contains protein from the cleared cell lysate; lane 2 contains protein from the first Q Sepharose step; Lane 3 contains protein from the second Q Sepharose step; Lane 4 contains protein from the hydroxyapatite step. Protein was visualized with Coomassie Brilliant Blue staining.

6.3.3. Steady state kinetic characterization of spectinomycin kinase.

The ability to overexpress and purify SK in good yield also permitted a detailed kinetic characterization of the catalytic mechanism of this enzyme. As a first step in this characterization, I determined the steady state kinetic parameters for both spectinomycin and ATP (Table 6.2). The K_ms for both substrates examined are in the low micromolar range, whereas the k_{cat}s for spectinomycin and ATP are quite high, approximately 20 s^{-1}, revealing that SK is a highly efficient enzyme, with k_{cat}/K_m values in the 10^6 $M^{-1}s^{-1}$ range. These values are at least an order of magnitude higher than those observed for the APH(3')-IIIa enzyme, which possesses a very broad substrate range (McKay *et al*, 1994a).

Table 6.2. Steady state kinetic parameters for spectinomycin kinase.

Substrate	K_m (μM)	k_{cat} (s^{-1})	K_i (mM)	k_{cat}/K_m ($M^{-1}s^{-1}$)
Spectinomycin[1]	21.5±3.0	24.2±1.0	3.1±0.8	$1.13x10^6$
ATP[2]	17.9±1.1	29.6±0.2	-	$1.09x10^6$

Additionally, I tested a number of AG antibiotics, including streptomycin, kanamycin A, neomycin B, butirosin, amikacin, and apramycin, to see if these compounds could act as substrates for the SK enzyme. However, no APH activity was observed when these AGs were assayed (Table 6.3), under conditions that were expected

Table 6.3. Other structurally unrelated AGs are neither substrates nor inhibitors of spectinomycin kinase.

Aminoglycoside	AG kinase activity[3] (nmoles/min)	Percent of spectinomycin control activity	Inhibitor activity[4] (nmoles/min)	Percent activity remaining
Spectinomycin	59.8±0.6	100	16.9±0.0	100
Streptomycin	0.6±0.1	1.0	19.7±1.0	117
Kanamycin A	0.4±0.1	0.8	18.3±0.8	108
Neomycin B	0.7±0.0	0.7	22.0±1.0	130
Butirosin	1.3±0.3	1.2	16.6±0.1	98
Amikacin	0.4±0.0	2.2	17.2±0.1	102
Apramycin	0.4±0.0	0.7	19.1±1.3	113
ATP only	0.6±0.2	1.0	ND	

[1] ATP was held constant at 1000 μM.
[2] Spectinomycin was held constant at 150 μM.
[3] The ability of spectinomycin kinase to phosphorylate the AG antibiotics listed was determined in the presence of 1 mM of the AG and 930 μM ATP.
[4] The ability of AG antibiotics (100 μM) to inhibit spectinomycin phosphorylation was determined in the presence of 100 μM spectinomycin and 930 μM ATP.

to be saturating for both ATP (930 μM) and the AGs tested (1 mM), as these concentrations are ~100-fold higher than the K_ms for both these substrates. Thus, SK is a highly specific enzyme that exclusively phosphorylates spectinomycin. I further tested the ability of streptomycin, kanamycin A, neomycin B, butirosin, amikacin, and apramycin to act as inhibitors of the reaction catalyzed by SK. These AGs were tested, at a concentration of 100 μM, and no inhibition was observed (Table 6.3), thereby confirming that the spectinomycin-binding site is highly specific for this AG, and excludes other structurally unrelated AGs.

6.3.4. The catalytic mechanisms of spectinomycin kinase and APH(3')-IIIa are similar.

Since the primary structures of SK and APH(3')-IIIa are distantly related, I hypothesized that the catalytic mechanism employed by SK would be similar to the one employed by APH(3')-IIIa. Therefore, I have employed a number of biochemical techniques, previously used on the APH(3')-IIIa enzyme, to establish the catalytic mechanism of SK.

6.3.4.1 The ATP binding pocket of spectinomycin kinase.

One technique employed to study the ATP binding pocket of SK was the use of FSBA. FSBA is an electrophilic analogue of ATP (Figure 6.3) that has previously been shown to inactivate APH(3')-IIIa, through the modification of Lys33 and Lys44, with Lys44 being the predominant site of covalent modification (McKay *et al*, 1994b). Similarly to APH(3')-IIIa, SK was also inactivated by FSBA in a time dependent manner (Figure 6.3).

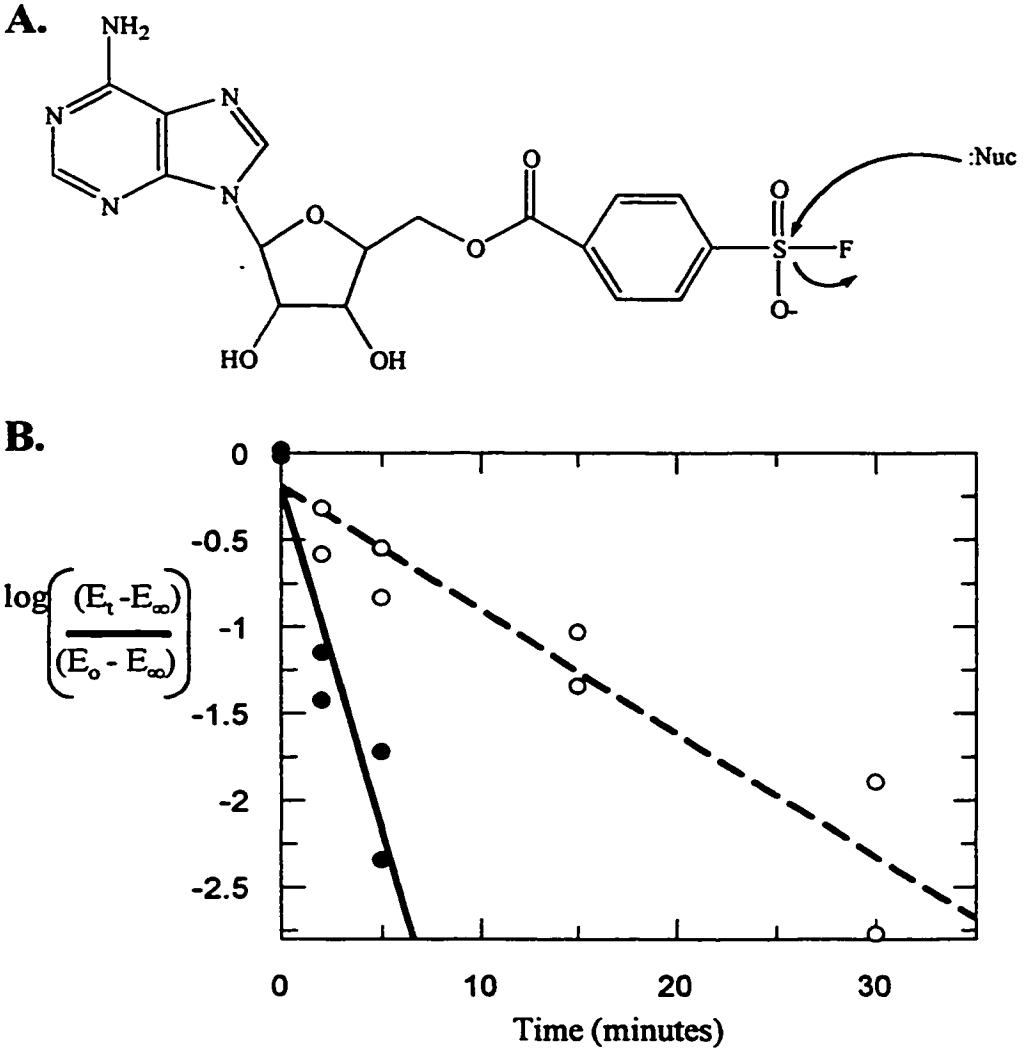

Figure 6.3. Inactivation of spectinomycin kinase by FSBA. A. The structure and mechanism of covalent modification. :Nuc represents an enzyme nucleophile. **B.** Inactivation of spectinomycin kinase by FSBA, in the absence (_____, •), or presence of ATP (— — — , o).

To ensure that the inactivation of SK was due to the covalent modification of a residue lining the ATP binding pocket of this enzyme, I monitored the progress of the inactivation reaction in the presence of ATP. While SK was still inactivated by FSBA, the progress of the inactivation reaction was dramatically slowed in the presence of ATP.

The ability of ATP to protect against the inactivation of this enzyme by FSBA, indicates that this agent specifically modifies a nucleophilic residue in the ATP binding pocket. Using the site of APH(3')-IIIa modification, Lys44, as a precedent, it was expected that the FSBA induced inactivation of SK was due to the modification of Lys52. Lys52 corresponds to Lys44 in primary structure alignments of APH(3')-IIIa and SK (Figure 6.4). Therefore, as a test of this possibility, I examined the ability of FSBA to inactivate the SK^{K52A} mutant in the presence and absence of ATP (Table 6.4). While FSBA also inactivated the SK^{K52A} mutant, in a 5-minute incubation, the inactivation was not complete, and ATP did not afford a significant level of protection. I take the lack of any observable ATP protection, as confirmation that the primary site of covalent modification by FSBA is Lys52. Thus, the ATP binding pockets of SK and APH(3')-IIIa are similar.

Table 6.4. Inactivation of the SK^{K52A} mutant by FSBA.

Reaction	Percent Activity Remaining
Control	100±0.2
+ FSBA	34.6±5.6
+ FSBA + ATP	38.0±1.7

In order to further probe the similarity of the SK and APH(3')-IIIa ATP binding pockets, I determined if H9 could act as an inhibitor of the SK enzyme, as H9 is a micromolar competitive inhibitor of ATP binding to APH(3')-IIIa. When the concentration of H9 was fixed at 1000 μM, the percent activity remaining was 84.0 ± 0.4, when compared to assays containing no H9. While H9 is a poor inhibitor of

spectinomycin phosphorylation, the fact that any inhibition was detected helps to further confirm the similarity of the ATP binding pockets of these two APHs.

```
APH(3')-IIIa      ------MAKMRISPELKKLIEKYRCVKDTEGM   26
SK                MLKQPIQAQQLIELLKVHYGIDIHTAQFIQGG   32
                                        •
APH(3')-IIIa SPAKVYKLVGENEN--LYLKMTDSRYKGTTYDVE-    57
SK           ADTNAFAYQADSESKSYFIKLKYGYHDEINLSIIR    67

APH(3')-IIIa ---REKDMMLWLEGK-LPVPKVLHFERHDGWSNLL    87
SK           LLHDSGIKEIIFPIHTLEAKLFQQLKHFKIIAYPF   102

APH(3')-IIIa MSEADGVLCSEEYEDE-QSPEKIIELYAECIRLFH   121
SK           IHAPNGFTQNLTGKQWKQLGKVLRQIHETSVPISI   137

APH(3')-IIIa SIDISDCPYTNSLDSRLAELDYLLNNDLADVDCEN   156
SK           QQQLRKEIYSPKWREIVRSFYNQIEFDNSDDKLTA   172

APH(3')-IIIa WEEDTPFKDPR--------ELYDFLKTEKPEEELV   185
SK           AFKSFFNQNSAAIHRLVDTSEKLSKKIQPDLDKYV   207
                    •
APH(3')-IIIa FSHGDLGDSNIFVKDGK--VSGFIDLGRSGRADKW   218
SK           LCHSDIHAGNVLVGNE--ESIYIIDWDEPMLAPKE   240

APH(3')-IIIa YDIAFCVRSIRED--IGEEQYVELFFDLLGIKPDW   249
SK           RDLMFIGGGVGN-VWNKPHEIQYFYEGYGEINVDK   272

APH(3')-IIIa EKI-----------------------------KY   257
SK           TILSYYRHERIVEDIAVYGQDLLSRNQNNQSRLES   309

APH(3')-IIIa YILLDELF----------------            264
SK           FKYFKEMFDPNNVVEIAFATEQAP            331
```

Figure 6.4. Primary sequence alignment of spectinomycin kinase and APH(3')-IIIa. While only the alignment of spectinomycin kinase with APH(3')-IIIa is shown, this overlap is based on an alignment of SK (Suter *et al*, 1997), APH(3')-Ia (Oka *et al*, 1981), APH(3')-Ib (Pansegrau *et al*, 1987), APH(3')-Ic (Lee *et al*, 1991),APH(3')-IIIa (Trieu-Cout & Courvalin, 1983), APH(3')-Va, (Thompson & Gray, 1983), APH(3')-Vb (Hoshiko *et al*, 1988), APH(3')-VIa (Martin *et al*, 1988), and APH(3')-VIIa (Tenover *et al*, 1989) using the program Clustal W (Thompson *et al*, 1994). Regions absolutely conserved between the APHs and ePKs are highlighted in bold blue, whereas spectinomycin kinase insert regions are highlighted in bold red. The positions of Lys52 and Asp212 are indicated, using a common bullet (•).

6.3.4.2. Kinetic analysis of spectinomycin kinase mutants.

Since Lys44 and Asp190, present in APH(3')-IIIa, are involved in nucleotide binding and substrate deprotonation, respectively (Hon *et al*, 1997; Chapter 4), primary structure alignments were performed to identify the corresponding residues in SK (Figure 6.4). This alignment putatively identified Lys52 and Asp212 in SK as residues corresponding to Lys44 and Asp190 in APH(3')-IIIa. I therefore generated the SK^{K52A} and SK^{D212A} mutants. The overexpression and purification of these mutant enzymes permitted a determination of their steady state kinetic parameters (Table 6.5), thereby enabling a better understanding of their respective contributions to catalysis.

Table 6.5. Steady state kinetic parameters for mutant spectinomycin kinase proteins.

	SK^{K52A}				
Substrate	K_m (μM)	$K_{m(mut)}/K_{m(WT)}$	k_{cat} (s^{-1})	$k_{cat(WT)}/k_{cat(mut)}$	$V/K_{WT}/V/K_{mut}$
ATP[5]	648±111	36	0.27±0.02	73	2600
Spectinomycin[6]	20.9±2.8	1.0	0.31±0.01	78	78

	SK^{D212A}				
Substrate	K_m (μM)	$K_{m(mut)}/K_{m(WT)}$	k_{cat} (s^{-1})	$k_{cat(WT)}/k_{cat(mut)}$	$V/K_{WT}/V/K_{mut}$
Spectinomycin[7]	ND		≤0.0016±0.0003	15125	-

[5]Spectinomycin was held constant at 150 μM.

[6] ATP was held constant at 1000 μM.

[7] Since the activity of the Asp212Ala was too low to determine steady state kinetic parameters for the phosphorylation of either spectinomycin or ATP, an estimation of the k_{cat} was made in the presence of 150μM spectinomycin and 930 μM ATP.

Consistent with the results obtained for the APH(3')-IIIa^{K44A} mutant (Hon *et al*, 1997), the SK^{K52A} mutant was significantly impaired in its ability to bind ATP. The K_m is increased 36.2-fold, which is comparable to the 26.4-fold effect observed for the APH(3')-IIIa^{K44A} mutant. While the effect on nucleotide binding is similar, the effect on k_{cat} is markedly different. For the SK^{K52A} mutant, the k_{cat} is decreased 78.1-fold, whereas the same mutation in APH(3')-IIIa does not cause a significant decrease in the observed rate of reaction. Thus, Lys52 appears to be required to promote catalysis, however, the manner in which this residue promotes catalysis is not known.

The kinetic parameters determined for the SK^{D212A} mutant indicated that the k_{cat} of this mutant is decreased ~15000-fold. These results parallel the results obtained with the APH(3')-IIIa^{D190A} mutant, as this mutant is 550-fold less active than the wild type enzyme; Asp190 in APH(3')-IIIa corresponds to Asp212 in SK (Hon *et al*, 1997; Chapter 4). Thus Asp212 is critical for the catalytic mechanism of SK, and it is therefore likely that this residue and Asp190, in APH(3')-IIIa, have similar roles in the promotion of phosphate transfer.

6.3.4.3. Metal and solvent isotope effects.

In order to further characterize the similarity of the catalytic mechanisms employed by SK and APH(3')-IIIa, I determined the solvent isotope effect, and as well, the effect of using Mn^{2+} in place of Mg^{2+}. The SK enzyme is quite active when Mn^{2+} is employed as the divalent cation, which is in stark contrast to the effect of this metal ion on the APH(3')-IIIa catalyzed reaction, as this enzyme is essentially inactive at high concentrations of Mn^{2+} (Chapter 4). Since SK is active in Mn^{2+}, the steady state kinetic

parameters, for the wild type SK enzyme, were determined in the presence of Mn^{2+}. While there was little effect on K_m when Mn^{2+} was substituted for Mg^{2+} (Table 6.6), the use of Mn^{2+} did have a rather dramatic effect on the k_{cat} of the reaction. The k_{cat} is decreased approximately 10-fold from the levels observed when Mg^{2+} is used as the divalent cation. Thus, similarly to APH(3')-IIIa, Mg^{2+} is the optimal divalent cation.

As we were interested in determining the contribution of proton abstraction to the rate-limiting step of SK, I determined the steady state kinetic parameters for both ATP and spectinomycin, using D_2O as the solvent and Mg^{2+} as the divalent cation (Table 6.6). When these parameters are compared to those determined in H_2O, one notes a 2.5- to 2.8-fold effect. Since the SK enzyme is also active in Mn^{2+}, I determined the solvent isotope effect in the presence of this metal ion. The effects on k_{cat} are similar, 2.4- to 2.9-fold. The significance of these effects is discussed below.

Table 6.6. Metal and solvent isotope effects.

Substrate	Divalent metal ion	$K_{m(x)}$ (μM)	$K_{m(x)}/K_{m(WT)}$	$k_{cat(x)}$ (s^{-1})	$k_{cat(WT)}/k_{cat(x)}$
H_2O					
Spectinomycin[8]	Mn^{2+}	7.7±2.6	0.4	2.01±0.14	12.1
ATP[9]	Mn^{2+}	8.0±0.49	0.5	2.24±0.02	8.8
D_2O					
Spectinomycin[8]	Mg^{2+}	5.4±1.0	0.3	8.75±0.26	2.8
Spectinomycin[8]	Mn^{2+}	3.5±1.0	0.5	0.85±0.03	2.4
ATP[9]	Mg^{2+}	9.2±1.4	0.5	8.00±0.18	2.5
ATP[9]	Mn^{2+}	10.5±1.5	1.3	0.78±0.01	2.9

[8] ATP was held constant at 1000 μM.
[9] Spectinomycin was held constant at 150 μM.

6.4. Discussion.

It was thought that a comparison of the catalytic mechanisms employed by other APHs to the one employed by APH(3')-IIIa would justify the use of APH(3')-IIIa as a model APH for the structure based design of APH inhibitors. This led to a study of the catalytic mechanism of SK, because I felt that if an APH with low sequence similarity to APH(3')-IIIa employed a similar phosphate transfer mechanism then there would be conclusive proof that the APH(3')-IIIa mechanism represented a paradigm for AG phosphorylation. Thereby, justifying our use of APH(3')-IIIa as a model APH. Thus, I began an initial characterization of the catalytic mechanism employed by SK.

The overexpression and purification of the SK enzyme facilitated the *in vitro* synthesis and purification of spectinomycin-phosphate. The availability of pure spectinomycin-phosphate further facilitated, through the use of electrospray ionization mass spectrometry, a determination of the stoichiometry of phosphorylation. SK catalyzes the transfer of a single phosphate group to spectinomycin. The availability of pure spectinomycin-phosphate also facilitated a determination of the regiospecificity of the spectinomycin kinase enzyme, by D.W. Hughes, in the Department of Chemistry, McMaster University, who, through the use of a variety of one and two dimensional ^{1}H, ^{13}C, and ^{31}P NMR techniques, identified the 9-hydroxyl as the exclusive site of phosphorylation (Figure 6.5). Thus, using the nomenclature of Shaw *et al* (1993) (see Chapter 1), SK will be referred to hereafter as APH(9)-Ia.

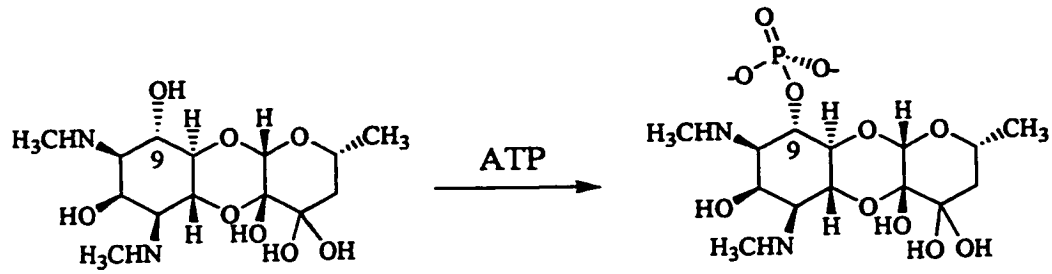

Figure 6.5. Regiospecificity of spectinomycin kinase. Phosphorylation occurs at the 9 hydroxyl, thus, this enzyme should be referred to as APH(9)-Ia, according to the nomenclature of Shaw *et al* (1993).

The overexpression, and purification, of APH(9)-Ia also facilitated the determination of the steady state kinetic parameters for ATP and spectinomycin. With k_{cat}/K_m values on the order of 10^6, APH(9)-Ia is a highly efficient enzyme. Furthermore, since no other AG substrate could be identified, the AG binding site on this enzyme must be highly tailored for spectinomycin binding. This stringent substrate specificity confirms previous results, which had shown, using crude cell lysates obtained from bacteria expressing this enzyme, that kanamycin, streptomycin and hygromycin are not substrates (Suter *et al*, 1997). This exclusive substrate preference, when compared to the broad substrate range of APH(3')-IIIa (McKay *et al*, 1994a), may generally be related to the larger size of this enzyme, as ~84% of the 7.5 kDa size difference is due to the presence of 3 insert regions, of 8 residues or more (Figure 6.4). Since the C-terminal half of APH(3')-IIIa forms the AG binding site (Thompson *et al*, 1999; Chapter 5), it is likely that the extra residues in the C-terminal half of APH(9)-Ia enzyme help form a tight AG binding pocket that precludes the binding of other structurally unrelated AGs. The presence of a 16 residue insert C-terminal to Phe314, in the primary sequence of APH(9)-Ia, suggests that, unlike the APH(3')-IIIa enzyme, there is no requirement for the C-

terminal carboxylate to be present at a position that corresponds with that of Phe264 in APH(3')-IIIa. Although it should be noted that Asp315 in APH(9)-Ia could be the functional equivalent of the APH(3')-IIIa C-terminal carboxylate in this enzyme.

For a more rigorous comparison of the catalytic mechanisms employed by APH3')-IIIa and APH(9)-Ia, I also applied a number of biochemical techniques, to my study of the APH(9)-Ia enzyme, which had previously been used to establish the catalytic mechanism of APH(3')-IIIa. These techniques included the use of an affinity label and site directed mutagenesis, as well as metal ion and solvent isotope effects.

FSBA is an ATP analogue that inactivates APH(3')-IIIa, and was successfully used to identify Lys44 (McKay *et al*, 1994b) as a residue that is present in the ATP binding pocket of APH(3')-IIIa. Therefore, it was felt that this ATP analogue would be a useful probe for comparing the ATP binding pockets of APH(9)-Ia and APH(3')-IIIa. The fact that ATP can specifically inhibit the rate of APH(9)-Ia inactivation, by FSBA, indicates that the inactivation of this enzyme is due to the covalent modification of a nucleophilic residue present in the ATP binding pocket. The fact that Lys52 aligns well with Lys44 in primary structure overlaps of APH(3')-IIIa and APH(9)-Ia, combined with the fact ATP does not inhibit the inactivation of the APH(9)-Ia^{K52A} mutant by FSBA, further indicates that Lys52 corresponds to Lys44, in APH(3')-IIIa. The determination of the steady state kinetic parameters for the APH(9)-Ia^{K52A} mutant confirms that this is indeed the case, as the affinity of this mutant enzyme for ATP is decreased 36-fold, which is similar to the effect observed for the corresponding APH(3')-IIIa mutant. Thus, Lys52, in APH(9)-Ia, corresponds to Lys44, in APH(3')-IIIa. Therefore, based on the

structure of the APH(3')-IIIa•ADP complex (Hon *et al*, 1997), Lys52, in APH(9)-Ia, coordinates the α- and β-phosphates of ATP.

In addition to the generation of the APH(9)-Ia^{K52A} mutant, I have employed site directed mutagenesis to study the role of Asp212 in the catalytic mechanism of this enzyme. Asp212 corresponds to Asp190 in primary structure overlaps of this enzyme and APH(3')-IIIa, and Asp190 is required for substrate deprotonation and metal ion coordination. The fact that the SK^{D212A} mutant is ~15000-fold less active than the wild type enzyme, indicates that Asp212 is critical for catalysis. While the effect on catalysis of removing the Asp212 carboxylate is 27-fold greater than the removal of the corresponding carboxylate, Asp190, in APH(3')-IIIa, the magnitude of this difference could be accounted for by differences in the kinetic mechanisms employed by these two enzymes. For APH(3')-IIIa, ADP release is fully rate limiting, indicating that the phosphate transfer step is at least an order of magnitude higher than the k_{cat} (McKay,& Wright, 1995; 1996), whereas for APH(9)-Ia the rate of the limiting step is not known. Thus, it is possible that for this enzyme phosphate transfer is rate limiting, and product release is not. If this is the case, then at least an order of magnitude of this difference could be accounted for by the kinetic mechanism of APH(9)-Ia. While this may indeed be true, the key fact to remember is that the Asp212 carboxylate is critical to the catalytic mechanism of APH(9)-Ia. Thus, Asp212 in APH(9)-Ia corresponds to Asp190 in APH(3')-IIIa. Therefore, based on the structure of APH(3')-IIIa (Hon *et al*, 1997), and our knowledge of the catalytic mechanism of this enzyme (Chapter 4), Asp212 in APH(9)-Ia is required for substrate deprotonation and metal binding.

Since metal ions play such a critical role in the phosphate transfer mechanism of APH(3')-IIIa, I was interested in determining the role of metal ions in the catalytic mechanism of APH(9)-Ia. Therefore, in an effort to further probe the role of metal ions, in the catalytic mechanism of this enzyme, I determined the effect on APH(9)-Ia activity of substituting Mg^{2+}, the normal divalent cation used in SK assays, with Mn^{2+}. While the APH(9)-Ia enzyme is active when Mn^{2+} is used as the divalent cation, there is approximately a 10-fold decrease in k_{cat}. The reason for the decrease in activity is not entirely clear, but likely reflects the electronic nature of Mn^{2+}, which could suggest that the Mn-ADP complex is tightly held by the enzyme, consequently making ADP release the rate limiting step. Such a situation is observed when Mn^{2+} is used as the divalent cation in APH(3')-IIIa assays (see Chapter 4). Thus, APH(3')-IIIa and APH(9)-Ia show similar, but not identical, metal ion dependencies.

To further compare the catalytic mechanisms of APH(3')-IIIa and APH(9)-Ia, I next examined the contribution of substrate deprotonation to the rate-limiting step of the APH(9)-Ia catalyzed reaction. In order to do this; I examined the effect of changing the bulk solvent to D_2O, on the steady state kinetic parameters of this enzyme. The finding that the APH(9)-Ia enzyme was also active in the presence of Mn^{2+} provided a further test of the role of substrate deprotonation in the catalytic mechanism of this enzyme. The results of these studies are suggestive of a significant role for substrate deprotonation during the formation of the TS. However, the solvent isotope effects observed, regardless of the metal ion used, are comparable to the effect observed for the APH(3')-IIIa

enzyme[10] (McKay & Wright, 1996). This fact indicates that the effects observed are not significant, as I have previously shown that substrate deprotonation does not contribute to the level of rate enhancement afforded by the APH(3')-IIIa enzyme. Further confirmation that the larger solvent isotope effect observed for the APH(9)-Ia enzyme, in comparison to APH(3')-IIIa, is not significant comes from studies of the PKA catalyzed reaction. For PKA, a large solvent isotope effect that is present during the steady state is not observed in the presteady state (Zhou & Adams, 1997). The sum of these results combines to suggest that other factors are the likely cause of the aberrantly large APH(9)-Ia solvent isotope effect. An example of such a factor is solvent viscosity, as Karsten *et al* (1995) have shown that the solvent isotope effect observed for the NAD-Malic enzyme is due to changes in solvent viscosity. Thus, substrate deprotonation does not contribute to the overall rate limiting step for either the APH(9)-Ia or APH(3')-IIIa enzymes, further proof that catalytic mechanisms of these two enzymes are similar (Figure 6.6).

6.5. Conclusions.

The characterizations of the ATP binding pocket and the catalytic mechanism of APH(9)-Ia have provided conclusive evidence that the catalytic mechanism employed by this enzyme is similar, if not identical, to the catalytic mechanism employed by APH(3')-IIIa. The finding that two APHs, with low primary structure identity, share similar

[10] The solvent isotope effects for the APH(3')-IIIa and APH(9)-Ia enzymes are comparable; ~1.5- to 1.7-fold for APH(3')-IIIa versus 2.4- to 2.9-fold for APH(9)-Ia.

catalytic mechanisms indicates that the catalytic mechanism of APH(3')-IIIa (see Chapter 4) is the paradigm for the phosphorylation of AG antibiotics by members of the APH

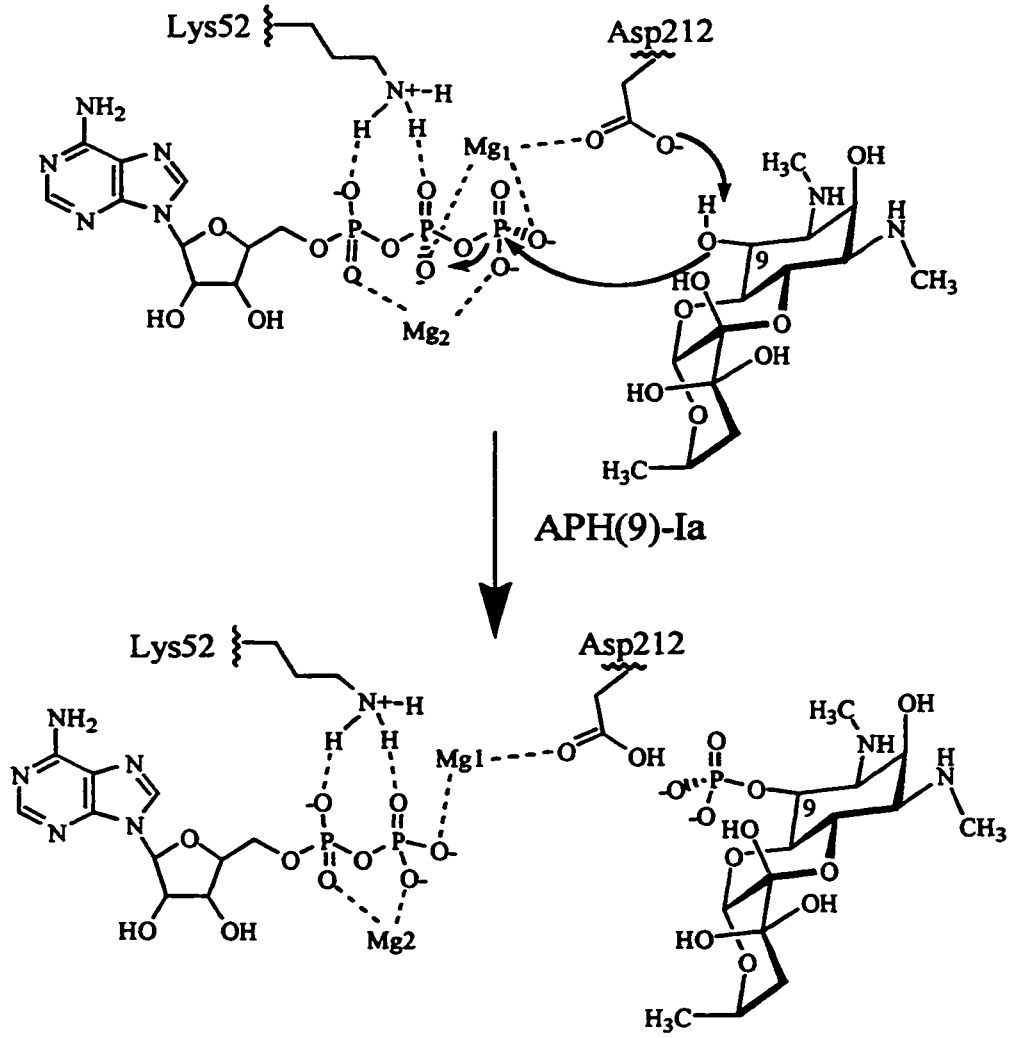

Figure 7.6. Catalytic mechanism of APH(9)-Ia. Lys52 and Asp212 play key roles in the catalytic mechanism of this enzyme. Lys52 likely coordinates the α- and β-phosphates of ATP, and Asp212 is likely involved in metal ion coordination and substrate deprotonation. While the catalytic mechanism is drawn in such a way that substrate deprotonation occurs prior to phosphate transfer, we have no evidence that this is the case, and based on the catalytic mechanism of APH(3')-IIIa, substrate deprotonation likely occurs after phosphate transfer.

family of enzymes. This justifies the use of APH(3')-IIIa as a model APH for the design of APH inhibitors. The fact that the catalytic mechanisms of these two APHs are similar, further indicates that the tertiary structure of the APH(9)-Ia enzyme will be similar to the structure of APH(3')-IIIa.

While the tertiary structures of these two enzymes are likely to be similar, clearly the AG binding domains are quite divergent, as APH(9)-Ia has a very limited substrate specificity, and APH(3')-IIIa has a very broad substrate specificity. The fact that APH(9)-Ia has such a stringent substrate specificity, which is unusual for an APH, leads one to question the evolutionary origins of this enzyme. While it is possible that this enzyme is required to mediate spectinomycin resistance in *L. pneumophila*, *Legionella sp.* are primarily aquatic organisms (Murray *et al*, 1994), whereas spectinomycin is produced by soil organisms, thereby suggesting that this enzyme is unlikely to be present to thwart an environmental toxin. Although this possibility cannot be ruled out, it is known that the APH(9)-Ia enzyme is unlikely to be an acquired form of resistance, as spectinomycin is not a part of the normal drug regimen (Murray *et al*, 1994; Onody *et al*, 1997). Therefore, it is possible that spectinomycin is not the natural substrate of this enzyme.

Since *L. pneumophila* is known to co-opt eukaryotic signal transduction pathways upon colonization of macrophages (Gao & Abu Kwaik, 1999; Susa & Marre, 1999), it is possible that the true substrate of APH(9)-Ia is a member of a signal transduction pathway, for example, a protein or lipid component. This hypothesis stems from the fact that APH(9)-Ia is structurally related to APH(3')-IIIa, an enzyme that is

structurally related to both the PIKs and ePKs (Hon *et al*, 1997; Rao *et al*, 1998). If this is indeed the case, then it suggests that APH(9)-Ia is secreted into the cytosol of macrophages, upon their infection by *L. pneumophila*. While a Type III protein secretion system has not yet been identified in *L. pneumophila*, the secretion of a bacterial enzyme into the cytosol of a eukaryote in order to subvert an immune response controlled by a eukaryotic signal transduction pathway is not without precedent. For example, Yersinia secretes a protein Tyr phosphatase into the macrophage cytoplasm, and this enzyme dephosphorylates a number of phospho-Tyr containing proteins (Bliska *et al*, 1991). Furthermore, YopJ, another Yersinia protein secreted into host cells, prevents the activation of mitogen activated protein kinase kinases through a direct interaction (Orth *et al*, 1999).

While such a role for the APH(9)-Ia enzyme is speculative, the suspected location of the *aph(9)-Ia* gene in an operon (Suter *et al*, 1997), suggests that this enzyme is synthesized for a specific cellular function, perhaps macrophage colonization. Thus, lending further support for a role other than spectinomycin phosphorylation. Unfortunately, confirmation of such a role waits further testing.

6.6. References.

Barker, J.E., & Farrell, I.D. (1990). The effects of single and combined antibiotics on the growth of *Legionella pneumophila* using time-kill studies. *J. Antimicrob. Chemother.* **26**, 45-53.

Bliska, J.B., Guan, K.L., Dixon, J.E., & Falkow, S. (1991). Tyrosine phosphate hydrolysis of host proteins by an essential Yersinia virulence determinant. *Proc. Natl. Acad. Sci. USA* **88**, 1187-1191 .

Bradford, M.M. (1976). A rapid and sensitive method for the quantitation of microgram

quantities of protein utilizing the principle of protein-dye binding. *Anal. Biochem.* **72**, 248-254.

Gao, L.Y., & Abu Kwaik, Y. (1999). Activation of caspase 3 during *Legionella pneumophila*-induced apoptosis. *Infect. Immun.* **67**, 4886-4894.

Hon, W-C., McKay, G.A., Thompson, P.R., Sweet, R.M., Yang, D.S.C., Wright, G.D. & Berghuis, A.M. (1997). Structure of an enzyme required for aminoglycoside resistance reveals homology to eukaryotic protein kinases. *Cell* **89**, 887-895.

Hoshiko, S., Nojiri, C., Matsunaga, K., Katsumata, K., Satoh, E., & Nagaoka, K. (1988). Nucleotide sequence of the ribostamycin phosphotransferase gene and of its control region in *Streptomyces ribosidificus*. *Gene* **68**, 285-296.

Karsten, W.E., Lai, C-J., & Cook, P.F. (1995). Inverse solvent isotope effects in the NAD-malic enzyme reaction are the result of the viscosity difference between D_2O and H_2O: implications for solvent isotope effect studies. *J. Am. Chem. Soc.* **117**, 5914-5918.

Leatherbarrow, R.J. (1992). *Grafit*, Ver 3.0, Erithacus Software Ltd., Staines, UK.

Lee, K.Y., Hopkins, J.D., & Syvanen, M. (1991). Evolved neomycin phosphotransferase from an isolate of *Klebsiella pneumoniae*. *Mol. Microbiol.* **5**, 2039-2046.

Martin, P., Jullien, E., & Courvalin, P. (1988). Nucleotide sequence of *Acinetobacter baumannii aphA-6* gene: evolutionary and functional implications of sequence homologies withnucleotide-binding proteins, kinases and other aminoglycoside-modifying enzymes. *Mol. Microbiol.* **2**, 615-625.

McKay, G.A., Thompson, P.R. & Wright, G.D. (1994a). Broad spectrum aminoglycoside phosphotransferase type III from *Enterococcus*: Overexpression, purification, and substrate specificity. *Biochemistry* **33**, 6936-6944.

McKay, G.A., Robinson, R.A., Lane, W.S., & Wright, G.D. (1994b). Active site labeling of an aminoglycoside antibiotic phosphotransferase (APH(3')-IIIa). *Biochemistry* **33**, 14115-14120.

McKay, G.A. & Wright, G.D. (1995). Kinetic mechanism of aminoglycoside phosphotransferase Type IIIa: Evidence for a Theorell-Chance kinetic mechanism. *J. Biol. Chem.* **270**, 24686-24692.

McKay, G.A. & Wright, G.D. (1996). Catalytic mechanism of enterococcal kanamycin kinase (APH(3')-IIIa): Viscosity, thio, and solvent isotope effects support a Theorell-Chance mechanism. *Biochemistry*, **35**, 8680-8685.

Murray, P.R., Kobayashi, G.S., Pfaller, G.S., & Rosenthal, K.S. (1994). *Legionella* and other miscellaneous Gram-negative bacilli. *Medical Microbiology*, 2nd Ed., pp279-283, Moseby, St. Louis.

Oka, A., Sugisaki, H., & Takanami, M. (1981). Nucleotide sequence of the kanamycin resistance transposon Tn903. *J. Mol. Biol.* **147**, 217-226.

Onody, C., Matsiota-Bernard, P., & Nauciel, C. (1997). Lack of resistance to erythromycin, rifampicin, ciprofloxacin in 98 clinical isolates of *Legionella pneumophila*. *J. Antimicrob. Chemother.* **39**, 815-816.

Orth, K., Palmer, L.E., Bao, Z.Q., Stewart, S., Rudolph, A.E., Bliska, J.B., & Dixon, J.E. (1999). Inhibition of the mitogen-activated protein kinase kinase superfamily by a Yersinia effector. *Science* **285**. 1920-1923.

Pansegrau, W., Miele, L., Lurz, R., & Lanka, E. (1987). Nucleotide sequence of the kanamycin resistance determinant of plasmid RP4: homology to other aminoglycoside 3'-phosphotransferases. *Plasmid* **18**. 193-204.

Rao, V.D., Misra, S., Boronenkov, I.V., Anderson, R.A., & Hurley, J.H. (1998). Structure of Type IIβ phosphatidylinositol phosphate kinase: a protein kinase fold flattened for interfacial phosphorylation. *Cell* **94**, 829-839.

Shaw, K.J., Rather, P.N., Hare, R.S., & Miller, G.H. (1993). Molecular genetics of aminoglycoside resistance genes and familial relationships of the aminoglycoside-modifying enzymes. *Microbiol. Rev.* **57**, 138-163.

Susa, M., & Marre, R. (1999). *Legionella pneumophila* invasion of MRC-5 cells induces tyrosine protein phosphorylation. *Infect. Immun.* **67**, 4490-4498.

Suter, T.M., Viswanathan, V.K., & Cianciotto, N.P. (1997). Isolation of a gene encoding a novel spectinomycin phosphotransferase from *Legionella pneumophila*. *Antimicrob. Agents Chemother.* **41**, 1385-1388.

Tenover, F.C., Gilbert, T., & O'Hara, P. (1989). Nucleotide sequence of a novel kanamycin resistance gene, aphA-7, from *Campylobacter jejuni* and comparison to other kanamycin phosphotransferase genes. *Plasmid* **22**, 52-58.

Thompson, C.J., & Gray, G.S. (1983). Nucleotide sequence of a streptomycete aminoglycoside phosphotransferase gene and its relationship to phosphotransferases encoded by resistance plasmids. *Proc. Natl. Acad. Sci. USA* **80**, 5190-5194.

Thompson, J.D., Higgins, D.G., & Gibson, T.J. (1994). CLUSTAL W: improving the sensitivity of progressive multiple sequence alignment through sequence weighting,

position-specific gap penalties and weight matrix choice. *Nucl. Acids Res.* **22**, 4673-4680.

Thompson, P.R., Hughes, D.W., Cianciotto, N.P., Wright, G.D. (1998). Spectinomycin kinase from *Legionella pneumophila*. Characterization of substrate specificity and identification of catalytically important residues. *J. Biol. Chem.* **273**, 14788-14795.

Thompson, P.R., Schwartzenhaur, J., Hughes, D.W., Berghuis, A.M., & Wright, G.D. (1999). The C-terminus of aminoglycoside phosphotransferase (3')-IIIa is critical for antibiotic recognition and resistance. *J. Biol. Chem.* **274**, 30697-30706.

Trieu-Cuot, P., & Courvalin, P. (1983). Nucleotide sequence of the *Streptococcus faecalis* plasmid gene encoding the 3'5"-aminoglycoside phosphotransferase type III. *Gene* **23**, 331-341.

Zhou, J., & Adams, J.A. (1997). Is there a catalytic base in the active site of cAMP-dependent protein kinase? *Biochemistry* **36**, 2977-2984.

Chapter 7

Conclusions, implications, and prospects for the future design of aminoglycoside phosphotransferase inhibitors.

All work described in this chapter was obtained by the author of this thesis.

CHAPTER 7: Conclusions, implications, and prospects for the future design of aminoglycoside phosphotransferase inhibitors.

7.1. From the past to the present - 1993-1999.

Our studies of APH(3')-IIIa, in collaboration with A.M. Berghuis and colleagues, have provided a wealth of information on the tertiary structure and catalytic mechanism of this enzyme. When we started our study of APH(3')-IIIa, a crystal structure of this, or for that matter any other APH, was not available and little was known about the catalytic mechanism of this enzyme. In fact, at the time that our study was initiated, even the regiospecificity of APH(3')-IIIa had not yet been definitively established. Furthermore, at that time, it was thought that the APHs employed a double displacement phosphoryl transfer mechanism with His188 (APH(3')-IIIa numbering) acting as the phosphate acceptor/donor (Martin *et al*, 1988; Kocabiyik & Perlin, 1992).

In the 6 years since we began our detailed characterization of the structure and catalytic mechanism of APH(3')-IIIa, the enzyme has been overexpressed and purified (McKay *et al*, 1994), the crystal structure bound to ADP solved (Hon *et al*, 1997), the kinetic mechanism determined (McKay & Wright, 1995; 1996), and a number of inhibitors identified (Daigle *et al*, 1997). In addition to the characterizations described above, I have been directly involved in characterizing both the regiospecificity and catalytic mechanism of APH(3')-IIIa. Through these studies, I have conclusively demonstrated that this enzyme does not employ a double displacement mechanism, but instead catalyzes the direct transfer of the γ-phosphate of ATP to either the

3'-hydroxyl, present on 4,6-disubstituted AGs, or to both the 3'- and 5" hydroxyls, present on 4,5-disubstitued AGs. For 4,5-disubstituted AGs that lack a 3'-hydroxyl, I have also been able to show that phosphorylation occurs exclusively at the 5"-hydroxyl (McKay *et al*, 1994; Thompson *et al*, 1996a; 1996b; Chapter 2 & 3).

The finding that the APH(3')-IIIa enzyme catalyzed the direct transfer of the γ-phosphate of ATP to an AG hydroxyl (Thompson *et al*, 1996b; Chapter 3) represented a new paradigm because these enzymes were thought to employ a double displacement mechanism, as mentioned above. As a result of this new paradigm, I began to explore the direct in-line phosphate transfer mechanism of this enzyme in greater detail. As one step in that direction, I examined the primary sequence homology that exists between APH enzymes, and, in so doing I identified an absolutely conserved aspartate residue, Asp190, that I felt was likely important for catalysis. The generation of an Asp190Ala mutant, and its subsequent kinetic characterization, confirmed that Asp190 was indeed critical for catalysis (Hon *et al*, 1997; Chapter 4). Fortuitously, this discovery occurred concomitantly with the determination of the APH(3')-IIIa•ADP crystal structure (Hon *et al*, 1997), which not only confirmed my kinetic evidence that Asp190 was critical for catalysis, but also suggested that this residue was involved in both substrate deprotonation and metal binding.

In addition to providing an explanation for the role of Asp190 in the catalytic mechanism of APH(3')-IIIa, the determination of the tertiary structure of this enzyme helped to identify potentially important catalytic residues. The identification of such residues was aided immeasurably by the finding that this enzyme is structurally related to

the ePKs, as the contribution of specific amino acid residues to catalysis, in such enzymes, has been very well studied (see Chapter 4 and Taylor *et al*, 1995, for a review). Thus, with the identification of catalytically important residues in APH(3')-IIIa, I was able to analyze the contribution of individual amino acid residues to the catalytic mechanism of this enzyme. This was accomplished by generating site directed mutants, and determining their steady state kinetic parameters.

The results, of this analysis, confirmed the accuracy of the APH(3')-IIIa crystal structure, and gave new insights into the catalytic mechanism employed by this enzyme. These studies indicated that the amide proton of Ser27 has a role in nucleotide binding, as does the functional group of this residue, although this occurs indirectly, as this hydroxyl is a ligand for Mg1, which coordinates the β- and γ-phosphates of ATP (Figure 4.3; Chapter 4). Similarly, the functional groups of Asn195 and Asp208 also have indirect roles in nucleotide binding, as these residues coordinate Mg2 and Mg1, respectively. While both of these residues contact metal ions, Asp208 is absolutely required for phosphate transfer (Daigle *et al*, 1999a; Chapter 4), suggesting that Mg1 is the catalytic metal ion. In addition to Ser27 and Asp208, Asp190 is also a metal ligand for Mg1. While Asp190 is also involved in deprotonating the AG substrate, solvent isotope effects for the wild type and mutant APH(3')-IIIa enzymes indicate that substrate deprotonation does not contribute to the rate limiting step of the enzyme. This fact suggests that the metal binding role of Asp190 is its critical role in the promotion of phosphate transfer, and not substrate deprotonation.

Since substrate deprotonation does not make a significant contribution to the rate-limiting step of APH(3')-IIIa, I concluded that this enzyme employs a dissociative-like TS (Chapter 4). But I wondered how this enzyme could generate such an intermediate. The answer came when I noted that Ser27, Asp190, and Asp208, all make contacts with the catalytic metal ion (Mg1). The fact that all these residues are Mg1 ligands, suggested that a metaphosphate-like intermediate could be generated by the concerted movement of these three residues in the same direction, which causes the directed movement of Mg1, away from P_β. And if P_β remains stationary, relative to Mg1, the elongation of the P_β-O-P_γ bond thereby generates the metaphosphate-like intermediate. This type of catalytic mechanism is best described as a biomechanical phosphate transfer mechanism.

During the time I pursued my studies on the catalytic mechanism of APH(3')-IIIa, I was also interested in identifying the specific residues in APH(3')-IIIa that were required for AG binding. Analogous to our identification of catalytically important residues, the identification of residues, required for AG binding, was facilitated by the determination of the crystal structure of the APH(3')-IIIa•ADP complex. This structure helped to identify a highly anionic pocket in the C-terminal region of this enzyme, which we felt would provide favorable electrostatic interactions for the binding of electropositive AG antibiotics. Therefore, the C-terminal region of the enzyme was examined, looking for residues that could help to form the putative AG binding pocket, for example, those residues whose functional groups are solvent exposed. One part of the C-terminal region that we could readily identify, as forming the AG binding pocket, was

the extreme C-terminal helix, which is composed of the sequence L_{260}DELF-COO^-. As this sequence is highly conserved among the APH(3) subfamily of APHs, it was decided to examine the role of the negatively charged residues in this peptide, as it was expected that these residues would be important for AG binding, due to their potential for forming complementary interactions with the positively charged AG substrates of this enzyme. Therefore, I again employed site directed mutagenesis to probe the roles of these residues in substrate binding and catalysis.

The results of this analysis provided concrete biochemical evidence to support the location of the AG binding pocket in the C-terminus of APH(3')-IIIa (Thompson *et al*, 1999; Chapter 5). Furthermore, we can now ascribe roles, for either substrate binding or catalysis, to Asp261, Glu262, and Phe264. Asp261 is required for stabilizing the C-terminal helix, and is therefore important for promoting catalysis, as helix stability is undoubtedly involved in properly orientating Glu262 and the Phe264 carboxylate, both of which are involved in substrate binding. Glu262 is required for binding 4,5-disubstituted AGs, such that the 5"-hydroxyl is phosphorylated, whereas the C-terminal carboxylate is required for binding 4,5-disubstituted AGs such that the 3'-hydroxyl is phosphorylated (Thompson *et al*, 1999; Chapter 5).

In addition to my work on APH(3')-IIIa, I have also characterized the catalytic mechanism of APH(9)-Ia, an enzyme from *L. pneumophila*, that specifically phosphorylates spectinomycin at the 9-hydroxyl group (Thompson *et al*, 1998; Chapter 6; Suter *et al*, 1997). Using a similar approach, to the one which we employed to examine the catalytic mechanism of APH(3')-IIIa, I have characterized the catalytic mechanism of

APH(9)-Ia, and found it to be identical to the one employed by APH(3')-IIIa. The fact that these two enzymes employ similar catalytic mechanisms (Thompson *et al*, 1998; Chapter 6), suggests that their tertiary structures are also likely to be similar. Since the tertiary structures of these enzymes are similar, it is reasonable to assume that the structures of all the APHs will resemble the tertiary structure of APH(3')-IIIa.

7.2. Where do we go from here?

While I have spent much time, and effort, describing our studies into the catalytic mechanisms of APH(3')-IIIa and APH(9)-Ia, the ultimate goal of these studies is the inhibition of the AG resistance mediated by APH enzymes, in general. As such, I feel it is now appropriate to discuss some of the implications of these studies for the design and synthesis of specific APH inhibitors. Such implications arise from studies regarding both the regiospecificities and catalytic mechanisms of several APH enzymes, including APH(3')-IIIa, APH(9)-Ia and AAC(6')-APH(2").

With regard to regiospecificity studies (Thompson *et al*, 1996a; Chapter 2; Daigle *et al*, 1999a); the finding that both APH(3')-IIIa and AAC(6')-APH(2") phosphorylate the 5"-hydroxyl of lividomycin A suggests that the synthesis of a 4"-nitro containing 4,5-disubtituted AG analogue (Figure 7.1), could form the basis for a broad specificity mechanism based inactivator of the APHs. Such a compound is based upon the work of Roestamadji *et al* (1999), who identified a 2'-nitro containing 4,6-disubstituted AG (Figure 7.1) as a mechanism based inactivator. The mechanism through which the 2'-nitro compound inactivates APH(9') enzymes is described in Chapter 1, Section 1.5. While the 2'-nitro substituted compounds failed to reverse resistance *in vivo* (Wright *et*

al, 1999), there is no reason to believe that the 4"-nitro compound proposed here, and in Thompson *et al* (1996a), would meet a similar fate. Thus, this compound should be synthesized and tested for *in vitro*, and *in vivo*, activity with all due haste.

A.

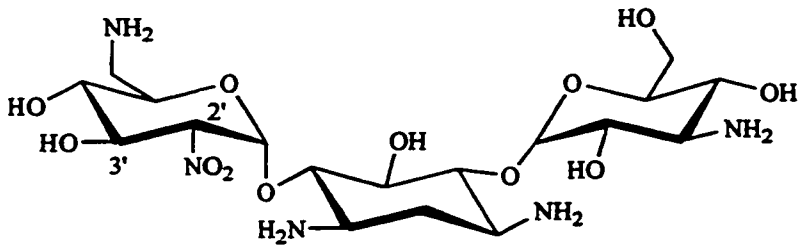

B.

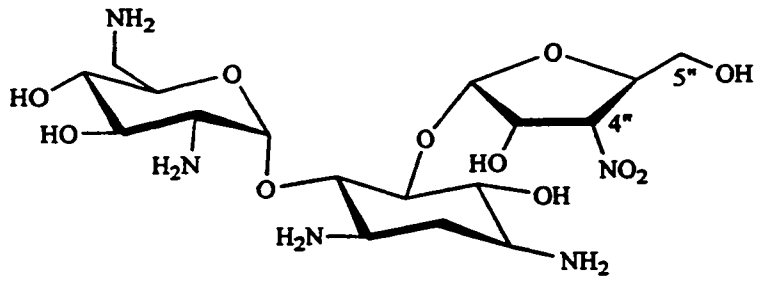

Figure 7.1. Regiospecific mechanism-based inactivators. The fact that the 2'-nitro derivative of kanamycin B (**A.**) could inactivate APH(3')-IIa, after phosphorylation of the 3'-hydroxyl (Roestamadji, *et al*, 1995), suggests that a 4"-nitro derivative of ribostamycin (**B.**) should also act as a mechanism-based inactivator of the 3'-APH enzymes, as the enzyme also catalyzes 5"-phosphorylation.

While regiospecificity studies, on a number of APHs, have not identified a plethora of potentially useful compounds to reverse resistance, our studies of the catalytic mechanism employed by APH enzymes have identified a number of compounds. For example, the usefulness of bi-substrate analogues was not previously examined, as it was

thought, prior to my studies on APH(3')-IIIa, that the APHs employed a double displacement mechanism; a mechanism which has no requirement for both substrates to remain bound to the enzyme during phosphate transfer. Therefore, my determination that APH(3')-IIIa employs a direct in-line phosphate transfer mechanism (Thompson *et al*, 1996b; Chapter 3) led us to explore the ability of bi-substrate analogues to act as inhibitors of APH(3')-IIIa. These compounds, which were the generous gift of S. Mobashery, Department of Chemistry, Wayne State University, Detroit, Michigan, and which link adenosine to neamine using various linker lengths (5-8 methylene units) (Figure 7.2), were subsequently tested for their ability to inhibit APH(3')-IIIa activity using the assay described in Chapter 4 (see Table 7.1 for details). Inhibition data, thereby derived, was fit by nonlinear least squares to either Equation 7.1,

$$v = V_{max}[S]/(K_m(1 + [I]/K_{is}) + [S]) \qquad \text{(Eq. 7.1)},$$

or Equation 7.2,

$$v = V_{max}[S]/(K_m(1 + [I]/K_{is}) + [S](1 + [I]/K_{ii} + [S]/K_I)) \qquad \text{(Eq. 7.2)},$$

depending on whether the pattern of inhibition observed was competitive or noncompetitive. While all of the compounds tested are low micromolar inhibitors of APH(3')-IIIa (Table 7.1), there is some variation in their effectiveness, as well, there are differences in the pattern of inhibition observed. These differences correlate well with the length of the linker, as bisubstrate analogues, with linkers that are 5 or 8 methylene units long are essentially competitive inhibitors towards ATP, thereby suggesting that the linker is either too long or too short. Thus, the ideal linker length is between 6 and 7 methylene units long.

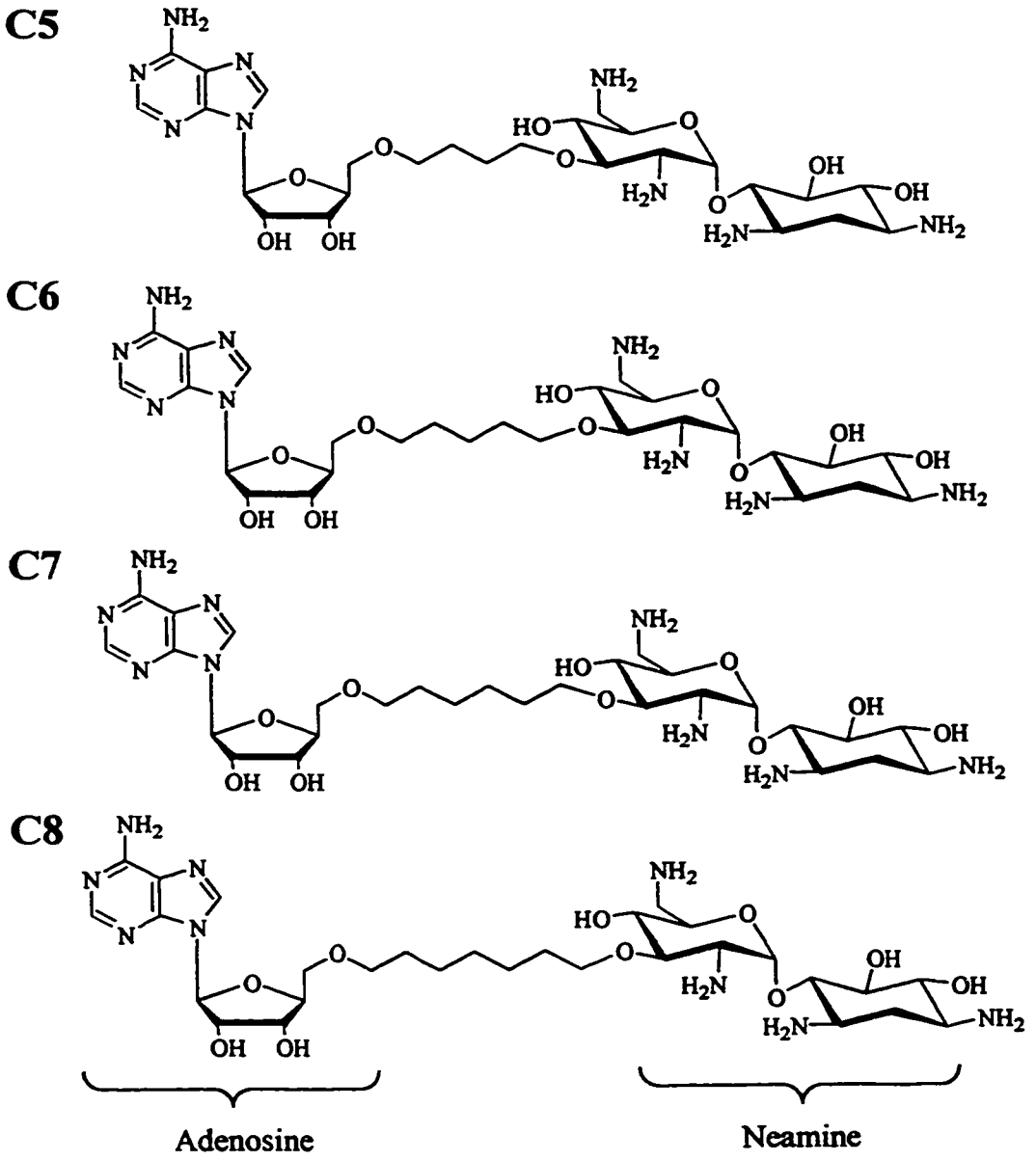

Figure 7.2. Bi-substrate analogues for the APH family of enzymes. Adenosine and neamine are linked together using a variable linker length. The linkers are either 5, 6, 7, or 8 methylene units long, and the compounds are named accordingly. These compounds were the generous gift of S. Mobashery.

A linker length of 6 or 7 methylene units is consistent with the distance between the 5'-hydroxyl of the ribose moiety and the 3'-hydroxyl of an AG substrate positioned

for phosphate transfer. Thus, these results suggest that modified compounds with linker lengths of 6 or 7 methylene units would be excellent starting points for the design and synthesis of more specific APH inhibitors.

Table 7.1. Bisubstrate analogue inhibition of APH(3')-IIIa[1].

Inhibitor	Substrate	K_{is} (μM)	K_{ii} (μM)	Pattern of Inhibition
C5	Kanamycin A[2]	4.16±1.76	15.1±2.2	NC
C5	ATP[3]	0.19±0.03	20.0±2.8	NC[4]
C6	Kanamycin A	14.4±7.5	25.9±4.3	NC
C6	ATP	0.73±0.19	34.9±7.5	NC
C7	Kanamycin A	12.8±3.5	34.9±4.6	NC
C7	ATP	0.74±0.25	52.8±16.2	NC
C8	Kanamycin A	36.7±37.1	224±120	NC
C8	ATP	0.34±0.09		C

One way to increase the specificity of these inhibitors would be to take advantage of the interactions that are known to occur between the enzyme and the triphosphate moiety of ATP. Such compounds should, for example, ideally provide complementary interactions for the positively charged Lys44 residue, and the negatively charged Asp208 residue, as these residues are absolutely conserved among the APH family of enzymes (Figure 4.3). This could be achieved by the placement of a negatively charged carboxylate, β to the 5'-hydroxyl of the ribose ring, in combination with the placement of a positively charged amino group, β to the 3'-hydroxyl of the linked AG

[1] Data was obtained in duplicate at 37° C.
[2] ATP was held at 1 mM.
[3] Kanamycin A was fixed at 100 μM.
[4] While the data shown here was derived using Eq 8.2, the data fits almost as well to a competitive inhibition plot.

(Figure 7.3). In order to maximize the Lys44 interaction, this distance between the newly added group and the bisubstrate linker is likely to be no more than 1 methylene unit, as the corresponding position in the APH(3')-IIIa•ADP structure is only 3.3 Å from the ε-amino group of this residue. For the Asp208 interaction this distance is likely to be 0-1 methylene units, as the closest βγ-non-bridge oxygen is 2.5-4.2 Å away from the carboxylate of Asp208. Thus, by examining the effect of increasing the distance between the newly added group and the bisubstrate linker it should be possible to further increase the affinity of these lead compounds for the active site of an APH enzyme.

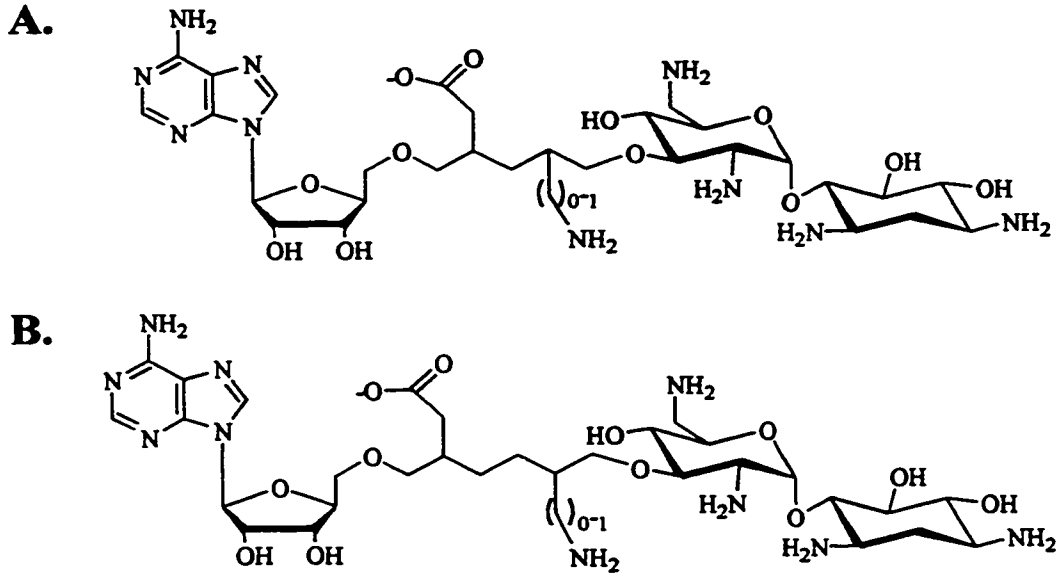

Figure 7.3. Derivatives of bisubstrate analogues.
A. Derivatives of C6. **B.** Derivatives of C7.

In addition to the bisubstrate analogues, study of the catalytic mechanism of APH(3')-IIIa led to the identification of a number of other lead inhibitory compounds. These compounds were identified because of the similarities that exist between the

structures and catalytic mechanisms of the APHs and the ePKs (Hon *et al*, 1997, Chapter 4; Daigle *et al*, 1999b), which suggested that protein kinase inhibitors might also inhibit APH(3')-IIIa (Daigle *et al*, 1997). The most effective of these compounds are the isoquinolinesulfonamides. Since several of these compounds were micromolar inhibitors of APH(3')-IIIa, and since my studies of the catalytic mechanisms of APH(3')-IIIa and APH(9)-Ia indicated that all of the APHs possessed similar tertiary structures, it was felt that these compounds would also inhibit the APH activity of AAC(6')-APH(2"). The *aac(6')-aph(2")* gene is the primary cause of AG resistance in *S. aureus* (Miller *et al*, 1997). Therefore, the ability of these compounds to inhibit the APH activity of this enzyme was examined. Similarly to what was observed for APH(3')-IIIa, the most effective inhibitors of AAC(6')-APH(2") were the isoquinolinesulfonamides. One of these compounds, H9 (Figure 7.4), inhibited both of these enzymes in the low micromolar range, and since H9 inhibition was competitive with respect to ATP, this compound likely binds tightly to the ATP binding pockets of both these enzymes.

With K_is, for H9 inhibition, on the order of 138±40 and 63±19 for the APH(3')-IIIa and AAC(6')-APH(2") enzymes, respectively (Daigle *et al*, 1997), H9 should provide an excellent framework for the design of more specific inhibitors. Since the isoquinoline ring of H9 is thought to mimic the adenosine ring of ATP (Daigle *et al*, 1997), it should be possible to provide more favorable interactions with an APH enzyme through the design of H9 derivatives that take advantage of the interactions that normally anchor the triphosphate moiety of ATP to the enzyme.

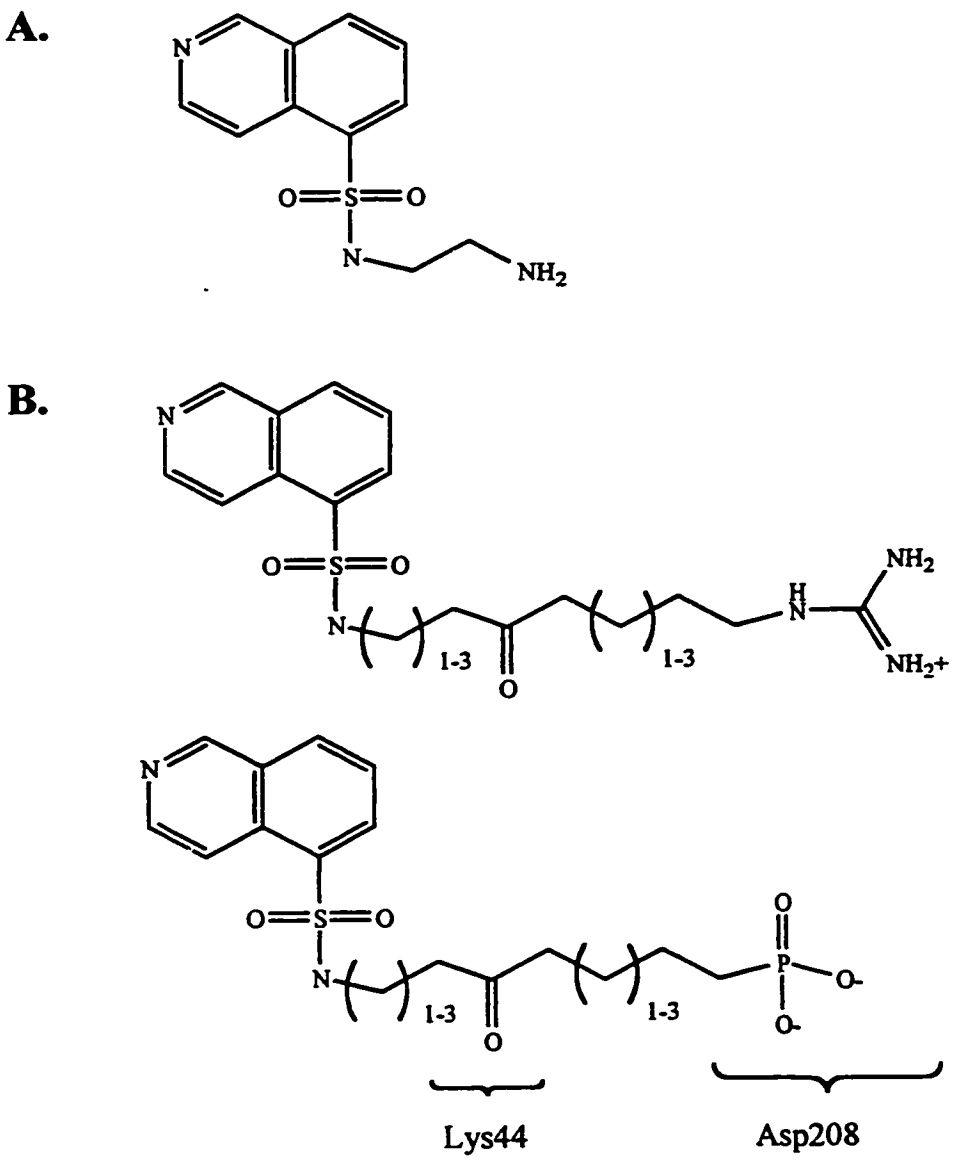

Figure 7.4. Structures of H9 (A) and potential higher affinity H9 derivatives (B). B. Postulated interactions between H9 derivatives and amino acid residues present in the active site of APH family members.

Similarly to the bi-substrate analogue derivatives described above, such H9 derivatives should have complementary interactions with key residues in the active site of the APHs, for example Lys44 and Asp208 (Figure 7.4). Such interactions could be

achieved by the placement of a carbonyl group within hydrogen bonding distance of Lys44, in combination with the placement of either a phosphinate group or a guanidinium group close to the carboxylate of Asp208. The use of a phosphinate presumes that a Mg^{2+} ion will bound to the Asp208 carboxylate in the absence of ATP, thereby bridging these two anions, whereas the use of the guanidinium group has no requirement for a bound metal ion. While the affinity of an APH for such derivatives of H9 are likely to be higher than that observed for H9, it should be noted that various combinations of linker lengths (see Figure 7.4) will have to be tested. Nevertheless, the strategy described above should be an effective process for the identification of an inhibitor with a high degree of specificity towards a clinically relevant APH.

In summary, the characterization of APH(3')-IIIa and APH(9)-Ia has immensely aided our ability to identify specific compounds that can inhibit members of the APH family of enzymes. The synthesis of the compounds described herein, or the design and synthesis of structurally related compounds will, undoubtedly, lead to the reversal of the AG resistance phenotype that is mediated by APHs in general. The design of even more specific compounds, tailored to a particular APH, will ultimately be aided by the determination of crystal structures for such inhibitors bound to APH(3')-IIIa and other clinically relevant APH enzymes. For example, AAC(6')-APH(2"), as the gene encoding this enzyme is the primary cause of AG resistance in *S. aureus* and *E. faecalis* (Brighty *et al*, 1993; Miller *et al*, 1997).

7.3. What does it all mean?

A number of important implications can be drawn from my studies of APH(3')-IIIa and APH(9)-Ia. First and foremost comes from my comparison of the catalytic mechanisms employed by these two enzymes. Since these mechanisms are so similar, it must be concluded that all of the APHs employ nearly identical catalytic mechanisms. Therefore, the catalytic mechanism first described for APH(3')-IIIa represents a paradigm for AG phosphorylation.

Secondly, the fact that APH(3')-IIIa is structurally related to the ePKs, and, as well the PIKs (Rao, *et al*, 1998), makes it likely that these three families of enzymes employ similar, if not identical, mechanisms of phosphoryl transfer. The findings that these three families of enzymes are structurally related and employ similar catalytic mechanisms, indicates that these families of enzymes are related in the distant past, thereby indicating the existence of an ancestral kinase. While it is possible that this primordial kinase had a specific phosphate accepting substrate, I have great difficulty believing that an enzyme, with such a high degree of substrate specificity, would have existed. This is especially true if one thinks of the current requirement for phosphotransferases in so many life-giving cellular processes, which suggests that the first kinases would also have been involved in many cellular processes. Therefore, what is more likely, to my mind, is that the primordial kinase phosphorylated many substrates, including proteins, lipids, and AG-like compounds, and as time passed, and cells evolved more elaborate regulatory networks, greater substrate specificity was required of this primordial catalyst. A process of gene duplication, the addition of family specific peptide

sequences, and mutation likely met this need for greater specificity. What is most amazing, is that throughout this process, the underlying structural and mechanistic properties of these enzymes remained intact!

7.4. A final word.

Conceptually, the idea that the PIKs, ePKs, and APHs all evolved, from a single primordial catalyst, has profound implications for the evolution of enzymes in general. It suggests that all enzymes, which employ a similar catalytic mechanism, are likely to have evolved from a single primordial enzyme that possessed the same core catalytic structure. While such an idea is not compatible with convergent evolution, it is difficult to envisage the development a new enzyme from a protein that simply binds a substrate, because for catalysis to occur an enzyme does not bind a substrate; it binds the TS for the reaction. While there may be examples of enzymes generated by convergent evolution, for example the serine proteases, I believe that the general principle, in evolution, is the adaptation of the structural and mechanistic properties of an old enzyme, to create a new one that can act on a different substrate.

7.5. References.

Brighty, K.E., Kohlbrenner, W., & McGuirk, P.R. (1993). Recent developments in antibacterial resistance mechanisms. *Ann. Rep. Med. Chem.* **28**, 141-147.

Daigle, D.M., McKay, G.A., & Wright, G.D. (1997). Inhibition of aminoglycoside resistance enzymes by protein kinase inhibitors. *J. Biol. Chem.***272**, 24755-24758.

Daigle, D.M., Hughes, D.W., & Wright, G.D. (1999a). Prodigious substrate specificity of AAC(6')-APH(2"), an aminoglycoside antibiotic resistance determinant in enterococci and staphylococci. *Chem. Biol.* **6**, 99-110.

Daigle, D.M., McKay, G.A., Thompson, P.R. & Wright, G.D. (1999b). Aminoglycoside antibiotic phosphotransferases are also serine protein kinases. *Chem. Biol.* **6**, 11-18.

Hon, W-C., McKay, G.A., Thompson, P.R., Sweet, R.M. Yang, D.S.C., Wright, G.D., & Berghuis, A.M. (1997). Structure of an enzyme required for aminoglycoside antibiotic resistance reveals homology to eukaryotic protein kinases. *Cell* **89**, 887-895.

Kocabiyik, S., & Perlin, M.H. (1992). Site-specific mutations of conserved C-terminal residues in aminoglycoside 3'-phosphotransferase II: phenotypic and structural analysis of mutant enzymes. *Biochem. Biophys. Res. Comm.* **185**, 925-931.

Martin, P., Jullien, E., & Courvalin, P. (1988). Nucleotide sequence of *Acinetobacter baumannii aphA-6* gene: evolutionary and functional implications of sequence homologies with nucleotide-binding proteins, kinases and other aminoglycoside-modifying enzymes. *Mol. Microbiol.* **2**, 615-625.

McKay, G.A., Thompson, P.R. & Wright, G.D. (1994a). Broad spectrum aminoglycoside phosphotransferase type III from *Enterococcus*: Overexpression, purification, and substrate specificity. *Biochemistry* **33**, 6936-6944.

McKay, G.A., Robinson, R.A., Lane, W.S., & Wright, G.D. (1994b). Active site labeling of an aminoglycoside antibiotic phosphotransferase (APH(3')-IIIa). *Biochemistry* **33**, 14115-14120.

McKay, G.A. & Wright, G.D. (1995). Kinetic mechanism of aminoglycoside phosphotransferase Type IIIa: Evidence for a Theorell-Chance kinetic mechanism. *J. Biol. Chem.* **270**, 24686-24692.

McKay, G.A. & Wright, G.D. (1996). Catalytic mechanism of enterococcal kanamycin kinase (APH(3')-IIIa): Viscosity, thio, and solvent isotope effects support a Theorell-Chance mechanism. *Biochemistry*, **35**, 8680-8685.

Miller, G.H., Sabatelli, F.J., Hare, R.S., Glupczynski, Y., Mackey, P., Schlaes, D., Shimizu, K., Shaw, K.J., & the Aminoglycoside Study Groups (1997). The most frequent aminoglycoside resistance mechanisms-changes with time and geographic area: a reflection of aminoglycoside usage patterns? *Clin. Infect. Dis.* **24(Suppl 1)**, S46-S62.

Rao, V.D., Misra, S., Boronenkov, I.V., Anderson, R.A., & Hurley, J.H. (1998). Structure of Type IIβ phosphatidylinositol phosphate kinase: a protein kinase fold flattened for interfacial phosphorylation. *Cell* **94**, 829-839.

Roestamadji, J., Grapsas, I., & Mobashery, S. (1995). Loss of individual electrostatic interactions between aminoglycoside antibiotics and resistance enzymes as an effective means to overcoming bacterial drug resistance. *J. Am. Chem. Soc.* **117**, 11060-11069.

Suter, T.M., Viswanathan, V.K., & Cianciotto, N.P. (1997). Isolation of a gene encoding a novel spectinomycin phosphotransferase from *Legionella pneumophila*. *Antimicrob. Agents Chemother.* **41**, 2135-2143.

Taylor, S.S., Radzio-Andzelm, E., & Hunter, T. (1995). How do protein kinases discriminate between serine/threonine and tyrosine? Structural insights from the insulin receptor protein-tyrosine kinase. *FASEB J.* **9**, 1255-1266.

Thompson, P.R., Hughes, D.W., & Wright, G.D. (1996a). Regiospecificity of aminoglycoside phosphotransferase from *Enterococci* and *Staphylococci* (APH(3')-IIIa). *Biochemistry* **35**, 8686-8695.

Thompson, P.R., Hughes, D.W. & Wright, G.D. (1996b) Mechanism of aminoglycoside 3'-phosphotransferase type IIIa: His188 is not a phosphate-accepting residue. *Chem. Biol.* **3**, 747-755.

Thompson, P.R., Hughes, D.W., Cianciotto, N.P., & Wright, G.D. (1998). Spectinomycin kinase from *Legionella pneumophila*. Characterization of substrate specificity and identification of catalytically important residues. *J. Biol. Chem.* **273**, 14788-14795.

Thompson, P.R., Schwartzenhaur, J., Hughes, D.W., Berghuis, A.M., & Wright, G.D. (1999). The C-terminus of aminoglycoside phosphotransferase (3')-IIIa is critical for antibiotic recognition and resistance. *J. Biol. Chem.* **274**, 30697-30706.

Wright, G.D., Berghuis, A.M., & Mobashery, S. (1999). Aminoglycoside antibiotics: structures, function and resistance. In *Resolving the antibiotic paradox: progress in drug design and resistance.* (Rosen, B.P., & Mobashery, S., eds), pp. 27-69, Plenum Publishing Corporation, New York, NY.